# *Design, Synthesis and Application of Ultrastable Rylene Dyes for Fluorescent Labeling of Biomolecules*

Dissertation zur Erlangung des Grades
„Doktor der Naturwissenschaften"
am Fachbereich Chemie und Pharmazie
der Johannes Gutenberg-Universität in Mainz

vorgelegt von

Kalina Peneva
geb. in Plovdiv, Bulgarien

Mainz, 2008

Dekan:

1. Berichterstatter:

2. Berichterstatter:

Tag der mündlichen Prüfung:

Science is a way of thinking much more than it is a body of knowledge.

*Carl Sagan*

Dedicated to my parents –
Nikolay Penev and Magdalena Peneva

## List of most used abbreviations

| | |
|---|---|
| SMS | Single molecule spectroscopy |
| PMI | Perylenemonoimide |
| TMI | Terrylenemonoimide |
| PDI | Perylenediimide |
| TDI | Terrylenediimide |
| QDI | Quaterrylenediimide |
| $\delta$ | Chemical shift [ppm] |
| d | Doublet |
| DCM | Dichloromethane |
| FCS | Fluorescence Correlation Spectroscopy |
| SPT | Single particle tracking |
| DMF | N,N-Dimethylformaide |
| DMSO | Dimethylsulfoxide |
| DNA | Deoxyribonucleic acid |
| e | Elementary charge |
| EDC | N'-(3-Dimethylaminopropyl)-N-ethylcarbodiimide Hydrochloride |
| FD | Field Desorption |
| HPLC | High performance liquid chromatography |
| IR | Infrared |
| J | Coupling constant [Hz] |
| m | Mass |
| MALDI-TOF | Matrix-Assisted Laser Desorption/Ionization-Time of Flight |
| MeOH | Methanol |
| MS | Mass spectroscopy |
| NHS | N-hydroxysuccinimide |
| NMR | Nuclear Magnetic Resonance |
| $Pd(PPh_3)_4$ | Tetrakis(triphenylphosphin)-Palladium(0) |
| PEG | Polyethylene glycol |
| Ph | Phenyl |
| $Ph_2O$ | Diphenyl ether |
| ppm | parts per million |

| | |
|---|---|
| RNA | Ribonucleic Acid |
| $R_H$ | Hydrodynamic radius |
| RT | Room temperature |
| s | Singlet |
| T | Temperature [K] |
| t | Triplett |
| NTA | Nitrilotriacetic acid |
| THF | Tetrahydrofuran |
| UV | Ultra violet |
| TRITC | Tetramethylrhodamine isothiocyanate |
| EGFP | Enhanced Green fluorescent protein |
| $\nu$ | Wave number [$cm^{-1}$] |
| Cys | cysteine |
| Lys | lysine |
| nm | nanometer |
| z | Charge |

# Contents

## *Chapter 4 – Water-soluble perylene and terrylene dyes: powerful labels for single enzyme tracking*

## Chapter 5 – Preparation of water-soluble perylene thioester for site-specific labeling of proteins

## Chapter 6 – Exploiting the nitrilotriacetic acid moiety for biolabeling using rylene dyes

## *Chapter 7*

## *Chapter 8*

# 1. Color and colorants

Color vision is based on a variety of physical, chemical, physiological, and psychological processes. The electromagnetic spectrum visible to man lies in the wavelength range of 400-700 nm. The different forms of light, whether directly coming from a light source, reflected from a surface or transmitted through a medium, reach the retina in the human eye, where a photochemical process is initiated, and a complex neurochemical information transfer between the eye and the brain finally leads to visual perception. Colors have always appealed to human beings. Colors not only influence emotions of individuals but are also an instrument of communication. Therefore, colorants have played an important role in the development of cultural history, and the synthetic manufacturing of dyestuffs was a major driving force in the industrial revolution of the 19th century.[1] Colorants are characterized by their ability to absorb or emit light in the visible range (400-700 nm). Man has used natural colorants since prehistoric times, as reflected by the cave drawings in Europe, Africa, in ancient Egypt and in China.[1] In 1856, Perkin's discovery of mauve marked the start of the modern synthetic dye industry. In the last 150 years, several million different colored compounds have been synthesized, with ca. 15 000 colorants, over time, produced on an industrial scale.[1] Colorants are either dyes or pigments. Pigments consist of small particles that are practically insoluble in those media in which they are applied; dyes on the other hand are applied from a liquid in which they are completely soluble.

Chromatic colors are generated when matter specifically absorbs (or reflects) light of a given wavelength, which leads to absorption bands with typical maxima and minima in the visible spectrum. (Figure 1.1) When material absorbs in the short wavelength around 400 – 430 nm, the corresponding body appears yellow to the eye. Analogously, absorption bands at 430-480, 480-550, 550-600 and 600-700 nm make the absorbing bodies appear orange, red, violet, and blue, respectively.
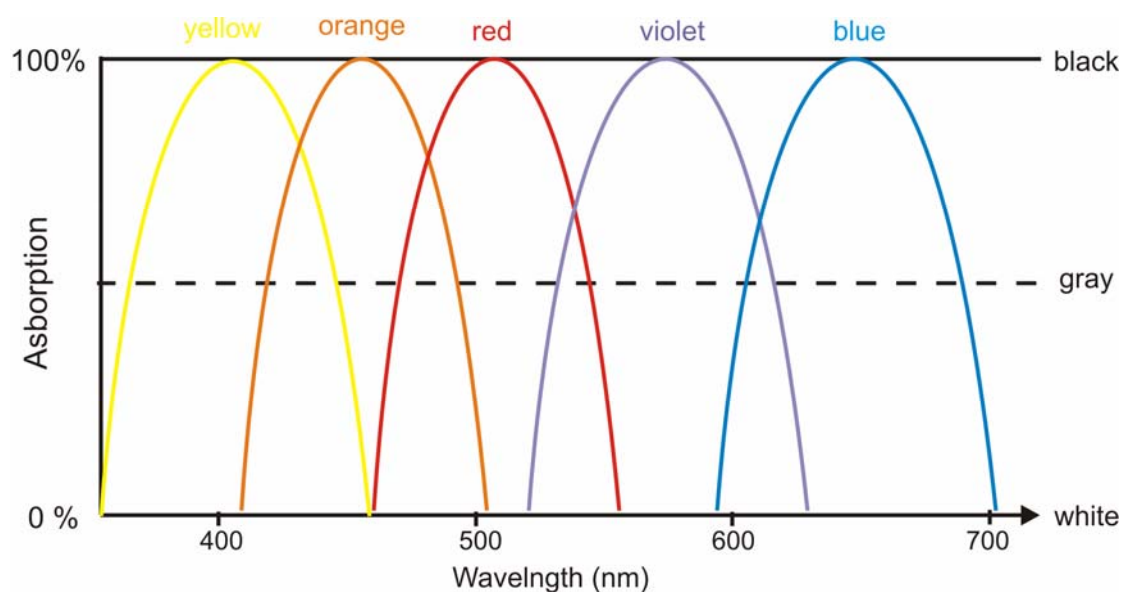
**Figure 1: Schematic representation of the light absorption of colored solids. [2]**

The perception of color by the human eye does not solely depend on absorption wavelength, although this is crucial, but also on the shape of the bands involved. The smaller the width and the steeper the slopes of a band, the purer and the more brilliant the color appears.

In recent times, the use of organic dyes and pigments for coloring textiles and other consumer goods was expanded to the field of the so called "functional dyes". In this context, the most important role is not played by the aesthetic appearance, but by the physical or chemical properties of the dyes such as light emission, photoelectric and photochemical activity as well as light induced polarization. Some of the resulting applications which make use of this new type of chromophore are fluorescent labels in biochemistry and medicine, laser dyes, electrophotography, xerography, data storage and sensitizers in photovoltaic devices. The integration of dyes in diverse high-technology fields dictates new and fascinating challenges for a materials-oriented organic synthesis.

## *1.1. Color model and color coordinates*

A color model is an abstract mathematical model describing the way colors can be represented as tuples of numbers, typically as three or four values or color components. When this model is associated with a precise description of how the components are to be interpreted (viewing conditions, etc.), the resulting set of colors is called a color space. In the study of the perception of color, one of the first mathematically defined color spaces was the CIE 1931 XYZ color space (also known as CIE 1931 color space), created by the International Commission on Illumination (CIE) in 1931.[1][2] Since the human eye has three types of color sensors that respond to different ranges of wavelengths, a full plot of all visible colors is a three-dimensional figure. However, the concept of color can be divided into two parts: brightness and chromaticity.
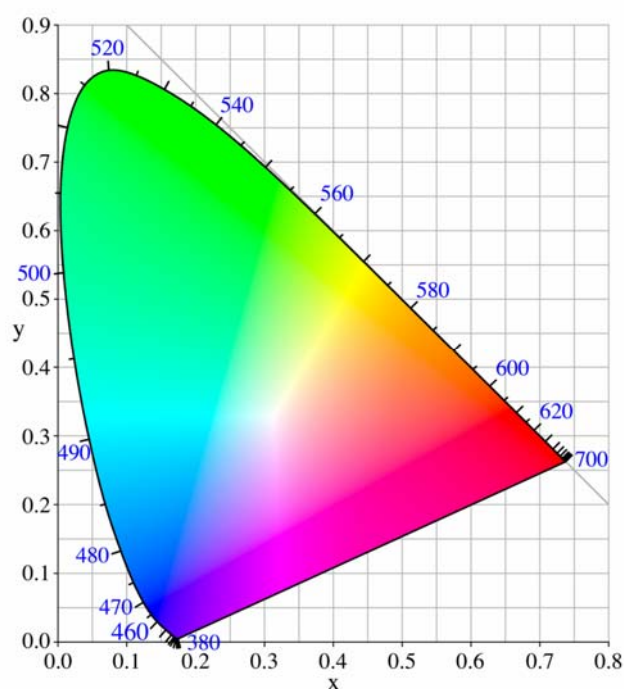


**Figure 1.1. The CIE 1931 color space chromaticity diagram. The outer curved boundary is the spectral (or monochromatic) locus, with wavelengths shown in nanometers. Note that the colors depicted depend on the color space of the device on which you are viewing the image, and no device has a gamut large enough to present an accurate representation of the chromaticity at every position.**

The diagram shown on figure 1.1 represents all of the chromaticities visible to the average person. These are shown in color and this region is called the gamut of human vision. The gamut of all visible chromaticities on the CIE plot is the tongue-shaped or horseshoe-shaped figure shown in color. The curved edge of the gamut is called the spectral locus and corresponds to monochromatic light, with wavelengths listed in nanometers. The straight edge on the lower part of the gamut is called the line of purples. These colors, although they are on the border of the gamut, have no counterpart in monochromatic light. Less saturated colors appear in the interior of the figure with white at the center. Mathematically, x and y are projective coordinates and the colors of the chromaticity diagram occupy a region of the real projective plane. If one chooses any two points on the chromaticity diagram, then all colors that can be formed by mixing these two colors lie between those two points, on a straight line connecting them. It follows that the gamut of colors must be convex in shape. All colors that can be formed by mixing three sources are found inside the triangle formed by the source points on the chromaticity diagram (and so on for multiple sources).

## *1.2 Rylene dyes and pigments*

Rylene dyes are based on naphthalene units linked in the peri-position, thus they can be named as poly(peri-naphthalene) (PPN). The nomenclature is explained in Figure 1.2. The basic structures of the materials described in this text consist of perylene **1.1** and the much more photostable perylenetetracarboxydiimides **1.2** (PDI), first prepared in 1912.[3] Particularly severe requirements for functional dyes are nowadays defined by single molecule spectroscopy (SMS) where the fluorescence of single emitter molecules rather than of their ensemble is recorded. The rylene chromophores have proved to be of outstanding value for SMS.



**1.1**

**1.2**
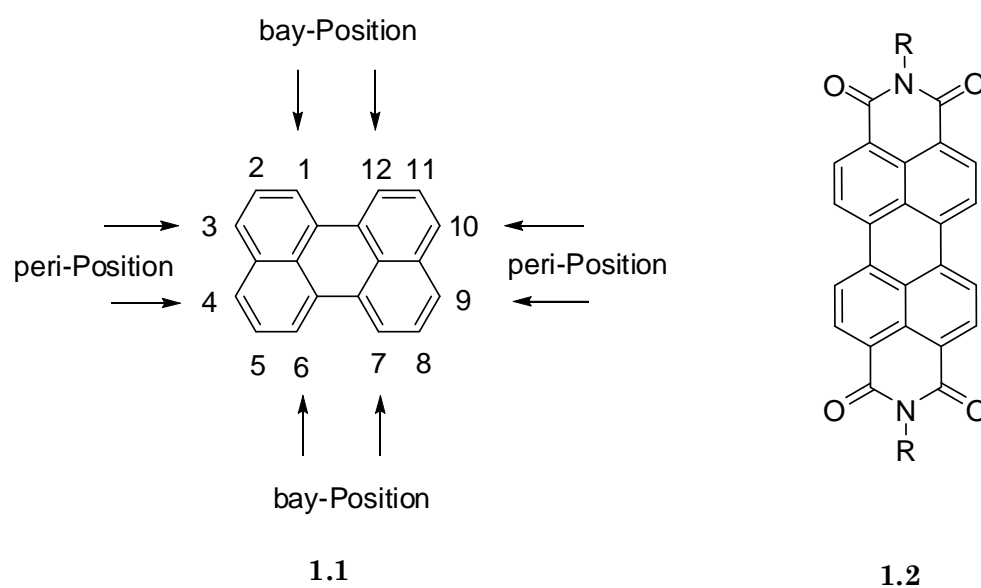
**Figure 1.2. Poly(peri-naphthalene) and perylene**

In this class of dyes, the most important representatives are the perylene-3,4,9,10-tetracarboxdimides (PDIs). Highly fluorescent PDIs are widely used as dyes and pigments due to their outstanding chemical, thermal and photochemical stability.[2, 4, 5] Therefore, they are utilized in the fields of paints and lacquers, particularly in the car industry, and as key chromophores for high-tech applications such as reprographic processes, fluorescent solar collectors,[6] optical switches[7] and

dye lasers.[8] Since PDI derivatives possess high electron mobilities,[9, 10] Friend and Müllen,[11, 12] as well as Gregg have fabricated high-efficiency organic photovoltaic devices by using a blend of electron-accepting PDI and a hole-accepting hexabenzocoronene as well as a polymer-PDI blend, respectively. The higher homologues of the rylene also have played key roles in single molecule spectroscopy (terrylene derivatives), and as NIR absorbers (quaterrylene derivatives).[13-16]

## *1.3 Perylene derivatives*
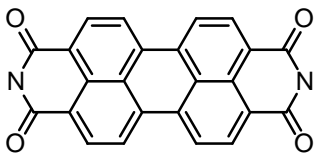
The industrial synthesis of perylene pigments and dyes is based on the patent in 1913 of M. Kardos (Scheme 1.1).[3] Acenaphthylene (**1.3**) is converted to 1,8-naphthalene-dicarboxanhydride (**1.4**) by oxidation with atmospheric oxygen using a vanadium oxide catalyst or with nitric acid. After imidization, the 1,8-naphthalenedicarboximide (**1.5**) is obtained. An oxidative dimerization is then carried out with alkali (e.g. a mixture of sodium hydroxide, potassium hydroxide and sodium acetate at 190~200°C) to give perylene-3,4,9,10-tetracarboxdiimide (**1.7**). Perylene-3,4,9,10-tetracarboxdianhydride (**1.8**) is obtained via the saponification of PDI **1.7** with sulfuric acid. By using aromatic or aliphatic amines, different N, N'-diaryl and N, N'-dialkyl substituted PDIs (**1.9**) respectively are then synthesized.[4, 17] Recently, new reaction conditions for the dimerization to produce PDI **1.9** are developed using a mixture of potassium *tert*-butoxide, 1,8-diazabicyclo[5.4.0]undec-7-ene (DBU), and diglyme under nitrogen atmosphere to give purer materials with almost quantitive conversion.[18]
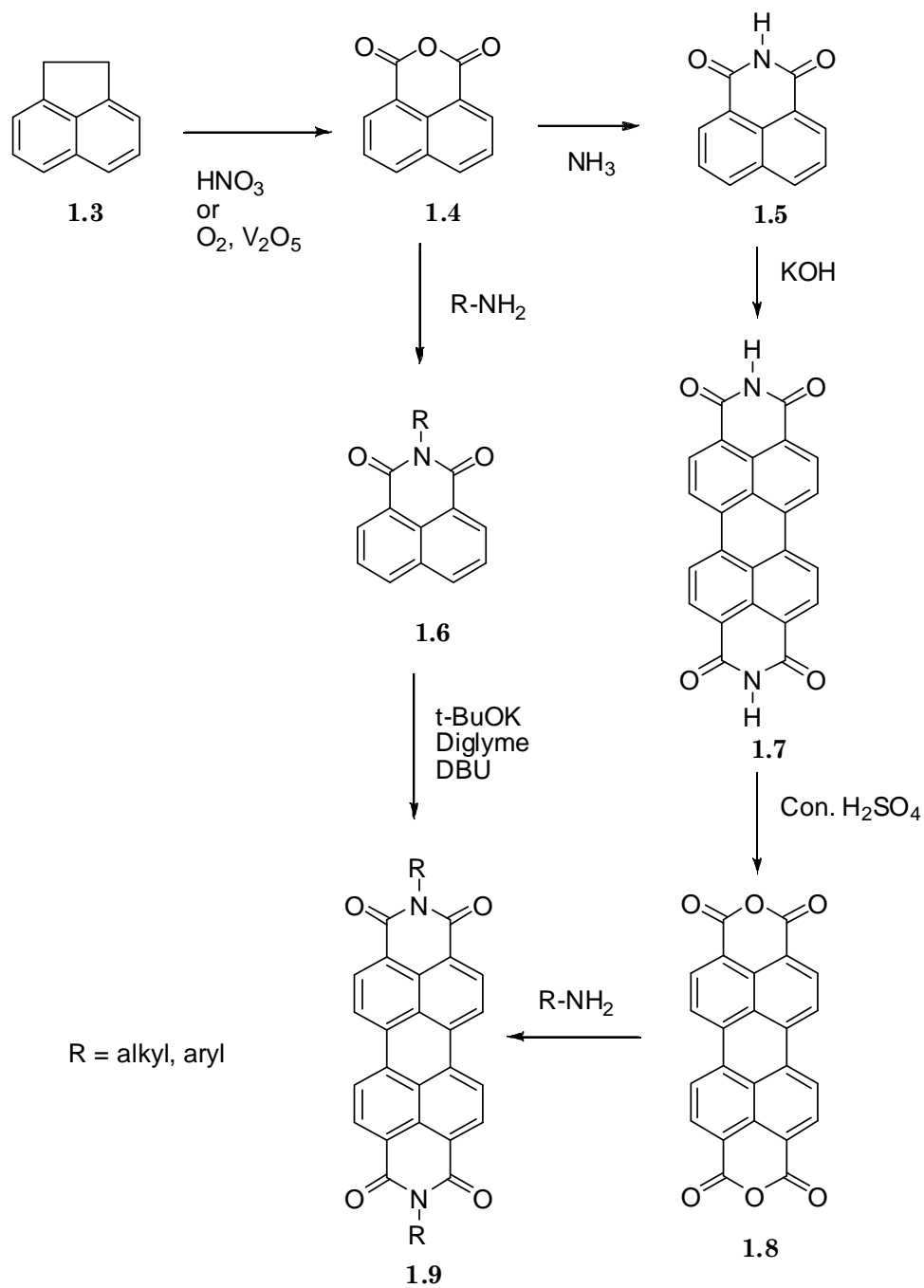
**Scheme 1.1. Synthetic route to perylene-3,4:9,10-tetracarboxdiimide 1.9.**

PDI pigments show high thermal and chemical stabilities, for example, their decomposition temperature is up to 350 °C. They are used to stain polymers such as polyethylene as well as various copolymers. A further advantage of perylene pigments is their broad range of colors, which can be controlled by using different substituents in the imide structure of PDIs. (Table 1.1) The reason for the large differences of color is hidden in the small differences of the imide substituents, and the influence of the respective crystal structure on the light absorption. For example, in the solid state, the space requirement of the imide structure of PDI suppresses the parallel stacking of the aromatic systems. X-ray crystal analysis of black pigments revolved a stronger aggregation of the individual aromatic systems than that of the red pigments.

**Table 1.1. Examples of red and black perylene pigments**

| | Substituent in the imides | Pigment | Industrial name |
|---|---|---|---|
|  | $CH_3$ | red | Indanthren Rot 2G |
| | H | Deep red | Pigment Violet 29 |
| | $CH_2CH_2Ph$ | black | Pigment Black 31 |

If particularly bulky imide substituents are used, the parallel stacking of PDI can be completely avoided due to the steric hindrance to give perylene dyes instead of perylene pigments.[5] PDIs substituted with 2,6-diisopropylphenyl and 2,5-di-tert-butylphenyl in the imides are highly soluble in common organic solvents and display a bright color with strong fluorescence.[19] Another method to transform perylene chromophores into dyes is to introduce phenoxy groups in the bay region of PDIs (Scheme 1.2). This substitution prevents the aggregation of the chromophores in solution resulting in a remarkable increase of the solubility.[20]

By selective chlorination in the bay region of perylenedianhydride **1.8** with chlorine gas in sulfuric acid or with thionyl chloride in nitrobenzene, tetrachloro-substituted perylene derivatives **1.10** and **1.11** can be synthesized. After nucleophilic exchange of the chlorines by phenolates, the desired tetraphenoxy-PDI **1.12** is obtained.[21] Phenoxylation with 4-isooctylphenol **1.13** bearing sterically demanding alkyl groups is accompanied by a bathochromic shift of the absorption maximum from c.a. 520 nm to 580 nm, and leads to 50-fold increase in the solubility of **1.13** in organic solvents. Solubility in aqueous medium can be achieved as a result of introduction of sulfonyl- or carboxyl groups in the phenol units of the bay-positions as realized for **1.14** and **1.15**, respectively. In addition, perylenedianhydride with four phenoxy substituents can be achieved via saponification using potassium hydroxide in ethanol and water at $90^{o}C$.[22] The soluble PDIs e.g. **1.9** and **1.12** exhibit brilliant orange and red color respectively as well as intensive fluorescence with nearly 100 % quantum yield in solution.[23]

Functionalization of the bay positions also enables an effective shielding of the chromophore, which otherwise exhibits a high tendency towards π-stacking. Encapsulation is realized by creating four terminal alkynes at the phenoxy groups, which are used for the build-up of polyphenylene dendrimers around compound **1.16** acting as a core molecule.[24-26]
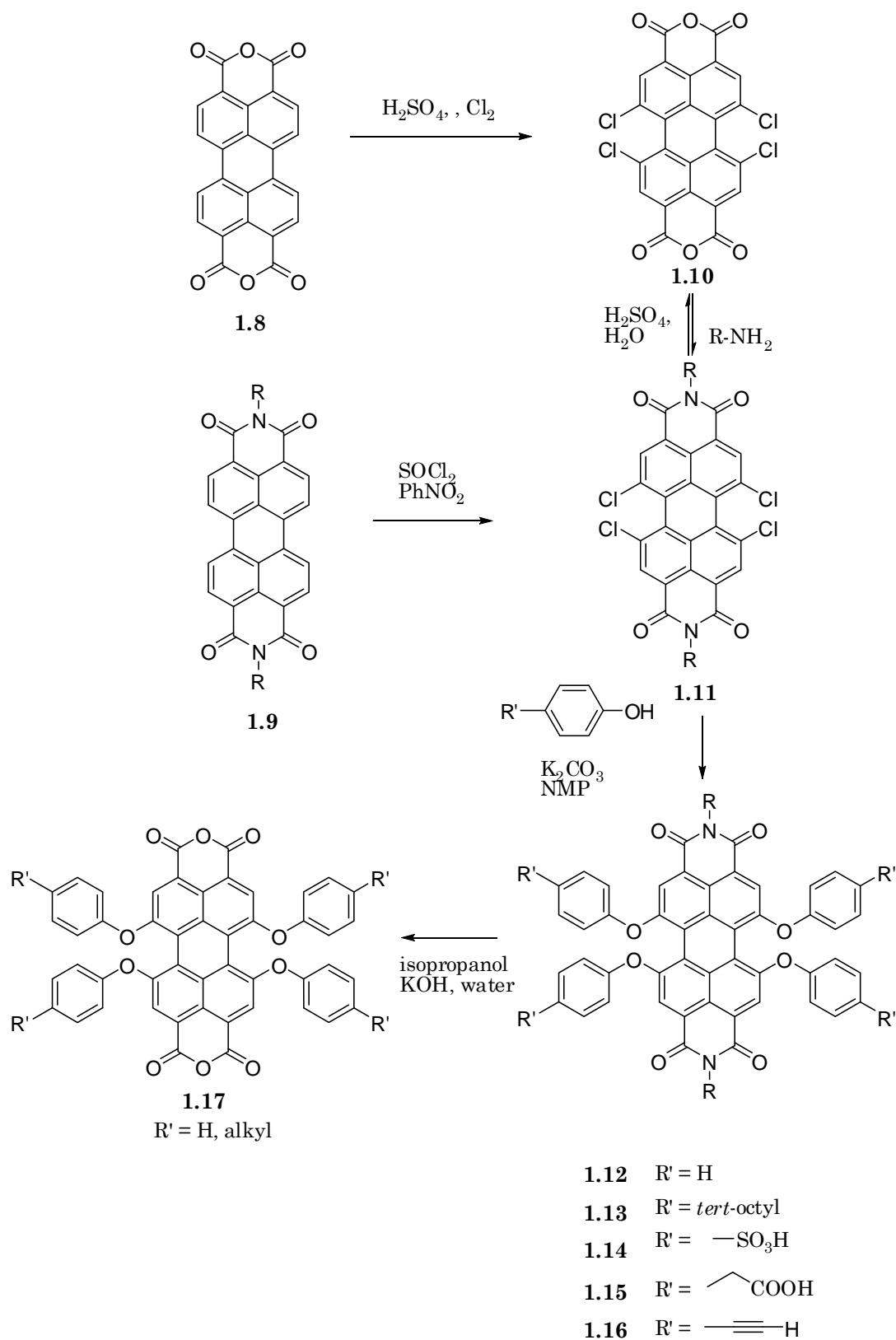
**Scheme 1.2. Synthesis of tetraphenoxyperylene-3,4,9:10-tetracarboxdiimides 1.12 and tetraphenoxyperylene-3,4,9,10-tetracarboxdianhydride 1.17.**

Instead of four halogen atoms, the bay positions can be functionalized with two bromine atoms by reacting perylenedianhydride **1.8** with bromine in sulphuric acid.[27] After an imidization reaction with alky- or arylamines, the dibromo PDI **1.19** is obtained. This compound allows easy access to a different class of chromophores - the coronenediimides.[27] In this synthesis, **1.19** is reacted in a palladium(0)-catalyzed Hagihara-Sonogashira reaction with various 1-alkynes to afford the bis(alkynyl)-substituted perylene-3,4:9,10-bis(dicarboximide)s, which upon treatment with strong, non-nucleophilic bases underwent an almost quantitative cyclization reaction to yield **1.21**. When **1.21** is substituted with appropriate alkyl chains, the coronenediimides form discotic mesophases and combine the properties of both dyes and liquid crystals. Using an alternative route, the coronene scaffold can be further extended. Instead of reacting terminal alkynes with **1.19**, the Suzuki coupling using 2-bromophenylboronic acid and subsequent palladium catalyzed dehydrohalogenation yields dibenzocoronene tetracarboxydiimide **1.20**. [28]
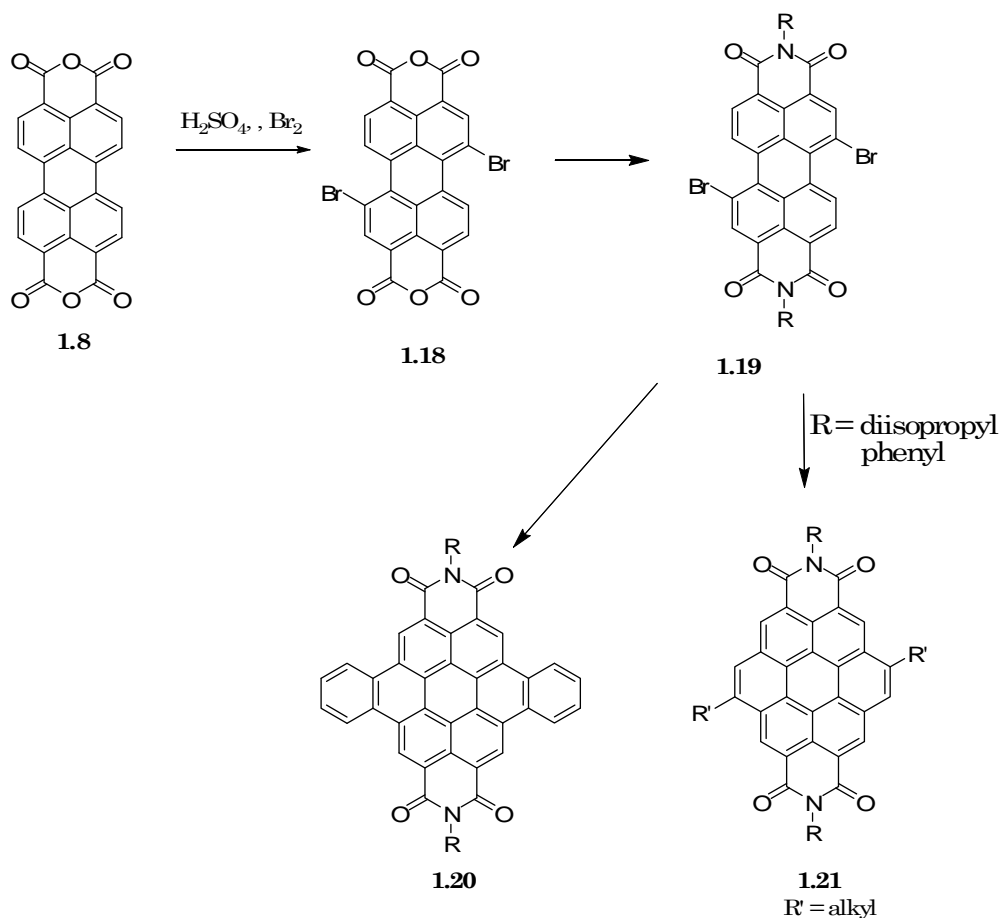


**Scheme 1.3. Synthesis of dibromoperylene-3,4:9,10-tetracarboxdiimides 1.19 and dibenzocoronene tetracarboxydiimide 1.20.**

Perylene-3,4-dicarboximide (PMI) can be synthesized from perylenedianhydride **1.8** and an aryl amine followed by decarboxylation using a procedure developed at BASF (Scheme 1.4). For that purpose, the perylenedianhydride **1.8** is subjected to an imidization reaction with 2,6-dialkylanilines, preferentially 2,6-diisopropylaniline, during which one of the two anhydride structures decarboxylates and the perylenemonoimide **1.22** is formed.[29] The reaction conditions involve very high temperatures and quinoline as solvent, whereupon the thermally less stable imide-anhydride spontaneously loses the anhydride structure.
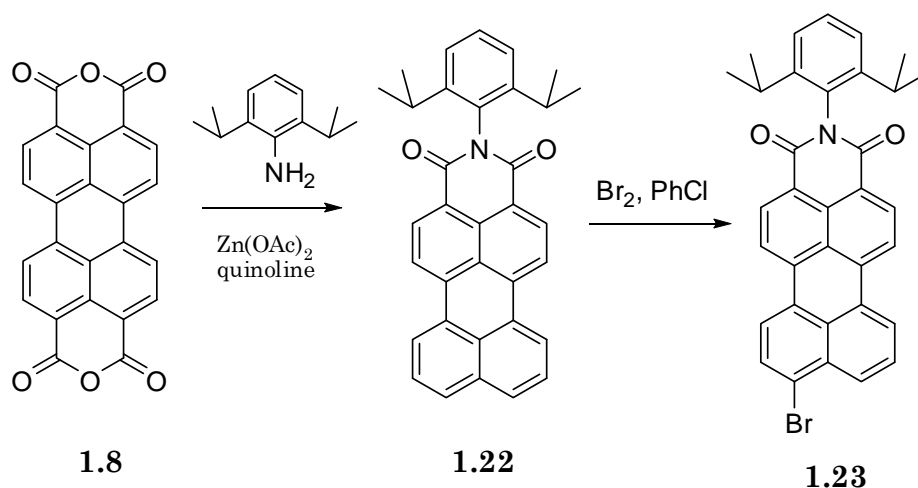


**Scheme 1.4. Synthesis of 9-bromo-perylene-3,4-dicarboximid 1.23**

The absorption spectrum of monoimide **1.22** with maxima at 487 and 507 nm exhibits a hypsochromic shift compared to **1.9**. More important are the facile routes by which **1.23** can be chemically functionalized as summarized in Scheme 1.5. Compound **1.22** is selectively brominated in the 9- position by applying a five-fold excess of bromine at 50 °C to yield **1.23**.[30, 31] More drastic reaction conditions and a larger excess of bromine result in the corresponding tribrominated perylenemonoimide **1.24**.[30, 31] In the case of **1.24**, introducing phenoxy groups with sterically demanding alkyl substituents as discussed for **1.13** leads to improved

solubility, which is of major importance for the preparation of more extended π-systems as described in regard to NIR absorbing dyes. Perylenedicarboximide bearing one bromine atom attached to the perylene core opens the way for fast and easy functionalization of the chromophore. A representative example is the conversion of **1.23** into the cyano derivative **1.26** applying the Rosemund von Braun reaction, which exhibits a brilliant yellow–orange color shade and a strong fluorescence in the solid state.[32] An elegant way for introducing an amino group in the 9-position consists of palladium mediated Buchwald coupling of **1.23** with benzophenonimine and subsequent deprotection of the amine **1.27** under acidic conditions.[33] Since metal catalyzed cross-coupling reactions are proven as powerful tool for the functionalization of perylene dyes, the chromophore itself was derivatized into the boronic ester **1.25** making building blocks readily available which can be applied in these type of reactions.
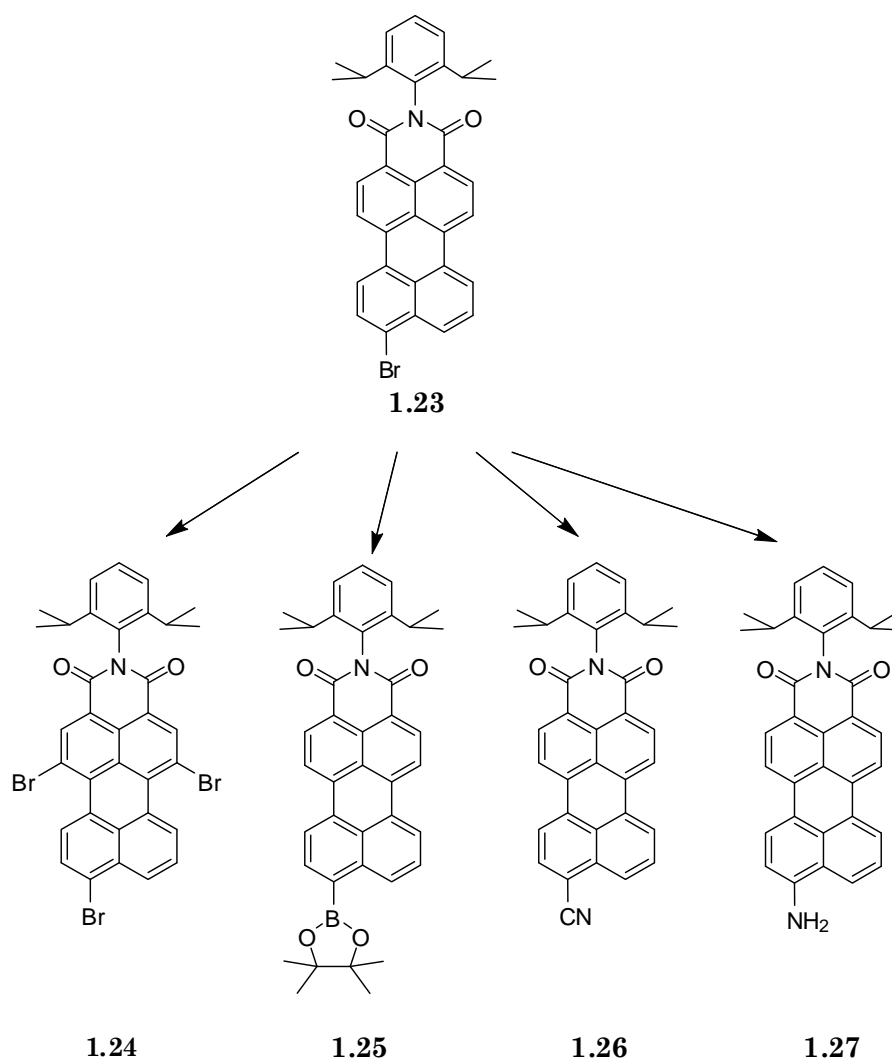


**Scheme 1.5. Synthesis of monosubstituted perylene-3,4-dicarboximides**

## 1.4. Higher rylene derivatives

The first attempts to shift the absorption maximum of **1.8** to longer wavelengths relied on condensation of perylenedianhydride 9 with o-diaminoarene compounds, which produced the corresponding imidazole derivatives as a mixture of *syn*- and *anti*-isomers (Scheme 1.6).[20, 34] Bathochromic shifts of up to 100 nm were achieved.



**1.8**

**1.28**

'anti'

**1.29**

'syn'
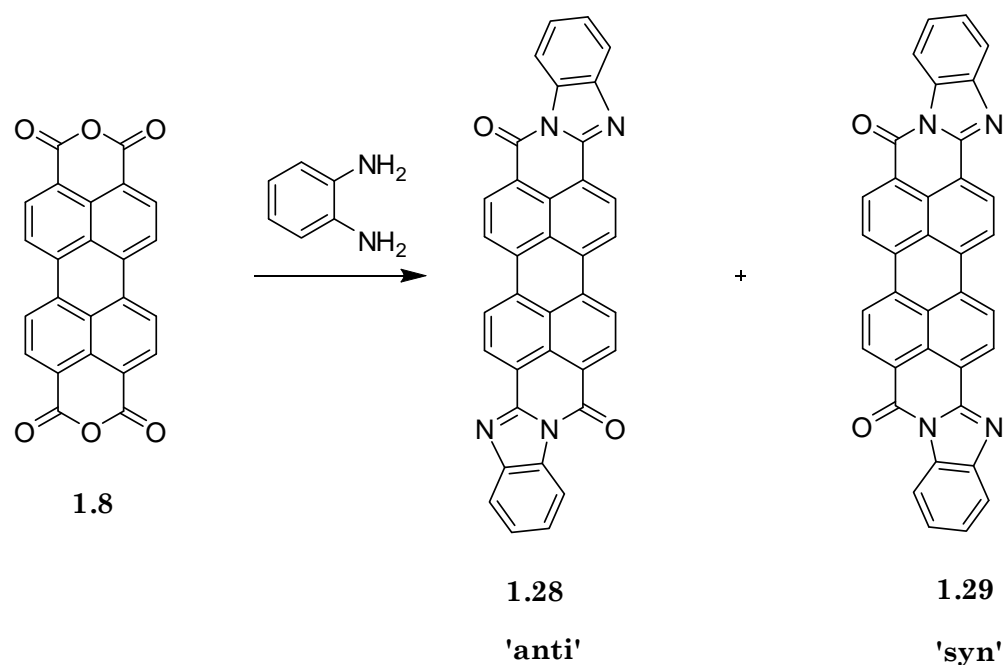
**Scheme 1.6. Synthesis of bisimidazole derivatives of 1.8**

An alternative concept to obtain longer wavelength absorbing perylene dyes is the successive incorporation of additional naphthalene units between the imide structures leading to the homologous series of rylenetetracarboxydiimides. Extension of PDI by one naphthalene results in the terrylenediimide **1.32** (TDI). **1.25** is reacted with **1.30** in a Suzuki coupling to form **1.32** .[35] This reaction proceeds efficiently to yield the terrylene precursor **1.31**, which can be fused by KOH and an oxidation reagent to the **1.32** (Scheme 1.7). Due to the high demand

for TDIs, a third route has been established. It is based on coupling perylenemonoimide **1.22** with naphthalenemonoimide **1.34** in a one-pot reaction in the presence of 1,5- diazabicyclo[4.3.0]non-5-ene (DBN) and t-BuONa. The advantages of this route are that it can be easily carried out on the 100 g scale and the purification by column chromatography is avoided.
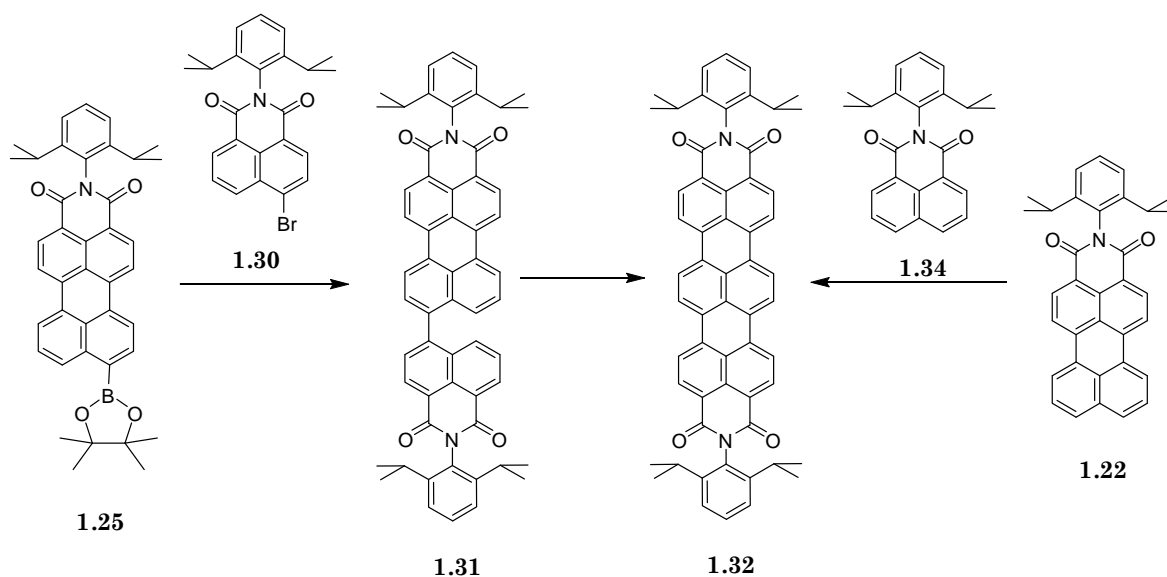


**Scheme 1.7. Synthesis of terrylene-3,4:11,12-tetracarboxdiimide 1.32**

The next higher homologue in the series of rylenetetracarboxydiimides is the quaterrylenediimide (QDI). The synthesis of this dye is even more straightforward since instead of a heterocoupling a homocoupling leads to the target molecule 28. Starting from brominated perylenemonoimides **1.23**, nickel(0)- induced dimerization leads to the bisperylenyl **1.35**, which can be planarized to **1.36** under the same conditions as described for the **1.32**.
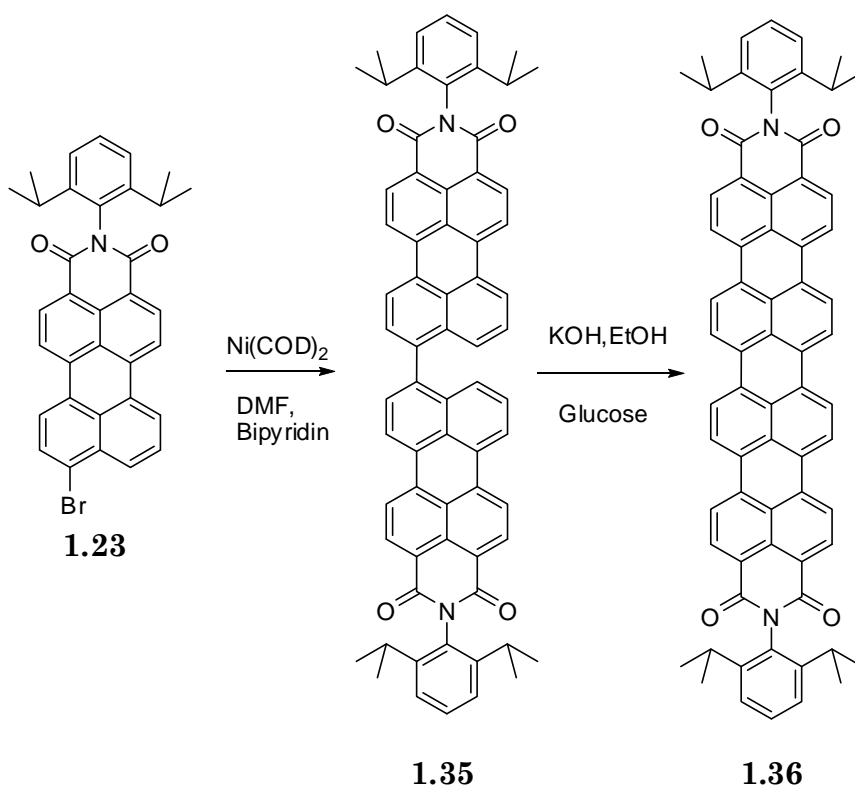
**Scheme 1.8  Synthesis of quaterrylene-3,4:13,14-tetracarboxdiimide 1-23 and 6,8(9),11,16,19,21-hexabromoquaterrylene-3,4,13,14-tetracarboxdiimide 1-24.**

Further extension along the long axis of the rylenediimides is achieved and two synthetic routes towards the penta- and hexarylenediimide have been developed.[36, 37] The first one, the so called "nitronaphthalene method", starts from the coupling product of the boronic ester of 1-bromo-5-nitronaphthalene and **1.23**. The bisaryl compound **1.37** is then cyclized to **1.38**, reduced to the amine **1.39**, and finally transformed into the iodo terrylenemonoimide **1.40** by a Sandmeyer reaction. From this building block, the hexarylenediimide **1.44** is obtained by homocoupling and subsequent cyclodehydrogenation. Similarly, the coupling of **1.40** with **1.23** yields the perylenemonoimide terrylenemonoimide bichromophore **1.41** and subsequent planarization results in the pentarylenedimide **1.43**. An alternative access to pentarylene and hexarylene, which will not be discussed any further here, the so called "bisbromorylene method" is based on building up triaryl precursor molecules consisting of three perylene units or two perylenes and a naphthalene which after cyclodehydrogenation result in the hexa- and pentarylendiimides, respectively.[38]

**1.37**  **1.38**  **1.39**  **1.40**

n = 0  **1.41**
n = 1  **1.42**
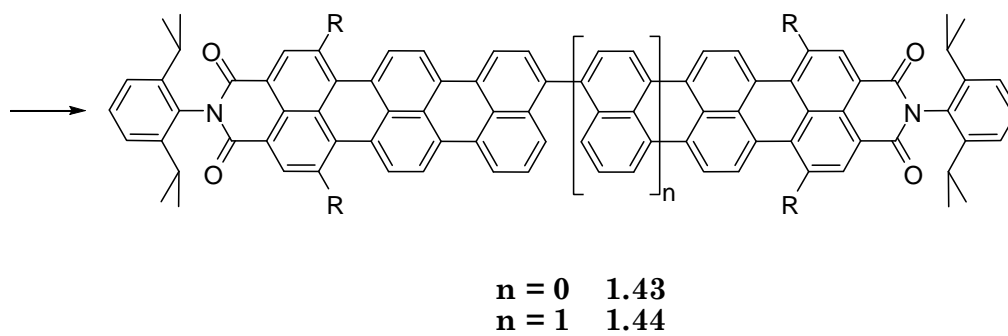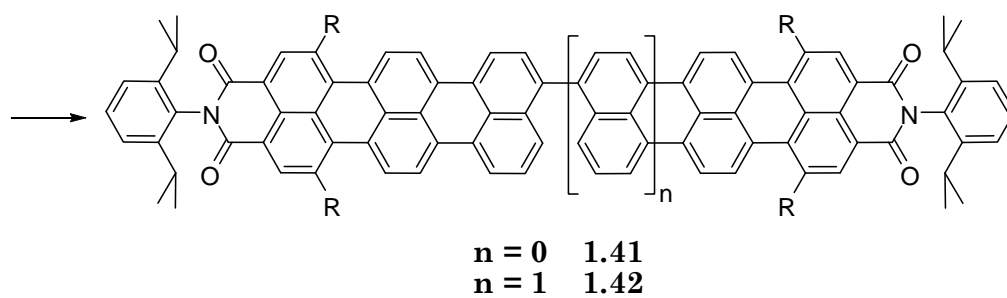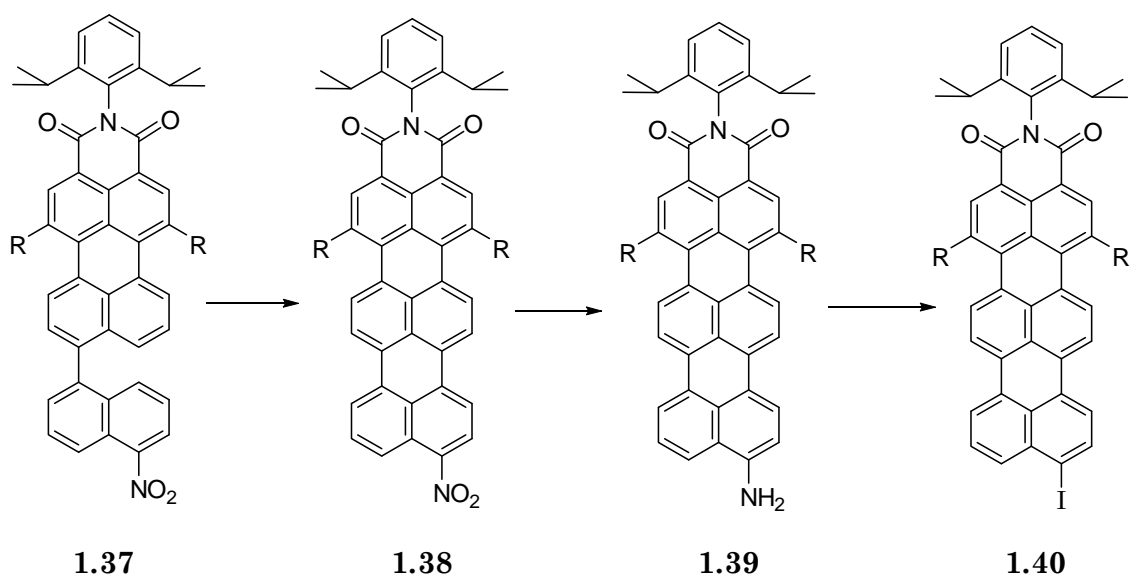
n = 0  **1.43**
n = 1  **1.44**

**Scheme 1.9: Synthesis of higher rylene dyes – pentarylenediimide (n=0) 1.43 and hexarylenediimide (n=0) 1.44**

Upon inspecting the absorption spectra of **1.9** and **1.32** a bathochromic shift of around 100 nm is detected (Figure 1.3). **1.32**, which is deeply blue colored, absorbs at 650 nm whereas **1.9** has a brilliant red color (abs. max. 550 nm). Even more important in the context of functional dyes is that upon going from PDI to TDI the fluorescent quantum yield remains almost unchanged at 90% for **1.32**. The emission maxima of TDI derivatives lie in the range from 670 to 710 nm depending on the substitution pattern in the bay regions.[39] Thus they are NIR emitting dyes, which is an important region of the electromagnetic spectrum for biological applications. In the case of QDI **1.36** the fluorescence quantum yield drops to 5% (em. max. 800 nm). The absorption maxima of QDI dyes with varying degree of phenoxylation are detected between 760 and 790 nm (Figure 1.3). In strong contrast to PDI and TDI, solutions of quaterrylenediimide appear to be almost colorless having a light greenish appearance, which is caused by the rising absorption band at around 600 nm. The absorption spectra of penta- and hexarylene derivatives **1.43** and **1.44** exhibit absorption maxima at 830–880 and 950 nm, respectively (Figure 1.3). As a result the penta- and hexarylenediimide are completely colorless in solution.

By extending the aromatic $\pi$-system also the absorption coefficients increase from $\varepsilon = 60\ 000\ M^{-1}\ cm^{-1}$ (PDI), $\varepsilon = 93\ 000\ M^{-1}\ cm^{-1}$ (TDI), $\varepsilon = 167\ 000\ M^{-1}\ cm^{-1}$ (QDI) trough $\varepsilon = 235\ 000\ M^{-1}\ cm^{-1}$ (pentarylendiimide) to $\varepsilon = 293\ 000\ M^{-1}\ cm^{-1}$ for the hexarylenediimide. For organic NIR-dyes such high absorption coefficients are unprecedented. In addition to these remarkable photophysical properties, all the presented NIR-absorbers still display the excellent chemical, photochemical and thermal stability seen for their smaller counterparts, the PDIs. For this reason, the pentarylene **1.43** and the hexarylene **1.44** are very well suited for a new technique for joining polymers called laser welding. In the process of overlap welding, the laser penetrates the upper workpiece and is absorbed by the lower part. The generated heat is transferred by heat conduction. The mutual melt pool achieves almost base material strength after solidification. For effective heat absorption within the polymer, absorbing additives are needed, which mostly exhibit an intrinsic color in the visible limiting the color range of the components.
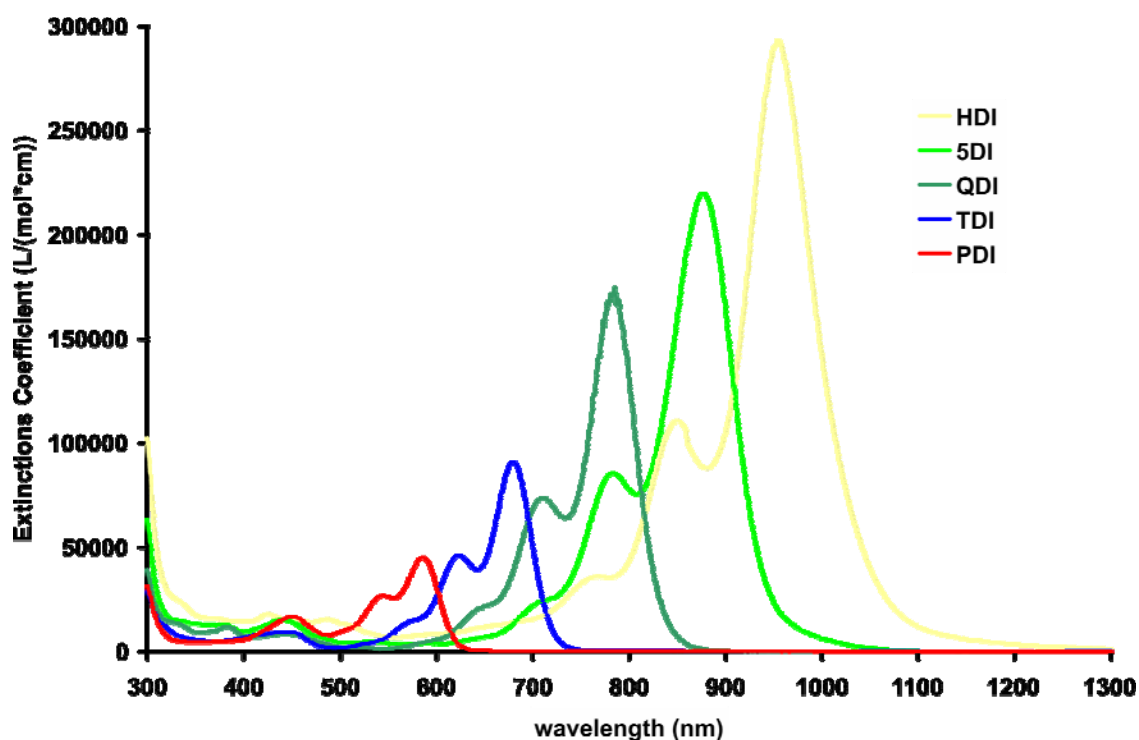
**Figure 1.3. UV/Vis absorption spectra of rylenediimides: Perylenediimide 1.9 (PDI), terrylenediimide 1.32 (TDI), quaterrylenediimide 1.36 (QDI), pentarylendiimide 1.43 (5DI), hexarylenediimide 1.44 (HDI).**

The most striking advantage of the NIR absorbing rylenecarboxdiimides for that purpose is that they do not absorb in the visible so that the process of laser welding would not be restricted anymore to the use of transparent or colored components.

Perylene dyes can be functionalized by a large variety of organic reactions to control their solubility, absorption and emission behavior, whereby PDI, perylenedianhydride and tetrachloro PDI act as starting materials. Especially metal-catalyzed cross-coupling reactions are proven as powerful synthetic tools in perylene chemistry. These types of reactions, beside functionalization, allow the build up of the homologous series of the rylenetetracarboxydiimides up to the hexarylene consisting of six naphthalene units, connected via their *peri*-positions leading to strong absorption in the NIR region.

Due to their outstanding chemical and photochemical stabilities as well as their high fluorescent quantum yields, perylene- and terrylene chromophores have been established as key chromophores for SMS. Photophysical processes like energy and electron transfer can now be investigated on the single molecule level over long observation times. Beside labeling and visualization of single proteins, terrylene dyes have been applied to study events taking place in living cells.

In the future, the rylene dyes will be further investigated in the context of biological systems including the visualization of protein-protein interactions or enzyme catalysis.

## *1.5. Fluorescent labels*

Fluorescence spectroscopy has proven as a powerful tool for determining the dynamic behavior of fluorescent probes or tracing individual molecules in living systems such as cellular structures.[40-43] Fluorescence is ideally suited for observing the location of molecules in cells as it is non-invasive and can be detected with high sensitivity and signal specificity.[44] The study of protein, or protein reactions in vivo with fluorescence microspectroscopy requires labeling of proteins, which can be achieved by chemical modification of a purified protein, site-specific covalent labeling of recombinant protein molecules inside cells or construction of fusion proteins with one of the green fluorescent protein (GFP) mutants.[44-47]

For in vivo staining experiments, the spectral properties of the fluorescent probe in aqueous media, its chemical stability with respect to cell metabolism, as well as low or no toxicity toward the cells are crucial criteria. Adequate label should combine absorption and emission maxima above 500 nm due to the background noise of fluorescent impurities and the auto-fluorescence of the cell, as well as high fluorescence quantum yields in aqueous solution.[48, 49] Furthermore, if sophisticated photophysical investigations such as single molecule spectroscopy are intended, a sufficient photostability of the chromophore becomes a key concern.

Different approaches were applied to meet all these criteria, such as the use of autofluorescent proteins or, more recently, of water-soluble quantum dots, each of these approaches possessing several advantages, as well as limitations.

In the last ten years, GFP was intensively used as an alternative to synthetic dyes. The high quantum yield (~0.8), the possibility for labeling of cellular proteins in situ, the GFP mutants (cyan fluorescent protein, blue fluorescent protein) that can be used to design constructs that undergo fluorescence energy transfer, and the discovery of the red-emitting protein DsRed12 are important reasons that promoted the use of autofluorescent proteins.[46, 47] The main disadvantage, when using GFP or its mutants to label other proteins is their relatively high molecular weight (27 000 Da) that can impair the normal dynamics (folding/unfolding) of the studied protein, especially if its molecular weight is not much higher than that of GFP. Other drawbacks of autofluorescent proteins come from their fast photobleaching and from their complex photophysical properties. Interconversion of the protonated and deprotonated form or structural changes (cis/trans isomerization of the chromophore) are possible in the GFP mutants, as well as intersubunit energy transfer in the DsRed. All these lead to multiexponential fluorescence decays and long dark states in single molecule experiments.[50-53]Water-soluble quantum dots are proposed as an alternative because they have a reduced spectral width compared to an organic fluorophore, they are almost 100 times more stable to photobleaching, and the fluorescence intensity of a single particle was equivalent to that of ~20 Rhodamine molecules.[54-57] One of their disadvantages could be that after functionalization more than one protein molecule is attached to a single particle (usually 2-5 protein molecules). In addition, their large size (~20 nm) and the dependence of their photophysical properties on the particle size can cause problems in biological labeling. Also, dendrimers built from amphiphilic units were used for gene transfer, for drug delivery in tumor cells, and for in vivo imaging of tumors with radioactive isotopes.[58-60] Because of their size (3 nm or more), the incorporation in living cells occurs probably by endocytosis or receptor-mediated endocytosis when a specific ligand (like folate) is attached. Dendrimers containing three bright fluorescent chromophores such as perylene monoimide, solubilized using labeling detergents, can be applied for very sensitive detection (at single molecule level) of cell surface markers by immunolabeling, or of surface receptors, on the condition that ligand-receptor interaction is not significantly perturbed.[61]

The use of porphyrins caged inside dendritic shells as compartmental pH sensors, of lanthanide complexes as an alternative to radioactive probes in immunoassay kits, or of aromatic flat fluorophores that replace the base in a

DNAlike structure demonstrates that people keep exploring different approaches to use aromatic chromophores in aqueous environments.[62-64]Therefore, classic fluorescent molecules will still be extensively used for measurements in living cells. Recently several single molecule studies of rylene chromophores performed in the groups of Prof. Bräuchle in LMU, Munich and Prof. Hofkens, Katholieke University, Leuven, have demonstrated their remarkable photophysical properties.[65, 66] The results showed exceptional photostability and extended survival times in comparison with some of the commercially available fluorophores. We will explain in greater details the photophysical behavior of the rylene chromophore, which suggested more extended use of these fluorophore especially in the field of single molecule detection and prompt the synthesis of new water-soluble rylene dyes decorated with functional groups for labeling of biomolecules.

## 1.5.1. Toward ultrastable fluorescent rylene dyes for single-molecule spectroscopy

Here we will discuss the photophysical properties of two recently introduced members of the rylene family, namely 1,6,7,12-tetra(4-sulfophenoxy)-N,N'-(2,6-diisopropylphenyl)-perylene-3,4:9,10-tetracarboxylidiimide **1.45** and 1,6,9,14-tetra(4-sulfophenoxy)-N,N'-(2,6-diisopropylphenyl)-terrylene-3,4:11,12-tetracarboxydiimide **1.46**. The structures of these chromophores are shown on Scheme 1.10. Details about the synthesis and introduction of functional groups into the perylene and terrylene scaffold will be given in the next chapter.

The absorbance and fluorescence spectra of **1.45** in water (Figure 1.4) has a similar shape as the spectra of other perylene(dicarboxidiimide)s in organic solvents. Two electronic transitions are visible in the absorbance spectrum, the $S_0$-$S_1$ transition (along the long axis) is situated between 480 nm and 625 nm, and $S_0$-$S_2$ transition (along the short axis) appears as second peak between 400 nm and 480 nm. The maximum of the emission spectrum (dotted line), taken with an excitation wavelength of 543 nm, is positioned at 625 nm.[65] Therefore, the 543 nm or 568 nm wavelengths can be used to excite this dye loaded into cells, obtaining a good

signal/noise ratio due to the reduced autofluorescence in the green region of the visible spectrum.



1.45                                    1.46
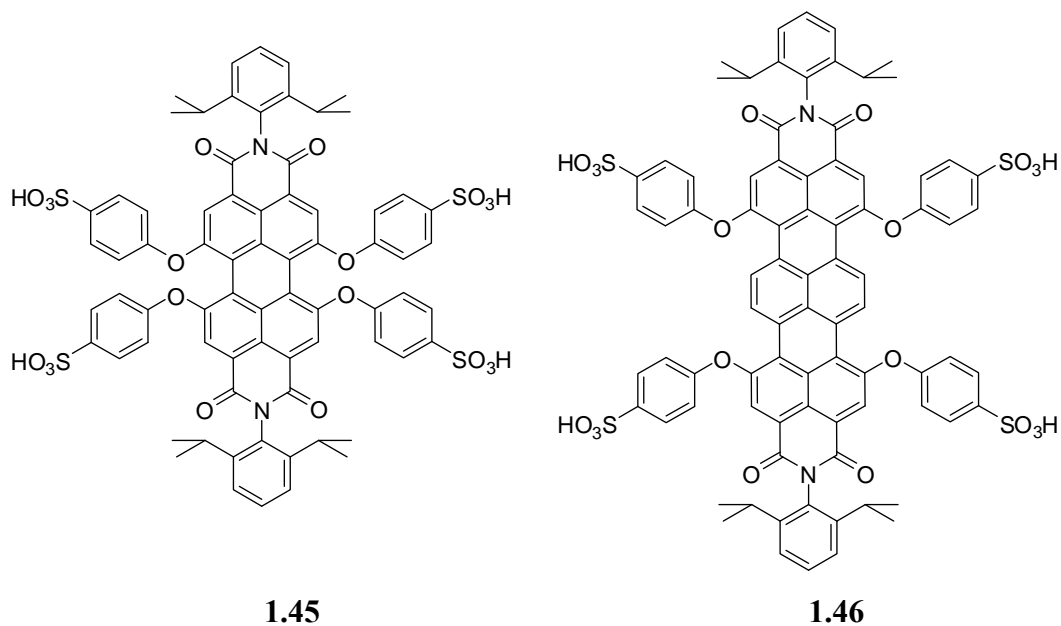
**Scheme 1.10. Chemical structure of the water-soluble perylene and terrylene tetracarboxydiimide**
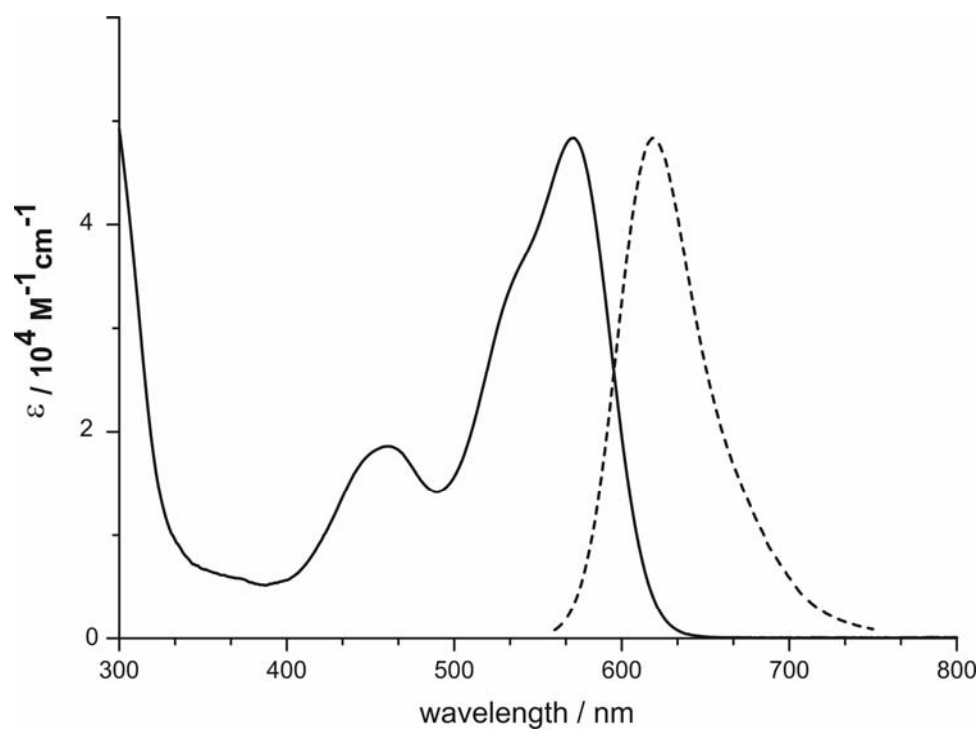


**Figure 1.4. Absorbance (solid line) and fluorescence (dotted line) spectra of 1.45 in water**

In water, the molar extinction coefficient of **1.45** is approximately 30 000 $M^{-1}cm^{-1}$, while the fluorescence quantum yield ($\Phi_f$) equals 0.6. The $\Phi_f$ value is higher than that reported for quantum dots (0.35-0.5)[57] or for cyanine dyes (0.2)[67], and is high enough for single molecule applications.

The chemical structure of the water-soluble terrylene chromophore – 1,6,9,14-tetra(4-sulfophenoxy)-N,N'-(2,6-diisopropylphenyl)-terrylene-3,4:11,12-tetracarboxi diimide **1.46** is shown on Scheme 1.10. This molecule shows an adequately balanced effect of the hydrophilic sulfonic groups and the hydrophobic core. The sulfonic groups are responsible for the water solubility; however, due to the large π-electron system of the rigid hydrophobic core, many of the molecules are still stacked, forming water-soluble aggregates.[68]
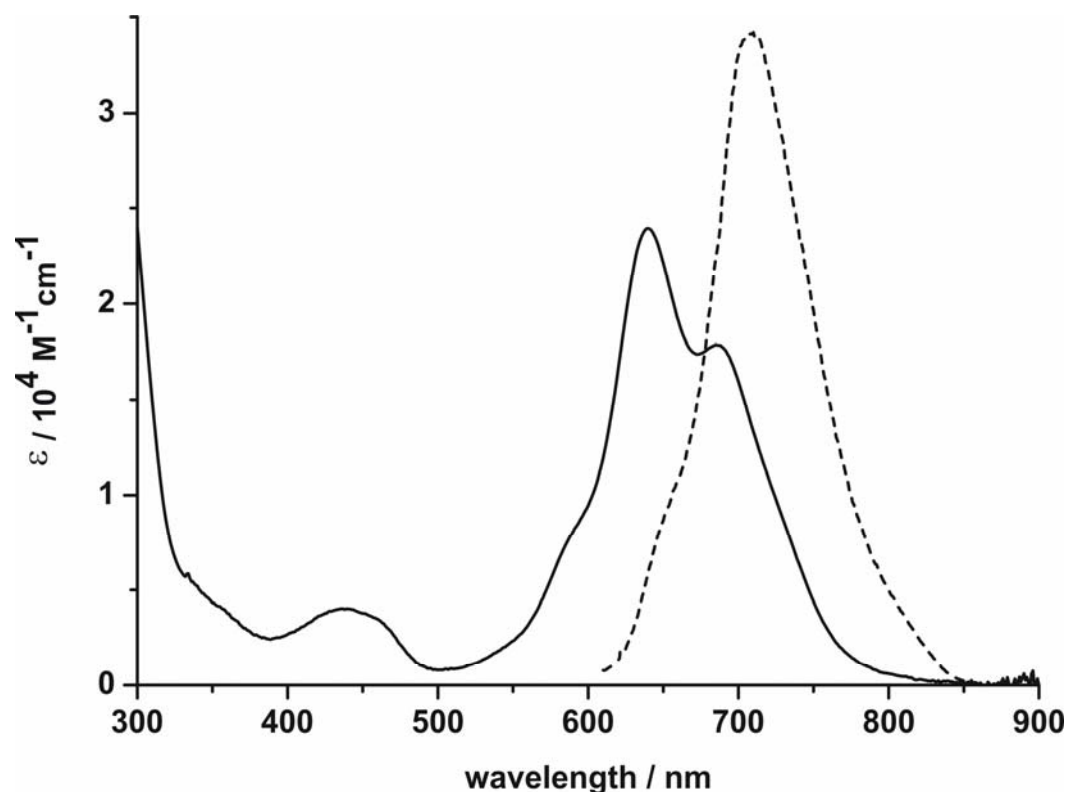


**Figure 1.5. Absorbance spectrum of 1.46 in water (solid line) and fluorescence spectrum in methanol (dotted line)**

The absorbance spectrum of **1.46** in water consists of a main band at a shorter wavelength of 637 nm and a weak band at 690 nm. Nearly no fluorescence emission signal is observed in water, due to the formation of aggregates. Self-

association of dyes in solution is a frequently encountered phenomenon in dye chemistry due to strong intermolecular forces.[69-71] The water-soluble terrylene dye is a relatively rigid molecule with a large planar π-electron system with hydrophobic nature and has a strong tendency to aggregate in polar solvents such as water. Previous studies have already characterized aggregates of π-π stacked perylene diimide dyes in solution,[72] which have a slightly smaller π-electron system than **1.46**. In general, aggregates in solution exhibit distinct changes in absorption and fluorescence properties compared to that in monomeric species. Molecular excitonic theory describes two main species of dye aggregates distinguished as H- and J-aggregates. H-Aggregates are formed by parallel stacking, whereas J-aggregates occur in a head-to-tail arrangement.[73] In H-aggregates, the absorption maximum is blueshifted with respect to the isolated chromophore and the fluorescence is normally quenched. However, J-aggregates usually show fluorescence, and both the absorption and emission maxima are red-shifted.[74] Comparing these statements with the experimental results, it can be concluded that **1.46** forms H-aggregates in water. Nevertheless, fluorescence signal can be detected in polar organic solvents like DMSO, methanol (Figure 1.5 dotted line) or in water solutions containing surfactants.[66]

## *1.5.2. Comparison with other fluorescent molecules for biological applications*

Single molecule studies of **1.45** and **1.46** performed in solution and in the solid state demonstrated that these chromophores have an improved stability to photobleaching than commonly used fluorescent labels like sulforhodamine and oxazine, and can represent a viable alternative to other water-soluble dyes used in biology and can be successfully applied for single molecule studies.[65, 66] Single molecule measurements performed in solution showed mean survival time for **1.45** to be 94 s, and the mean number of total detected photons being around 750 000.

One of the disadvantages related to the study of single biomolecules is the short observation time (usually between 10 and 20 s) due to the photobleaching of the chromophores used as labels. These times are too short to follow, for instance, the folding of a single protein over the full range of relevant time scales.[75] Measurements of **1.45** show that these molecules can provide longer observation times than other available water-soluble chromophores even without the use of oxygen scavengers, which cannot be applied in all experiments because of possible interference with cellular processes. In Table 1.2 are summarized photophysical data obtained from Hofkens et al for **1.45** and other commonly used chromophores in SMS studies.[65]

| Chromophore | Survival time | No. detected photons | Environment | Excitation power |
|:---:|:---:|:---:|:---:|:---:|
| **1.45** | 94 s | 750 000 | PVA | 1.4 kW/cm$^2$ |
| Rhodamine 6G | 15 s | 500 000 | Trehalose | 0.4 kW/cm$^2$ |
| TRITC | 11 s | | PVA | 4.5 kW/cm$^2$ |
| Cy5 | | 30 000 | glass surface | 500 w/cm$^2$ |
| *EGFP* | 0.5-2 s | 25 000 | PVA | 350 w/cm$^2$ |

**Table 1.2. Survival time and number of detected photons for fluorescent dyes commonly used in biology.** [TRITC: tetramethylrhodamine isothiocyanate; EGFP: enhanced green fluorescent protein; PVA: poly(vinyl alcohol)]

Bräuchle et al. made a similar comparison between **1.46** and fluorophores that have corresponding absorption and emission maxima like oxazine-1, sulforhodamine-B, and also **1.45**.[66] The chemical structures, absorbance and emission maxima are given on Scheme 1.11. They have immobilized single molecules of the fluorophores in polymer matrix and studied their photophysical properties. During these experiments the total emitted photons (TEP) and the survival time (ST, time to the irreversible photobleaching) was determined. The

distributions of these two parameters characterize the fluorescence capability and the photostability of a fluorescent dye.

The average TEP for **1.46** in PVA was calculated to be $63.7 \times 10^6$, and the average ST – 40 s. The fluorescence capability of **1.46** was compared with the above mentioned chromophores under the same experimental conditions. The water-soluble terrylene chromophore **1.46** emits about 8, 18 and 53 times more photons before photobleaching and lives 3, 5, and 37 times longer than **1.45**, sulforhodamine-B, and oxazine-1, respectively.[66]



Sulforhodamine B
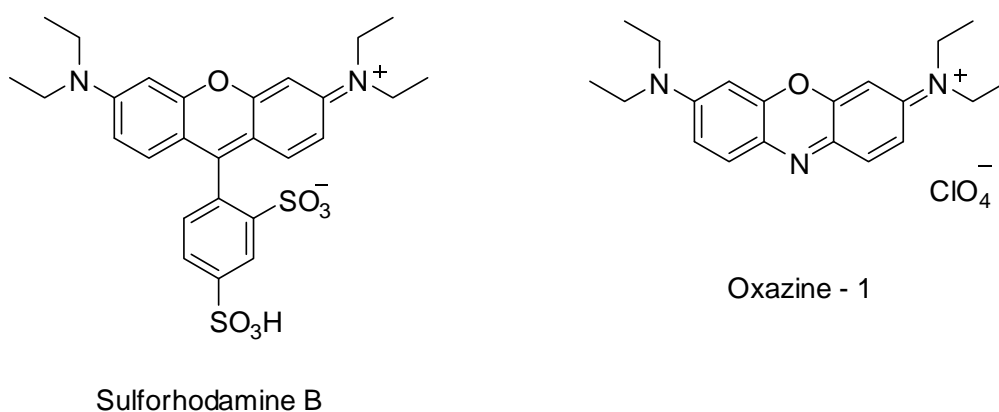
Oxazine - 1

**Scheme 1.11. Chemical structure of sulforhodamine-B ($\lambda_{abs}$ = 565 nm/ $\lambda_{em}$= 586 nm) and Oxazine-1 ($\lambda_{abs}$ = 646 nm/ $\lambda_{em}$= 670 nm)**

Rhodamine and oxazine molecules are currently among the best performing water-soluble dyes.[76-80] The presented results however, clearly showed that **1.46** emit much more photons over a longer period of time than the other dyes measured. The high number of emitted photons and the superior photostability combined with the absorption in the red spectral region (650 nm, avoiding, for example, autofluorescence in live cell imaging experiments) made **1.46** very promising for single molecule experiments.

The single molecule experiments performed with symmetrical water-soluble perylene and terrylene chromophores pointed out that these molecules posses an exceptional photophysical behavior.

# 1.6 References

[1] H. Zollinger, *Zollinger, H. Color Chemistry: Syntheses, Properties and Applications of Organic Dyes and Pigments. Xii+367p. Vch Publishers, Inc.: New York, New York, USA; Vch Verlagsgesellschaft Mbh: Weinheim, West Germany. Illus* **1987**, XII+367P, *Color Chemistry Syntheses Properties and Applications of Organic Dyes and Pigments*.

[2] H. Langhals, *Color Chemistry. Synthesis, Properties and Applications of Organic Dyes and Pigments. 3rd revised edition, by Heinrich Zollinger, Vol. 43*, **2004**.

[3] M. Kardos DR P276357. DR P276357, 1913.

[4] Y. Nagao, T. Misono, *Dyes Pigm.* **1984**, *5*, 171, *Synthesis and properties of N-alkyl-N'-aryl-3,4:9,10-perylenebis(dicarboximide)*.

[5] A. Rademacher, S. Maerkle, H. Langhals, *Chem. Ber.* **1982**, *115*, 2927, *Soluble perylene fluorescent dyes with high photostability*.

[6] H. Langhals, *Nachrichten aus Chemie, Technik und Laboratorium* **1980**, *28*, 716, *Dyes for fluorescent solar collectors*.

[7] M. P. O'Neil, M. P. Niemczyk, W. A. Svec, D. Gosztola, G. L. Gaines, III, M. R. Wasielewski, *Science (Washington, DC, U. S.)* **1992**, *257*, 63, *Picosecond optical switching based on biphotonic excitation of an electron donor-acceptor-donor molecule*.

[8] M. Sadrai, L. Hadel, R. R. Sauers, S. Husain, K. Krogh-Jespersen, J. D. Westbrook, G. R. Bird, *J. Phys. Chem.* **1992**, *96*, 7988, *Lasing action in a family of perylene derivatives: singlet absorption and emission spectra, triplet absorption and oxygen quenching constants, and molecular mechanics and semiempirical molecular orbital calculations*.

[9] R. Gvishi, R. Reisfeld, Z. Burshtein, *Chem. Phys. Lett.* **1993**, *213*, 338, *Spectroscopy and laser action of the \"red perylimide dye\" in various solvents*.

[10] C. W. Struijk, A. B. Sieval, J. E. J. Dakhorst, M. van Dijk, P. Kimkes, R. B. M. Koehorst, H. Donker, T. J. Schaafsma, S. J. Picken, A. M. van de Craats, J. M. Warman, H. Zuilhof, E. J. R. Sudholter, *J. Am. Chem. Soc.* **2000**, *122*, 11057, *Liquid crystalline perylene diimides: Architecture and charge carrier mobilities.*

[11] L. Schmidt-Mende, A. Fechtenkotter, K. Müllen, E. Moons, R. H. Friend, J. D. MacKenzie, *Science (Washington, DC, U. S.)* **2001**, *293*, 1119, *Self-organized discotic liquid crystals for high-efficiency organic photovoltaics.*

[12] A. J. Breeze, A. Salomon, D. S. Ginley, B. A. Gregg, H. Tillmann, H. H. Horhold, *Appl. Phys. Lett.* **2002**, *81*, 3085, *Polymer-perylene diimide heterojunction solar cells.*

[13] S. Mais, J. Tittel, T. Basche, C. Braeuchle, W. Goehde, H. Fuchs, G. Müller, K. Müllen, *J. Phys. Chem. A* **1997**, *101*, 8435, *Terrylenediimide: A Novel Fluorophore for Single-Molecule Spectroscopy and Microscopy from 1.4 K to Room Temperature.*

[14] S. Kummer, T. Basche, C. Brauchle, *Chem. Phys. Lett.* **1994**, *229*, 309, *Terrylene in P-Terphenyl - a Novel Single-Crystalline System for Single-Molecule Spectroscopy at Low-Temperatures.*

[15] T. Christ, F. Kulzer, T. Weil, K. Müllen, T. Basche, *Chem. Phys. Lett.* **2003**, *372*, 878, *Frequency selective excitation of single chromophores within shape-persistent multichromophoric dendrimers.*

[16] A. Herrmann, K. Müllen, *Chem. Lett.* **2006**, *35*, 978, *From industrial colorants to single photon sources and biolabels: the fascination and function of rylene dyes.*

[17] A. Rademacher, S. Markle, H. Langhals, *Chemische Berichte-Recueil* **1982**, *115*, 2927, *Soluble Perylene Fluorescent Dyes with High Photostability.*

[18] T. Sakamoto, C. Pac, *J. Org. Chem.* **2001**, *66*, 94, *A \"green\" route to perylene dyes: direct coupling reactions of 1,8-naphthalimide and related compounds under mild conditions Using a \"new\" base complex reagent, t-BuOK/DBN.*

[19] H. Langhals, *Chem. Ber.* **1985**, *118*, 4641, *Synthesis of highly pure perylene fluorescent dyes in large scale amounts - specific preparation of atropic isomers.*

[20] H. Quante, Y. Geerts, K. Müllen, *Chem. Mater.* **1997**, *9*, 495, *Synthesis of Soluble Perylenebisamidine Derivatives. Novel Long-Wavelength Absorbing and Fluorescent Dyes.*

[21] J. Qu, C. Kohl, M. Pottek, K. Müllen, *Angew. Chem. Int. Ed.* **2004**, *43*, 1528, *Ionic perylenetetracarboxdiimides: highly fluorescent and water-soluble dyes for biolabeling.*

[22] C. Kohl, Johannes-Gutenberg University (Mainz), **2003**.

[23] G. Seybold, G. Wagenblast, *Dyes Pigm.* **1989**, *11*, 303, *New Perylene and Violanthrone Dyestuffs for Fluorescent Collectors.*

[24] J. Qu, J. Zhang, A. C. Grimsdale, K. Müllen, F. Jaiser, X. Yang, D. Neher, *Macromolecules* **2004**, *37*, 8297, *Dendronized Perylene Diimide Emitters: Synthesis, Luminescence, and Electron and Energy Transfer Studies.*

[25] D. Liu, S. De Feyter, M. Cotlet, U.-M. Wiesler, T. Weil, A. Herrmann, K. Müllen, F. C. De Schryver, *Macromolecules* **2003**, *36*, 8489, *Fluorescent Self-Assembled Polyphenylene Dendrimer Nanofibers.*

[26] G. Mihov, D. Grebel-Koehler, A. Luebbert, G. W. M. Vandermeulen, A. Herrmann, H.-A. Klok, K. Müllen, *Bioconjugate Chem.* **2005**, *16*, 283, *Polyphenylene Dendrimers as Scaffolds for Shape-Persistent Multiple Peptide Conjugates.*

[27] U. Rohr, P. Schilichting, A. Bohm, M. Gross, K. Meerholz, C. Brauchle, K. Müllen, *Angew. Chem., Int. Ed.* **1998**, *37*, 1434, *Liquid crystalline coronene derivatives with extraordinary fluorescence properties.*

[28] S. Mueller, K. Müllen, *Chem. Commun. (Cambridge, U. K.)* **2005**, 4045, *Facile synthetic approach to novel core-extended perylene carboximide dyes.*

[29] L. Feiler, H. Langhals, K. Polborn, *Liebigs Annalen* **1995**, 1229, *Synthesis of perylene-3,4-dicarboximides - novel highly photostable fluorescent dyes.*

[30] H. Quante, K. Müllen, *Angew. Chem., Int. Ed. Engl.* **1995**, *34*, 1323, *Quaterrylenebis(dicarboximides).*

[31] Y. Geerts, H. Quante, H. Platz, R. Mahrt, M. Hopmeier, A. Bohm, K. Müllen, *J. Mater. Chem.* **1998**, *8*, 2357, *Quaterrylenebis(dicarboximide)s: near infrared absorbing and emitting dyes.*

[32] A. Boehm, P. Blaschka, W. Helfer, D. Hammel, P. Schlichting, K. Müllen 9-Cyano-3,4-perylenedicarboximide dyes, their production and their use. 2004.

[33] S. Becker, A. Bohm, K. Müllen, *Chem.--Eur. J.* **2000**, *6*, 3984, *New thermotropic dyes based on amino-substituted perylendicarboximides*.

[34] Y. Nagao, N. Ishikawa, Y. Tanabe, T. Misono, *Chem. Lett.* **1979**, 151, *Synthesis of unsymmetrical perylenebis(dicarboximide) derivatives*.

[35] F. Nolde, J. Qu, C. Kohl, N. G. Pschirer, E. Reuther, K. Müllen, *Chem.--Eur. J.* **2005**, *11*, 3959, *Synthesis and modification of terrylenediimides as high-performance fluorescent dyes*.

[36] N. G. Pschirer, C. Kohl, K. Müllen Hexarylene and pentarylene tetracarboxylic acid diimides. 2006.

[37] N. G. Pschirer, C. Kohl, F. Nolde, J. Qu, K. Müllen, *Angew. Chem., Int. Ed.* **2006**, *45*, 1401, *Pentarylene- and hexarylenebis(dicarboximide)s: near-infrared-absorbing polyaromatic dyes*.

[38] N. G. Pschirer, C. Kohl, F. Nolde, J. Qu, K. Müllen, *Angew. Chem. Int. Ed.* **2006**, *45*, 1401, *Pentarylene- and hexarylenebis(dicarboximide)s: near-infrared-absorbing polyaromatic dyes*.

[39] F. O. Holtrup, G. Lieser, K. Müllen, *Colloid Polym. Sci.* **2000**, *278*, 385, *Packing behavior of benzoylterryleneimide in the solid state*.

[40] T. Vosch, J. Hofkens, M. Cotlet, F. Kohn, H. Fujiwara, R. Gronheid, K. Van Der Biest, T. Weil, A. Herrmann, K. Müllen, S. Mukamel, M. Van der Auweraer, F. C. De Schryver, *Angew. Chem., Int. Ed.* **2001**, *40*, 4643, *Influence of structural and rotational isomerism on the triplet blinking of individual dendrimer molecules*.

[41] M. Lor, J. Thielemans, L. Viaene, M. Cotlet, J. Hofkens, T. Weil, C. Hampel, K. Müllen, J. W. Verhoeven, M. Van der Auweraer, F. C. De Schryver, *J. Am. Chem. Soc.* **2002**, *124*, 9918, *Photoinduced electron transfer in a rigid first generation triphenylamine core dendrimer substituted with a peryleneimide acceptor*.

[42] W. E. Moerner, M. Orrit, *Science* **1999**, *283*, 1670, *Illuminating single molecules in condensed matter*.

[43] S. Weiss, *Science* **1999**, *283*, 1676, *Fluorescence spectroscopy of single biomolecules*.

[44] P. I. H. Bastiaens, A. Squire, *Trends in Cell Biology* **1999**, *9*, 48, *Fluorescence lifetime imaging microscopy: spatial resolution of biochemical processes in the cell*.

[45] P. I. H. Bastiaens, T. M. Jovin, in *Cell Biology - a Laboratory Handbook, 2nd Edition, Vol 3*, **1998**, pp. 136.

[46] B. A. Griffin, S. R. Adams, R. Y. Tsien, *Science* **1998**, *281*, 269, *Specific covalent labeling of recombinant protein molecules inside live cells.*

[47] R. Y. Tsien, *Annu. Rev. Biochem.* **1998**, *67*, 509, *The green fluorescent protein.*

[48] M. Hopeross, L. A. Yannuzzi, E. S. Gragoudas, D. R. Guyer, J. S. Slakter, J. A. Sorenson, S. Krupsky, D. A. Orlock, C. A. Puliafito, *Ophthalmology* **1994**, *101*, 529, *Adverse Reactions Due to Indocyanine Green.*

[49] S. Mordon, J. M. Devoisselle, S. Soulie-Begu, T. Desmettre, *Microvascular Research* **1998**, *55*, 146, *Indocyanine green: Physicochemical factors affecting its fluorescence in vivo.*

[50] M. Chattoraj, B. A. King, G. U. Bublitz, S. G. Boxer, *Proc. Natl. Acad. Sci. U. S. A.* **1996**, *93*, 8362, *Ultra-fast excited state dynamics in green fluorescent protein: Multiple states and proton transfer.*

[51] M. Cotlet, J. Hofkens, F. Kohn, J. Michiels, G. Dirix, M. Van Guyse, J. Vanderleyden, F. C. De Schryver, *Chem. Phys. Lett.* **2001**, *336*, 415, *Collective effects in individual oligomers of the red fluorescent coral protein DsRed.*

[52] M. Cotlet, J. Hofkens, M. Maus, T. Gensch, M. Van der Auweraer, J. Michiels, G. Dirix, M. Van Guyse, J. Vanderleyden, A. Visser, F. C. De Schryver, *J. Phys. Chem. B* **2001**, *105*, 4999, *Excited-state dynamics in the enhanced green fluorescent protein mutant probed by picosecond time-resolved single photon counting spectroscopy.*

[53] W. E. Moerner, *J. Chem. Phys.* **2002**, *117*, 10925, *Single-molecule optical spectroscopy of autofluorescent proteins.*

[54] D. R. Larson, W. R. Zipfel, R. M. Williams, S. W. Clark, M. P. Bruchez, F. W. Wise, W. W. Webb, *Science* **2003**, *300*, 1434, *Water-soluble quantum dots for multiphoton fluorescence imaging in vivo.*

[55] W. C. W. Chan, D. J. Maxwell, X. Gao, R. E. Bailey, M. Han, S. Nie, *Curr. Opin. Biotechnol.* **2002**, *13*, 40, *Luminescent quantum dots for multiplexed biological detection and imaging.*

[56] B. Dubertret, P. Skourides, D. J. Norris, V. Noireaux, A. H. Brivanlou, A. Libchaber, *Science (Washington, DC, U. S.)* **2002**, *298*, 1759, *In vivo imaging of quantum dots encapsulated in phospholipid micelles.*

[57] W. C. W. Chan, S. M. Nie, *Science* **1998**, *281*, 2016, *Quantum dot bioconjugates for ultrasensitive nonisotopic detection.*

[58] R. Esfand, D. A. Tomalia, *Drug Discovery Today* **2001**, *6*, 427, *Poly(amidoamine) (PAMAM) dendrimers: from biomimicry to drug delivery and biomedical applications.*

[59] M. S. Shchepinov, I. A. Udalova, A. J. Bridgman, E. M. Southern, *Nucleic Acids Res.* **1997**, *25*, 4447, *Oligonucleotide dendrimers: synthesis and use as polylabelled DNA probes.*

[60] S. D. Konda, S. Wang, M. Brechbiel, E. C. Wiener, *Investigative Radiology* **2002**, *37*, 199, *Biodistribution of a Gd-153-folate dendrimer, generation=4, in mice with folate-receptor positive and negative ovarian tumor xenografts.*

[61] C. Minard-Basquin, T. Weil, A. Hohner, J. O. Raedler, K. Müllen, *J. Am. Chem. Soc.* **2003**, *125*, 5832, *A polyphenylene dendrimer-detergent complex as a highly fluorescent probe for bioassays.*

[62] O. Finikova, A. Galkin, V. Rozhkov, M. Cordero, C. Hagerhall, S. Vinogradov, *J. Am. Chem. Soc.* **2003**, *125*, 4882, *Porphyrin and tetrabenzoporphyrin dendrimers: Tunable membrane-impermeable fluorescent pH nanosensors.*

[63] M. H. V. Werts, J. W. Verhoeven, J. W. Hofstraat, *Journal of the Chemical Society-Perkin Transactions 2* **2000**, 433, *Efficient visible light sensitisation of water-soluble near-infrared luminescent lanthanide complexes.*

[64] M. H. V. Werts, R. H. Woudenberg, P. G. Emmerink, R. van Gassel, J. W. Hofstraat, J. W. Verhoeven, *Angewandte Chemie-International Edition* **2000**, *39*, 4542, *A near-infrared luminescent label based on Yb-III ions and its application in a fluoroimmunoassay.*

[65] A. Margineanu, J. Hofkens, M. Cotlet, S. Habuchi, A. Stefan, J. Qu, C. Kohl, K. Müllen, Y. Engelborghs, T. Gensch, F. C. De Schryver, *J. Phys. Chem. B* **2004**, *108*, 12242, *Photophysics of a Water-Soluble Rylene Dye: Comparison with Other Fluorescent Molecules for Biological Applications.*

[66] C. Jung, B. K. Müller, D. C. Lamb, F. Nolde, K. Müllen, C. Bräuchle, *J. Am. Chem. Soc.* **2006**, *128*, 5283, *A New Photostable Terrylene Diimide Dye for Applications in Single Molecule Studies and Membrane Labeling.*

[67] T. Ha, *Methods* **2001**, *25*, 78, *Single-molecule fluorescence resonance energy transfer.*

[68] C. Jung, B. K. Müller, D. C. Lamb, F. Nolde, K. Müllen, C. Braeuchle, *J. Am. Chem. Soc.* **2006**, *128*, 5283, *A New Photostable Terrylene Diimide Dye for Applications in Single Molecule Studies and Membrane Labeling.*

[69] S. B. Brichkin, M. A. Kurandina, T. M. Nikolaeva, V. F. Razumov, *High Energy Chemistry* **2004**, *38*, 373, *Effects of surfactants on the spectral properties of carbocyanine dyes in solutions.*

[70] T. Tang, K. Peneva, K. Müllen, S. E. Webber, *J. Phys. Chem. A* **2007**, *111*, 10609, *Photophysics of Water Soluble Perylene Diimides in Surfactant Solutions.*

[71] S. Das, K. G. Thomas, K. J. Thomas, V. Madhavan, D. Liu, P. V. Kamat, M. V. George, *J. Phys. Chem.* **1996**, *100*, 17310, *Aggregation behavior of water soluble bis(benzothiazolylidene)squaraine derivatives in aqueous media.*

[72] F. Würthner, C. Thalacker, S. Diele, C. Tschierske, *Chemistry-a European Journal* **2001**, *7*, 2245, *Fluorescent J-type aggregates and thermotropic columnar mesophases of perylene bisimide dyes.*

[73] E. G. McRae, M. Kasha, *J. Chem. Phys.* **1958**, *28*, 721, *Enhancement of Phosphorescence Ability Upon Aggregation of Dye Molecules.*

[74] J. Franck, E. Teller, *J. Chem. Phys.* **1938**, *6*, 861, *Migration and photochemical action of excitation energy in crystals.*

[75] S. E. Radford, *Trends Biochem. Sci.* **2000**, *25*, 611, *Protein folding: progress made and promises ahead.*

[76] C. Lefevre, H. C. Kang, R. P. Haugland, N. Malekzadeh, S. Arttamangkul, R. P. Haugland, *Bioconjugate Chem.* **1996**, *7*, 482, *Texas Red-X and Rhodamine Red-X, New Derivatives of Sulforhodamine 101 and Lissamine Rhodamine B with Improved Labeling and Fluorescence Properties.*

[77] R. P. Haugland, W. Szalecki Reactive derivatives of sulforhodamine 101 with enhanced hydrolytic stability, their conjugates, and labeling kits containing them. 1997.

[78] H. C. Kang Conjugates of sulforhodamine fluorophores with enhanced fluorescence. 1998.

[79] M. Börsch, M. Diez, B. Zimmermann, M. Trost, S. Steigmiller, P. Graber, *Proceedings of SPIE-The International Society for Optical Engineering* **2003**, *4962*, 11, *Stepwise rotation of the g-subunit of EF0F1-ATP synthase during ATP synthesis: a single-molecule FRET approach.*

[80] R. Kasper, M. Heilemann, P. Tinnefeld, M. Sauer, in *Biophotonics 2007: Optics in Life Science, Vol. 6633* (Eds.: J. Popp, G. VonBally), **2007**, pp. Z6331.

# 2. Motivation and objectives

The wide-spread use of fluorescent dyes in molecular diagnostics and fluorescence microscopy together with new developments such as single-molecule fluorescence spectroscopy provide researchers from various disciplines with an ever expanding toolbox. Single-molecule spectroscopy relies to a large extent on extraordinary bright organic fluorescent dyes such as rhodamine- or cyanine-derivatives. While in the last decade single-molecule equipment and methodology have significantly advanced and in some cases reached theoretical limits (e.g. detectors approaching unity quantum yields), instable emission ("blinking") and photobleaching become more and more the bottleneck of further developments and spreading of single-molecule fluorescence studies. In recent years, agents and recipes have been developed to increase the photostability of conventional fluorophores.

Studies of organic fluorescent dyes are experiencing a renaissance related to the increasing demands posed by new microscopy techniques for high resolution and high sensitivity. Such studies aim at a detailed understanding of the chromophores photophysics, their interactions with the environment and their photochemistry, inevitably leading to photobleaching. In particular, under close to physiological conditions, i.e. in aqueous environment, fluorescent dyes show noticeably different properties than in solid matrices and are often less photostable but therefore exhibit more homogeneous properties less influenced by inhomogeneous broadening.

One critical issue in observing biological entities on the single molecule level is the label. It should be water-soluble, highly fluorescent in aqueous environment, and have a reactive group to be attached to the bio-molecule, e.g. protein or enzyme. Moreover the attachment should not affect the bio-molecule's structure or function, or

in the case of an enzyme, its activity. Finally, an exceptional photostability of the label is needed to visualize or track for a sufficient period of time.
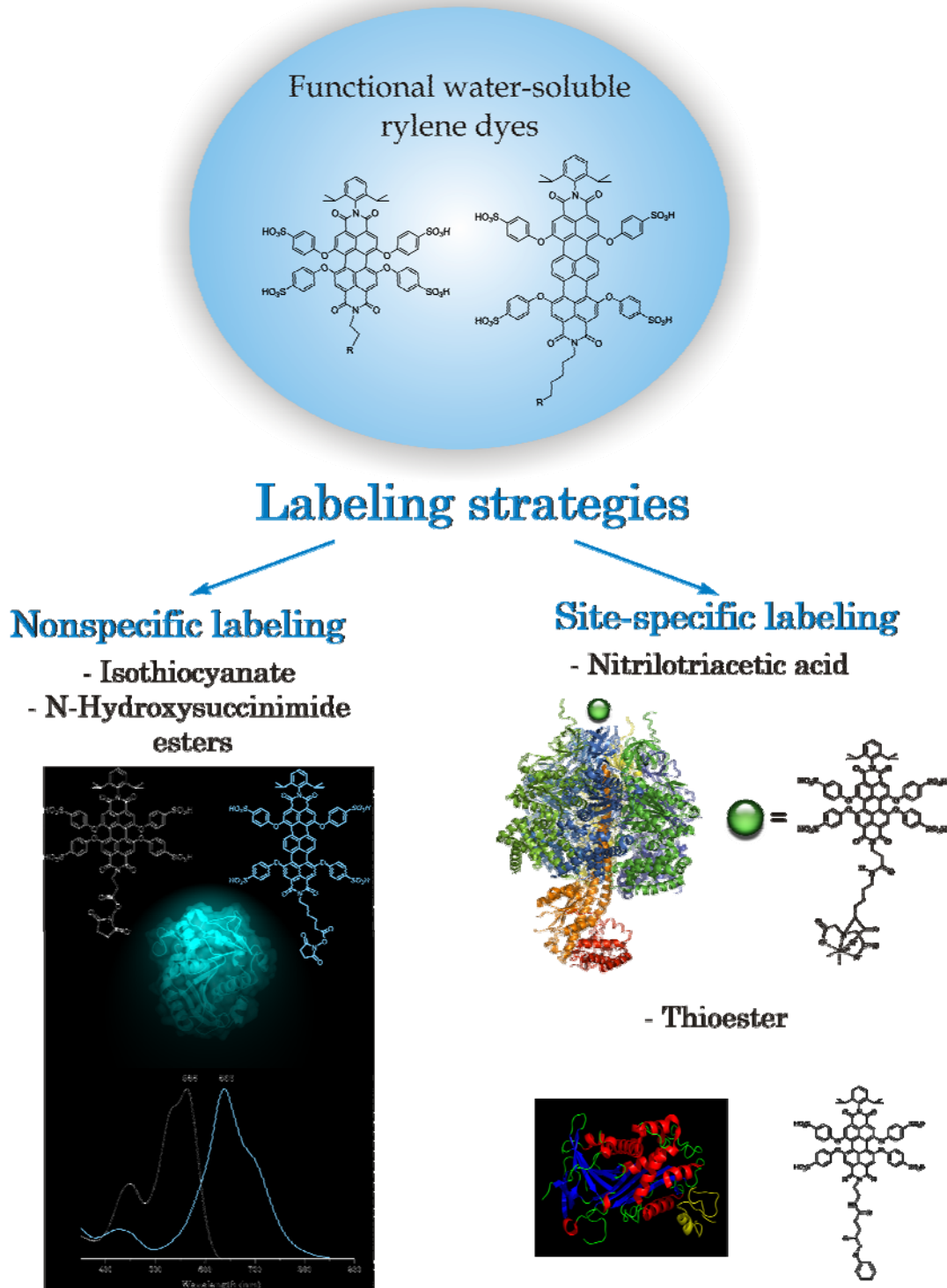
All of these above mentioned demanding studies could benefit from the extraordinary properties of the rylene dyes, mentioned in Chapter 1. In this regard it should be pointed out again that, in such experiments (e.g. protein labeling), reactive functional groups play a leading role. Hence the combination of rylene dye plus functional group could generate new improved fluorescent probes.

Therefore, the main goal of this work is the synthesis of new ultrastable fluorophores based on rylene dyes. This required the development of new synthetic strategies for the decoration of perylene and terrylene dyes with various reactive groups, like isothiocyanates, maleimides, N-hydroxysuccinimides, thioesters or nitrilotriacetic acids. The corresponding conjugates with proteins where applied to study the photophysical behavior of the new chromophores.[1-5]

The next chapters of the present thesis are structured as follows.

Chapter 3 describes newly developed synthetic concepts affording water-soluble perylene and terrylene fluorophores bearing functional groups for non-specific labeling of proteins. The reactivity and photophysical properties of these new chromophores are studied in aqueous medium. The most suitable chromophores were further derivatized with amine or thiol reactive groups, suitable for chemical modification of proteins. The next chapters are devoted to the application of the water-soluble monofunctional rylene dyes, as labels.

In chapter 4 the performance of perylene and terrylene possessing N-hydroxysuccinimide esters was assessed by single molecule enzyme tracking of phospholipase acting on phospholipid supported layers. Moreover, novel convenient procedure for the removal of unreacted dye from labeled enzymes is described.

Chapter 5 and 6 are devoted to site-specific labeling of proteins. Chapter 5 reviews the available strategies for site-specific labeling of proteins and illustrates the synthesis and application of perylene bearing thioester functional group. Native chemical ligation was exploited for the attachment of a fluorescent label at the N-

terminus of plasminogen activator inhibitor. Chapter 6 is elucidating the synthesis of nitrilotriacetic acid functionalized perylene chromophore and its complexation with His-tagged proteins. Studies of the photophysical properties of this new chromophore revealed that for the first time the complexation of nickel ions did not influence the fluorescence quantum yield of the fluorophore.

Finally, Chapter 7 summarizes the results obtained with a set of ultrastable fluorophores and outlines some of their future applications.

## 2.1 References:

[1] K. Peneva, A. Herrmann, K. Müllen Water-soluble rylene dyes, methods for preparing the same and uses thereof as fluorescent labels for biomolecules. EP07022521, 2007.

[2] K. Peneva, G. Mihov, F. Nolde, S. Rocha, J. Hotta, K. Braeckmans, J. Hofkens, H. Uji-i, A. Herrmann, K. Müllen, *Angew. Chem. Int. Ed.* **2008**, *120*, 3420, *Water-soluble monofunctional perylene and terrylene dyes: powerful labels for single enzyme tracking*.

[3] K. Peneva, G. Mihov, A. Herrmann, N. Zarrabi, M. Börsch, T. Duncan, K. Müllen, *J. Am. Chem. Soc.* **2008**, *130*, 5398, *Exploiting the nitrilotriacetic acid moiety for biolabeling with ultrastable perylene dyes*.

[4] S. Rocha, J. Hutchison, K. Peneva, A. Herrmann, K. Müllen, M. Skjøt, C. Jørgensen, A. Svendsen, J. Hofkens, H. Uji-i, *Proc. Natl. Acad. Sci. U. S. A.* **2008**, *submitted*, *Linking phospholipase mobility to activity by single molecule wide-field microscopy*.

[5] K. Peneva, G. Mihov, A. Herrmann, M. Börsch, K. Müllen, *Org. Biomol. Chem.* **2008**, *to be submitted*, *Site-specific labeling of plasminogen activator inhibitor at amine terminal cysteine with water-soluble perylene thioester*.

# 3. Design and synthesis of new water-soluble monofunctional rylene chromophores

## *3.1. Ionic water-soluble perylenetetracarboxydiimides*

General characteristics of a chromophore (e.g. high extinction coefficient, high quantum yield), as well as particularities of biological systems, need to be considered when new fluorescent dyes are introduced. Adequate chromophores combine absorbance and emission maxima above 500 nm due to the background noise of fluorescent impurities and the auto-fluorescence of the cell, high fluorescent quantum yield in aqueous solutions, as well as functional group for attachment to a biomolecule. In this chapter we focus on the synthesis of novel water-soluble rylene(dicarboximide) chromophores, possessing several functional groups suitable for labeling of proteins.

Chromophores carrying hydrophilizing substituents are already described in our group, for instance, peptide star polymers **3.1** with a PDI chromophore in the center,[1] a PMI chromophore **3.2** bearing a single polyethylene glycol (PEG) chain, [2] a dendronized PDI **3.3** [3] with PEG chains in the rim and PDI substituted by sulfonated phenoxy in the bay region. These polymers or dendrimers are water soluble; however, their fluorescence quantum yields are in all cases very low (~ 19%).

a: R = ⌒COO⁻

b: R = ⌒⌒NH₂*HBr

n = 10, 50, 100, 200

**3.1**



**3.2**   **3.3**

R = � structure⌯ₙ

Mw = 5000

R = a structure

**Figure 3.1. Water soluble perylene chromophores bearing peptides and glycol chains.**

Moreover, PDIs attached hydrophilic groups e.g. sulfonyl groups **3.4**, quaternized amines **3.5** or crown ethers, within the imide structure of the chromophore also have been reported (Figure 3.2). [4, 5] In all cases, these perylene chromophores revealed very low fluorescence in water. This behavior has been

attributed to their high tendency in aqueous media to form aggregates with strong intermolecular π-interactions.[6]
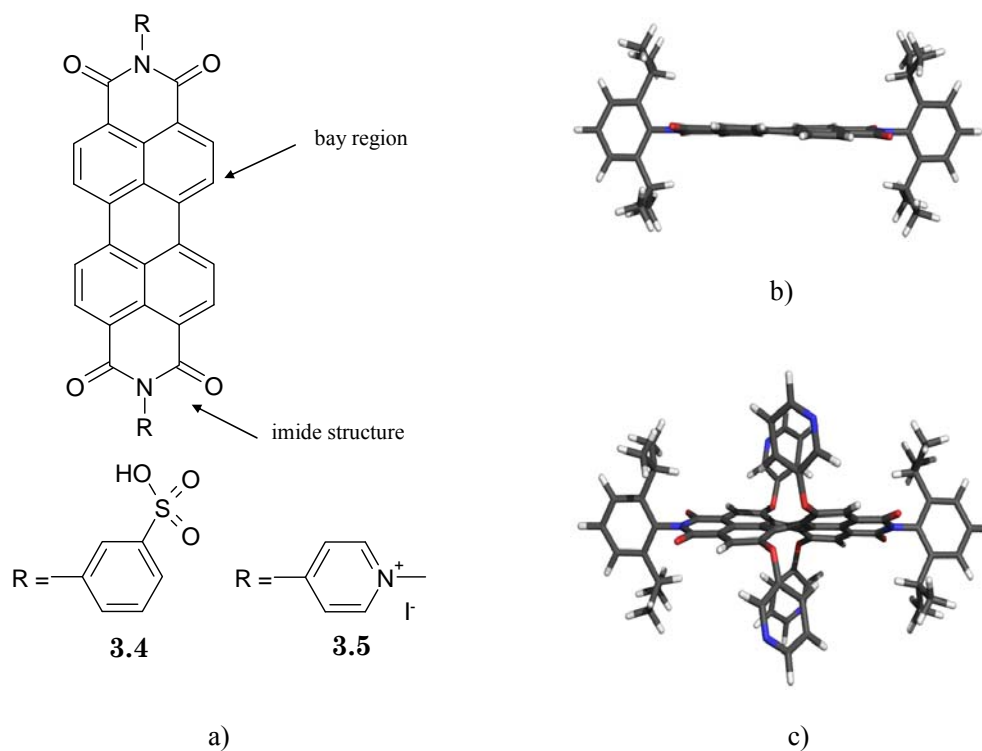


**Figure 3.2: a) PDI bearing substituents in the imide structure; b) 3D structure of PDI with no substituents in the bay region (planar scaffold) – view in the direction of the bay region; c) 3D structure with four substituents in the bay region (twisted scaffold).**

Since PDI chromophores bearing charged substituents in the imide structure of the chromophore displayed low fluorescence quantum yields in water,[1-3] these substituents were introduced in the bay region of the chromophore (Figure 3.2a). The functionalization of the bay region led to a non-planar and twisted aromatic scaffold (Figure 3.2c).[7] Quante in the group of Prof. Müllen first reported water soluble PDI with negative charges in the region, tetrasulfonyl perylenetetracarboxydiimides (**3.6**), however, their fluorescence properties in his study were not described.[8] Recently, Kohl repeated this reaction to obtain **3.7**,

which showed good water solubility ($10^{-2}$ M) and high fluorescence quantum yield in water. This indicated that the charged groups could improve the fluorescence quantum yield of PDI in water.[9]



**3.6**                **3.7**
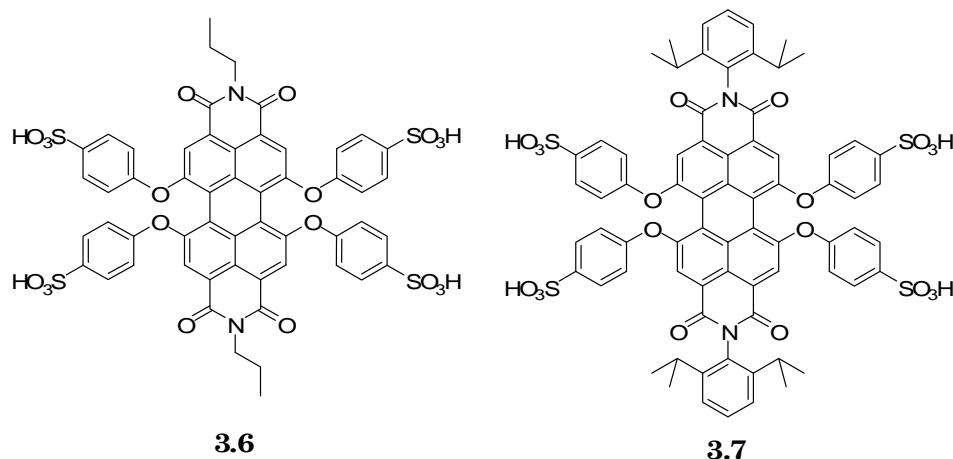
By using the same design mentioned above, Kohl and Qu have first introduced various hydrophilic substituents in the bay region, which results in a nonplanar, twisted aromatic chromophore scaffold.[9, 10] These waters-soluble perylene diimides bearing carboxylic groups, sulfonic acid, as well as positively charged branches was prepared by treatment of N,N'-bis(2,6-diisopropylphenyl)-1,6,7,12-tetrachloro perylene-3,4:9,10-tetracarboxylic acid diimide, available on the gram scale, with different *para*-substituted phenols.[11] (Scheme 3.1)



**3.8**                **3.9**

**3.10**

**3.11**

**3.12**
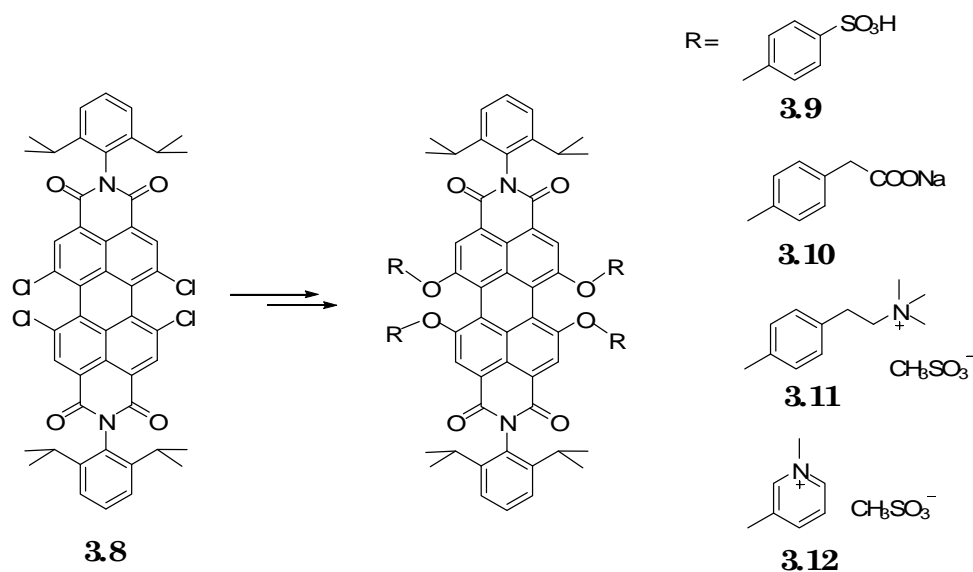
**Scheme 3.1. Synthesis of water-soluble perylene diimides bearing polar substituents in the bay region**

All of the above mentioned ionic PDI chromophores have good water solubility, ranging between $10^{-4}$ to $10^{-2}$ mol/l. The absorbance spectra of all ionic PDIs in water in a concentration range of 10 mg/mL exhibit the same vibrational fine structure of PDI, which suggest that ionic PDIs are present as monomers in high concentrations. The charged PDIs exhibit high fluorescence quantum yields in water 0.58 for **3.9** and 0.66 for **3.12**, measured using Cresyl violet in methanol as reference. One of the most important requirements for a fluorescent label is the occurrence of a functional group for covalent attachment to a protein or nucleic acid. For this reason the development of new and efficient routes for the synthesis of desymmetrized PDIs which contain one functional group was essential. The presence of more than one chemically reactive groups very often leads to cross conjugation, and therefore is undesirable. Monofunctional PDIs bearing ionic substituents in the bay region were first introduced by Qu et al.[11, 12] The desymmetrization was accomplished by statistical imidization of 1,6,7,12-tetrachloroperylene-3,4:9,10-tetracarboxylic acid dianhydride **3.13** using two different arylamines in propionic acid. (Scheme 3.2) The reaction proceeds in low yield (30 %) and leads to the formation of several products, thus it does not represent a good synthetic strategy for the preparation of monofunctional perylene dyes. Furthermore, an additional step is required for the introduction of different ionic substituents by subsequent phenoxylation.
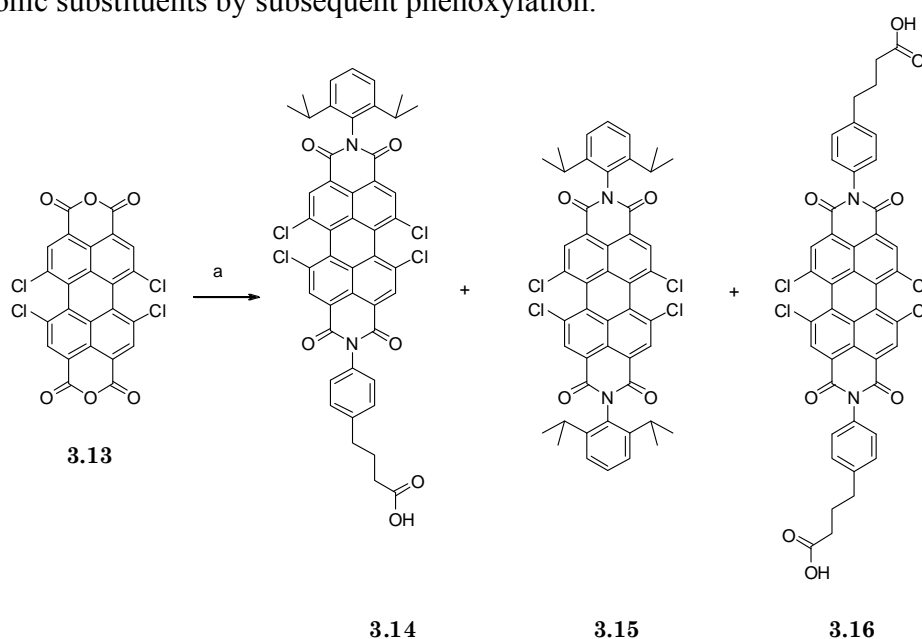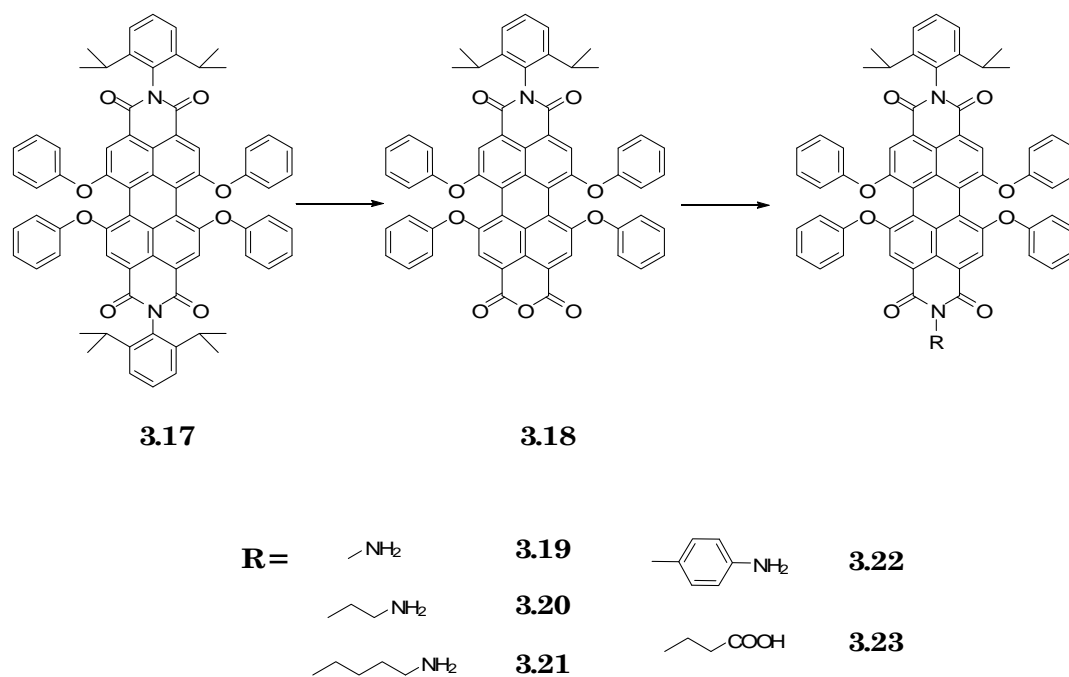


**Scheme 3.2. Synthesis of 3.14: a) 2,6-diisopropylaniline, 4-(butyric acid)aniline, propionic acid, 140°C, 5h, 30%.**

## *3.2. Preparation of new monofunctional water-soluble perylene dyes*

As main scaffold for the synthesis of new monofunctional water-soluble PDIs 1,6,7,12-tetra(4-sulfophenoxy)-N,N'-(2,6-diisopropylphenyl)-perylene-3,4:9,10-tetracarboxydiimide **1.45** was selected. A different route was chosen for the preparation of water-soluble desymmetrized perylenetetracarboxydiimides. The synthesis of the herein described perylene derivatives starts from the symmetrical perylene diimide **3.17**. (Scheme 3.3) One of the imide structures was saponified under strongly basic conditions and was further reacted with hydrazine **3.19**, 1,2-ethylenediamine **3.20**, 1,4-diaminobutane **3.21**, 1,4-diaminobenzene **3.22** and 3-aminopropanoic acid **3.23**, respectively, to give the corresponding monofunctionalized perylenes. The imidization reaction for **3.19**, **3.20** and **3.21** was carried out in toluene at 60°C for 3 hours to afford the desired products in high yields, (**3.21** was obtained in 70 % yield). In order to achieve the successful incorporation of p-phenylenediamine (**3.22**) the imidization was performed in quinoline at 160°C for 12 hours. The introduction of beta-alanine was performed in propionic acid at 140°C for 3 hours. In all cases, the desired products were easily separated by column chromatography due to the high polarity of the carboxylic acid or amine groups. Dichloromethane was used at first to remove the PDIs carrying no polar groups, and then the desired products were obtained using a mixture of dichloromethane/ethanol (10:3).

The molecular structures are confirmed by applying NMR spectroscopy, FD and/or MALDI-TOF mass spectrometry. Furthermore, ^{1}H- and ^{13}C-NMR spectra, FDMS and elementary analysis proved the purity of the compounds. One exemplary ^{1}H-NMR spectrum of **3.23** in dicloromethane-$d_2$ is given on Figure 3.3 together with the signal assignment.

**Scheme 3.3. Synthesis of desymmetrized perylenetetracarboxydiimides**



**Figure 3.3.** $^1$H-NMR spectrum of **3.23** in dichloromethane-$d_2$ at room temperature (300 MHz).
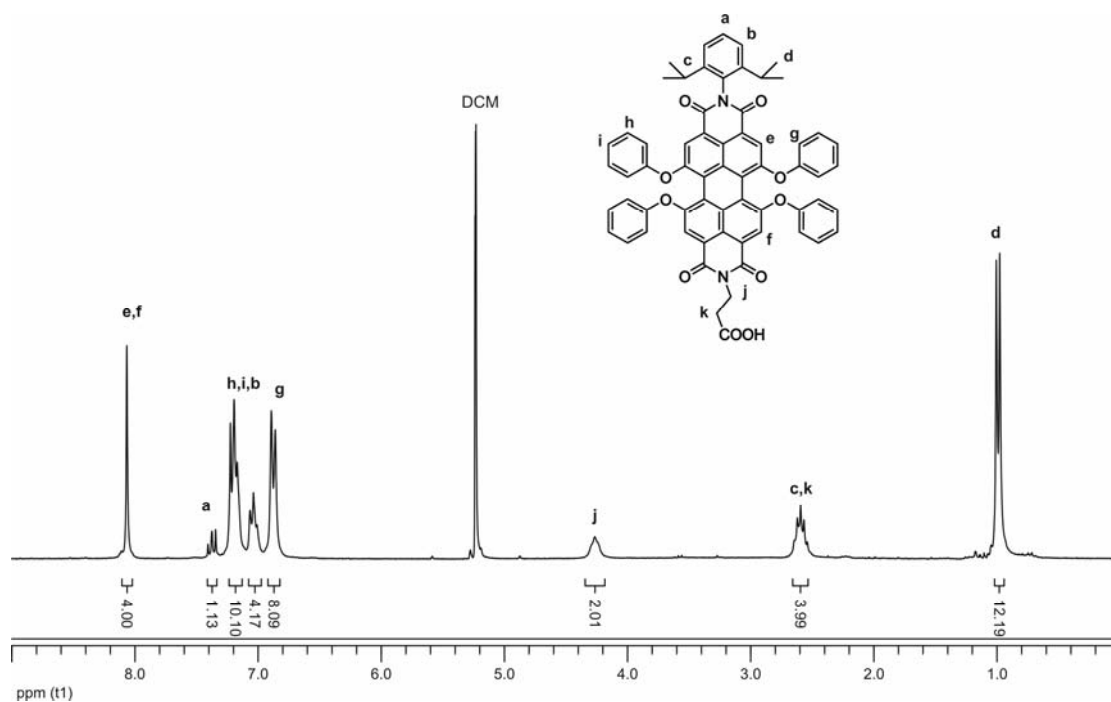
Water solubility was achieved by introducing sulfonyl substituents in the phenoxy rings of the already desymmetrized PDIs. The sulfonation of the above

mentioned perylene derivatives was chosen as the last step in the synthesis, since the sulfonated N-(2,6-diisopropylphenyl)-1,6,7,12-tetraphenoxyperylene-3,4:9,10-tetra carboxy-9,10-monoanhydride-3,4-monoimide **(3.24)** is not active in imidization reactions (Scheme 3.4).



**3.24**
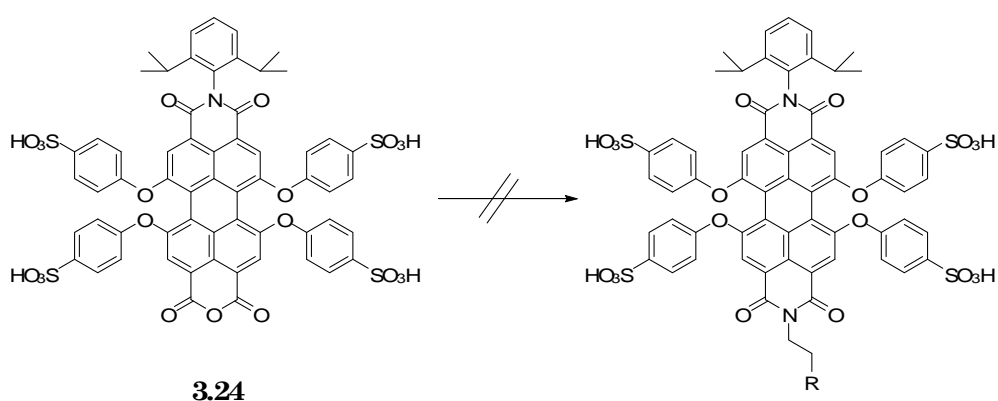
**Scheme 3.4. Sulfonated PDIs with one imide structure and one anhydride**
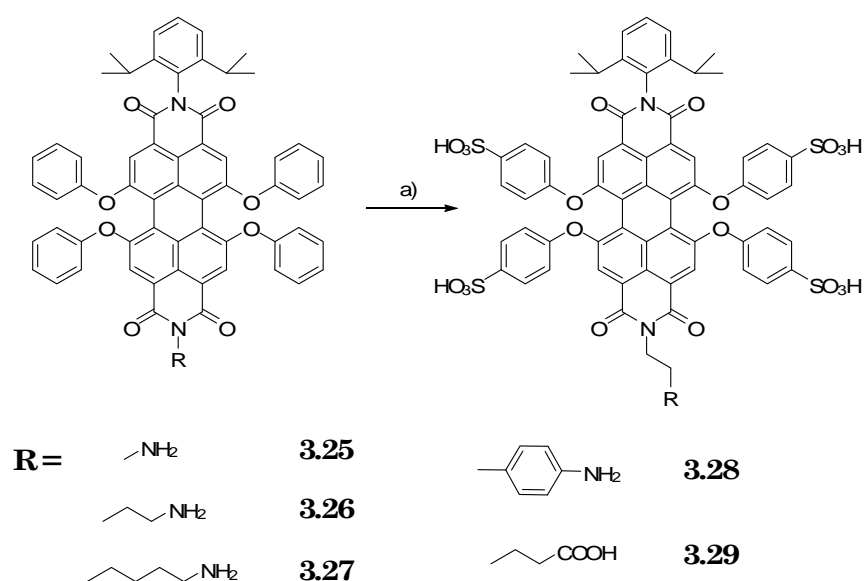


**Scheme 3.5. a) Concentrated H$_2$SO$_4$, room temperature, 24 h, 98 %**

The sulfonation was accomplished by treatment of the monofunctionalized perylenetetracarboxydiimides with concentrated sulphuric acid at room temperature for 24 hours (Scheme 3.5). The purification was accomplished by slowly adding

water to the reaction mixture and then the solution was dialyzed against water for 96 hours to remove the sulphuric acid.

The molecular structures and purity of the sulfonated desymmetrized perylene chromophores are confirmed by ^{1}H and ^{13}C-NMR spectroscopy, FD mass spectrometry and/or MALDI-TOF spectrometry and elemental analysis. One exemplary mass spectrum of **3.26** with four sulfonyl substituents is given in Figure 3.6, showing one single peak corresponding to the molecular mass and one corresponding to the molecular mass plus sodium. The agreement between the calculated (m/z calculated = 1282) and experimentally determined m/z ratios (m/z observed = 1283) confirms the purity of this monofunctional water soluble dye. The NMR spectrum of **3.29** exhibits well-separated and clearly assignable signals and their intensity ratios of all peaks perfectly agree with the theoretically expected. (Figure 3.7) In addition, since the protons in phenoxy groups (o and p) show two double peaks, respectively, the desymmetrization, the number of sulfonyl substituents as well as the substitution pattern of the phenyl ring (para substitution) are proven via NMR experiments.
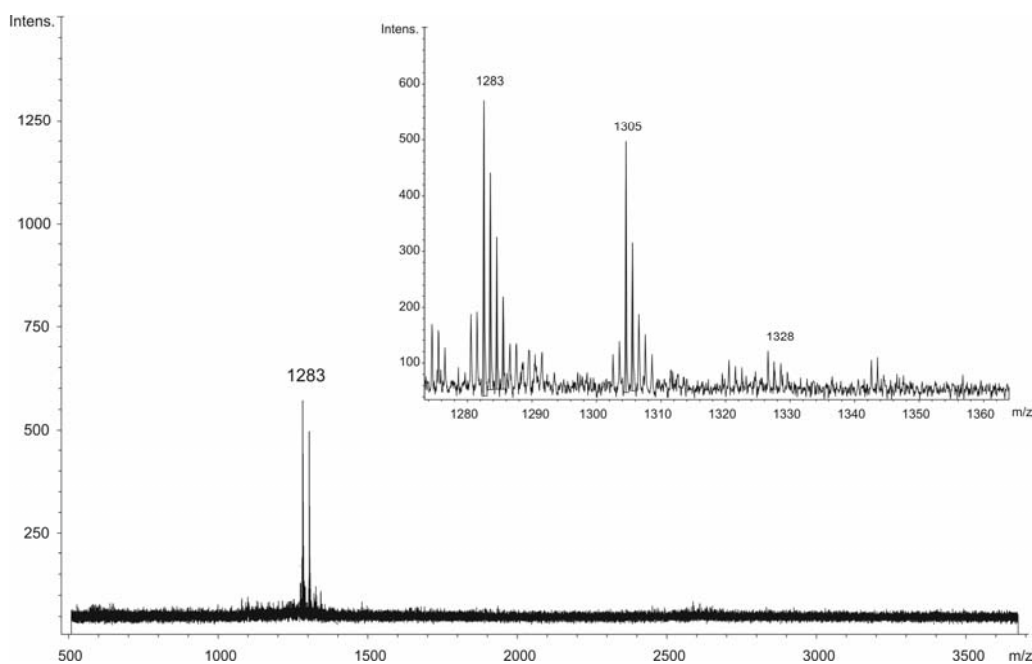


**Figure 3.6.** MALDI-TOF mass spectrum of **3.26** (1282[M]+, 1305[M+Na]+).
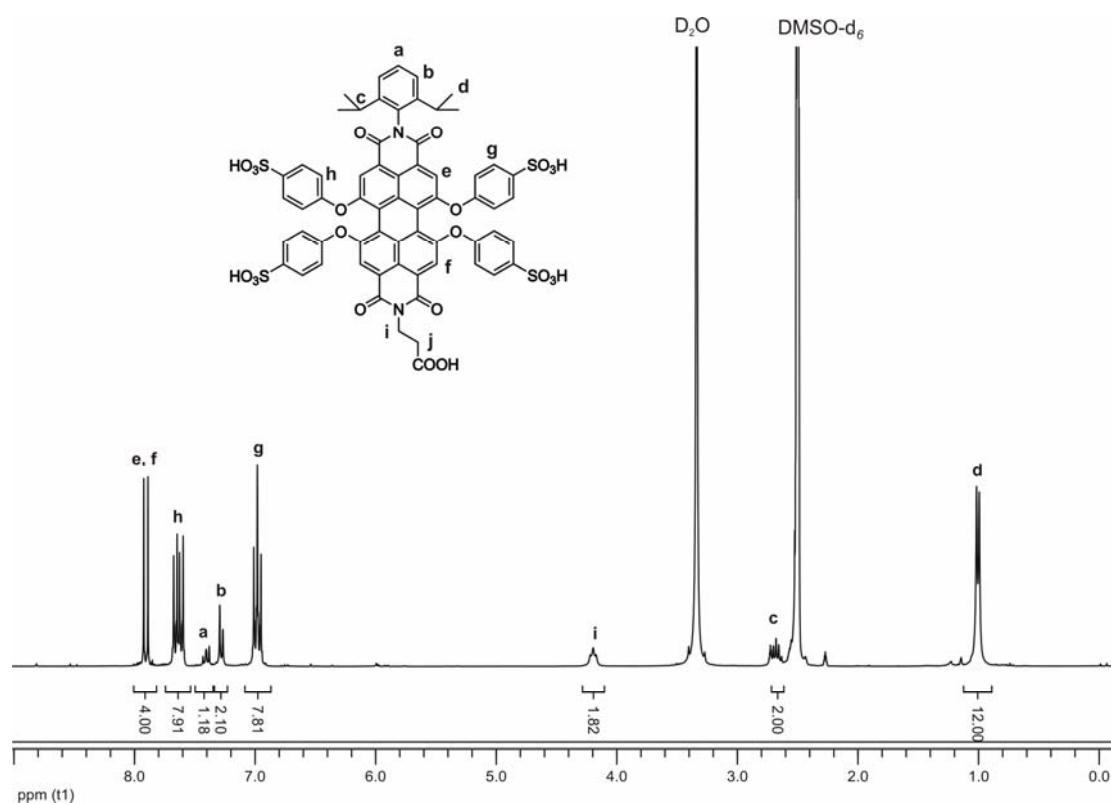
**Figure 3.7.** <sup>1</sup>H-NMR spectrum of 3.29 in dimethylsulfoxide-*d₆* at room temperature (300 MHz).

The optical properties of monofunctional PDI chromophores **3.26** and **3.29** were investigated in water. Their absorption and emission spectra are very similar to those of symmetric PDIs **1.45**. (Figure 3.8), the perylene chromophore containing carboxylic acid group, i.e. **3.29** showed an absorption maxima at 564 nm. Due to the broad and strong absorption band to yield intense fluorescence, they can be excited by the 488 and 514 nm (Ar), 532 nm (Nd:YAG) laser lines, as well as the 546 nm mercury arc line. These dyes possess high $\Phi_f$ as measured using Cresyl Violet in methanol as a reference. However, the values for the amine functionalized PDIs (0.39 for **3.26**) are slightly lower than the values for symmetric PDIs **3.11** (0.66) and the same for the carboxylic acid functionalized one **3.29** (0.66).
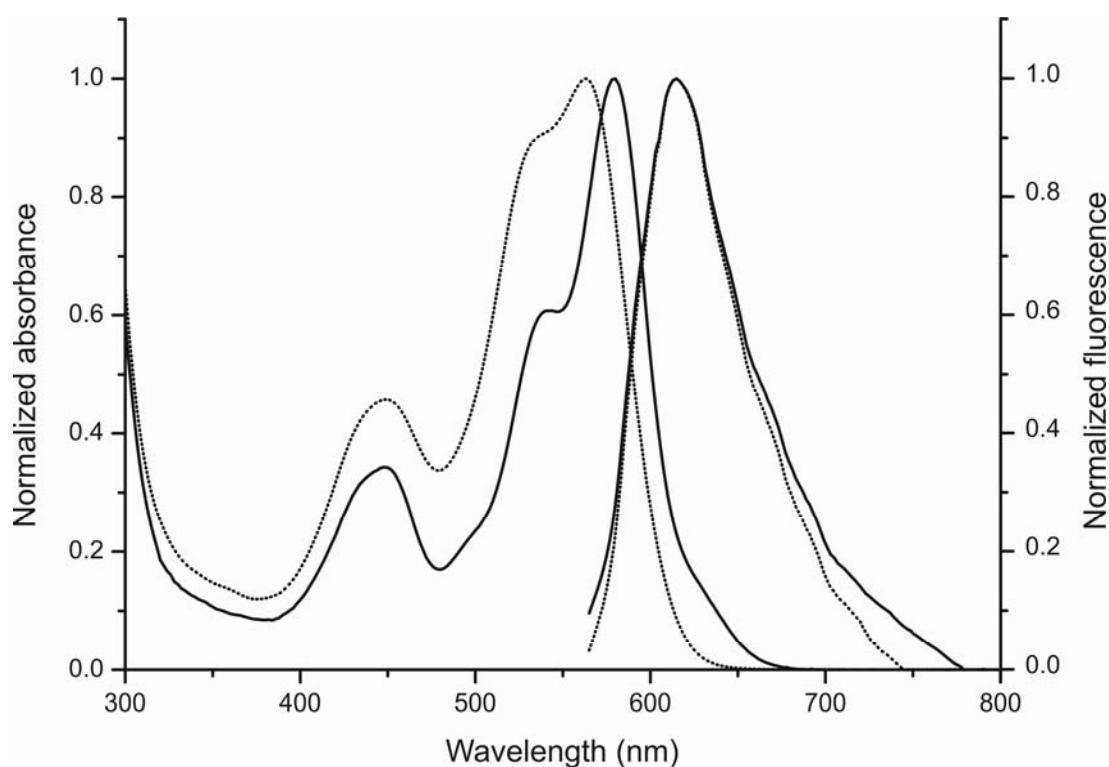
**Figure 3.8: Normalized absorption and emission spectra of amine and acid functionalized PDIs 3.26 (dotted line) and 3.29 (solid line) in water.**

## *3.3. Synthesis of monofunctional water-soluble perylene dyes containing activated groups*

The creation of bioconjugate reagents with spontaneously reactive or selectively reactive functional groups forms the basis for simple and reproducible cross-linking or tagging of target molecules. [13] The next section is focused on the synthesis of water-soluble monofunctional perylene dyes, possessing reactive groups for covalent attachment to biomolecules.

Two perylene chromophores were chosen as key compounds for the synthesis of the fluorophores containing reactive groups **3.26** and **3.29**. These two fluorophores were the starting point for the introduction of different functional

groups like isothiocyanate, N-hydroxysuccinimide, thioester functionality, maleimide group. (Scheme 3.6)
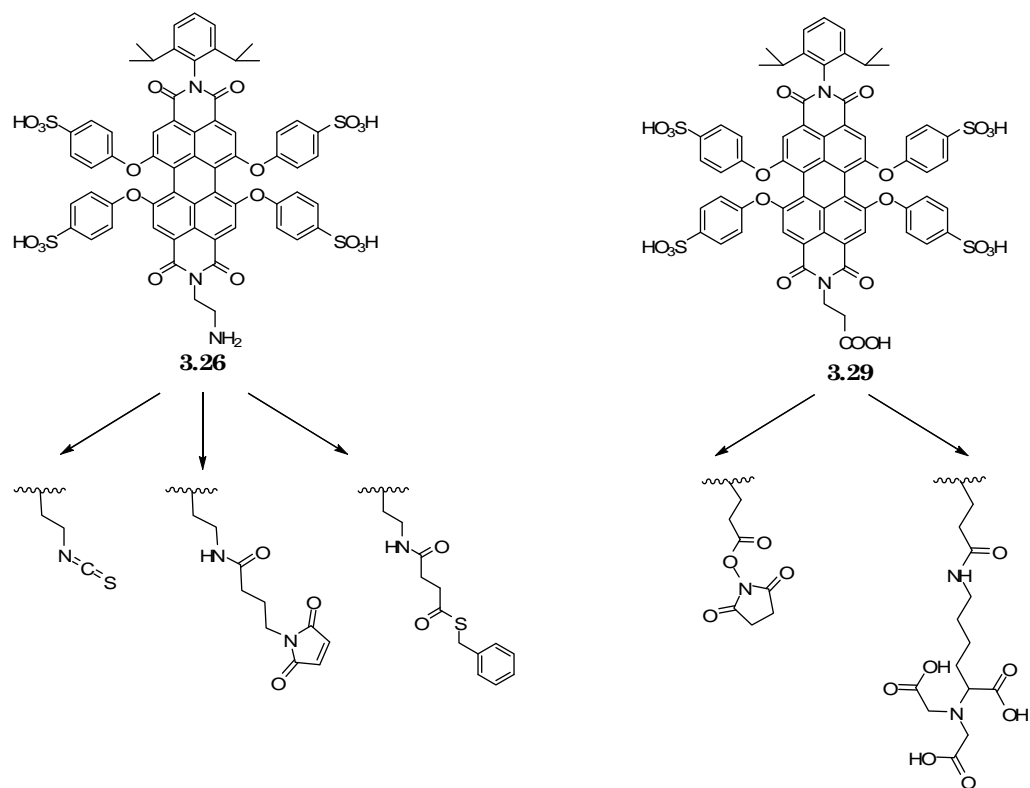


**Scheme 3.6. Perylene chromophore decorated with functional groups**

## 3.3.1. Introduction of amine reactive groups

## 3.3.1.1. Synthesis of isothiocyanate functionalized perylene tetracarboxydiimide

Reactive groups able to couple with amine-containing molecules are by far the most common functional groups present in bioconjugate chemistry.[13] An amine-coupling process can be used to conjugate with nearly all protein or peptide molecules as well as a host of other macromolecules. The primary coupling chemical reactions for modification of amines proceed by one of two routes: acylation or alkylation. Most of these reactions are rapid and occur in high yield to give stable amide or secondary amide bonds.

Isothiocyanates can be formed by the reaction of an aromatic or aliphatic amine with thiophosgene.[14] The group reacts with nucleophiles such as amines, sulfhydryls, and the phenolate ion of tyrosine side chains.[15] The only stable product of these reactions, however, is with primary amine groups. Therefore, isothiocyanate compounds are almost entirely selective for modifying ε- and N-terminal amines in proteins.[16] The reaction involves attack of the nucleophile on the central, electrophilic carbon of the isothiocyanate group (Scheme 3.7). The resulting electron shift and proton loss creates a thiourea linkage between the isothiocyanate-containing compound and the amine with no leaving group involved.

$$R_1N{=}C{=}S \ + \ R_2NH_2 \ \longrightarrow \ R_1HN{-}\overset{\overset{\textstyle S}{\|}}{C}{-}NHR_2$$

**Scheme 3.7. Representation of the reaction between isothiocyanate and primary amine**

The isothiocyanate functionalized dyes have been widely used for labeling of proteins.[16-19] Their usage was not only limited to conjugation to proteins, but they have been used also for incorporation of dye molecules into silica

nanoparticles.[20] A similar synthetic approach was used for the production of water-soluble perylene chromophore bearing an isothiocyanate group, and the one soluble solely in organic solvents. (Scheme 3.8) A solution of **3.20** or **3.26** in dry acetone was placed in a sealed tube filled with argon, followed by the addition of thiophosgene, and the reaction mixture was stirred for 24 hours at room temperature.



| R = | −H | **3.20** |
| | −SO₃H | **3.26** |

| R = | −H | **3.30** |
| | −SO₃H | **3.31** |
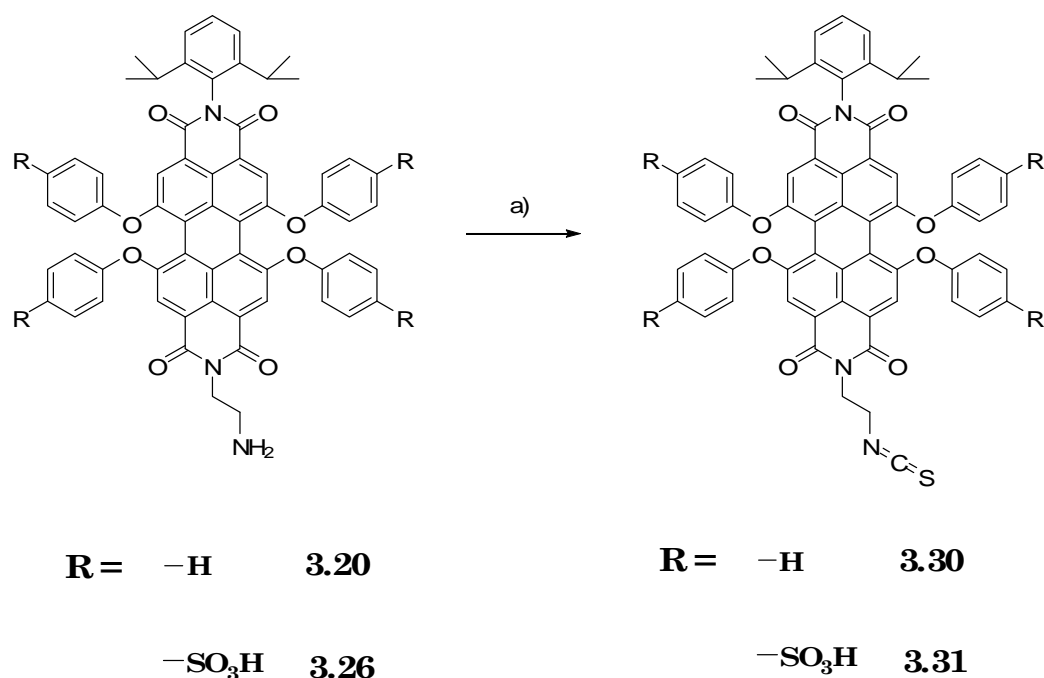
**Scheme 3.8. a) Thiophosgene, dry acetone, room temperature**

After precipitation in a small amount of hexane, the solid was washed with hexane; the hexane solution was collected and evaporated under reduced pressure to give the pure isothiocyanate. The ^{1}H NMR spectrum and the FD mass spectrometry supported the proposed structure and also proved the purity of the compound. The ^{1}H-NMR spectra of **3.20** and **3.30** are compared in Figure 3.4. The introduction of the isothiocyanate group leads to a shift of the characteristic signal of the methylene protons neighboring the amine group - from 3.44 ppm to 3.98 ppm. A smaller shift can be noticed for the methylene protons next to the imide structure – from $\delta = 4.23$ ppm to $\delta = 4.41$ ppm.
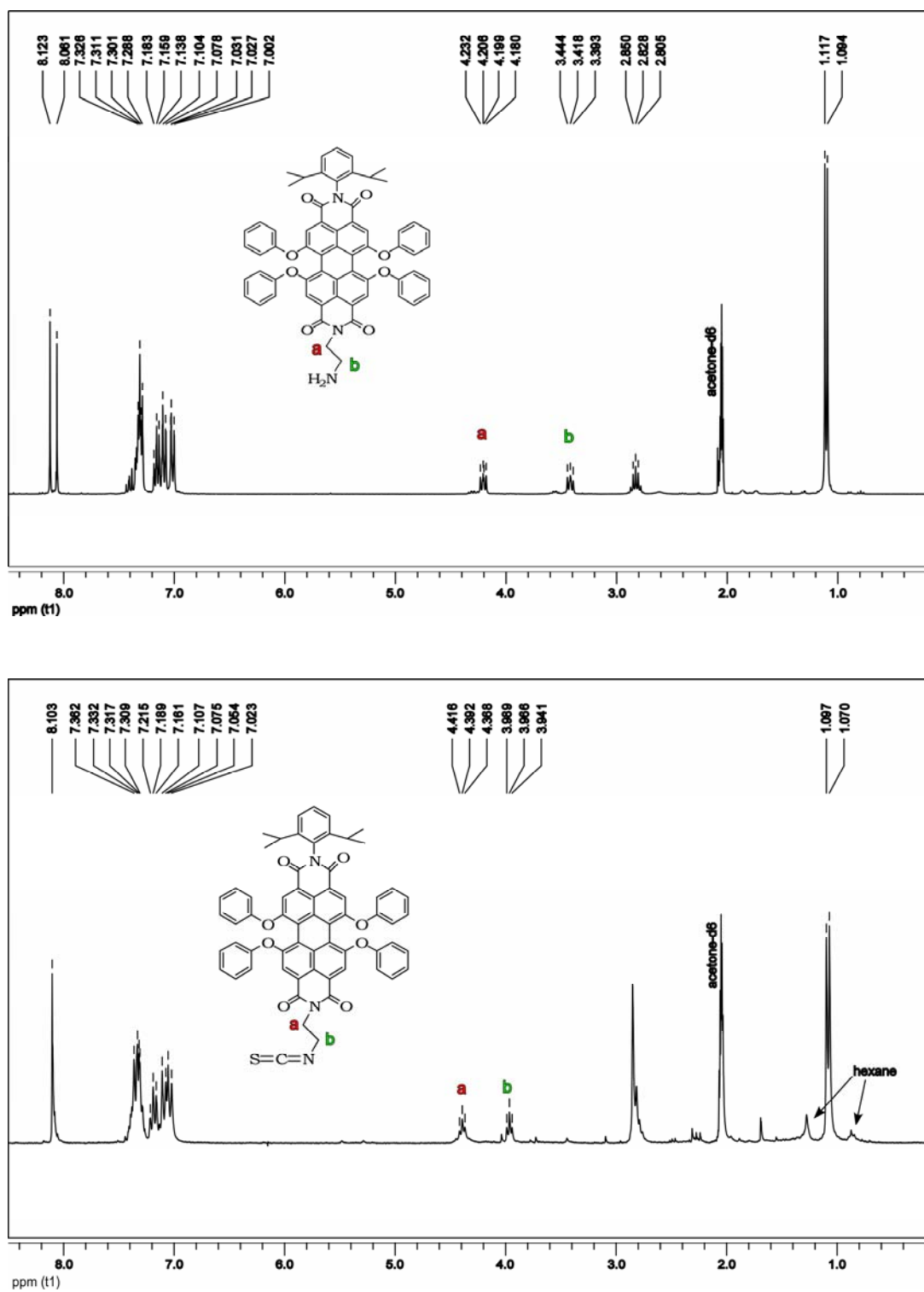
**Figure 3.4.** ¹H-NMR spectra of 3.20 and 3.30 in acetone-*d₆*, room temperature (300 MHz)

The water soluble perylene chromophore containing an isothiocyanate group was synthesized using a slightly modified procedure. **3.26** was dissolved in dry acetone, containing a small amount of dry dimethyl sulfoxide to ensure good solubility of the starting material. The reaction tube was sealed and filled with argon, then thiophosgene (10 fold excess) was added dropwise. After stirring for 24 hours at room temperature, the product was precipitated in cold ether. The precipitate was filtered and dried in vacuum, dissolved in a minimum amount of methanol and again precipitated in cold ether. The precipitation in cold ether was repeated twice and finally **3.31** was dried in vacuum. The $^1$H and $^{13}$C-NMR spectra and the MALDI MS supported the proposed structure of the compound. The chemical structure of **3.31** was confirmed by IR spectra as well, which showed a characteristic sharp band at 2 355 cm$^{-1}$. (Figure 3.5)
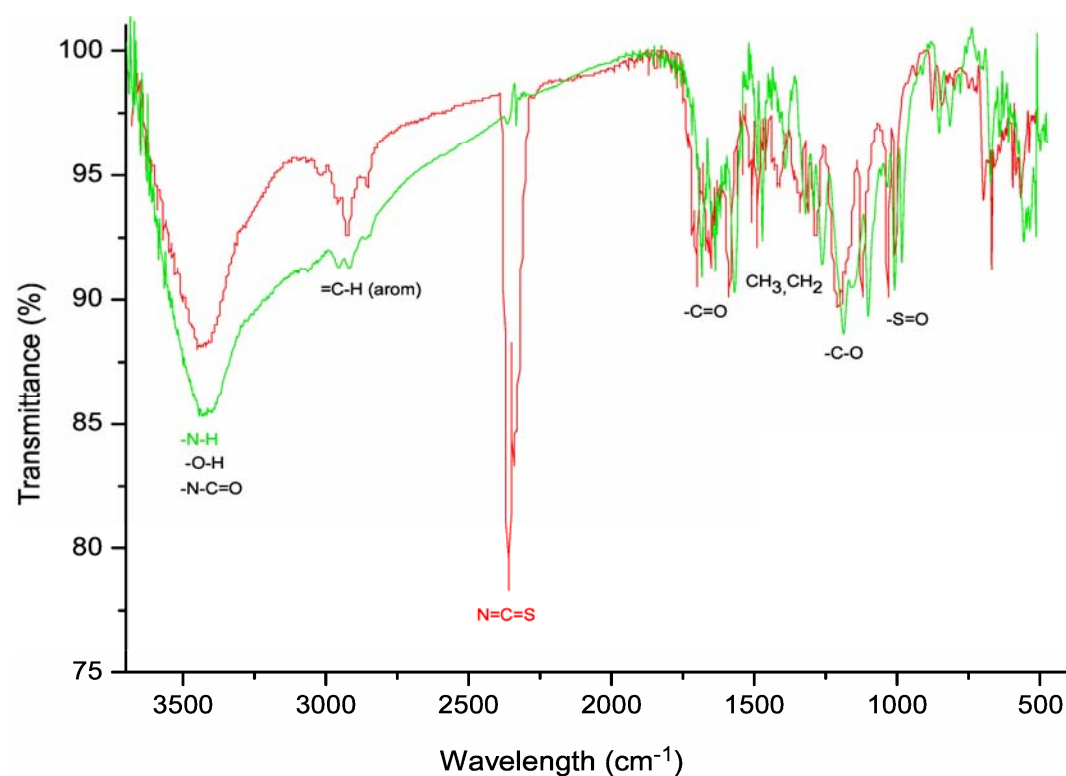


**Figure 3.5. Infrared spectra of 3.26 (green line) and 3.31 (red line) (KBr palettes)**

## 3.3.1.2. Synthesis of N-hydroxysuccinimide functionalized perylenetetracarboxydiimide

Nowadays, the great majority of commercially available amine-reactive cross-linking or modification reagents utilize NHS esters. An NHS ester may be formed by the reaction of a carboxylate with NHS in the presence of a carbodiimide. [21-26] To prepare stable NHS ester derivatives, the activation reaction must be done in nonaqueous conditions using condensing agents, such as N,N'-dicyclohexylcarbodiimide (DCC).[23]

NHS or sulfo-NHS ester-containing reagents react with nucleophiles with release of the NHS or sulfo-NHS leaving group to form an acylated product.[13, 23] (Scheme 3.9) the reaction of such esters with a sulfhydryl or hydroxyl group does not yield stable conjugates, forming thioesters or ester linkages, respectively. Both of these bonds hydrolyze in aqueous environments. Histidine side-chain nitrogens of the imidazolyl rings also may be acylated with an NHS ester reagent, but they too hydrolyze rapidly.[13, 24, 27-30]
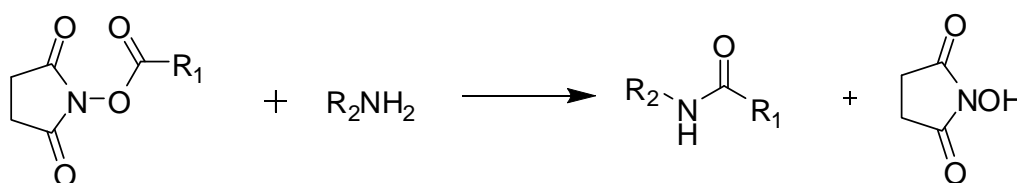


**Scheme 3.9. Reaction between NHS ester containing compound and primary amine**

Reaction with primary and secondary amines, however, creates stable amide and imide linkages, respectively, that do not readily break. Thus in protein

molecules, NHS ester cross-linking reagents couple principally with the α-amines at the N-terminals and the one of lysine side chains.[23]

Active esters are applied to form peptide bonds under mild conditions in both liquid-phase and solid-phase synthesis. In liquid-phase synthesis, most frequently the activation of the carboxyl group of amino acids utilizes N-hydroxysuccinimides. N-Hydroxysuccinimide (NHS) esters are the most useful reagents for coupling to proteins.[26, 31] The preferred residue for attachment is lysine, since modification of other functional groups frequently leads to inactivation of the protein. NHS functionalized water soluble perylene is very valuable chromophore, which combines the photostability of the rylene dyes and reactive group for covalent attachment to proteins. Further application of this chromophore will be discussed in Chapter 5. The first attempts for the synthesis include coupling of a sulfonated perylene, functionalized with an aliphatic acid **3.29** and N-hydroxysuccinimide, in the presence of dicyclohexyl carbodiimide (DCC). DCC is one of the most commonly used coupling agents, and it is most often used to synthesize active ester-containing cross-linking and modifying reagents. This approach however does not result in formation of the desired compound, probably due to high water content of the sulfonated perylenes, which lead to fast hydrolysis of the target compound. To form the active ester is used N,N,N',N' – tetramethyl (succinimido) uranium tetrafluoroborate (TSTU) which can transfer the carboxyl groups into their corresponding hydroxysuccinimide esters very fast and efficiently even in the presence of water.[32] (Scheme 3.10)

**3.29**

**3.32**
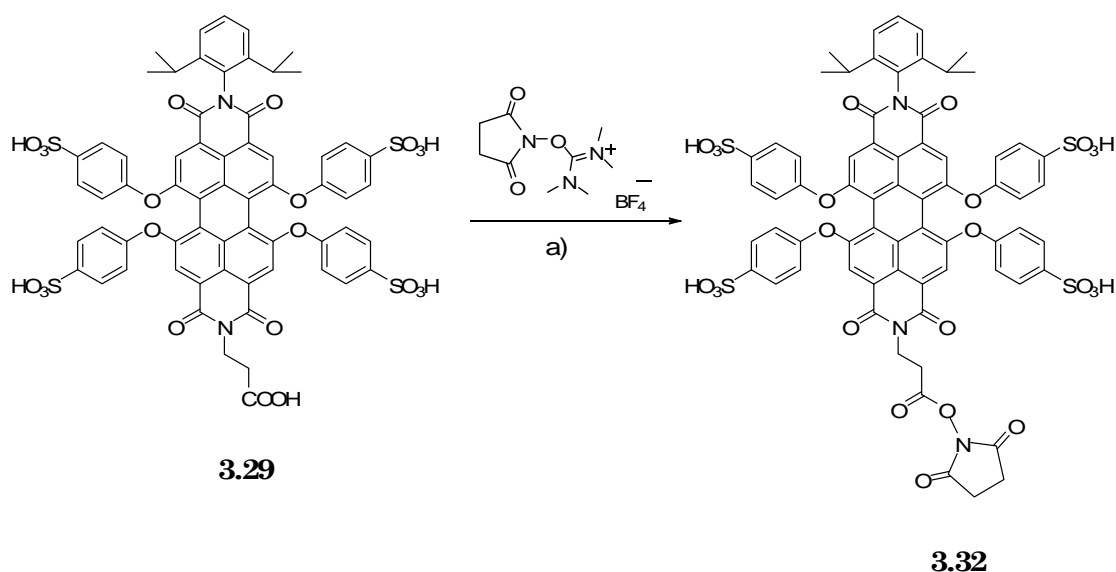
**Scheme 3.10. a) N,N,N',N' – tetramethyl(succinimido)uranium tetrafluoro borate, diisopropylethylamine, dimethyl formamide, dioxane, water, 1h, 85 %**

A mixture of dimethyl formamide (DMF), dioxane and water was used as solvent to ensure the solubility of all the reagents. **3.29** and TSTU was stirred in this mixture for 1 hour at room temperature. Following the removal of the solvent mixture under vacuum, a small amount of water was added and the product lyophilized.

Physical data (MALDI-TOF MS, ^{1}H NMR and ^{13}C NMR spectra) confirmed the proposed structure of the compound. The ^{13}C NMR spectrum was the most convenient method to verify the identity of the new functional group and the attachment of the N-hydroxysuccinimide. Comparing the ^{13}C NMR spectra of **3.32**, and a mixture containing N-hydroxysuccinimide and **3.29** measured at the same conditions, showed that the spectrum of **3.32** exhibits chemical shifts at $\delta = 169$ and $\delta = 166$ ppm as well as the signal at 25 ppm corresponding to the two identical carbon atoms from the NHS. Whereas the spectrum containing mixture of NHS and **3.29** display only signals belonging to the two compounds, without any change in the signals neighboring the NHS group (spectrum not shown here).

## *3.3.2. Introduction of thiol reactive groups*

## 3.3.2.1. Synthesis of maleimide functionalized perylene tetra carboxydiimide

Maleic acid imides (maleimides) are derivatives of the reaction of maleic anhydride and ammonia. This functional group is a popular constituent of many heterobifunctional cross-linking agents.[33-36] The double bond of maleimides may undergo an alkylation reaction with sulfhydryl groups to form stable thioether bonds. One of the carbons close to the maleimide double bond undergoes nucleophilic attack by the thiolate anion to generate the addition product. (Scheme 3.11) Maleimide reactions are specific for sulfhydryl groups in the pH range 6.5-7.5. At pH 7, the reaction of the maleimide with sulfhydryl proceeds at a rate 1000 times greater than its reaction with amines.[37, 38] At higher pH values some cross-reactivity with amino groups takes place and a selectivity is not detected.[39]
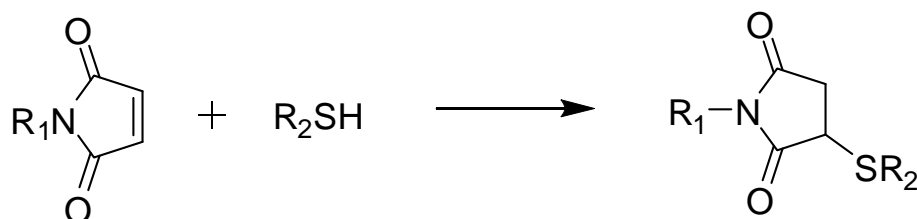


**Scheme 3.11 Formation of a thioether bond between sulfhydryl compound and maleimide derivative**

Herein is described the synthesis of maleimide functionalized water-soluble perylene dye. A special feature of the reactivity of maleimides is their susceptibility to additions across the double bond either by Michael additions or via Diels-Alder reactions. Maleimides linked to polyethylene glycol chains are often used as flexible linking molecules to attach proteins to surfaces. The double bond readily reacts with the thiol group found on cysteine to form a stable carbon-sulfur bond. Attaching the

other end of the polyethylene chain to a bead or solid support allows easy separation of the protein from other molecules in solution, provided these molecules do not also possess thiol groups.[13]

Maleimides are excellent reagents for thiol-selective modification, quantitation and analysis.[40, 41] In most proteins, the sites of reactions are at cysteine residues that are either intrinsically present, or result from reduction. As it is explained in Chapter 3, in this reaction, the thiol is added across the double bond of the maleimide to yield a thioether. Applications of fluorescent and chromophoric analogs of N-ethylmaleimide (NEM) strongly overlap those of iodoacetamides, although unlike iodoacetamides, maleimides do not react with histidines, tyrosine and methionines under physiological conditions. Reaction of maleimides with amines usually requires a higher pH than reaction of maleimides with thiols.

The synthesis of the maleimide functionalized chromophore is accomplished in one step using N-(γ-maleimidobutyryloxy)succinimide ester (GMBS) and the desired product is obtained in very high yield (Scheme 3.12). GMBS is a heterobifunctional crosslinking agent that contains an NHS ester on one end and a maleimide group on the other.[42, 43] GMBS is often used for multistep conjugation protocols wherein an amine-containing molecule is first modified via the NHS ester end (its most liable functional group) to create a stable amide bond. This derivative contains reactive maleimide groups able to couple with the available sulfhydryl groups of a second protein or molecule. In a similar way we take advantage of the NHS ester end to create an amide bond linkage between the amine functionalized perylene and the GMBS. GMBS is water-insoluble and therefore the conjugation is performed in dry DMF in the presence of triethylamine (TEA). Initially the reaction is done using excess of the GMBS; however an interesting discovery regarding the phase behavior of the final compound changed our synthetic strategy. As mentioned before the GMBS is soluble in DMSO, DMF and well soluble in dichloromethane, on the other hand the sulfonated perylene dyes are completely insoluble in organic solvents like chloroform, dichloromethane, hexane etc. Surprisingly we discovered that the maleimide functionalized water-soluble perylene is soluble not only in water, but in organic solvents as well. This ambipolar behavior of the perylene maleimide can be observed only if the maleimide group is not hydrolyzed. The hydrolysis of the active group leads to a change of the solubility and the hydrolyzed product is soluble only in water and polar solvents, similar to **3.26**.

**3.26**                                                      **3.33**
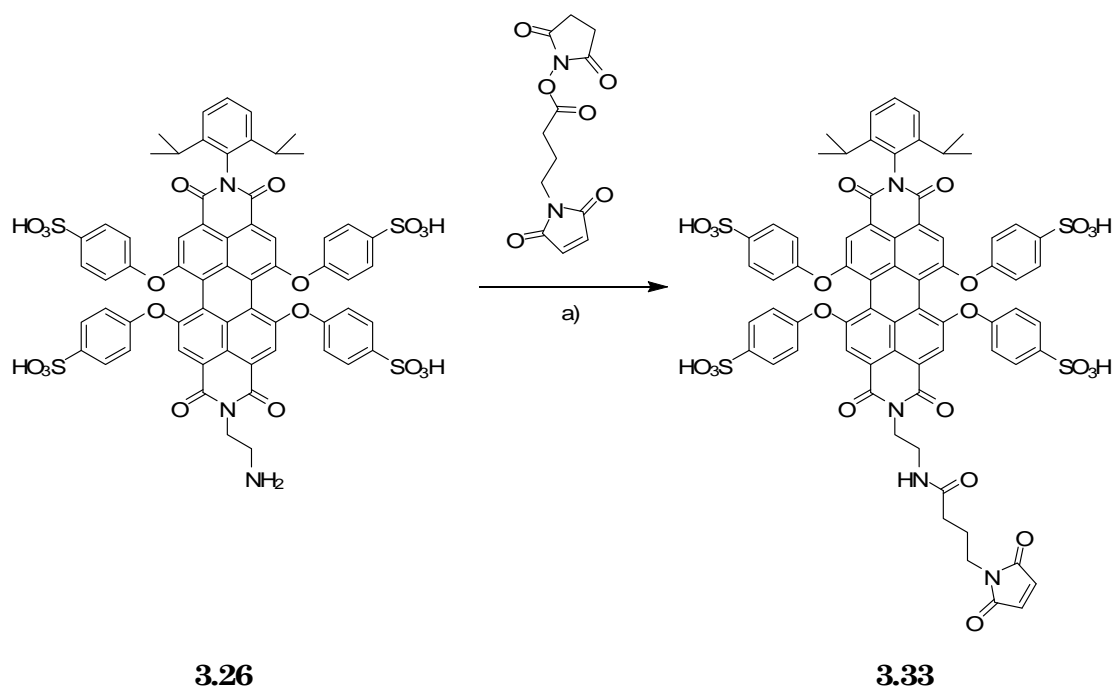
**Scheme 3.12. a) N-(γ-maleimidobutyryloxy)succinimide ester, triethylamine, dry dimethylformamide, 5h, 95 %**

The reaction was performed applying small excess of the perylene **3.26**; the reaction completion was followed by formation of intensively red colored product soluble in dichloromethane. After 5 hours the reaction was complete, the solvent evaporated under reduced pressure, then the solid residue dissolved in dichloromethane and additionally filtered to remove the starting material. Applying this simple procedure the target compound was obtained in high purity and high yield (95 %). The stability of the maleimide group can be monitored by checking the solubility of the product in dichloromethane. The target compound remained active for more than one year kept at – 20°C.

The ^{1}H NMR spectrum and the MALDI MS support the proposed structure of the compound. The agreement between the calculated (m/z calculated = 1447.45) and experimentally determined m/z ratios (m/z observed = 1448) confirms the purity of this monofunctional water soluble dye. Further support for the attachment of the maleimide group comes from ^{13}C NMR spectrum. The spectrum exhibits the signals from the GMBS as well as the signals from the perylene chromophore and the signals of the amide carbon atom is detected at δ = 173 ppm.

### *3.4. Preparation of new monofunctional water-soluble terrylene dyes*

### 3.4.1. Ionic water-soluble terrylenetetracarboxydiimides

Stable, highly fluorescent perylene-3,4:9,10-tetracarboxdiimides are widely used as dyes or pigments, depending on the substituent R at the N-imide position. They are suitable for demanding applications such as photovoltaic devices,[44] dye lasers,[45, 46] light-emitting diodes (LEDs)[47] and molecular switches.[48] By extending the core π-conjugated system, higher homologues of perylenediimide are synthesized in our group, that is, terrylenediimide (TDI) [49] and quaterrylenediimide (QDI).[8, 50] The absorption maxima of the deep blue terrylenediimides are shifted bathochromically in comparison to perylenediimide. Terrylenediimides exhibit brilliant color, high extinction coefficients, high fluorescence quantum yields of 90%,[49] and high thermal, chemical, and photochemical stabilities, which are generally required for practical use.
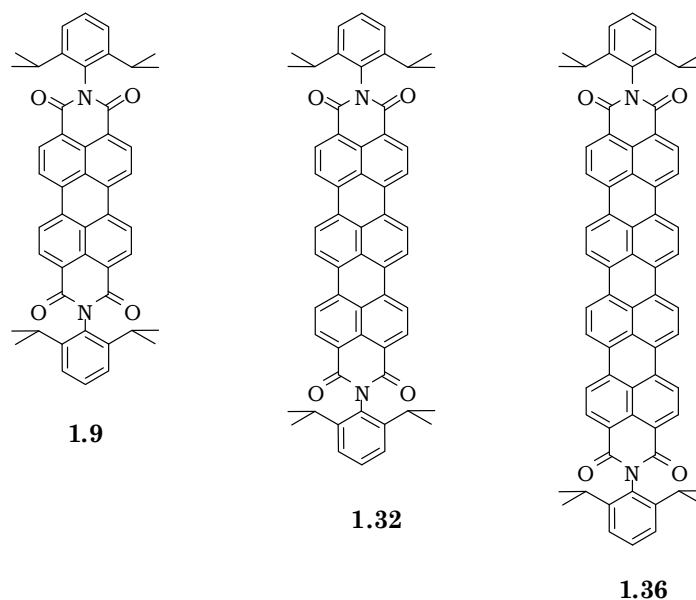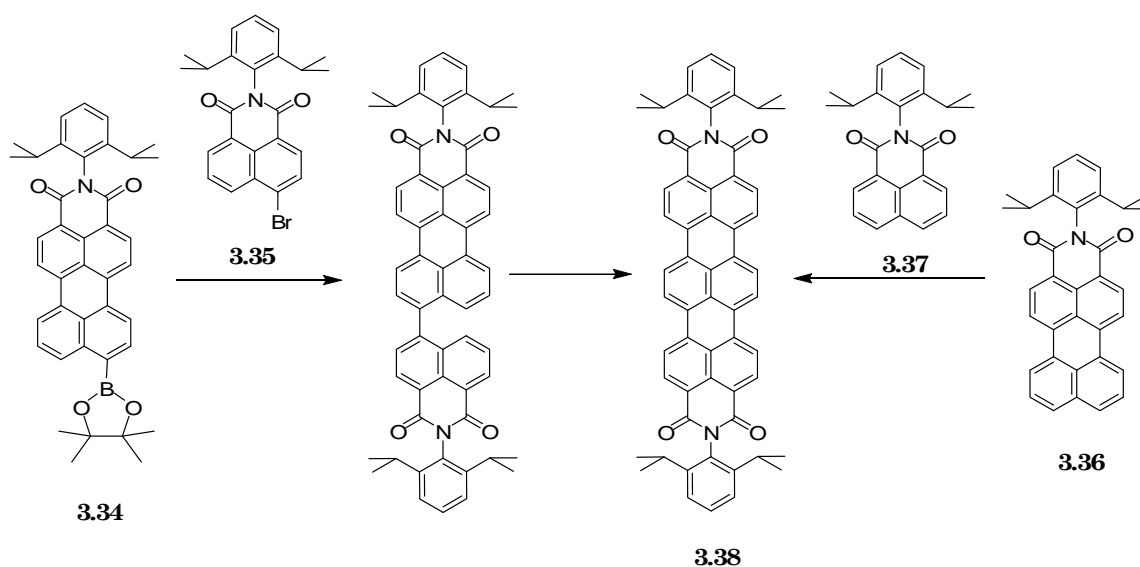


**Scheme 3.13. Perylenedicarboximide (1.9) and its higher homologues terrylenetetracarboxydiimide (1.32) and quaterrylenetetracarboxydiimide (1.36)**

The number of organic compounds showing intense fluorescence like terrylenediimide in the red and deep red spectral region of the electromagnetic spectrum is rather limited.[10][51] A great advantage of this spectral region is that inexpensive and effective excitation sources such as the HeNe laser (633 nm), krypton-ion laser (647, 676 nm) and common diode lasers are available, which is important for fluorescent labels.[52] In addition to the photophysical properties such as high extinction coefficients and photochemical stability, the negligible population of the triplet bottleneck, low photobleaching efficiency at room temperature, and weak electron–phonon coupling at low temperature qualify terrylenediimide as an ideal chromophore for single-molecule spectroscopy.[53]Furthermore, fluorescent dyes are often used in "live cell imaging" experiments where single proteins, virions, drugs or other single bio-particles are labeled in order to follow the pathway and/or the interactions of these particles inside the living cell.[54-57] Up to now, there are very few, if any, water-soluble fluorophores available in this spectral region with high photostability.

Water-soluble terrylenediimides have been achieved only in our group by introducing peptide chains or positive and negative charges in the bay region. The negatively charged terrylene dye is first prepared by Qu[10] and the positively charged one, as well as monofunctional water-soluble terrylene dyes are introduced by Nolde.[58, 59] Starting from the monofunctional water-soluble terrylenediimide introduced by Nolde, the synthesis of water-soluble terrylene chromophores bearing reactive groups for protein labeling will be demonstrated. The details regarding the preparation of the monofunctional terrylenediimide are given in the thesis of Fabian Nolde, for that reason the synthesis of the above mentioned dyes will be only outlined.

Monofunctional terrylenetetracarboxidiimide can be synthesized by two ways, both of them developed in our group. The first synthetic strategy involves Suzuki cross-coupling of boronic ester **3.34** and 4-bromonaphtahlenedicarboximide **3.35** perylenemonoimide with naphthalene monoimide, followed by a cyclodehydrogenation step under mild conditions. (Scheme 3.14) The second route is even simpler because it utilizes a one-pot procedure which is reminiscent of the direct coupling reaction of 1,8-naphthalenedicarboximides affording the corresponding perylenedicarboximide. Heating a mixture of perylenedicarboximide

**3.36**, naphthalenedicarboximide **3.37**, 1,5-diazabicyclo[4.3.0]non-5-ene (DBN) and tBuONa in diglyme delivers terrylenediimide **1.32**.



**Scheme 3.14. Alternative strategies for the preparation of terrylene tetracarboxydiimide**

The base-promoted one-pot reaction is also the simplest monofunctionalization method for terrylenediimides. The use of a perylenedicarboximide and a naphthalenedicarboximide with different substituents in the imide structures affords an asymmetric terrylenediimide in one-pot synthesis (Scheme 3.14).

The monocarboxyl-substituted terrylenediimide used here was prepared following the one-pot procedure. Monocarboxyfunctionalized terrylenediimide (**3.39**) was synthesized by using N-(5-carboxypentyl)-naphthalenedicarboximide (**3.40**) and perylenedicarboximide **3.36** under the same conditions (tBuONa/DBN, diglyme) used in the one-pot synthesis for the symmetrical terrylenediimide. The reaction mixture of the coupling reaction was poured into a small amount of water to obtain the sodium salt of monocarboxyl-substituted terrylenediimide **3.39**. A very convenient way of purifying the sodium salt is by washing away all byproducts and starting materials with chloroform. The sodium salt is insoluble in nonpolar solvents (e.g., chloroform, as used here). The dark blue precipitate is then redissolved in

methanol and acidified with hydrochloric acid to give the desired pure monocarboxyfunctionalized terrylenediimide **3.39** in 36% yield. (Scheme 3.15)
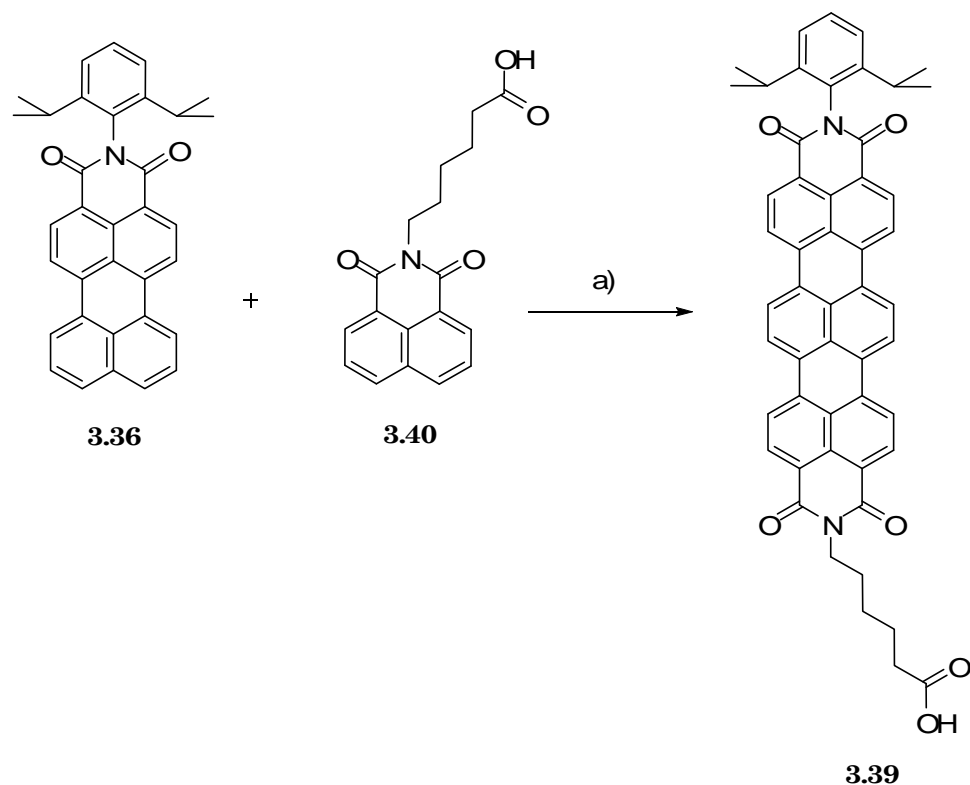


**Scheme 3.15. a) Sodium *tert*-butoxide/ 1,5-diazabicycl[4.3.0]nonene-5, diglyme, 2 h, 36 %**

The naked monocarboxyfunctionalized terrylenediimide was brominated by treating **3.39** with elementary bromine in chloroform (Scheme 3.16). A small amount of methanol was added to the reaction mixture, in order to increase the solubility of **3.39**. The addition of methanol also changed the carboxy group of **3.39** into the corresponding methyl ester **3.41**. The substitution under basic conditions of **3.41** with phenol produced **3.42** in high yield. The presence of the methyl ester made easier the purification of **3.41** and **3.42** using column chromatography, thus these precursors were obtained in high purity as confirmed by $^1$H and $^{13}$C-NMR spectra, FD MS and/or MALDI MS and elemental analysis.
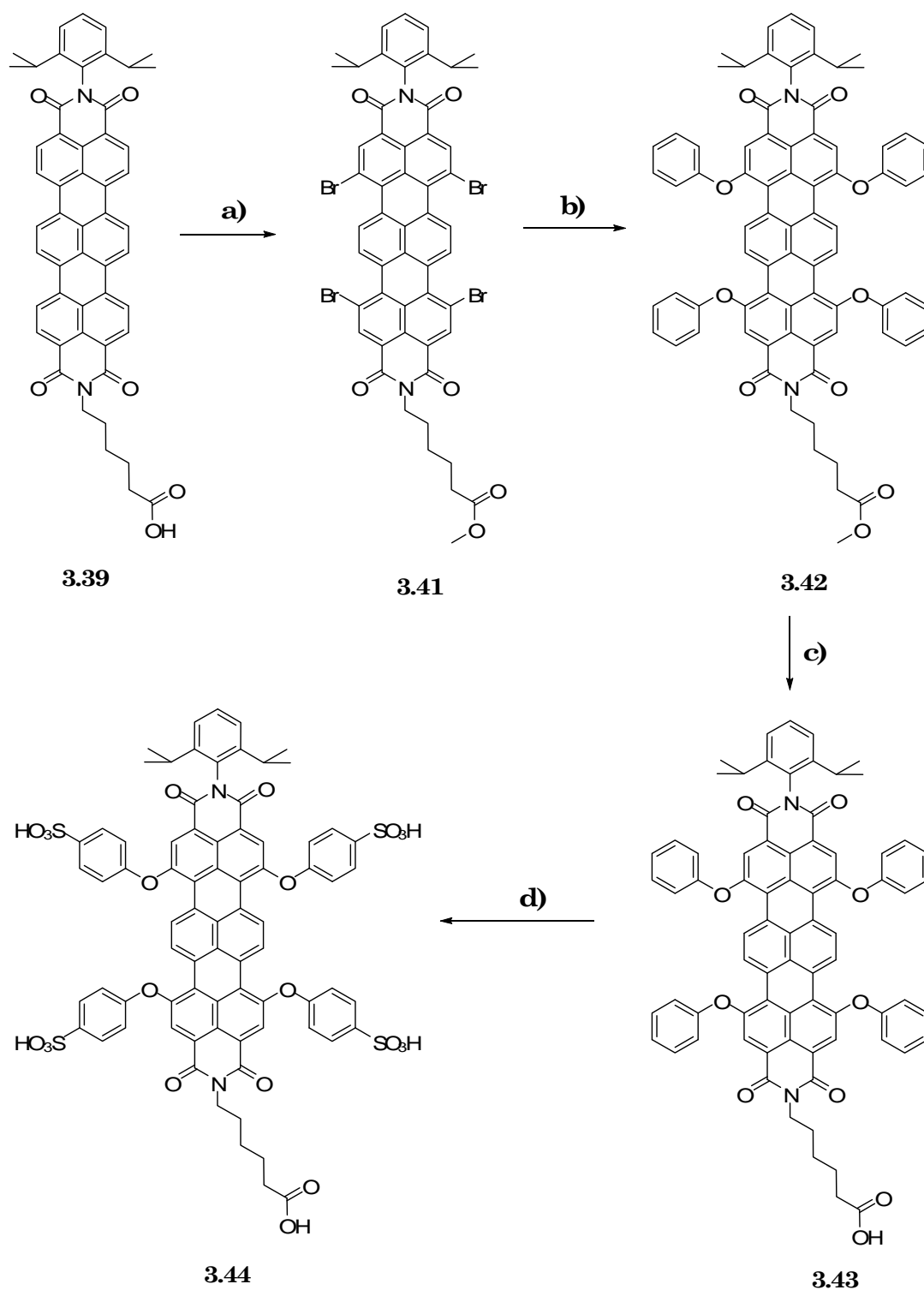
**Scheme 3.16: a) Br₂, chloroform, methanol, 48 h, 55°C, 61%; b) phenol, K₂CO₃, NMP, 15 h, 80°C, 73%; c) LiOH, H₂O, THF, 12h, 80°C, 90%; d) H₂SO₄, RT, 48 h, 95%**

The methyl ester group was removed by treating **3.42** with a water solution of LiOH in THF for 12 hours at 80°C to obtain the carboxyfunctionalized terrylenetetracarboxidiimide **3.43** (Scheme 3.16). Further, **3.43** was sulfonated with concentrated sulphuric acid at room temperature to afford **3.44**. The purification was accomplished by slowly adding water to the reaction mixture and the solution was dialyzed against water for 96 hours.

The water-soluble terrylenediimide, bearing carboxy group, **3.44** was used for the synthesis of N-hydroxysuccinimide-functionalized derivative applying the same procedure used for the preparation of perylene derivative (Scheme 3.17). **3.44** was reacted with TSTU in a mixture of dimethyl formamide (DMF), dioxane for 1 hour at room temperature. Following the removal of the solvent mixture under vacuum, small amount of water was added and the product lyophilized.
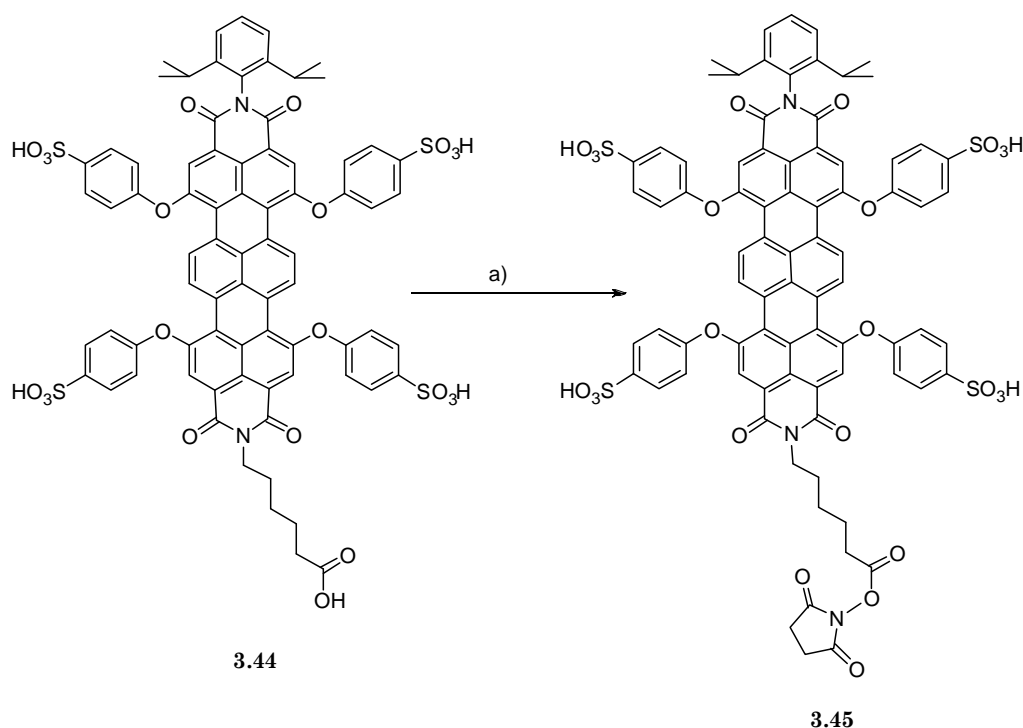


**Scheme 3.17: a) N,N,N',N' – tetramethyl (succinimido) uranium tetrafluoroborate, diisopropylethylamine, dimethyl formamide, dioxane, water, 1h, RT, 80%**

The $^1$H NMR and $^{13}$C NMR spectra and the MALDI MS support the proposed structure. $^1$HNMR spectrum of **3.45** exhibits clearly assignable signals and their intensity ratios of all peaks perfectly agree with the theoretically expected ones (Figure 3.6).
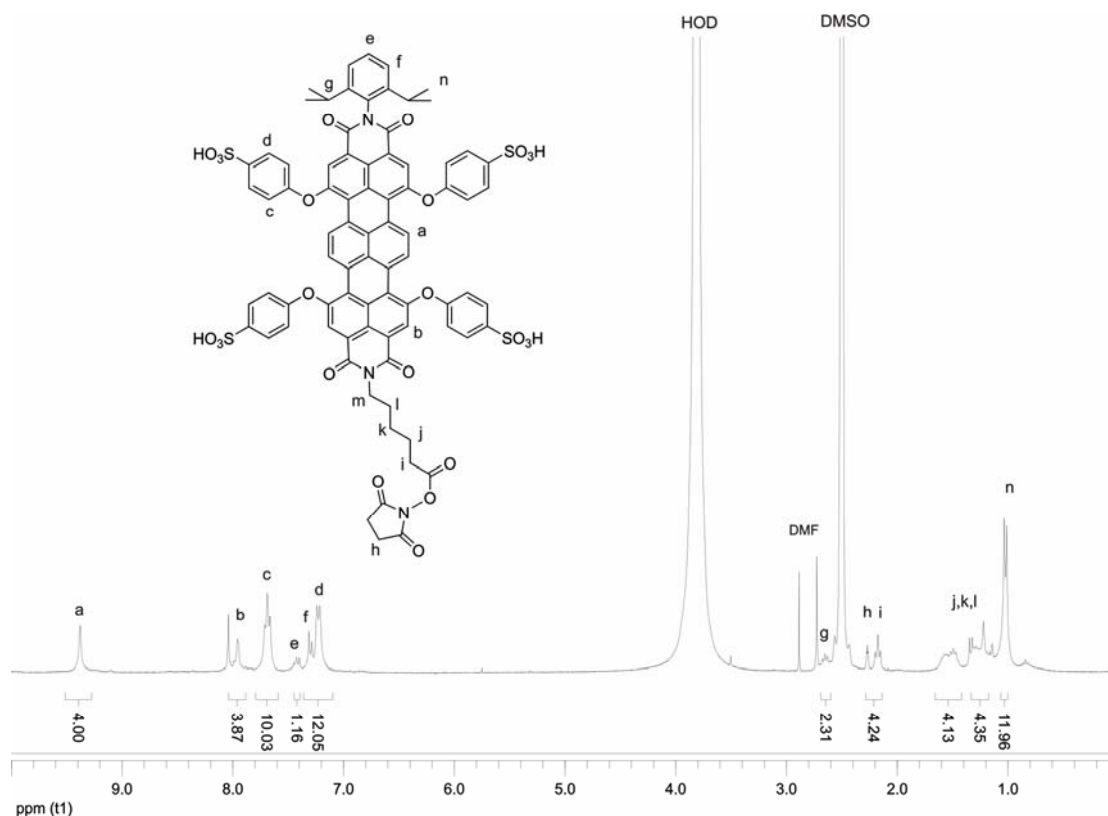


**Figure 3.6.** $^1$**H-NMR spectrum of 3.45 in dimethylsulfoxide-$d_6$ at room temperature (500 MHz).**

A different synthetic route was chosen for the synthesis of the maleimide functionalized terrylenediimide. **3.45** was treated with 1-(2-aminoehtyl)pyrrol-2,5-dion in DMF in the presence of TEA at room temperature for 5 hours (Scheme 3.18). The terrylene maleimide demonstrated the same ambipolar behavior as **3.33** and the desired product was extracted and purified using dichloromethane. The maleimide functionalized terrylenetetracarboxydiimide was obtained in 90% yield. The $^1$H-NMR and $^{13}$C NMR spectra and the MALDI MS supported the proposed structure.
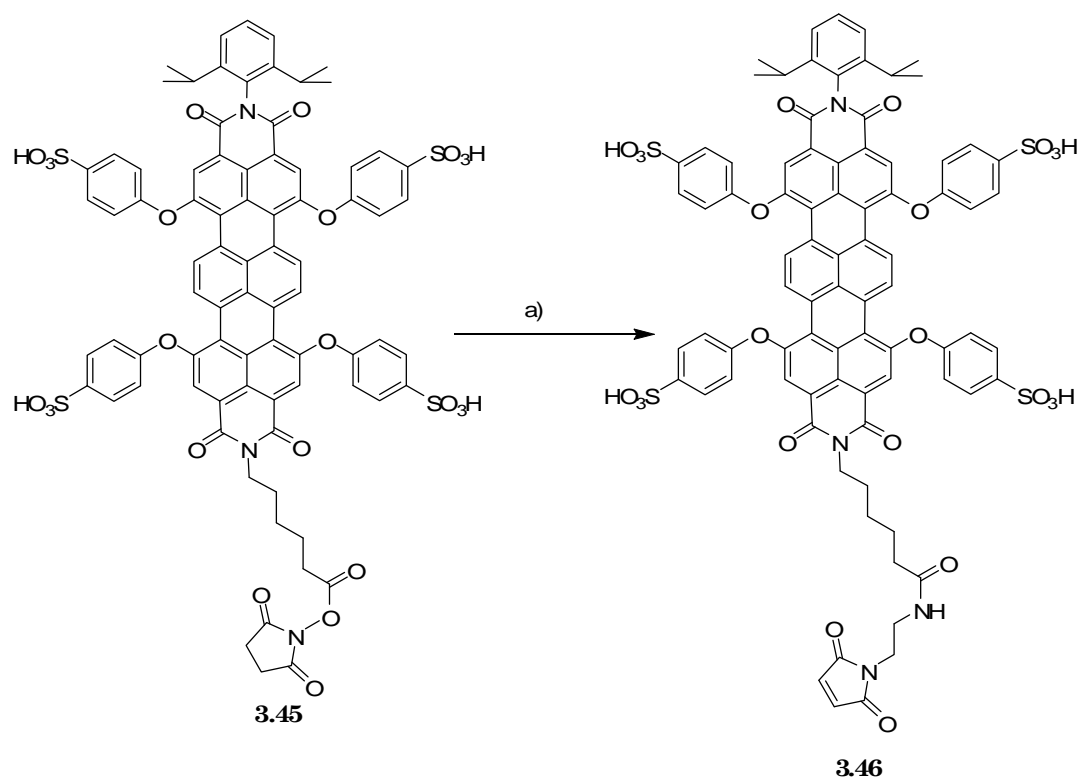
**Scheme 3.18: a) 1-(2-aminoehtyl)pyrrol-2,5-dione, DMF, TEA, 5 h, RT, 90%**

One exemplary mass spectrum of **3.46** with four sulfonyl substituents is depicted on Figure 3.7, showing only two single peaks corresponding to the molecular mass plus three sodium ions (sodium ions were added during the sample preparation for MALDI MS analysis, in order to increase the signal intensity) and molecular mass minus the maleimide group. The molecular weight of 1545 m/z indicates fragmentation of the molecule during the MALDI MS measurements. The agreement between the calculated (m/z calculated = 1665.59) and experimentally determined m/z ratios (m/z observed = 1665) confirms the purity of this monofunctional water-soluble dye.
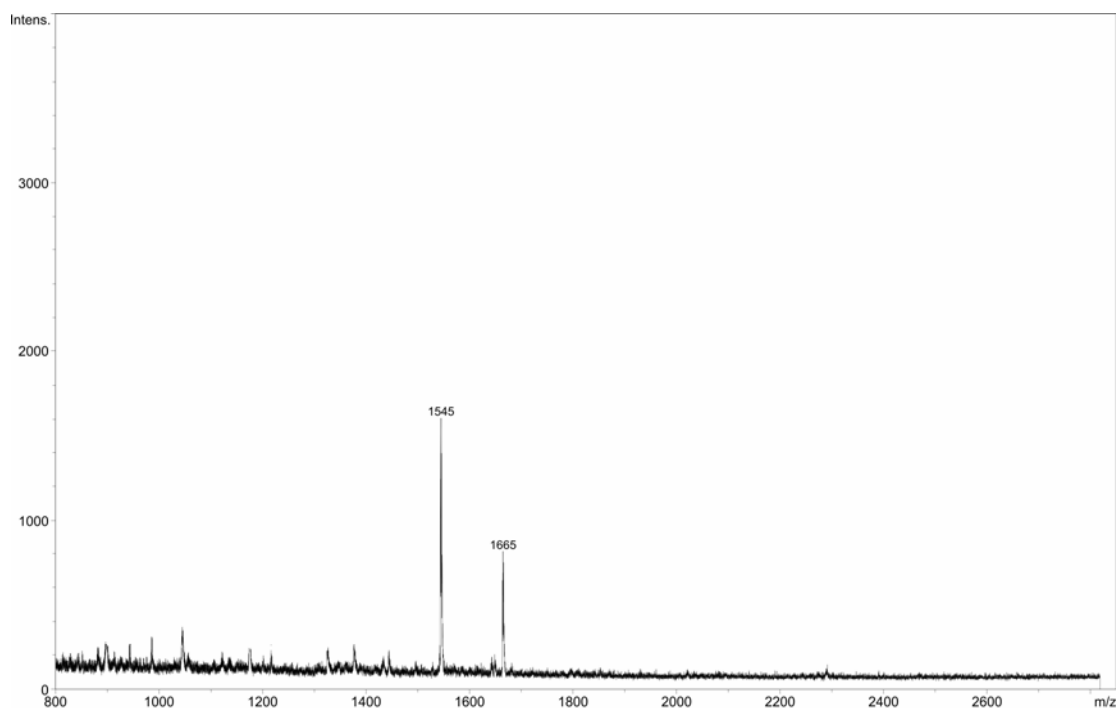
**Figure 3.7. MALDI-TOF mass spectrum of 3.45 (1665[M+3Na]+).**

## *3.5. Optical characterization of monofunctional perylene and terrylenediimides*

All the above described perylene and terrylene chromophores containing reactive groups have excellent water solubility. Thus, their optical properties are studied in aqueous medium (an overview is given in Table 3.1) and compared with water-soluble perylene and terrylene chromophore bearing no functional groups, in order to evaluate the influence of newly introduced chemical groups. The symmetrical perylenetetracarboxydiimide displays three absorption maxima at 571, 541 and 461 nm and one emission maximum at 620 nm in water. The absorbance spectra of **3.26** and **3.29** in water show high extinction coefficients and distinct vibronic fine structures of PDI. The same behavior is observed for the conjugate with NHS ester and maleimide, which indicates that the substitution in the imide structure does not influence significantly the absorbance spectrum of the chromophore. The fluorescence quantum yield of **3.29** is slightly higher than the one measured for **1.45** and remains unchanged for **3.32**. The amine functionalized

perylenetetracarboxydiimide **3.26** displays a fluorescence quantum yield faintly lower than **1.45**. This is due to the intramolecular charge transfer as explained in details in the previous section.

**Table 3.1. Absorption ($\lambda_{max, abs}$) and fluorescence ($\lambda_{max, flu}$) maxima as well as fluorescence quantum yields ($\Phi_f$)(a) in water**

| Compound | $\lambda_{max}$, abs [nm] (extinction coefficient [M-1cm-1]) | $\lambda_{max}$, flu [nm] | $\Phi_f$ [a] |
|---|---|---|---|
| **1.45** | 461 (10708), 541 (21026), 571 (27800) | 619 | 0.58 |
| **3.26** | 450 (10 850), 534 (21 825), 562 (22 243) | 620 | 0.39 |
| **3.29** | 450 (11 454), 534 (22 510), 564 (25 059) | 620 | 0.66 |
| **3.32** | 450 (9951), 534 (18 867), 566 (21 071) | 622 | 0.58 |
| **3.33** | 450 (8367), 534 (16 199), 566 (16 569) | 620 | 0.40 |
| **1.46** | 638 (23 899), 685 (17875) | - | - |
| **3.45**[b] | 426 (4569), 638 (24 468) | - | - |
| **3.46**[b] | 426 (2 782), 638 (16 633) | - | - |

[a] $\Phi_f$ was measured at room temperature using Cresyl Violet et in methanol ($\Phi_f$ =0.54) as a reference. [b] The water-soluble terrylene derivatives form nonfluorescent H aggregates in water under the conditions employed here. However, when highly diluted they are well suited for single-molecule studies.
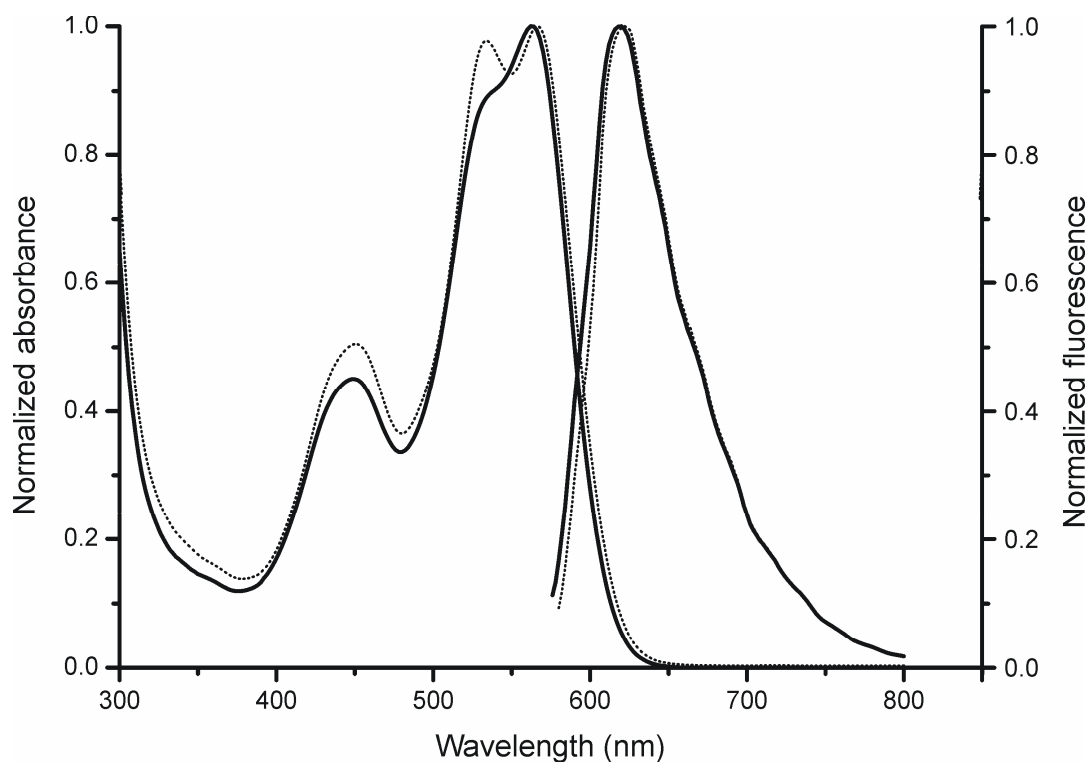
**Figure 3.8. Comparison between the absorbance and fluorescence spectra of 3.32 (solid line) and 3.33 (dotted line)**
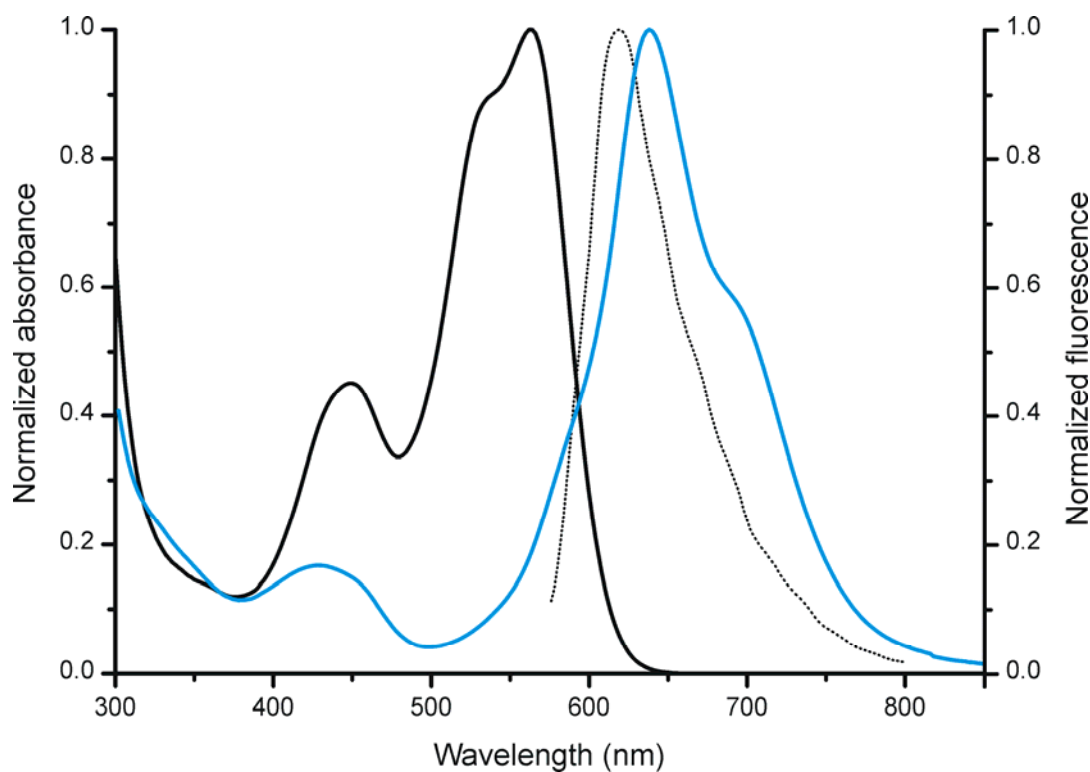


**Figure 3.9. Absorbance spectra of 3.32 (solid line), 3.46 (blue line) and fluorescence spectrum of 3.32 (dotted line)**

On Figure 3.8 are compared the absorbance and fluorescence spectra of **3.32** and **3.33**. The absorbance spectrum of **3.33** shows slight increase of the absorbance intensity at 534 nm. Fluorescence excitation measurement in fact displayed that the fluorescence excitation maxima for **3.33** is situated at 534 nm, and not at 566 nm as expected. The absorbance spectrum of **3.46** is depicted in Figure 3.9. The terrylenetetracarboxydiimide show absorbance maxima bathochromically shifted with 75 nm in comparison with the perylenetetracarboxydiimide.

The water-soluble monofunctionalized PDIs and TDIs, represent very promising couple for FRET experiments. The PDIs – like **3.32** have high extinction coefficients, and large stocks shifts, moreover the fluorescence of **3.32** overlaps with the absorbance maxima of **3.46**, for example (as shown on Figure 3.9). These two chromophores – **3.32** and **3.46**, have two different functional groups – the possible donor possesses NHS ester group, which allows attachment of several dye molecules on the surface of a protein, due to the frequent occurrence of lysine residues. The acceptor in this couple – **3.46** has a maleimide function, which can be used for site-specific introduction of the dye on proteins having one cysteine residue in their structure.

## *3.6 References*

[1] H.-A. Klok, J. R. Hernandez, S. Becker, K. Müllen, *J. Polym. Sci., Part A: Polym. Chem.* **2001**, *39*, 1572, *Star-shaped fluorescent polypeptides*.

[2] T. Weil, M. A. Abdalla, C. Jatzke, J. Hengstler, K. Müllen, *Biomacromolecules* **2005**, *6*, 68, *Water-Soluble Rylene Dyes as High-Performance Colorants for the Staining of Cells*.

[3] T. Weil, Johannes Gutenberg-University (Mainz), **2002**.

[4] H. Langhals Water-soluble perylenetetracarboxylic acid bisimide fluorescent dyes. 1988.

[5] H. Langhals, W. Jona, F. Einsiedl, S. Wohnlich, *Adv. Mater. (Weinheim, Ger.)* **1998**, *10*, 1022, *Self-dispersion. Spontaneous formation of colloidal dyes in water*.

[6] H. Quante, P. Schlichting, U. Rohr, Y. Geerts, K. Müllen, *Macromol. Chem. Phys.* **1996**, *197*, 4029, *Novel perylene-containing polymers*.

[7] A. Herrmann, T. Weil, V. Sinigersky, U.-M. Wiesler, T. Vosch, J. Hofkens, F. C. De Schryver, K. Müllen, *Chem.--Eur. J.* **2001**, *7*, 4844, *Polyphenylene dendrimers with perylene diimide as a luminescent core*.

[8] H. Quante, Johannes Gutenberg University (Mainz), **1995**.

[9] C. Kohl, Johannes-Gutenberg University (Mainz), **2003**.

[10] J. Qu, Johannes Gutenberg University (Mainz), **2004**.

[11] C. Kohl, T. Weil, J. Qu, K. Müllen, *Chem.--Eur. J.* **2004**, *10*, 5297, *Towards highly fluorescent and water-soluble perylene dyes*.

[12] J. Qu, C. Kohl, M. Pottek, K. Müllen, *Angew. Chem. Int. Ed.* **2004**, *43*, 1528, *Ionic perylenetetracarboxdiimides: highly fluorescent and water-soluble dyes for biolabeling*.

[13] G. T. Hermanson, G. T. Hermanson, *Bioconjugate techniques* **1996**, xxvii+785p, *Bioconjugate techniques*.

[14] A. Rifai, S. S. Wong, *J. Immunol. Methods* **1986**, *94*, 25, *Preparation of Phosphorylcholine-Conjugated Antigens*.

[15] D. Podhradsky, L. Drobnica, P. Kristian, *Experientia* **1979**, *35*, 154, *Reactions of Cysteine, Its Derivatives, Glutathione, Coenzyme-a, and Dihydrolipoic Acid with Isothiocyanates*.

[16] A. Jobbagy, K. Kiraly, *Biochim. Biophys. Acta* **1966**, *124*, 166, *Chemical Characterization of Fluorescein Isothiocyanate-Protein Conjugates*.

[17] A. Jobbagy, *Kiserletes Orvostudomany* **1972**, *24*, 442, *Labeling of serum proteins with fluorescein isothiocyanate*.

[18] E. Majima, M. Ishida, S. Miki, Y. Shinohara, H. Terada, *J Biol Chem FIELD Full Journal Title:The Journal of biological chemistry* **2001**, *276*, 9792, *Specific labeling of the bovine heart mitochondrial phosphate carrier with fluorescein 5-isothiocyanate: roles of Lys185 and putative adenine nucleotide recognition site in phosphate transport*.

[19] H. G. Patzwaldt, I. Markuse, *Kommentare zum Arzneibuch der Deutschen Demokratischen Republik* **1978**, *4*, 68, *Test serums labeled with fluorescein isothiocyanate*.

[20] H. Ow, D. R. Larson, M. Srivastava, B. A. Baird, W. W. Webb, U. Wiesner, *Nano Lett.* **2005**, *5*, 113, *Bright and stable core-shell fluorescent silica nanoparticles*.

[21] P. D. Bragg, C. Hou, *Arch. Biochem. Biophys.* **1975**, *167*, 311, *Subunit Composition, Function, and Spatial Arrangement in Ca2+-Activated and Mg2+-Activated Adenosine Triphosphatases of Escherichia-Coli and Salmonella-Typhimurium*.

[22] A. J. Lomant, G. Fairbanks, *J. Mol. Biol.* **1976**, *104*, 243, *Chemical Probes of Extended Biological Structures - Synthesis and Properties of Cleavable Protein Cross-Linking Reagent [Dithiobis(Succinimidyl-S-35 Propionate)*.

[23] A. R. Katritzky, K. Suzuki, S. K. Singh, *ARKIVOC (Gainesville, FL, United States)* **2004**, 12, *N-acylation in combinatorial chemistry*.

[24] Cuatreca.P, I. Parikh, *Biochemistry* **1972**, *11*, 2291, *Adsorbents for Affinity Chromatography - Use of N-Hydroxysuccinimide Esters of Agarose*.

[25] A. Kambegawa, *Nippon Rinsho FIELD Full Journal Title:Nippon rinsho. Japanese journal of clinical medicine* **1995**, *53*, 2160, *Enzyme labeling methods and it's specificities*.

[26] E. Terpetschnig, H. Szmacinski, A. Ozinskas, J. R. Lakowicz, *Anal Biochem FIELD Full Journal Title:Analytical biochemistry* **1994**, *217*, 197, *Synthesis of squaraine-N-hydroxysuccinimide esters and their biological application as long-wavelength fluorescent labels*.

[27] F. Fujisaki, M. Oishi, K. Sumoto, *Chem. Pharm. Bull.* **2007**, *55*, 124, *A conventional new procedure for N-acylation of unprotected amino acids*.

[28] N. Abello, H. A. M. Kerstjens, D. S. Postma, R. Bischoff, *J. Proteome Res.* **2007**, *6*, 4770, *Selective Acylation of Primary Amines in Peptides and Proteins*.

[29] C. K.-F. Chiu, D. A. Griffith Preparation of an imidazopiperazinedione drug intermediate. 2000.

[30] D. L. Duenweber, I. H. Jensen, L. B. Hansen Method for producing acylated peptides. 2004.

[31] B. Oswald, L. Patsenker, J. Duschl, H. Szmacinski, O. S. Wolfbeis, E. Terpetschnig, *Bioconjugate Chem.* **1999**, *10*, 925, *Synthesis, Spectral Properties, and Detection Limits of Reactive Squaraine Dyes, a New Class of Diode Laser Compatible Fluorescent Protein Labels*.

[32] R. Chinchilla, D. J. Dodsworth, C. Najera, J. M. Soriano, M. Yus, *ARKIVOC (Gainesville, FL, United States)* **2003**, 41, *Uronium salts from polymeric N-hydroxysuccinimide (P-HOSu) as new solid-supported peptide coupling reagents*.

[33] H. Ohta, *Seitai no Kagaku* **1989**, *40*, 313, *m-Maleimidebenzoyl-N-hydroxysuccinimide ester*.

[34] S. Fujita, P. J. Redei, T. Toru Preparation of maleamidic acids and maleimides. 1999.

[35] R. M. de Figueiredo, P. Oczipka, R. Froehlich, M. Christmann, *Synthesis* **2008**, 1316, *Synthesis of 4-maleimidobutyric acid and related maleimides*.

[36] S. N. Sisson, *Bact. Immunoglobulin-Binding Proteins* **1990**, *2*, 197, *Use of fluorescent-conjugated bacterial immunoglobulin-binding proteins*.

[37] J. R. Heitz, C. D. Anderson, B. M. Anderson, *Arch. Biochem. Biophys.* **1968**, *127*, 627, *Inactivation of Yeast Alcohol Dehydrogenase by N-Alkylmaleimides*.

[38] G. Gorin, P. A. Matic, G. Doughty, *Arch. Biochem. Biophys.* **1966**, *115*, 593, *Kinetics of Reaction of N-Ethylmaleimide with Cysteine and Some Congeners*.

[39] M. D. Partis, D. G. Griffiths, G. C. Roberts, R. B. Beechey, *J. Protein Chem.* **1983**, *2*, 263, *Cross-Linking of Protein by Omega-Maleimido Alkanoyl N-Hydroxysuccinimido Esters*.

[40] P. Graceffa, R. Dominguez, *J. Biol. Chem.* **2003**, *278*, 34172, *Crystal structure of monomeric actin in the ATP state - Structural basis of nucleotide-dependent actin dynamics*.

[41] Y. H. Tong, G. S. Brandt, M. Li, G. Shapovalov, E. Slimko, A. Karschin, D. A. Dougherty, H. A. Lester, *Journal of General Physiology* **2001**, *117*, 103, *Tyrosine decaging leads to substantial membrane trafficking during modulation of an inward rectifier potassium channel*.

[42] K. Fujiwara, N. Matsumoto, S. Yagisawa, H. Tanimori, T. Kitagawa, M. Hirota, K. Hiratani, K. Fukushima, A. Tomonaga, K. Hara, K. Yamamoto, *J. Immunol. Methods* **1988**, *112*, 77, *Sandwich Enzyme-Immunoassay of Tumor-Associated Antigen Sialosylated Lewis-X Using Beta-D-Galactosidase Coupled to a Monoclonal-Antibody of Igm Isotype*.

[43] K. Fujiwara, T. Saita, T. Kitagawa, *J. Immunol. Methods* **1988**, *110*, 47, *The Use of N-[Beta-(4-Diazophenyl)Ethyl]Maleimide as a Coupling Agent in the Preparation of Enzyme-Antibody Conjugates*.

[44] L. Schmidt-Mende, A. Fechtenkotter, K. Müllen, E. Moons, R. H. Friend, J. D. MacKenzie, *Science (Washington, DC, U. S.)* **2001**, *293*, 1119, *Self-organized discotic liquid crystals for high-efficiency organic photovoltaics*.

[45] M. Sadrai, L. Hadel, R. R. Sauers, S. Husain, K. Krogh-Jespersen, J. D. Westbrook, G. R. Bird, *J. Phys. Chem.* **1992**, *96*, 7988, *Lasing action in a family of perylene derivatives: singlet absorption and emission spectra, triplet absorption and oxygen quenching constants, and molecular mechanics and semiempirical molecular orbital calculations*.

[46] R. Reisfeld, G. Seybold, *Chimia* **1990**, *44*, 295, *Solid-state tunable lasers in the visible, based on luminescent photoresistant heterocyclic colorants*.

[47] J. Kalinowski, P. Di Marco, V. Fattori, L. Giulietti, M. Cocchi, *J. Appl. Phys.* **1998**, *83*, 4242, *Voltage-induced evolution of emission spectra in organic light-emitting diodes*.

[48] M. P. O'Neil, M. P. Niemczyk, W. A. Svec, D. Gosztola, G. L. Gaines, III, M. R. Wasielewski, *Science (Washington, DC, U. S.)* **1992**, *257*, 63, *Picosecond optical switching based on biphotonic excitation of an electron donor-acceptor-donor molecule.*

[49] F. O. Holtrup, G. R. J. Müller, H. Quante, S. De Feyter, F. C. De Schryver, K. Müllen, *Chem.--Eur. J.* **1997**, *3*, 219, *Terrylenimides: new NIR fluorescent dyes.*

[50] H. Quante, K. Müllen, *Angew. Chem., Int. Ed. Engl.* **1995**, *34*, 1323, *Quaterrylenebis(dicarboximides).*

[51] S. Daehne, U. Resch-Genger, O. S. Wolfbeis, Editors, *Near-Infrared Dyes for High Technology Applications. (Proceedings of the NATO Advanced Research Workshop, held 24-27 September 1997, in Trest, Czech Republic.) [In: NATO ASI Ser., Ser. 3, 1998; 52]*, **1998**.

[52] J. Arden-Jacob, J. Frantzeskos, N. U. Kemnitzer, A. Zilles, K. H. Drexhage, *Spectrochim Acta A Mol Biomol Spectrosc FIELD Full Journal Title:Spectrochimica acta. Part A, Molecular and biomolecular spectroscopy* **2001**, *57*, 2271, *New fluorescent markers for the red region.*

[53] S. Mais, J. Tittel, T. Basche, C. Braeuchle, W. Goehde, H. Fuchs, G. Müller, K. Müllen, *J. Phys. Chem. A* **1997**, *101*, 8435, *Terrylenediimide: A Novel Fluorophore for Single-Molecule Spectroscopy and Microscopy from 1.4 K to Room Temperature.*

[54] J. Lippincott-Schwartz, E. Snapp, A. Kenworthy, *Nat. Rev. Mol. Cell Biol.* **2001**, *2*, 444, *Studying protein dynamics in living cells.*

[55] G. Seisenberger, M. U. Ried, T. Endress, H. Buning, M. Hallek, C. Bräuchle, *Science* **2001**, *294*, 1929, *Real-time single-molecule imaging of the infection pathway of an adeno-associated virus.*

[56] C. Brauchle, G. Seisenberger, T. Endress, M. U. Ried, H. Buning, M. Hallek, *ChemPhysChem* **2002**, *3*, 299, *Single virus tracing: visualization of the infection pathway of a virus into a living cell.*

[57] G. J. Schutz, M. Sonnleitner, P. Hinterdorfer, H. Schindler, *Mol. Membr. Biol.* **2000**, *17*, 17, *Single molecule microscopy of biomembranes (Review).*

[58] C. Jung, B. K. Müller, D. C. Lamb, F. Nolde, K. Müllen, C. Bräuchle, *J. Am. Chem. Soc.* **2006**, *128*, 5283, *A New Photostable Terrylene Diimide Dye for Applications in Single Molecule Studies and Membrane Labeling.*

[59] F. Nolde, J. Qu, C. Kohl, N. G. Pschirer, E. Reuther, K. Müllen, *Chem.--Eur. J.* **2005**, *11*, 3959, *Synthesis and modification of terrylenediimides as high-performance fluorescent dyes*.

# 4. Water-soluble monofunctional perylene and terrylene dyes: powerful labels for single enzyme tracking

Fluorescence microscopy is the most widely used tool for visualizing subcellular structures and for localizing proteins within cells.[1] Single-molecule spectroscopy (SMS) has gone beyond that and has revealed information about complex biological molecules and processes which are difficult to obtain from ensemble measurements.[2] Single proteins, virions, drugs or other single bio-particles were labeled and their pathway and interactions were followed inside living cells.[3, 4] One critical issue of observing biological entities on the single molecule level is the label. It should be water-soluble, highly fluorescent in aqueous environment, and have a reactive group to be attached to the bio-molecule, e.g. protein or enzyme. Moreover the attachment should not affect the bio-molecule's structure or function, or in the case of an enzyme, its activity. Finally, an exceptional photostability of the label is needed to visualize or track for a sufficient period of time.

In this chapter N-hydroxysuccinimide ester functionalized perylene and terrylene dyes and the corresponding conjugates with proteins are employed for tracking single phospholipases on their native substrate by real time wide-field fluorescence microscopy. The aim of the experiments reported here is to study the capability of the water-soluble perylene and terrylenetetracarboxydiimides as fluorescent labels and to compare their photophysical properties with some of the existing chromophores. A new affinity based purification technique is developed and successfully applied for separation of the fluorescent conjugate of rylene dye and phospholipase PLA1. The labeled enzyme was employed for tracking single phospholipase enzyme molecule on its native substrate using wide-field microscopy. The single molecule wide-field microscopy and fluorescence correlation spectroscopy experiments were performed in the group of Prof. Johan Hofkens, Katholieke Universiteit, Leuven. The labeling experiments were done in cooperation with Dr. Gueorgui Mihov, Max Planck Institute for Polymer Research.

## *4.1. Experimental methods*

## 4.1.1. Wide-field fluorescence microscopy

The wide-field reflected light fluorescence microscope has been a fundamental tool for the examination of fluorescently labeled cells and tissues since the late 1940s. Furthermore, advances in synthetic fluorophore design coupled to the vast array of commercially available primary and secondary antibodies have provided the biologist with a powerful arsenal, by in which he can to probe the small structural details of living organisms with this technique. The simplest method to observe single-molecule fluorescence is to use wide-field microscopy. A laser or arc lamp is used to illuminate an area several microns in diameter, as in a traditional microscope. Proper filtering is used to eliminate excitation light and to pass the single molecule fluorescence to a two-dimensional array detector, usually a charged-couple device (CCD) as described above, although the best single molecule emitters can even be observed with unaided eye. Performing SMS in this fashion has two major advantages: many individual chromophores can be observed simultaneously, and the position of chromophores can be monitored at near video rates, allowing researchers to observe translation of single molecules in real time.

In the following chapter an inverted wide-field epi-fluorescence microscope was used for imaging of individual single enzymes labeled with the perylene(dicarboximide). It was equipped with a 60x TIRF (total internal reflection fluorescence) objective and a cooled Electron Multiplying-CCD (cascade 512B, Princeton Instruments Inc.). A typical experimental setup of epi-fluourescent microscope is depicted on Figure 4.1.
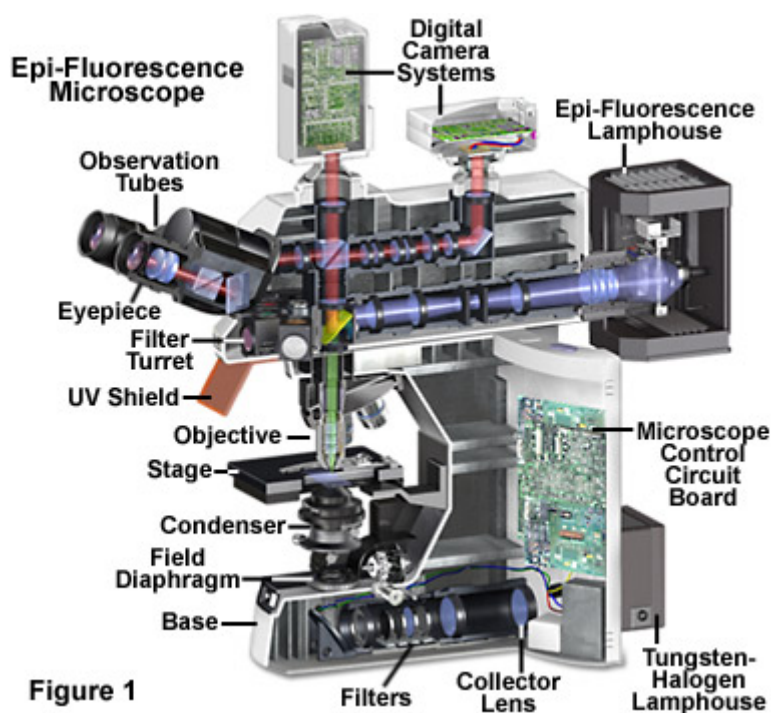
**Figure 4.1. Typical experimental setup of epi-fluorescent microscope (source Olympus)**

As presented in Figure 4.1, the reflected light vertical illuminator comprises an arc-discharge lamphouse at the rear end (usually a mercury or xenon burner). Excitation light travels along the illuminator perpendicular to the optical axis of the microscope, passes through collector lenses and a variable, centerable aperture diaphragm, and then through a variable, centerable field diaphragm ( Figure 4.1). The light then impinges upon the excitation filter where selection of the desired band and blockage of unwanted wavelength occurs. The selected wavelengths, after passing through the excitation filter, reach the dichromatic beamsplitting mirror, which is a specialized interference filter that efficiently reflects shorter wavelength light and efficiently passes longer wavelength light. The dichromatic beamsplitter is tilted at a 45-degree angle with respect to the incoming excitation light and reflects this illumination at a 90-degree angle directly through the objective optical system and onto the specimen. Fluorescence emission produced by the illuminated specimen is gathered by the objective, now serving in its usual image-forming function. Because the emitted light consists of longer wavelengths than the

excitation illumination, it is able to pass through the dichromatic mirror and upward to the observation tubes or electronic detector.

In wide-field microscopy a CCD camera is used to record movies of the events taking place in the several hundred square micrometers large excitation area. The resolvable spots are again diffraction limited, but now represent a larger excitation volume due to a decreased resolution, mainly in the z-direction, reducing the SNR. The time resolution for large domain imaging is limited by the frame transfer rate of the used CCD camera (millisecond or sub-millisecond range) and is lower than for the aforementioned point detectors. Working with total internal reflection illumination implies excitation by an evanescent field. The reduced excitation volume results in an increased SNR. Wide-field microscopes are most commonly used to study diffusion and other dynamic processes taking place over an extended area. An additional advantage is that many molecules can be studied in parallel; hence statistical relevant numbers of molecules can be sampled much faster then in a confocal approach.

## *4.2. Labeling of phospholipase A1 with perylene and terrylene(dicarboximide)s and purification of the corresponding conjugates*

### *4.2.1. Phospholipase A1*

Phospholipases are ubiquitous and diverse enzymes that induce changes in membrane composition, activate the inflammatory cascade and alter cell signaling pathways.[5] These enzymes contain specific structural features that allow them to interact effectively with the target phospholipid interface. The rate of substrate hydrolysis depends on the rate of formation of an interfacial enzyme/substrate complex, on the catalytic turnover rate, and on the rates of adsorption, desorption and diffusion of the enzyme on the substrate, greatly complicating a full kinetic characterization.[6] Despite numerous studies performed in this area, the relation between the hydrolysis reaction and the interfacial mobility of phospholipases is still not fully understood. Here we demonstrate how phospholipase A1 interacts with and catalyses the hydrolysis of, 1-palmitoyl-2-oleoyl-sn-glycero-3-phosphocholine layers at the single molecule level. Our approach allows us to visualize and distinguish events such as free diffusion, docking and catalytic activity of an interfacial enzyme on its natural substrate. Direct relationship between the interaction of a single phospholipase enzyme molecule with its native substrate layer and the subsequent hydrolysis was established. Our results shed new light on the mode of action of phospholipases, while these methods represent a new and promising approach to the study of interfacial enzyme kinetics.

The enzyme used in this study is a mutant from Thermomyces lanuginosus lipase (TLL) developed by Novozymes (for details see experimental section). It cleaves the ester bond of the phospholipid at the sn-1 position being therefore designated phospholipase A1 (PLA1) (Figure 4.2).
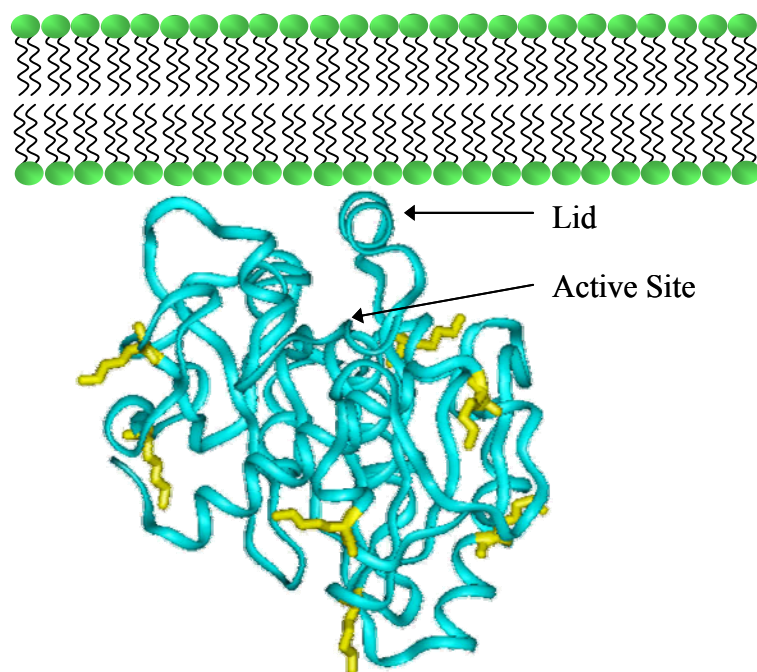
**Figure 4.2. PLA1 model backbone in cyan and the 7 lysines in yellow. The active site and the lid are indicated by black arrows. After phospholipid surface contact occurs (top), the enzyme lid opens and the enzyme penetrates slightly into the phospholipid layer.**

N-Hydroxysuccinimide perylene(dicarboximide) derivative **3.32** was used for the labeling of PLA1, targeting the seven solvent exposed lysines of the enzyme (Scheme 4.1). Therefore, **3.32** was applied in 20-fold excess to the enzyme.



**3.32**                    **3.45**
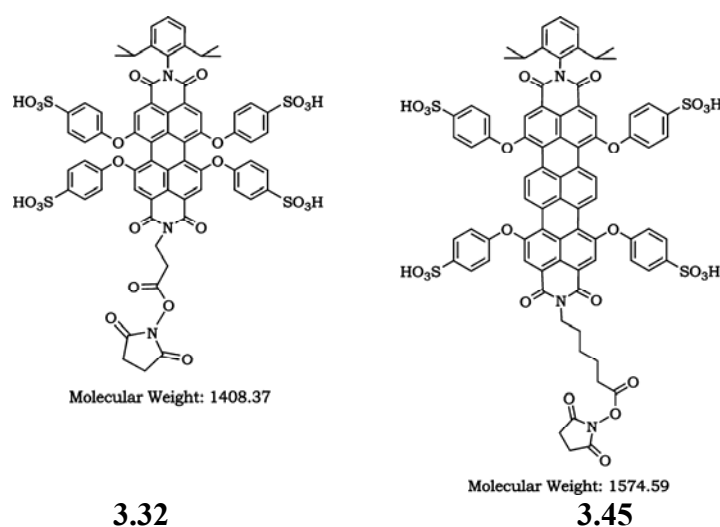
**Scheme 4.1. Chemical structures of the N-hydroxysuccinimide functionalized perylene and terrylene (dicarboximide)s**

A solution of phospholipase-A1 in 10 mM succinic acid, 0,4M NH$_4$SO$_4$, pH 6 was reacted at 4 °C for one hour with **3.32,** freshly dissolved in 0.01 M NaHCO$_3$. The dye showed excellent reactivity and after incubation for one hour at 4°C the labeling was completed. For the purification of the labeled enzyme, new affinity based purification technique was developed.[7, 8]
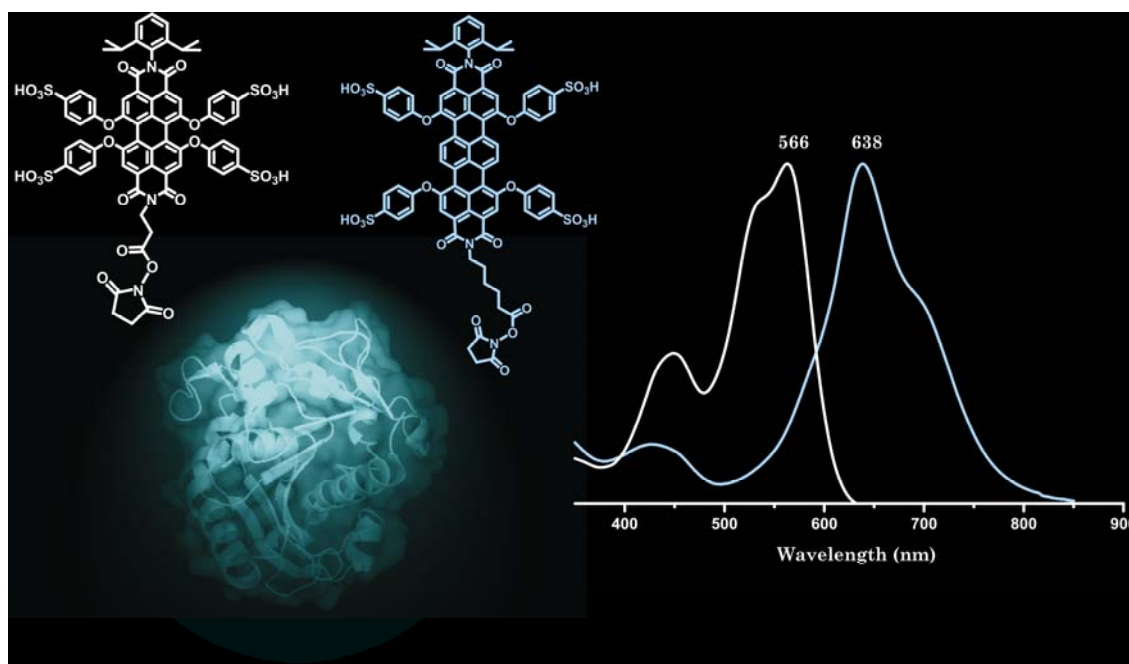


**Figure 4.3. Absorbance and fluorescence spectra of 3.32 (white line) and 3.46 (blue lineleft side), model of PLA1 used in this study, based on crystal structure of the enzyme**

The purification of the conjugates was accomplished by coupling the unreacted dye to a solid support. The resin consisted of a low crosslinked polystyrene matrix onto which polyethylene glycol containing a free terminal amino group was grafted. Usually such resins are employed for solid-phase organic synthesis. Here the non-reacted dye was covalently captured after addition of the support to the labeling solution and the labeled enzyme isolated by filtration.
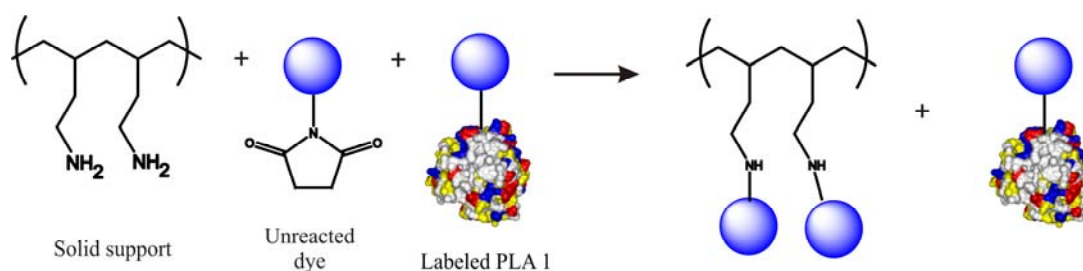
**Figure 4.4. Schematic representation of the purification of the labeled PLA1**

The amine functionalized resin was added directly to the reaction mixture containing the labeled enzyme and the excess of the free dye. (Figure 4.4) Very few purification techniques provide the researchers with easy and fast separation of the conjugate, similar to the technique discussed here. The reaction time necessary for the unreacted dye to be completely captured by the support was five minutes (monitored by SDS-PAGE gel electrophoresis). This short reaction time indicates again the excellent reactivity of the dye, and proves this technique as one of the fastest and most efficient ways for purification of fluorescently labeled conjugates. The addition of the resin directly to the reaction mixture allows efficient protein recovery, since the labeled enzyme is separated form this mixture simply by filtration. This approach can be utilized for the purification of any bioconjugate, providing that the solid support is carrying the necessary reactive group – e.g. resin bearing thiol groups for the capturing of the excess of the maleimide functionalized fluorophore, or any other "couple" of reactive groups allowing covalent attachment of the unreacted chromophore. This novel strategy for the purification of bioconjugates allowed convenient and fast separation of labeled enzymes without the need for performing time consuming chromatographic or electrophoretic purification steps.

The gel electrophoretic analysis confirmed that the unreacted label was removed very efficiently (Figure 4.5).
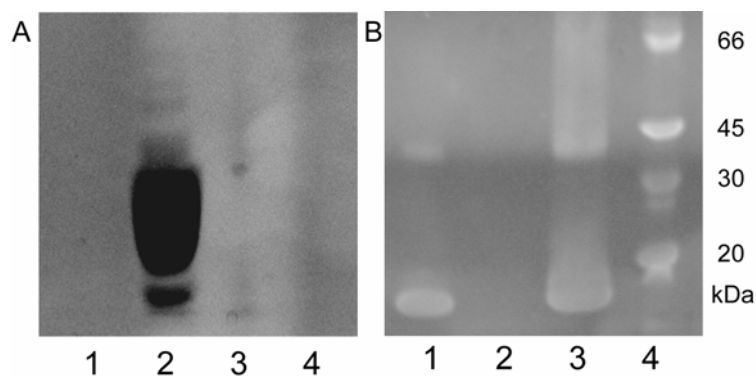
**Figure 4.5.** SDS-PAGE electrophoresis of the labeled enzyme. Panel A corresponds to UV-transillumination visualization and Panel B was stained with Coomassie blue. Lane 4 is the protein molecular weight standard. Lane 2 contains compound **3.32**. Lane 1 is the phospholipase and lane 3 the labeled enzyme.

Further evidence for effective removal of unreacted dye was obtained by performing fluorescence correlation spectroscopy measurements (for technical details see experimental section). For the free dye a diffusion coefficient of $2.3 \times 10^{-6}$ $cm^2/s$ was measured, whereas for the labeled protein a value of $1 \times 10^{-6}$ $cm^2/s$ was found. The values were in agreement with calculations based on the molecular weight of the protein; the results are summarized in Table 4.1.

**Table 4.1.** Diffusion time and constants for the reference and the target molecules

|  | **Diffusion time** | **Diffusion constant** |
|---|---|---|
|  | $(\tau)$ **($\mu$s)** | $(D)$ **($cm^2/s$)** |
| Rhodamine 101 | 30.0 | $3 \times 10^{-6}$ |
| **3.32** | $39.7 \pm 1.14$ | 2.3 x 10-6 |
| PDI 1 labeled PLA1 | $90.1 \pm 1.84$ | $1 \times 10^{-6}$ |

In a similar way labeling with terrylene(dicarboximide) N-hydroxysuccinimide derivative **3.45** was achieved. A solution of phospholipase A1 in 10 mM succinic acid, 0.4M $NH_4SO_4$, pH 6 was reacted at 4 °C for one hour with

**3.45** freshly dissolved in 0.01 M NaHCO$_3$. The unreacted dye was removed applying the above mentioned purification and the labeled enzyme again isolated in high purity (99 % purity confirmed by SDS-PAGE and FCS).

**A**                                                                **B**
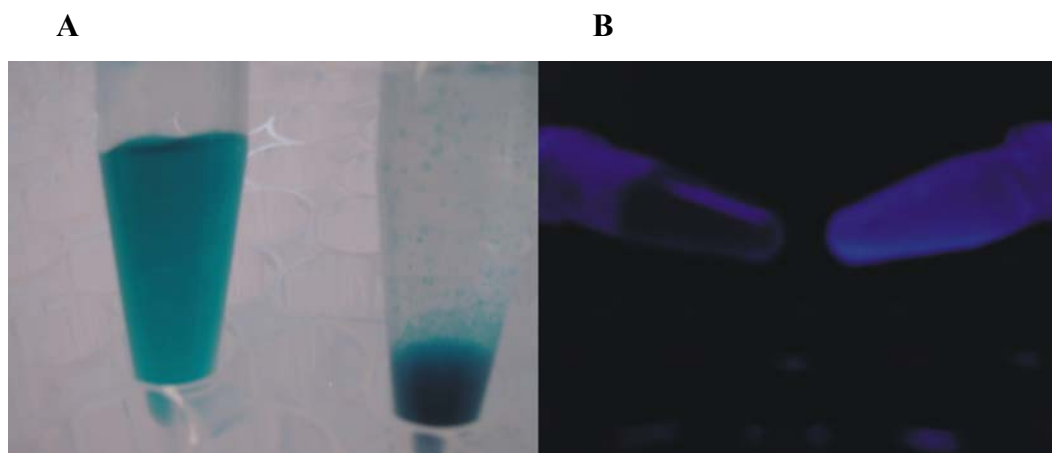


**Figure 4.6. Panel A: Buffer solutions of the water-soluble terrylene (dicarboximide) N-hydroxysuccinimide ester (3.45) – before and after the addition of the resin. Panel B: Fluorescence illumination of the same solutions – the water-soluble terrylene(dicarboximide) is non-fluorescent in water due to the formation of aggregates, after the formation of the covalent bond between the dye and the resin, the fluorescence properties of the chromophore changes due to the disappearance of these aggregates.**

The water-soluble terrylene chromophore, decorated with N-hydroxysuccinimide can be used to demonstrate the covalent binding of the unreacted dye to the solid support. As described in Chapter 1 and Chapter 3, the water-soluble terrylene derivatives forms a nonfluorescent aggregate in water.[9] The covalent attachment of the terrylene dye to the resin destroys the H-aggregates, the fluorescence is again restored and can be observed (Figure 4.6).[9]

The bulk activity of the labeled enzyme is tested. Thereby, PLA1 catalyzes the saponification of the acetate groups of the fluorescein derivative that is non-fluorescent (Figure 4.7a). The hydrolysis of the substrate can be followed via the increase in the fluorescence intensity due to the formation of the fluorescent product upon the enzymatic reaction. Figure 4.7bb shows fluorescence intensity changes of a similar solution of pro-fluorescent substrate as a function of time without the enzyme (o), after adding non-labeled enzyme (x), and after adding the labeled enzyme (Δ), respectively. The rate constants of the hydrolysis were estimated to be

3001.3 ± 29.1 (s$^{-1}$) and 3083.1 ± 38.1 (s$^{-1}$) for the labeled enzyme and the non-labeled enzyme, respectively. The autohydrolysis of 5-CFDA was measured as 110 ± 17.9 (s$^{-1}$). The result clearly shows that no activity was lost by the labeling.
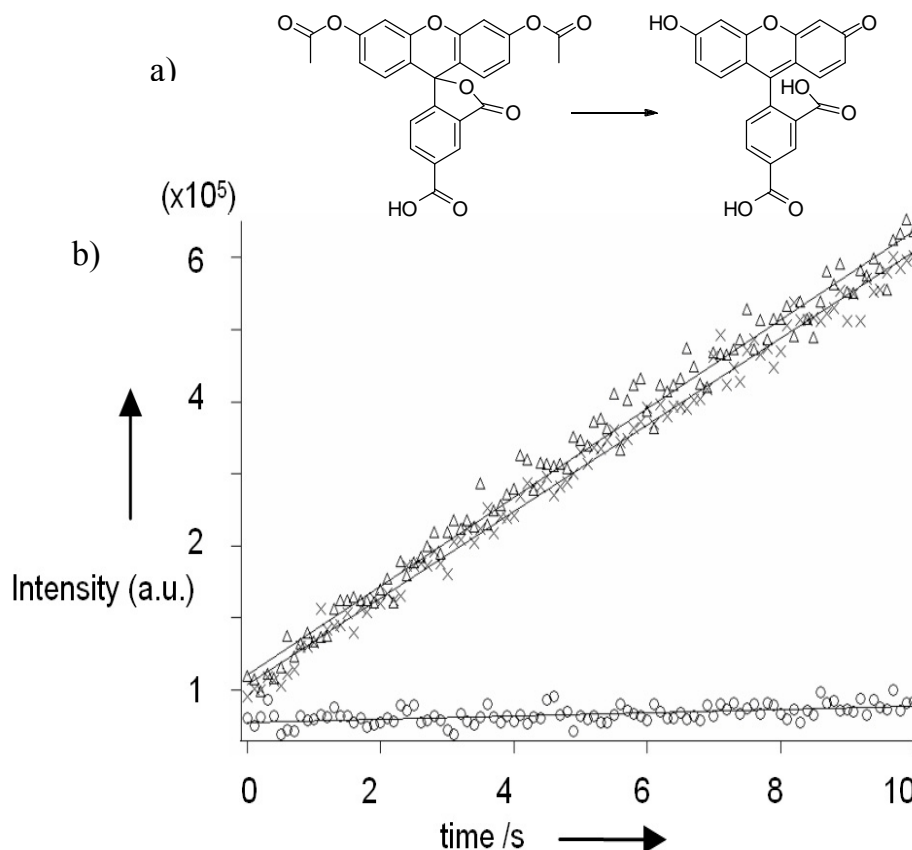


**Figure 4.7. Relative enzymatic activity in bulk. Using a pro-fluorescent substrate it is possible to follow the reaction kinetics trough the increase in the fluorescent intensity (a) Scheme of the hydrolysis of non-fluorescent 5-carboxyfluorescein diacetate (5-CDFA) yielding the fluorescent product 5-carboxyfluorescein (5-FAM). (b) Fluorescence intensity of 5-FAM as function of time. For the activation of the surface enzyme in solution (e.g., in order to open the lid protecting the active site), Triton X-100 was added to the solution. 5-CDFA: 0.7mM; Triton X-100: 0.5mM (x) non-labeled PLA1 (3E$^{-8}$ M), 3001.3 ± 29.1 s$^{-1}$ (Δ) PLA1 labeled with N-hydroxysuccinimide perylene derivative 3.32 (3E$^{-8}$ M), 3083.1 ± 38.1 s$^{-1}$ (o) 5-CFDA autohydrolysis 110.54 ± 17.9 s$^{-1}$. From the figure it shows that the labeling of the enzyme with NHS-PDI has no affect on its activity towards 5-CFDA.**

To compare the photostability of the rylene dyes with other commercially available chromophore PLA1 was labeled with ATTO 647N NHS ester using standard procedure for protein labeling. The survival time of the PLA1 labeled with ATTO 647N NHS was approximately 0.2 s with about 1 kW/cm$^2$ of excitation power (using 628.8 nm line of a He-Ne laser to excite the dye molecules). This is considerably lower than the survival time of the PDI label **3.32,** despite the fact that the ATTO 647N is excited using a laser power about 5 times lower than the one use for **3.32**). With such a short survival time, it is hard to distinguish between dye photobleaching and enzyme desorption during single particle tracking. Therefore, such short-lived dye is not suitable for experiments as the single enzyme tracking on a natural substrate layers.

## 4.3. Single enzyme tracking using wide-field microscopy

Recent advances in optical microscopy have made it possible to detect fluorescence emission from single molecules and to follow their behavior over time. Single molecule fluorescence spectroscopy (SMFS) allows deeper insight into locally inhomogeneous molecular behavior not otherwise available from ensemble measurements, making it ideally suited to the study of complex biological systems.[2]

The study of enzyme kinetics on a single molecule level is usually performed using confocal microscopy on immobilized enzyme molecules using either enzymes with fluorescent co-factors or pro-fluorescent substrates.[10-12] Temporal fluctuations and memory effects in catalytic turnover have been detected as a common feature for many different enzymes.[11-13] These fluctuations were attributed to the existence of several conformations of the enzyme, each with different catalytic activity.[13] However, it remains unclear whether these fluctuations are caused solely by conformational changes or if they are at least in part an artefact arising from either the immobilization of the enzymes or the use of non-natural (and large) substrates.

Wide-field SMFS has the potential to resolve this question as the technique allows for the study of enzymes on their natural substrates, as has been elegantly demonstrated for a number of DNA enzymes.[14-16] Further advantage of wide-field SMFS is that it offers information not only on catalytic rates but also on diffusion behavior which can be a critical component of interfacial enzyme action.

In this work wide-field SMFS was applied to the study of a phospholipase on its natural substrate. Similar experiments have been performed previously by means of atomic force microscopy (AFM), however by using SMFS the possible perturbation of the phospholipid layers by contact with the AFM probe tip is avoided and better time resolution can be achieved (milliseconds for wide-field imaging versus seconds for AFM measurements).[17, 18]
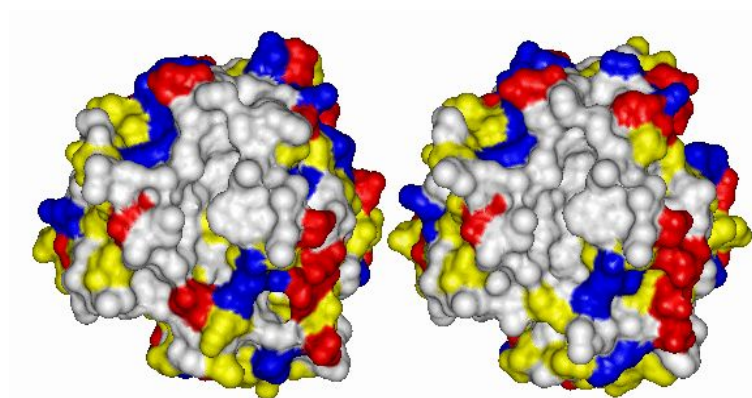


**Figure 4.8. Comparison of the open TLL structure (right) and a model of the open structure of PLA1 (left). The model of the open structure of PLA1 is constructed from the X-ray structure of the PLA1 backbone except at the open part of the lid region, where it is modeled on the open part of the TLL structure. The properties of the surface residues are indicated by color-coding. The hydrophobic residues are shown in white, hydrophilic residues in yellow, positively-charged residues in blue and negatively-charged residues in red.**

As a substrate, supported membranes of 1-palmitoyl-2-oleoyl-sn-glycero-3-phosphocholine (POPC) were used. Due to its relatively high fluidity at room temperature, POPC serves as a good model for cellular membranes. Fluorescent substrate layers were prepared by the re-hydration method, using POPC solutions mixed with a fluorescent dye and a mica support.[19]
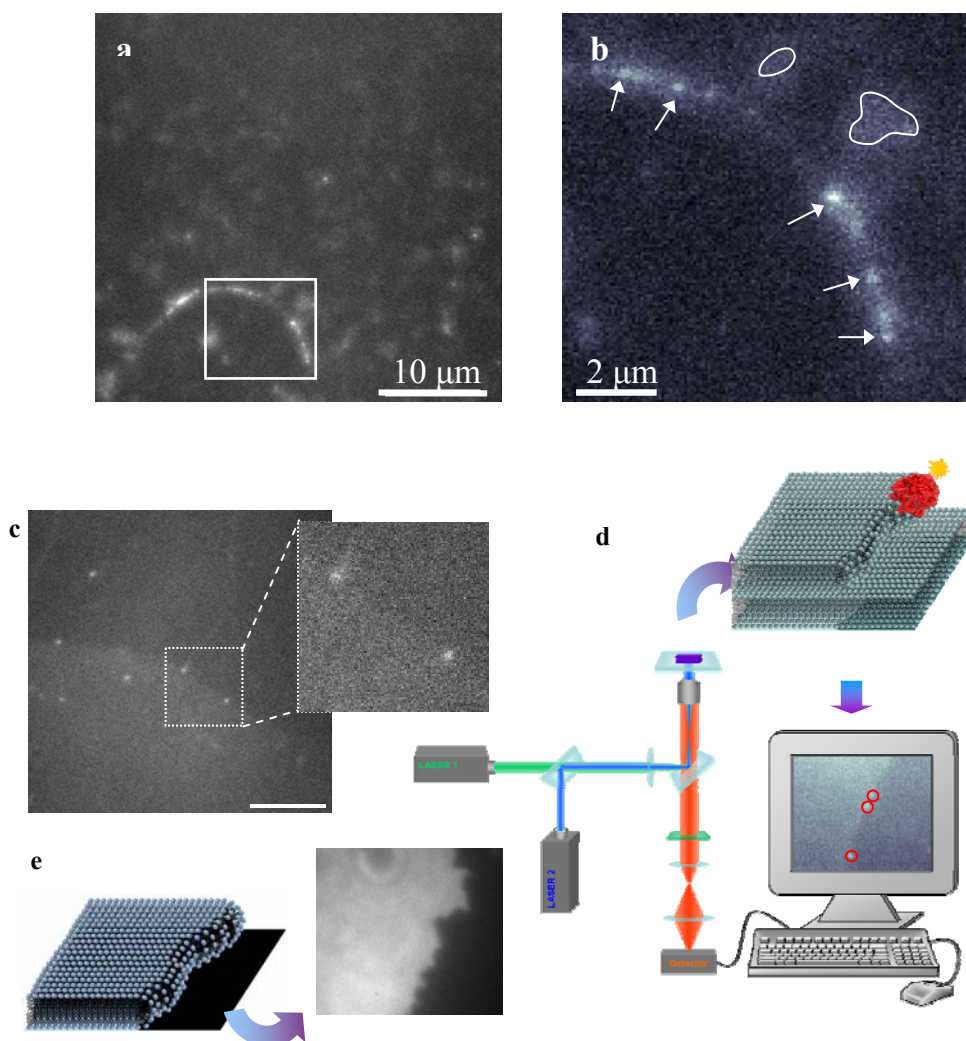
**Figure 4.9. Fluorescence image of individual labeled enzymes on POPC layers. (a) 4.33 labeled PLA1 on a non-labeled POPC layer (b) Magnification of the area in image (a) indicated by the white square. The arrows indicate clearly distinguishable individual enzymes located on the edge of the layer. Note that the signal-to-noise is much higher than for the not adsorbed molecules diffusing in solution (indicated by the circles). c) Action of phospholipase A1 on phospholipid layers imaged by fluorescence microscopy. Discrimination of single enzymes is possible. (d) Setup used for the simultaneous excitation of the dye-labeled substrate and the PDI-labeled enzyme. The image on the monitor cartoon shows labeled POPC multilayers in the presence of labeled PLA1 (indicated by the red circles) (e) When only a single labeled phospholipid bilayer is present, the mica support appears as a black area (almost no background emission).**

In order to link the diffusion of the labeled enzyme with hydrolysis of POPC layers, 3,3'-dioctadecyloxacarbocyanine perchlorate (DiO) was incorporated into the phospholipid layers to render them fluorescent, albeit at a different emission wavelength than the label. The use of labeled phospholipid layers allows a clear visualization of the edge between two consecutive layers or between a bilayer and the support (Figure 4.9a). Labeled POPC multilayers and labeled PLA1 (PDI-PLA1) were imaged simultaneously using two color excitation (Figure 4.9dd).

Furthermore, hydrolysis of the layers can also be followed due to the drop in the quantum yield of DiO caused by the increase of cis-trans isomerization when freely diffusing in aqueous solution. When PDI-PLA1 (~$10^{-7}$ M) was added to a labeled multilayer, the desorption of phospholipid molecules was indicated by a retreat of the uppermost layer (Figure 4.9b). Bright emission due to the enzyme can be seen clearly against the background fluorescence of the multilayer and is concentrated at the layer edges. Even in these difficult conditions for SMS (introduction of fluorescent background), the new labels allow to obtain sufficient signal-to-noise ratio to discriminate and track individual enzymes on the labeled POPC layers (Figure 4.9a-b). The observed desorption rate is not constant over time. Temporal fluctuations in enzymatic activity are observed here for a phospholipase on its natural substrate, having already been reported several times in confocal microscopy studies of enzymes on non-natural substrates.[11-13] The fluctuations can be explained by the existence of several enzyme conformations with different catalytic turnover rates.[13] In the case of interfacial enzymes, the fluidity of the layer is also likely to affect the catalysis rate over time by influencing the packing of substrate molecules.

Figure 4.10c shows the trajectory of an enzyme diffusing along the edge of the layer (see supporting movie). The diffusion coefficient can be quantified by calculating the mean square displacement from these trajectories. The diffusion constant of the phospholipase molecule on the trajectory present on Figure 4.8 is 1.276 ± 0.014 µm2/s. Due to the interaction between enzymes and the substrate layers, the value of the diffusion constant is lower than the usual values obtained for free diffusion of proteins in solution (~102 µm2/s).

Most of the enzymes in the recorded movies stayed on the layers for less than 0.3 seconds. It has been shown that the water-soluble perylene label **3.32** has a survival time of 120 s when immobilized in polyvinylalcohol. Therefore, the

disappearance of the labeled enzymes after 0.3 s is probably linked to enzyme activity as well as its mode of action (non processive hydrolysis of the layers).
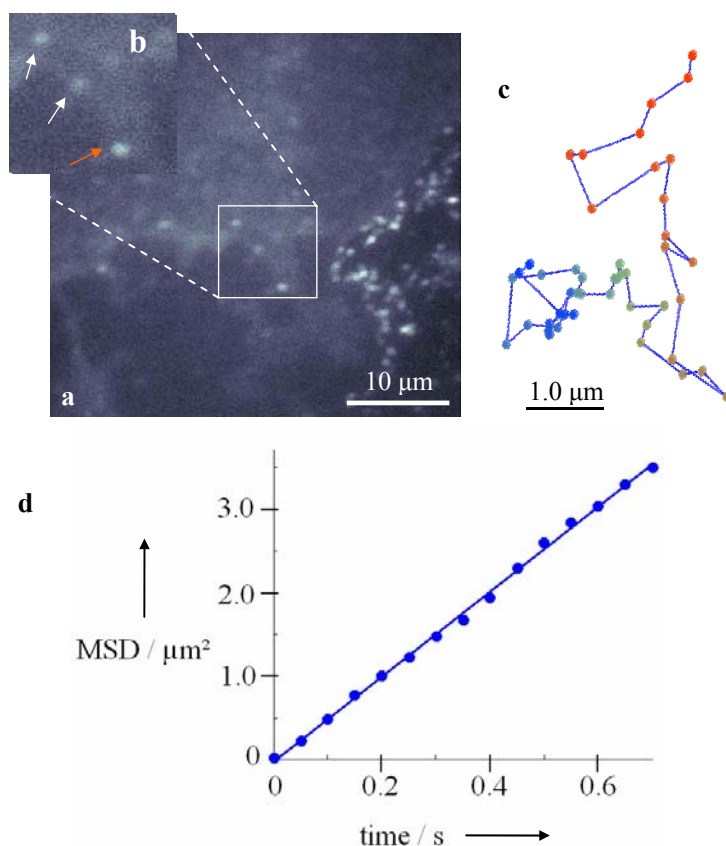


**Figure 4.10. Fluorescence image of individual PDI 5 labeled enzymes on POPC layers labeled with DiO. The PDI label allows obtaining sufficient photons to discriminate individual enzymes even with fluorescence background from the layers. (a) Labeling of the layers allows visualization of steps in the layers as well as preferential adsorption of the enzyme molecules at the steps. The image results from accumulating 8 frames (400 ms) (b) Magnification of the area indicated by the white square in image A. Single enzyme molecules are indicated by arrows. Exposure time for each frame was 50ms; Excitation wavelength for PDI and DiO were 532 and 488 nm, respectively. The fluorescence from both dyes is detected through the same filters, see experimental section. (c) Trajectory described by the enzyme on the edge of a POPC layer labeled with DiO indicated by the orange arrow on (b) (d) Plot of the mean square displacement (MSD) of the enzyme for the first points of the track. From these data, it is possible to calculate the diffusion constant of a single active enzyme: 1.28 ± 0.02 μm2/s**

## 4.4. Conclusions and outlook

In summary, N-hydroxysuccinimide functionalized perylene and terrylene dyes have been attached to phsopholipase-A1. In regard to protein labeling, a convenient procedure for the removal of unreacted dye from labeled enzymes has been developed which involves capturing excess dye with a solid support. This novel strategy for purification of bioconjugates allows convenient and fast separation of labeled proteins without the need for performing time consuming chromatographic or electrophoretic purification steps. The application of this approach is not only limited to amine reactive probes, but can be applied to any fluorescent reporter, which contains a functional reactive group. The labeled biomolecule can be recovered very fast and in high purity, thus making this approach one of the most convenient ways for isolating modified biomolecules.

The performance of the new fluorescent probes was assessed by single-particle tracking. The measurements revealed that single enzymes could even be visualized on a fluorescently labeled substrate. The outstanding photostability of the dyes and their extended survival times under strong illumination conditions allow the actions of enzymes to be characterized on their natural substrates, in this case, phospholipase acting on phospholipid-supported layers. By using this approach, enzyme mobilities could be correlated with the catalytic activity. Furthermore, this assay allows the validation of the influence of the layer composition, fluidity, etc. on both parameters (enzyme mobility and activity).

## 4.5. References

[1] J. W. Lichtman, J. A. Conchello, *Nature Methods* **2005**, *2*, 910, *Fluorescence microscopy.*

[2] P. Tinnefeld, M. Sauer, *Angew. Chem. Int. Ed.* **2005**, *44*, 2642, *Branching out of single-molecule fluorescence spectroscopy: Challenges for chemistry and influence on biology.*

[3] G. Seisenberger, M. U. Ried, T. Endress, H. Buning, M. Hallek, C. Bräuchle, *Science* **2001**, *294*, 1929, *Real-time single-molecule imaging of the infection pathway of an adeno-associated virus.*

[4] C. Bräuchle, G. Seisenberger, T. Endress, M. U. Ried, H. Buning, M. Hallek, *ChemPhysChem* **2002**, *3*, 299, *Single virus tracing: visualization of the infection pathway of a virus into a living cell.*

[5] I. Sitkiewicz, K. E. Stockbauer, J. M. Musser, *Trends Microbiol.* **2007**, *15*, 63, *Secreted bacterial phospholipase A(2) enzymes: better living through phospholipolysis.*

[6] A. Aloulou, J. A. Rodriguez, S. Fernandez, D. van Oosterhout, D. Puccinelli, F. Carriere, *Biochimica Et Biophysica Acta-Molecular and Cell Biology of Lipids* **2006**, *1761*, 995, *Exploring the specific features of interfacial enzymology based on lipase studies.*

[7] K. Peneva, A. Herrmann, K. Müllen Water-soluble rylene dyes, methods for preparing the same and uses thereof as fluorescent labels for biomolecules. EP07022521, 2007.

[8] K. Peneva, G. Mihov, F. Nolde, S. Rocha, J. Hotta, K. Braeckmans, J. Hofkens, H. Uji-i, A. Herrmann, K. Müllen, *Angew. Chem. Int. Ed.* **2008**, *120*, 3420, *Water-soluble monofunctional perylene and terrylene dyes: powerful labels for single enzyme tracking.*

[9] C. Jung, B. K. Müller, D. C. Lamb, F. Nolde, K. Müllen, C. Braeuchle, *J. Am. Chem. Soc.* **2006**, *128*, 5283, *A New Photostable Terrylene Diimide Dye for Applications in Single Molecule Studies and Membrane Labeling*.

[10] H. P. Lu, L. Y. Xun, X. S. Xie, *Science* **1998**, *282*, 1877, *Single-molecule enzymatic dynamics*.

[11] K. Velonia, O. Flomenbom, D. Loos, S. Masuo, M. Cotlet, Y. Engelborghs, J. Hofkens, A. E. Rowan, J. Klafter, R. J. M. Nolte, F. C. de Schryver, *Angew. Chem. Int. Ed.* **2005**, *44*, 560, *Single-enzyme kinetics of CALB-catalyzed hydrolysis*.

[12] O. Flomenbom, K. Velonia, D. Loos, S. Masuo, M. Cotlet, Y. Engelborghs, J. Hofkens, A. E. Rowan, R. J. M. Nolte, M. Van der Auweraer, F. C. de Schryver, J. Klafter, *Proc. Natl. Acad. Sci. U. S. A.* **2005**, *102*, 2368, *Stretched exponential decay and correlations in the catalytic activity of fluctuating single lipase molecules*.

[13] H. Engelkamp, N. S. Hatzakis, J. Hofkens, F. C. De Schryver, R. J. M. Nolte, A. E. Rowan, *Chem. Commun.* **2006**, 935, *Do enzymes sleep and work?*

[14] J. Elf, G. W. Li, X. S. Xie, *Science* **2007**, *316*, 1191, *Probing transcription factor dynamics at the single-molecule level in a living cell*.

[15] J. Yu, J. Xiao, X. J. Ren, K. Q. Lao, X. S. Xie, *Science* **2006**, *311*, 1600, *Probing gene expression in live cells, one protein molecule at a time*.

[16] J. B. Lee, R. K. Hite, S. M. Hamdan, X. S. Xie, C. C. Richardson, A. M. van Oijen, *Nature* **2006**, *439*, 621, *DNA primase acts as a molecular brake in DNA replication*.

[17] M. Grandbois, H. Clausen-Schaumann, H. Gaub, *Biophys. J.* **1998**, *74*, 2398, *Atomic force microscope imaging of phospholipid bilayer degradation by phospholipase A(2)*.

[18] L. K. Nielsen, J. Risbo, T. H. Callisen, T. Bjornholm, *Biochimica Et Biophysica Acta-Biomembranes* **1999**, *1420*, 266, *Lag-burst kinetics in phospholipase A(2) hydrolysis of DPPC bilayers visualized by atomic force microscopy*.

[19] A. C. Simonsen, L. A. Bagatolli, *Langmuir* **2004**, *20*, 9720, *Structure of Spin-Coated Lipid Films and Domain Formation in Supported Membranes Formed by Hydration*.

# 5. Preparation of water-soluble perylene thioester for site-specific covalent labeling of proteins

## 5.1. Site-specific labeling of proteins

When a protein is being labeled, the goal is to introduce a fluorescent label while preserving the native function and properties of the protein itself. Ideally, one should be able to attach covalently a precise number of chromophores to one or more specific locations on the surface of any molecule in solution. Currently, the most general approach is to use electrophilic reagents that can react with nucleophilic groups on the surface of a target protein; however, this tends to yield a heterogeneous mixture of products since almost all proteins carry a number of nucleophilic groups on their surface. To overcome this problem the researchers have developed numerous strategies for site-specific labeling of proteins, defining new and efficient ways for attaching a chromophore at precise position.[1-4]

A good labeling strategy should ideally satisfy the following criteria: (1) possess a high signal-to-noise ratio (i.e. high specificity for target protein); (2) uphold the integrity of the labeled protein; (3) not interfere with the biochemical functions or cellular localization of the labeled protein and (4) have minimal perturbation to the normal cellular processes.

Various novel strategies for specific labeling of proteins with small molecular probes have recently been reported.[5-10] The cell permeability, non-toxicity, specific reactivity and wide spectrum of "colors" are some of the important features that have made the small fluorescent probes an attractive alternative to the fluorescent proteins.[11-14]

One of the earliest methods for site-specific labeling of recombinant proteins with small organic molecules within live cells was developed by Tsien et al.[5] This method exploits the well-known specificity of organoarsenicals with pairs of thiols.

A short peptide sequence CCXXCC (in which X is a non-cysteine amino acid) was genetically fused to the protein of interest, which was subsequently recognized and labeled by a cell permeable fluorescein derivative.

Biarsenical tags have numerous advantages, including cell permeability, and unique fluorescence properties which are "lighted" up only upon specific binding with the tetracysteine protein target. Nevertheless, a major limitation to the strategy is that micromolar concentrations of dithiols (e.g. ethanedithiol) are required as agonists in order for specific labeling to occur.

We have exploited two strategies for site-selective labeling of proteins in regard of further functionalization of the rylene derivatives described in Chapter 3, based on site-specific covalent and noncovalent labeling. The first method is based upon nitrilotriacetic acid derivatized fluorophores, which represents one of a few techniques for noncovalent fluorescent labeling with well-defined localization of the attached dye currently available. It is based on the well-known interaction between polyhistidine sequences and the $Ni^{2+}$-NTA moiety, in which a small organic fluorophore is conjugated to nitrilotriacetic acid (NTA) moiety.[15] This site-specific, fast and reversible approach is successfully applied to determine the topology of membrane proteins in living cells without the need for fixation and/or permeabilization of the cells and is suitable for studying the protein-protein interactions within cellular signaling. The main disadvantage is the severe quenching of the fluorescence upon binding to the nickel ions. The application of this strategy using the ultrastable rylene chromophores and its surprising photophysical behavior will be discussed in further details in Chapter 6.

The second method for site-selective labeling of proteins which we applied has attracted attention in the last decade and is taking advantage of the chemoselective reaction of native chemical ligation. This approach provides efficient covalent incorporation of fluorescent probe at the N-terminal cysteine residue, via the formation of native amide bond between the protein of interest and a chromophore, bearing thioester functional group. The use of the perylene(dicarboximide) derivatized as thioester and its application for site-selective labeling of Plasminogen Activator Inhibitor, bearing N-terminal cysteine will be discussed in the following section.

## *5.2. Experimental methods*

### 5.2.1. Fluorescence Correlation Spectroscopy

The Fluorescence Correlation spectroscopy (FCS) experiments were done in cooperation with Dr. Michael Börsch (University of Stuttgart).

Fluorescence correlation spectroscopy (FCS) is one of the many different modes of high-resolution spatial and temporal analysis of extremely low concentrated biomolecules. In contrast to other fluorescence techniques, the parameter of primary interest is not the emission intensity itself, but rather spontaneous intensity fluctuations caused by the minute deviations of the small system from thermal equilibrium. In general, all physical parameters that give rise to fluctuations in the fluorescence signal are accessible by FCS. It can be applied for determination of local concentrations, mobility coefficients or characteristic rate constant of inter- or intramolecular reactions of fluorescently labeled biomolecules in nanomolar concentrations. FCS is taking advantage of very small spontaneous fluctuations of physical parameters that are reflected by the fluorescence emission of the molecules. Such fluctuations are continuously occurring at ambient temperatures and are represented as noise patterns of the measured signal. The fluctuations can be quantified in their strength and duration by temporally autocorrelating the recorded signal, a mathematical procedure that gives the technique its name.

A typical experimental setup (Figure 5.1a) consists of a high numerical aperture (NA) objective which focuses a laser beam into the sample (e.g., single cells or solution). The diffraction-limited beam waist in the objective focal plane is on the order of the illumination wavelength $\lambda_x$ in the lateral dimension (i.e., typically 0.5 μm). Fluorescence is collected through the same objective, separated from the excitation light by both a dichroic mirror and emission filters, and then focused by a tube lens onto a confocal aperture (either an optical fiber or a pinhole) that precedes a detector for depth discrimination. Avalanche photodiodes (APDs) or photomultiplier tubes (PMTs) are used for fluorescence detection. Most PMTs tend

to have lower quantum efficiencies and a low dark count rate compared to those of APDs, which are highly sensitive but exhibit higher dark count rates. The excitation intensity profile and detection optics (in particular, the confocal aperture) define the $10^{-15}$ *l* observation volume (Figure 5.1b), from which fluorescence photons are detected. The detector signal is then processed with a PC correlator card to calculate the autocorrelation curve (Figure 5.1). The correlation decay curve is then fitted with an analytic function, which accounts for the mechanism and kinetics of the fluorescence fluctuations. Those processes include translational diffusion of particles through the observation volume [16], rotational diffusion within that volume [17-19], intersystem crossing [20], chemical reactions [21], conformational fluctuations [22, 23], and photobleaching [24, 25].

The capability of FCS as an analytical tool extends beyond the measurements of molecular concentrations and diffusion times. Kinetic parameters of molecular dynamics or chemical reactions are also accessible when they cause fluorescence fluctuations on time scales faster than the diffusion time. This includes unimolecular reactions, intersystem crossing, triplet state dynamics, photoconversion, and reversible photobleaching.

FCS measurements were carried out on a confocal setup based on an Olympus IX71 inverted microscope. A solid-state laser (JIVE, Cobolt AB, Stockholm, Sweden) with emission at 561 nm was used and attenuated to 85 µW or 150 µW before focusing into the buffer solution by a water immersion objective (60x, N.A. 1.2, Olympus). The solution was placed on a microscope coverslide as a droplett of 30 µl. Scattered laser light was blocked by a dichroic beam splitter (DCXR 575, AHF, Tübingen, Germany) and out-of-focus fluorescence was rejected by an 150 µm pinhole in the detection pathway. Fluorescence was collected in the spectral range from 575 to 648 nm using an interference filter (AHF). Single photons were detected by an avalanche photodiode (SPCM AQR-14, Perkin Elmer) and registered by a TCSPC device (PC card SPC-630, Becker & Hickl, Berlin, Germany) for software calculation of the autocorrelation functions, $g^{(2)}(t_c)$.[26] Sulforhodamine B (Sigma) in $H_2O$ was used for the calibration of the confocal volume.
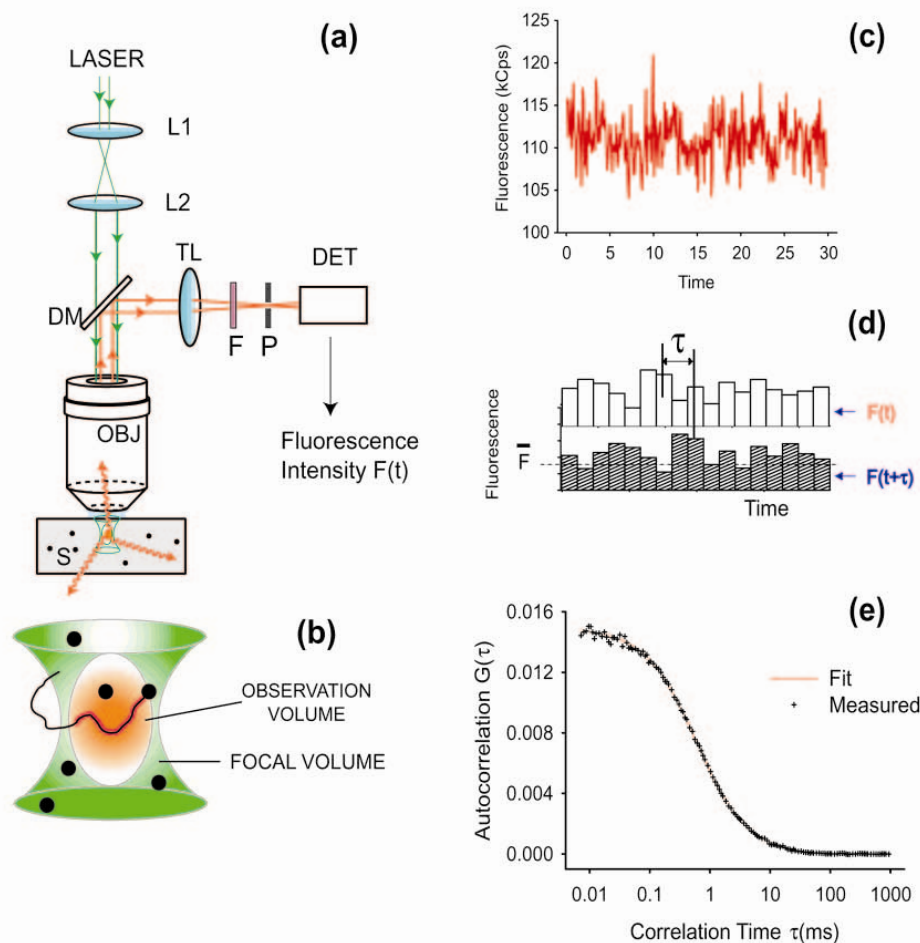
**Figure 5.1: (Left) Experimental setup for FCS. (a) A laser beam is first expanded by a telescope (L1 and L2), and then focused by a high-NA objective lens (OBJ) on a fluorescent sample (S). The epifluorescence is collected by the same objective, reflected by a dichroic mirror (DM), focused by a tube lens (TL), filtered (F), and passed through a confocal aperture (P) onto the detector (DET). (b) Magnified focal volume (green) within which the sample particles (black circles) are illuminated. (Right) (c) A typical fluorescence signal, as a function of time, measured for rhodamine green (RG) with a $\lambda_x$ of 488 nm. (d) Portion of the same signal in panel c, binned, with an expanded time axis and average fluorescence $\overline{F}$. The signal is correlated with itself at a later time (t + $\tau$) to produce the autocorrelation G($\tau$). (e) Measured G($\tau$) describing the fluorescence fluctuation of RG molecules due to diffusion only as observed by FCS.**

## 5.3. Synthesis of thioester functionalized perylene (dicarboximide)

Different classes of chromophores have been synthesized and utilized for site-specific covalent labeling of proteins, cells and other biomolecules.[5, 27] For an increasing number of applications the photostability of the label is crucial. The rylene chromophores have proven to be a class of chromophores possessing exceptional thermal and photochemical stabilities. Their unique sets of photophysical properties have provoked many studies in the area of single molecule spectroscopy. They have been used efficiently as label in single enzyme tracking using real time wide field microscopy of single enzymes as shown in Chapter 4.[28] The nitrilotriacetic acid functionalized perylene dye has shown an unexpected behavior in the presence of nickel ions and no change in the quantum yield was observed as it will be demonstrated in Chapter 6.[29] In this chapter we focus on the preparation of rylene chromophore that possesses thioester function to employ the native chemical ligation for site-specific labeling of proteins, in order to extend our toolbox of labeling strategies.

So far no derivative of the rylene series is known to exhibit an appropriate functionality for covalently labeling either the N- or C-terminus of proteins selectively. Therefore, we decided to synthesize a water soluble perylenediimide functionalized as a thioester to achieve covalent attachment to an N-terminal cysteine of proteins.

Available methods for the preparation of suitable thioesters range from biochemical approaches to solid phase synthesis using modified resins.[30, 31] Among all of them two easy and straightforward route have provoked the preparation of thioester functionalized chromophores. A simple protocol for the synthesis of

thioester derivatives starting from succinimidyl esters was presented by Pannell et al.[32] This method was successfully applied for the preparation of Cy5-thioester and the chromophore conjugated to a short peptide, containing N-terminal cysteine. Initially, the aluminum reagent was prepared from an equimolar mixture of trimethylaluminum and benzyl mercaptane in a protocol similar to the one described by Hatch in 1977. These aluminum compounds are known to react with a variety of esters at room temperature to produce the respective thioesters in good yield and can be used without further purification. It was therefore attempted to use this very simple procedure to generate the benzyl thioester of water-soluble perylene(dicarboximide).(Scheme 5.1) The incubation of perylene(dicarboximide) N-hydroxysuccinimide ester with the reaction mixture containing compound **3.32** resulted in a colorless solution, possibly via interaction of the chromophore with the aluminum compounds. It did not regain its color after dilution in aqueous solution and the analytical data showed no evidence for the formation of the desired product.



**3.32**                    **3.47**
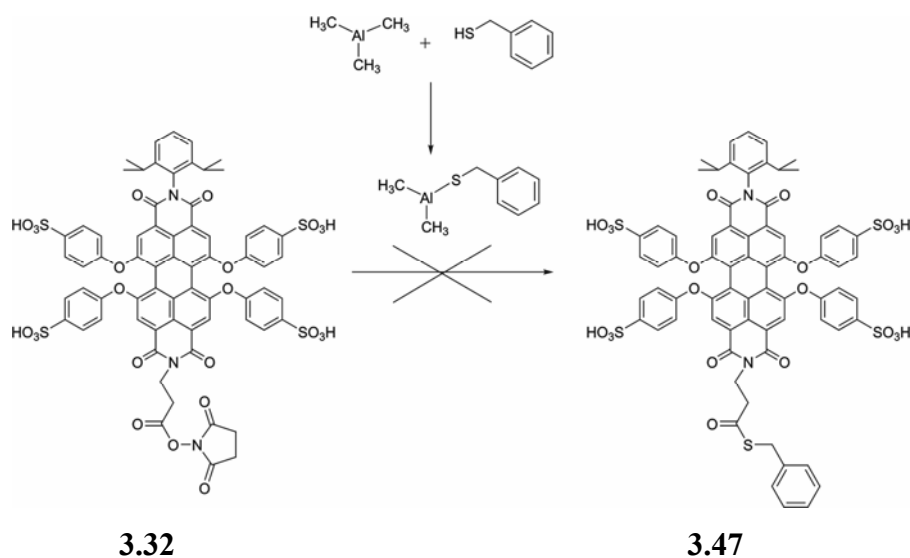
**Scheme 5.1. Conversion of perylene(dicarboximide) N-hydroxysuccinimide ester via activation of benzyl mercaptane with trimethylaluminum**

The synthesis of perylene(dicarboximide) thioester was achieved via one-pot procedure for the preparation of thioesters from primary amines developed by Mapp et al.[33] Water-soluble perylene(dicarboximide) functionalized with primary amine was reacted with thiolane-2,5-dione and subsequent addition of benzyl bromide at slightly acidic conditions resulted in formation of the thioester in 50% yield.



**3.26**                          **3.47**
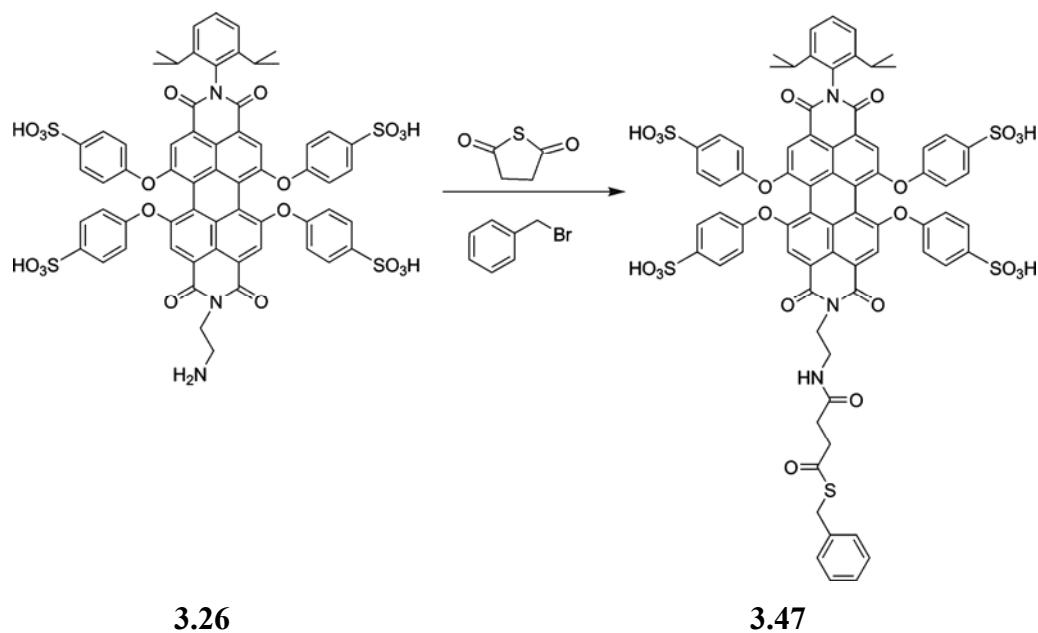
**Scheme 5.2. Preparation of perylene thioester via reaction with thiolane-2,5-dione and subsequent addition of benzyl bromide**

^{13}C NMR spectroscopy was the most convenient method for analysis; the formation of the amide bond lead to the shift of the $C_c$ signal from $\delta$ = 155 ppm to $\delta$ = 171 ppm. After the transformation of **3.26** into **3.47** new signals appeared at $\delta$ =178.14 and 174.02 ppm pointing to the new **C**=O segments. Moreover, **3.47** displays two resonances from **C**H$_2$S at $\delta$ = 48.79 and one from **C**H$_2$CH$_2$ at $\delta$ = 42.07 ppm. The ^{13}C NMR spectra of **3.26** and **3.47** are compared in Figure 5.2. The proposed structure was confirmed also from ^{1}H NMR and MALDI-TOF MS.
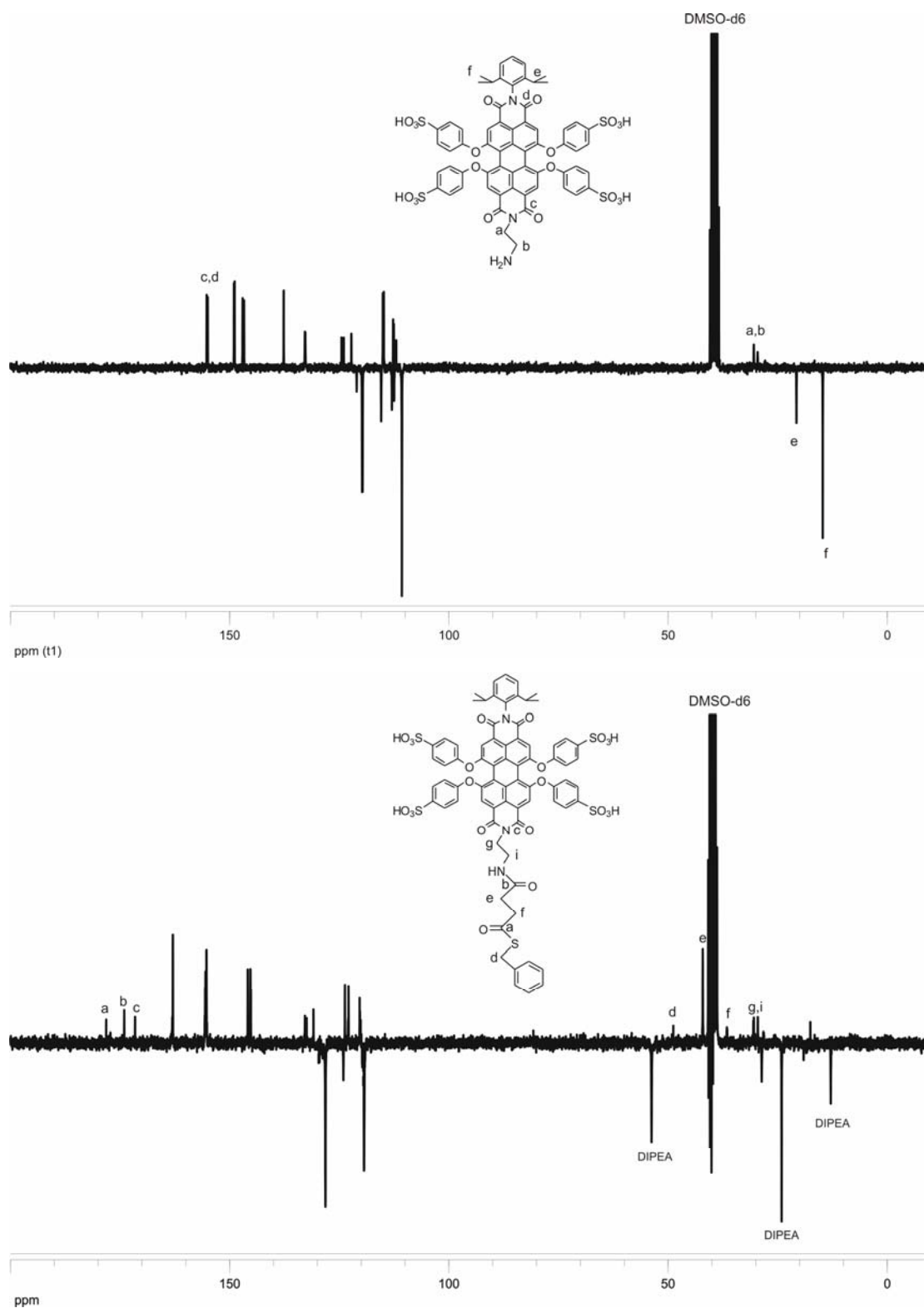
**Figure 5.2.** **¹³C NMR spectra of 3.26 and 3.47 in DMSO-*d₆*, room temperature (300 MHz)**

The perylene thioester is excellently soluble in water and exhibits an absorption maximum at 568 nm ($\varepsilon$ = 23 400 M$^{-1}$ cm$^{-1}$) and an emission maximum at 622 nm. The perylene thioester **3.47** shows high fluorescence quantum yield ($\Phi_f$) of 54 % in aqueous medium measured at room temperature using Cresyl Violet in methanol as reference.[34] Normalized absorbance and fluorescence spectra of the perylene chromophore are shown on Figure 5.3.



**Figure 5.3. Normalized absorption (solid line) and emission (dotted line) spectra of perylene thioester in aqueous medium**

To prove the suitability of the perylene thioester for labeling of proteins using the native chemical ligation, series of experiments with peptides, containing N-terminal cysteine were performed.

## *5.3. Site-specific labeling of proteins via native chemical ligation*
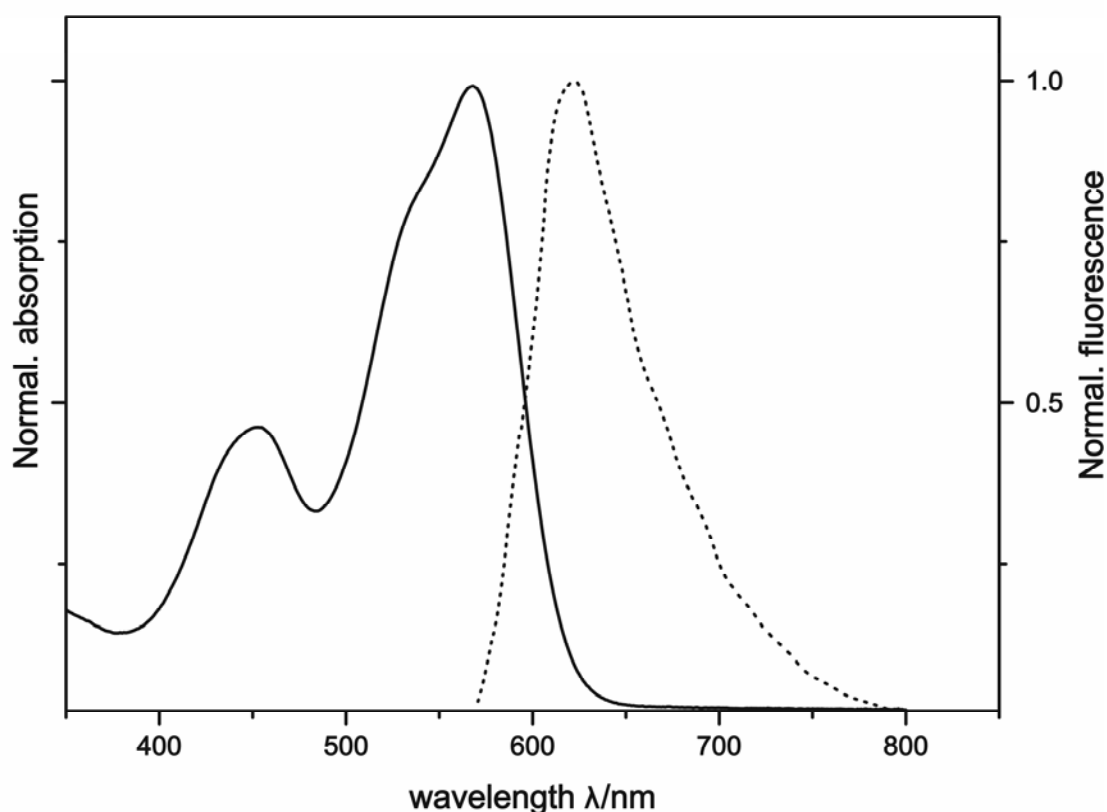
The labeling experiments were done in cooperation with Dr. Gueorgui Mihov, Max Planck Institute for Polymer Research.

Native chemical ligation (NCL) involves the chemoselective reaction of two unprotected peptides in aqueous solution to give a single covalently linked ligation product.[30, 35-37] A peptide-thioester is reacted with a Cys-peptide to give a product polypeptide with a native peptide bond at the ligation site. The reaction is envisioned to occur according to the reaction scheme shown in Figure 5.4. Peptide-R-thioester is reacted with a peptide containing an N-terminal cysteine residue; transthioesterification with the side chain thiol of the N-terminal cysteine residue results in a thioester-linked intermediate, which spontaneously rearranges through a favorable five-membered ring intramolecular nucleophilic attack by the cysteine R-amino group to form a native amide bond at the Xxx-Cys ligation site.
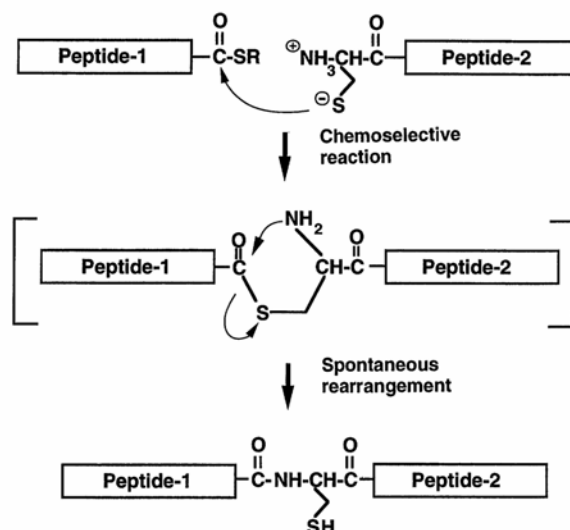


**Figure 5.4 Mechanism of the native chemical ligation.**

As model system was chosen a small peptide, containing only six amino acids with N-terminal cysteine residue. The peptide **P1** consists of the following sequence: Cys-Leu-Ser-Arg-Ala-Gly with molecular weight of 605. The protein was synthesized by Dr. Anke Lübbert, Max Planck Institute for Polymer Research using standard solid-phase peptide synthesis. A solution of the dye was incubated with the peptide overnight using standard conditions for native chemical ligation (Scheme 5.3). Unfortunately monitoring or separation of the reaction mixture was not possible using RP-HPLC. Previous observations and experience with sulfonated rylene chromophores has shown that separation of conjugates using reverse-phase HPLC is not possible, most probably due to the formation of aggregates.



Molecular Weight: 1488.57

Molecular Weight: 605.71

Molecular Weight: 1970.07
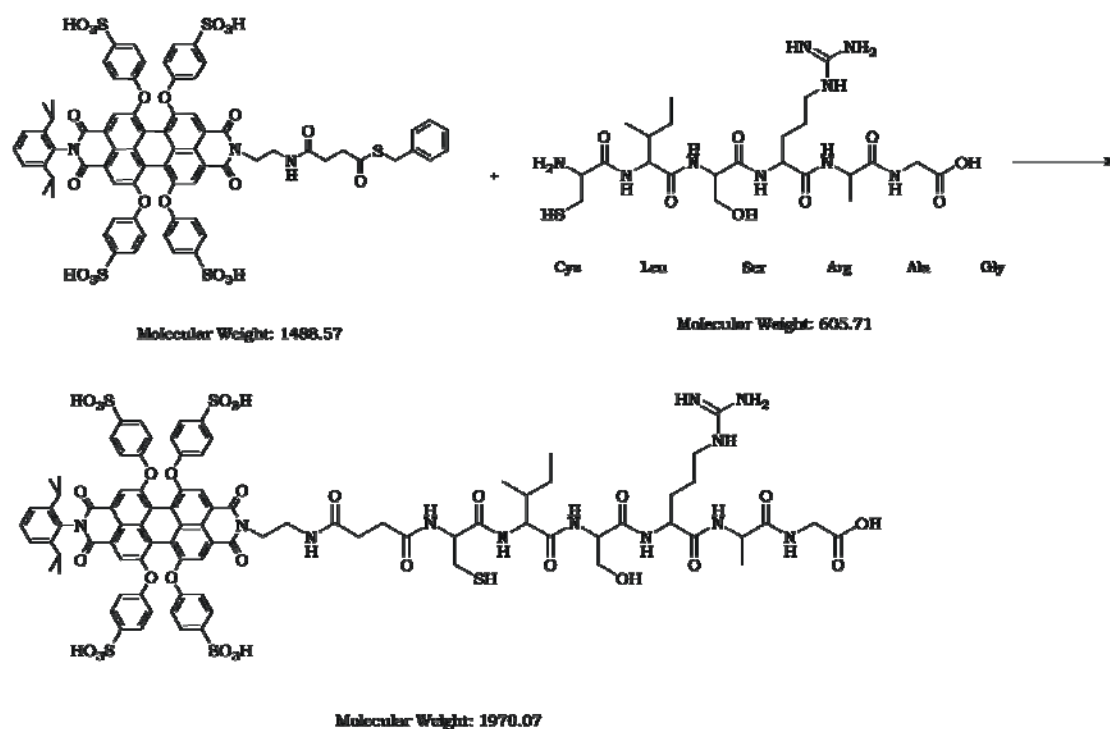
**Scheme 5.3. Native chemical ligation between 3.47 and a model hexapeptide**

While confirmed that separation or monitoring of the reaction between water-soluble perylene thioester and hexapeptide with HPLC is not possible, another polypeptide was chosen in order to be able to check the conjugation also by gel electrophoresis. A polypeptide **P2** consisting of twenty-six amino acid residues was selected. The sequence is a part of malaria antigen (Boykins A.R. et al.,

Peptides 2000, 21, 9.), and possesses more than ten polar groups to ensure good solubility of the peptide and N-terminal cystein residue is incorporated to enable the native chemical ligation. The peptide has the following sequence: Cys-Asn-Glu-Asn-Leu-Asp-Asp-Leu-Asp-Glu-Gly-Ile-Glu-Lys-Ser-Ser-Glu-Glu-Leu-Ser-Glu-Glu-Lys-Ile, and molecular weight of 2795 (Scheme 5.4).
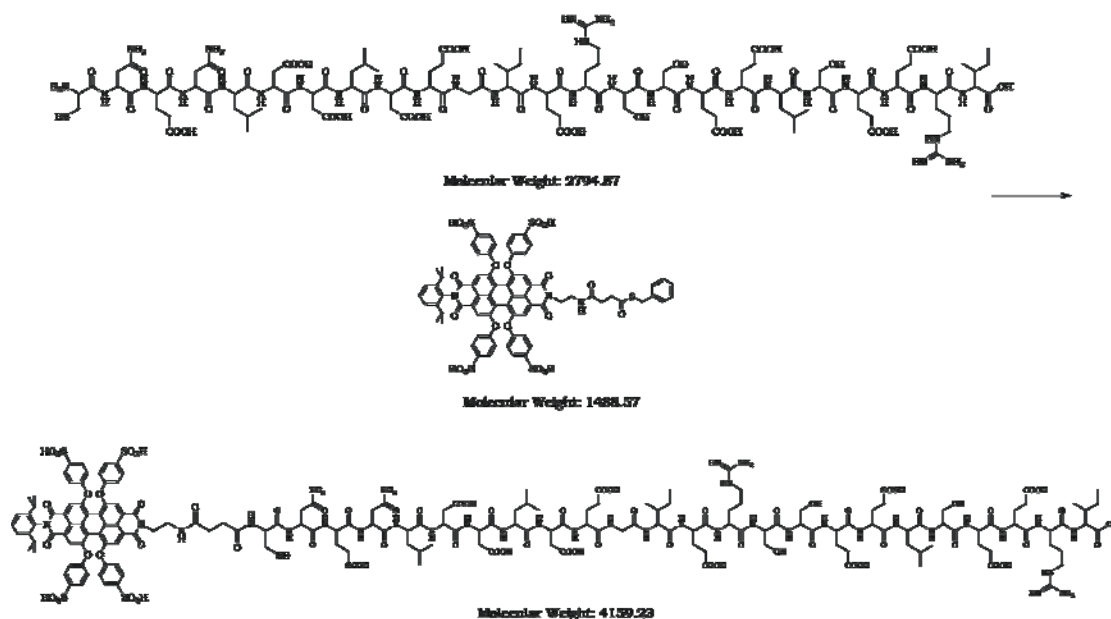


**Scheme 5.4 Native chemical ligation between 3.47 and polypeptide chemical structure of polypeptide P2 and bioconjugate**

Since the **P2** has a higher molecular weight than the previously used hexapeptide **P1** slightly different conditions were used for the ligation. The peptide was first incubated for five minutes with Tris-(2-carboxyethyl)-phosphine (TCEP) in order to reduce any disulfide bonds to sulfhydryls. Afterwards, buffer solution of the dye was added to the peptide and incubated at room temperature for 24 hours. The mixture was analyzed by analytical SDS-PAGE.

Surprisingly the dye and the protein showed the same electrophoretic mobility. The dye has a molecular weight of 1488 and four positive charges, the peptide P2 has a molecular weight of 2795, although it is expected that the conjugate would have molecular weight of 4160. The difference in molecular

weight and number of charges should cause different mobility of these three molecules on the gel, however the expected separation was not observed.

Generally, when new labeling strategy is evaluated a model peptide, containing the target functional group is incubated with a label and the subsequent conjugation is monitored by means of HPLC chromatography. If the monitoring of the labeling is not possible the conjugate is separated and characterized by gel-electrophoresis, HPLC chromatography or MS spectroscopy. Normally, small proteins or peptides are chosen as models, since they are easy to prepare by solid-phase synthesis on large scale and do not possess complicated secondary structures, which can interfere with the conjugation. For these reasons we have initially chosen two small peptides, prepared by solid-phase peptide synthesis, as model biomolecules for the conjugation via native chemical ligation. Our unsuccessful attempts to monitor or separate the labeled peptide, has provoked the choice of a considerably different model; the details for the labeling experiment will be given in the next section.

## 5.4. Native chemical ligation between perylene-thioester and plasminogen activator inhibitor with N-terminal cysteine residue.

To overcome the unexpected problems with the product separation of the native chemical ligation, different biomolecule was chosen - significantly larger protein. Plasminogen Activator Inhibitor 1 (PAI-1), a stable mutant, containing N-terminal cysteine residue was used in a native chemical ligation with the perylene thioester. PAI-1 is a glycoprotein found in plasma that is implicated in the processes of angoigenisis, hemostasis, tumor metastasis, fibrionlysis, ovulation, embryonic development and inflammation (Figure 5.5). The elevation of PAI-1 has shown to correlate with the prognosis of many cancers including breast cancer. PAI-1 is activated by the glycoprotein vitronectin. Vitronectin binds to PAI-1 and modulates fibrinolysis and cell migration. This binding has proven to be an important inhibitor

of the activated form of proteinC (APC). The PAI-1 is a member of the SERine Protease Inhibitor superfamily (SERPINS) and exhibits a molecular weight of 43 kDa.[38] The N-terminal cysteine containing PAI-1 was chosen as model protein in this study.
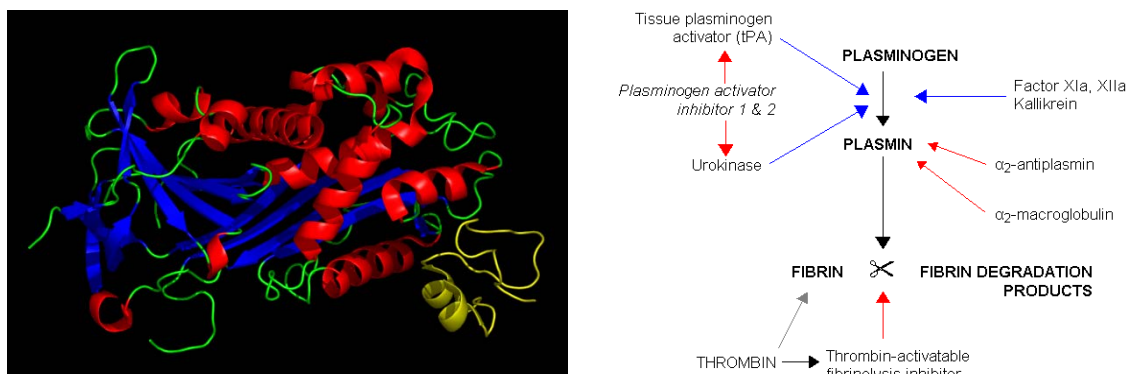


**Figure 5.5. Plasminogen activator inhibitor type 1 (left side); Fibrinolysis (simplified). Blue arrows denote stimulation and red arrows inhibition (right)**

The method and conditions applied for the labeling of the PAI-1 are the same as described by Dawson et al., 1994, which are often referred to as "standard native chemical ligation conditions".[35, 39] The conjugation is usually performed under very strongly denaturing conditions, which causes the reactivity of the N-terminal cysteine residue to be independent from the three-dimensional structures of the polypeptides in their native state. These strongly denaturing conditions ensure that the reactivity of the N-terminal cysteine is independent from the three-dimensional structure of the protein in its native state. Additionally, 4% thiophenol is included in the reaction mixture. This has been shown to accelerate the reaction and increase reaction yields due to the formation of the more reactive phenyl thioester through in situ transesterification. Excess thiol keeps cysteine side chains reduced and catalyzes the reversal of unproductive thioester formation.

Under these conditions transesterification of the thioester **3.47** with the cysteine thiol of the protein occurs, followed by an S-N acyl shift to generate the conjugate that exhibits a stable amide bond. (Scheme 5.5)
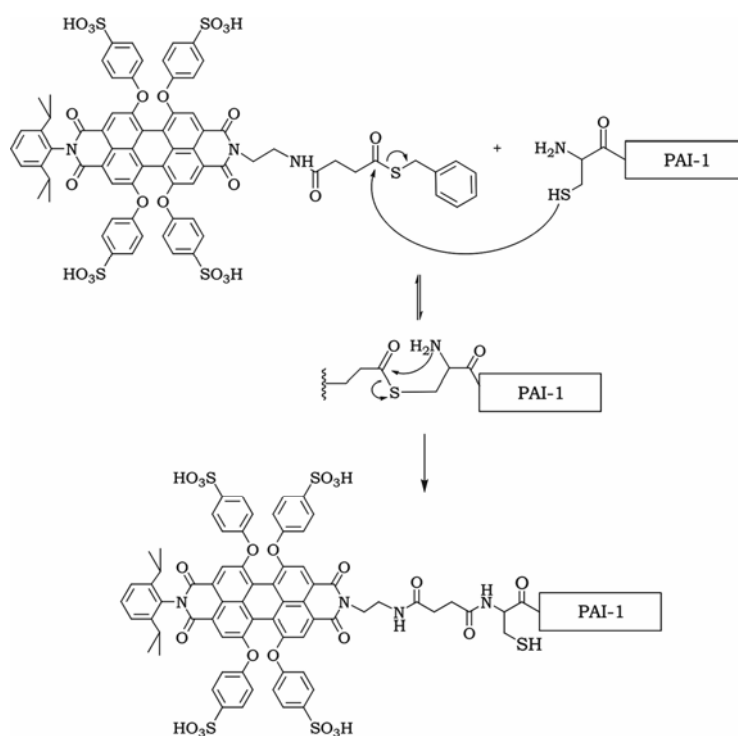
**Scheme 5.5 Conjugation between PAI-1 N-terminal cysteine and 3.47**

The PAI-1 N-terminal cystein mutant was dissolved in 100 mM phosphate buffer, containing 6 M GdmCl, 4 % v/v thiophenol and 100 mM sodium phosphate at pH 7,6 to a final protein concentration of 2 mM. An equimolar amount of the dye was dissolved in the same buffer and added to the protein solution. Then the reaction mixture was incubated at room temperature for 24 hours. An analytical SDS-PAGE electrophoresis confirmed the successful labeling of the PAI-1, with compound **3.47** (Figure 5.6)

The gel showed undoubtedly the presence of a lane with molecular weight slightly higher than the starting protein, a lane moving slower than the PAI-1 itself and having lower electrophoretic mobility. Since the reaction was performed at strongly denaturing condition, after the addition of the buffer containing 6 M GdmCl, the protein precipitated.
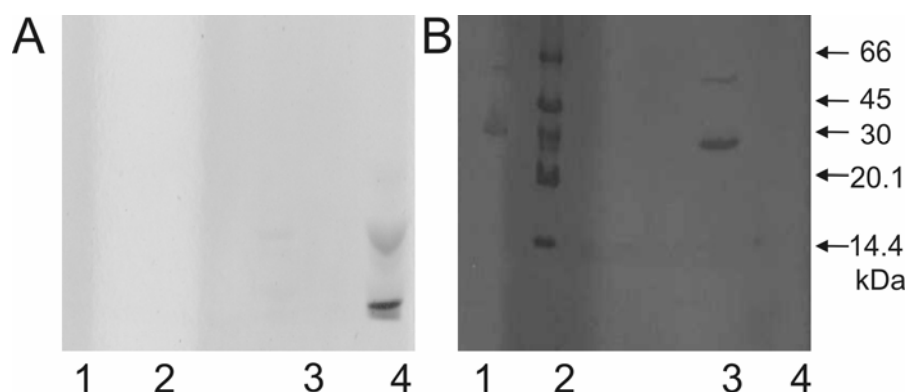
**Figure 5.6. SDS-PAGE electrophoresis of the labeled PAI-1. Panel A corresponds to UV-transillumination visualization. Panel B was stained with Coomassie Blue. Lane 1 is the labeled PAI-1. Lane 4 contains compound 3.47. Lane 3 is the N-terminal cystein PAI-1 and lane 2 is a molecular weight marker.**

Denatured Perylene- PAI-1 conjugate was refolded by dialysis (2 h, 4°C) in 20 mM Na-acetate, 1 M NaCl, 0.01% Tween-80 (v/v), pH 5,6 followed by a second dialysis step (overnight, 4°C). The protein was subsequently concentrated and analyzed.

The successful refolding of the Perylene-PAI-1 conjugate was confirmed by fluorescence correlation spectroscopy (FCS) analysis of the protein solution. (Figure 5.7) The diffusion time of the refolded Perylene-PAI-1 was 1.7 times larger than for the Perylene-thioester **3.47**, and 3.3 times larger than sulforhodamine B at 150 µW excitation power. Using low excitation power of 85 µW, the diffusion time of the refolded Perylene-PAI-1 was 2.6±0.4 times larger compared to sulforhodamine B and 3.0±0.35 times larger compared to perylene-thioester **3.47**. PAI-1 is a barrel-shaped protein of 43 kDa with a height of 7.4 nm and a diameter of 4.5 nm.[40] Two estimation approaches were applied to correlate the diffusion times of Perylene-PAI-1 with its structure. First, approximating similar densities for protein and dyes, the relative diffusion time increase compared to perylene-thioester can be estimated from the ratio of molecular weights by a factor 3.1, and compared to sulforhodamine B by a factor 4.3, which are both in agreement with the measured FCS data. Secondly, the effective hydrodynamic radius $R_H$ of a folded perylene-

PAI-1 was calculated using the crystallographic dimensions of a cylinder.[41] $R_H$ = 3.04 nm corresponded to a diffusion time increase by a factor 5 compared to sulforhodamine B assuming a hydrodynamic radius $R_H$ = 0.6 nm similar to rhodamine 6 G.[42] In contrast the unfolded protein consisting of 379 amino acids is expected to behave like a random-coil polymer and to exhibit a radius of gyration $R_G$ = 4.63 nm.[43] Accordingly a diffusion time increase of at least factor 7 compared to sulforhodamine B is expected for the denatured PAI-1. Taking both estimation approaches together, the measured diffusion times of perylene-labeled PAI-1 can be related only to the folded, more compact protein, but not a denatured protein with random coil structure.
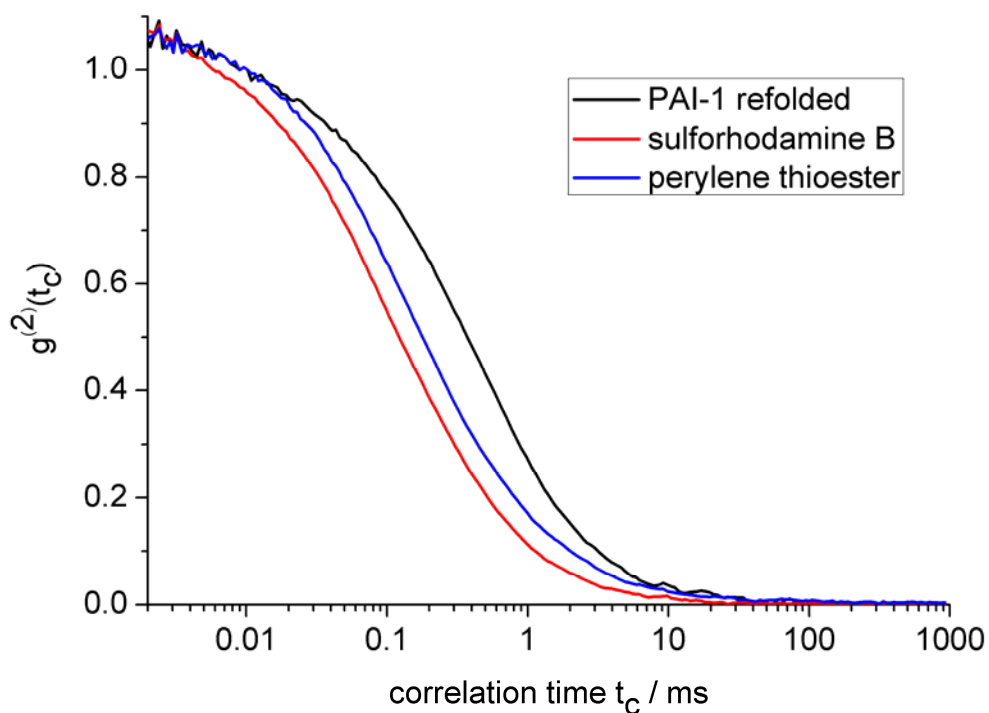


**Figure 5.7. Normalized autocorrelation functions $g^{(2)}(t_c)$ of sulforhodamine B in water (red curve), perylene-thioester (blue) as well as the refolded protein PAI-1 labeled with perylene-thioester (black), measured in PBS buffer at 22°C. $t_c$ = correlation time.**

The FCS analysis of perylene-thioester showed only half the molecular brightness compared to a single sulforhodamine B. However the extinction coefficient of the perylene is only one third of sulforhodamine B at laser excitation wavelength of 561 nm. Accordingly the molecular brightness of a single perylene-thioester as measured by FCS indicates a fluorescence quantum yield similar to sulforhodamine B. After binding to PAI-1 the brightness of the perylene dye slightly decreased by 15 percent. This indicates an almost independent fluorescence quantum yield from the local protein environment, which makes the perylene dye a very attractive new label for N-terminal cysteines in proteins.

In summary, the powerful reaction of native chemical ligation is exploited for site-specific labeling of proteins with water-soluble perylene, bearing thioester group. This required the preparation of a water-soluble perylene chromophore, decorated with thioester functional group. Fluorescent probes, suitable for native chemical ligation, were previously reported by Yao et al.[44] They are based on fluorescein and rhodamine, and even though they have high extinction coefficient and reactive group for specific attachment; they suffer from low water-solubility and low photostability. The fluorophore presented here combines excellent water-solubility, high fluorescence quantum yield, functional groups for selective labeling and excellent photostability. The perylene thioester underwent reaction under standard "native chemical ligation" conditions with a protein having an amino-terminal cysteine. The successful attachment was proven by gel electrophoresis and fluorescence correlation spectroscopy. By applying the latter technique it was also demonstrated that the perylene chromophore maintains its excellent photophysical properties in the presence of the protein environment.

## 5.5. References

[1] H. Jung, R. Lopez, C. Altenbach, W. L. Hubbell, H. R. Kaback, *Biophys. J.* **1993**, *64*, A14, *Site-Directed Spin and Fluorescent Labeling of the Lactose Permease of Escherichia-Coli*.

[2] M. R. Eftink, *Methods of Biochemical Analysis* **1991**, *35*, 127, *Fluorescence Techniques for Studying Protein-Structure*.

[3] J. Brunner, *Annu. Rev. Biochem.* **1993**, *62*, 483, *New Photolabeling and Cross-Linking Methods*.

[4] V. W. Cornish, D. R. Benson, C. A. Altenbach, K. Hideg, W. L. Hubbell, P. G. Schultz, *PNAS* **1994**, *91*, 2910, *Site-Specific Incorporation of Biophysical Probes into Proteins*.

[5] B. A. Griffin, S. R. Adams, R. Y. Tsien, *Science* **1998**, *281*, 269, *Specific covalent labeling of recombinant protein molecules inside live cells*.

[6] S. R. Adams, R. E. Campbell, L. A. Gross, B. R. Martin, G. K. Walkup, Y. Yao, J. Llopis, R. Y. Tsien, *J. Am. Chem. Soc.* **2002**, *124*, 6063, *New biarsenical Ligands and tetracysteine motifs for protein labeling in vitro and in vivo: Synthesis and biological applications*.

[7] G. Gaietta, T. J. Deerinck, S. R. Adams, J. Bouwer, O. Tour, D. W. Laird, G. E. Sosinskyl, R. Y. Tsien, M. H. Ellisman, *Science (Washington, DC, U. S.)* **2002**, *296*, 503, *Multicolor and electron microscopic imaging of connexin trafficking*.

[8] U. Lauf, B. N. G. Giepmans, P. Lopez, S. Braconnot, S.-C. Chen, M. M. Falk, *Proc. Natl. Acad. Sci. U. S. A.* **2002**, *99*, 10446, *Dynamic trafficking and delivery of connexons to the plasma membrane and accretion to gap junctions in living cells*.

[9] A. Keppler, S. Gendreizig, T. Gronemeyer, H. Pick, H. Vogel, K. Johnsson, *Nat. Biotechnol.* **2003**, *21*, 86, *A general method for the covalent labeling of fusion proteins with small molecules in vivo*.

[10] A. Juillerat, T. Gronemeyer, A. Keppler, S. Gendreizig, H. Pick, H. Vogel, K. Johnsson, *Chem. Biol.* **2003**, *10*, 313, *Directed Evolution of O6-Alkylguanine-DNA Alkyltransferase for Efficient Labeling of Fusion Proteins with Small Molecules In Vivo*.

[11] E. A. Lipman, B. Schuler, O. Bakajin, W. A. Eaton, *Science* **2003**, *301*, 1233, *Single-molecule measurement of protein folding kinetics*.

[12] B. Schuler, E. A. Lipman, W. A. Eaton, *Nature* **2002**, *419*, 743, *Probing the free-energy surface for protein folding with single-molecule fluorescence spectroscopy*.

[13] J. A. Schmid, A. Birbach, *Thromb. Haemostasis* **2007**, *97*, 378, *Fluorescent proteins and fluorescence resonance energy transfer (FRET) as tools in signaling research*.

[14] B. Zimmermann, M. Diez, N. Zarrabi, P. Graeber, M. Börsch, *EMBO J.* **2005**, *24*, 2053, *Movements of the e-subunit during catalysis and activation in single membrane-bound H+-ATP synthase*.

[15] A. N. Kapanidis, Y. W. Ebright, R. H. Ebright, *J. Am. Chem. Soc.* **2001**, *123*, 12123, *Site-specific incorporation of fluorescent probes into protein: Hexahistidine-tag-mediated fluorescent labeling with (Ni2+:Nitrilotriacetic Acid)n-fluorochrome conjugatesfluorescent probes*.

[16] D. Magde, E. L. Elson, W. W. Webb, *Biopolymers* **1974**, *13*, 29, *Fluorescence Correlation Spectroscopy .2. Experimental Realization*.

[17] Ehrenber.M, R. Rigler, *Chem. Phys.* **1974**, *4*, 390, *Rotational Brownian-Motion and Fluorescence Intensity Fluctuations*.

[18] S. R. Aragon, R. Pecora, *J. Chem. Phys.* **1976**, *64*, 1791, *Fluorescence correlation spectroscopy as a probe of molecular dynamics*.

[19] P. Kask, K. Palo, D. Ullmann, K. Gall, *Proc. Natl. Acad. Sci. U. S. A.* **1999**, *96*, 13756, *Fluorescence-intensity distribution analysis and its application in biomolecular detection technology*.

[20] J. Widengren, U. Mets, R. Rigler, *J. Phys. Chem.* **1995**, *99*, 13368, *Fluorescence correlation spectroscopy of triplet states in solution: a theoretical and experimental study*.

[21] B. Rauer, E. Neumann, J. Widengren, R. Rigler, *Biophys. Chem.* **1996**, *58*, 3, *Fluorescence correlation spectrometry of the interaction kinetics of tetramethylrhodamine a-bungarotoxin with Torpedo californica acetylcholine receptor.*

[22] G. Bonnet, O. Krichevsky, A. Libchaber, *Proc. Natl. Acad. Sci. U. S. A.* **1998**, *95*, 8602, *Kinetics of conformational fluctuations in DNA hairpin-loops.*

[23] U. Haupts, S. Maiti, P. Schwille, W. W. Webb, *Proc. Natl. Acad. Sci. U. S. A.* **1998**, *95*, 13573, *Dynamics of fluorescence fluctuations in green fluorescent protein observed by fluorescence correlation spectroscopy.*

[24] J. Widengren, R. Rigler, *Bioimaging* **1996**, *4*, 149, *Mechanisms of photobleaching investigated by fluorescence correlation spectroscopy.*

[25] C. Eggeling, J. Widengren, R. Rigler, C. A. M. Seidel, *Anal. Chem.* **1998**, *70*, 2651, *Photobleaching of fluorescent dyes under conditions used for single-molecule detection: evidence of two-step photolysis.*

[26] M. G. Düser, N. Zarrabi, Y. Bi, B. Zimmermann, S. D. Dunn, M. Börsch, *Proceedings of SPIE-The International Society for Optical Engineering* **2006**, *6092*, 60920H/1, *3D-localization of the a-subunit in F0F1-ATP synthase by time resolved single-molecule FRET.*

[27] C. Lefevre, H. C. Kang, R. P. Haugland, N. Malekzadeh, S. Arttamangkul, R. P. Haugland, *Bioconjugate Chem.* **1996**, *7*, 482, *Texas Red-X and Rhodamine Red-X, New Derivatives of Sulforhodamine 101 and Lissamine Rhodamine B with Improved Labeling and Fluorescence Properties.*

[28] K. Peneva, G. Mihov, F. Nolde, S. Rocha, J. Hotta, K. Braeckmans, J. Hofkens, H. Uji-i, A. Herrmann, K. Müllen, *Angew. Chem. Int. Ed.* **2007**, *accepted*, *Water-soluble monofunctional perylene and terrylene dyes: powerful labels for single enzyme tracking.*

[29] K. Peneva, G. Mihov, A. Herrmann, N. Zarrabi, M. Börsch, T. Duncan, K. Müllen, *J. Am. Chem. Soc.* **2008**, *130*, 5398, *Exploiting the nitrilotriacetic acid moiety for biolabeling with ultrastable perylene dyes.*

[30] T. W. Muir, D. Sondhi, P. A. Cole, *Proc. Natl. Acad. Sci. U. S. A.* **1998**, *95*, 6705, *Expressed protein ligation: A general method for protein engineering.*

[31] Y. Shin, K. A. Winans, B. J. Backes, S. B. H. Kent, J. A. Ellman, C. R. Bertozzi, *J. Am. Chem. Soc.* **1999**, *121*, 11684, *Fmoc-based synthesis of*

*peptide-(alpha)thioesters: Application to the total chemical synthesis of a glycoprotein by native chemical ligation.*

[32] B. Schuler, L. K. Pannell, *Bioconjugate Chem.* **2002**, *13*, 1039, *Specific Labeling of polypeptides at amino-terminal cysteine residues using Cy5-benzyl thioester.*

[33] A. K. Mapp, *Tetrahedron Lett.* **2000**, *41*, 9451, *Preparation of thioesters for the ligation of peptides with non-native substrates.*

[34] J. R. Lakowicz, *Principles of Photoluminescence Spectroscopy*, 2nd ed. ed., Kluwer Academic/Plenum Publishers, Dordrecht, **1999**.

[35] P. E. Dawson, T. W. Muir, I. Clarklewis, S. B. H. Kent, *Science* **1994**, *266*, 776, *Synthesis of Proteins by Native Chemical Ligation.*

[36] P. E. Dawson, M. Churchill, M. R. Ghadiri, S. B. H. Kent, *J. Am. Chem. Soc.* **1997**, *119*, 4325, *Modulation of Reactivity in Native Chemical Ligation through the Use of Thiol Additives.*

[37] T. M. Hackeng, J. H. Griffin, P. E. Dawson, *Proc. Natl. Acad. Sci. U. S. A.* **1999**, *96*, 10068, *Protein synthesis by native chemical ligation: Expanded scope by using straightforward methodology.*

[38] M. C. Alessi, P. J. Declerck, M. Demol, L. Nelles, D. Collen, *Eur. J. Biochem.* **1988**, *175*, 531, *Purification and Characterization of Natural and Recombinant Human-Plasminogen Activator Inhibitor-1 (Pai-1).*

[39] P. E. Dawson, M. J. Churchill, M. R. Ghadiri, S. B. H. Kent, *Journal of the American Chemical Society*
 **1997**, *119*, 4325, *Modulation of reactivity in native chemical ligation through the use of thiol additives.*

[40] H. Nar, M. Bauer, J. M. Stassen, D. Lang, A. Gils, P. J. Declerck, *J. Mol. Biol.* **2000**, *297*, 683, *Plasminogen activator inhibitor 1. Structure of the native serpin, comparison to its other conformers and implications for serpin inactivation.*

[41] K. Ding, F. E. Alemduroglu, M. Börsch, R. Berger, A. Herrmann, *Angew. Chem., Int. Ed.* **2007**, *46*, 1172, *Engineering the structural properties of DNA block copolymer micelles by molecular recognition.*

[42] G. Porter, P. J. Sadkowski, C. J. Tredwell, *Chem. Phys. Lett.* **1977**, *49*, 416, *Picosecond Rotational Diffusion in Kinetic and Steady-State Fluorescence Spectroscopy.*

[43] J. E. Kohn, I. S. Millett, J. Jacob, B. Zagrovic, T. M. Dillon, N. Cingel, R. S. Dothager, S. Seifert, P. Thiyagarajan, T. R. Sosnick, M. Z. Hasan, V. S. Pande, I. Ruczinski, S. Doniach, K. W. Plaxco, *Proc. Natl. Acad. Sci. U. S. A.* **2004**, *101*, 12491, *Random-coil behavior and the dimensions of chemically unfolded proteins*.

[44] D. S. Y. Yeo, R. Srinivasan, M. Uttamchandani, G. Y. J. Chen, Q. Zhu, S. Q. Yao, *Chem. Commun.* **2003**, 2870, *Cell-permeable small molecule probes for site-specific labeling of proteins*.

# 6. Exploiting the nitrilotriacetic acid moiety for biolabeling using rylene dyes

In the following chapter we exploit oligohisitidine sequences as recognition elements for site-selective labeling. These genetically encoded tags can be introduced into regions of the amino acid sequence where they do not disturb the protein's structure and function such as at the termini or in loops. Oligohisitidine sequences are widely applied in combination with NTA for purification, in vitro detection and surface immobilization of recombinant proteins. The preparation of new nitrilotriacetic acid modified perylene chromophore is described and its photophysical properties studied. The ability of the new chromophore to label proteins will be demonstrated. The Fluorescence Correlation spectroscopy (FCS) experiments were done in cooperation with Dr. Michael Börsch, Universität Stuttgart, Stuttgart, Germany. The $His_6$-tagged $F_1$ complex of $F_oF_1$-ATP synthase was prepared and supplied by Dr. Thomas M. Duncan, Department of Biochemistry and Molecular Biology, SUNY Upstate Medical University, Syracuse, NY, USA.

In the current era of proteome research, generic tools for labeling, handling, modifying and organizing proteins are increasingly demanded. Numerous methodologies for selective, site-specific conjugation of proteins with reporter molecules, such as organic fluorophores, spin labels or nanoparticles have been reported.[1-3] Non-covalent conjugation has most frequently served as an engineering principle for a selective and specific attachment to proteins.[4-9] Biological recognition units such as antibodies have reached high affinity and unmatched specificity towards their targets by an optimal interplay of many weak noncovalent forces such as hydrophobic interactions, hydrogen bonding, electrostatics, π-π stacking or cation-π interactions.

Chemical and biological labeling is essential for the exploration of protein function, as fluorescent probes allow detection of molecular interactions, mobilities and conformational changes.

Especially fluorescence resonance energy transfer (FRET) has become an important tool to study conformational distributions and dynamics of biomacromolecules[10]. This however, requires the ability to introduce fluorescent reporters at specific sites[10]. One of the most frequently used approaches for selective labeling of proteins is to introduce a non-native cysteine at a desired location, while the chromophore possesses a thiol reactive group. This approach suffers from the disadvantage that the number and position of native cysteines are practically important for the structure and biological function of various proteins like cysteine-based oxidoreductases, phosphatases and proteases [11].

## 6.1. Nitrilotriacetic acid functionalized chromophores

The most widely used genetically encoded tag is the polyhistidine tag, which usually consists of 2-6 consecutive histidine residues[12, 13]. It was originally developed for the purification of recombinant proteins by immobilized metal-affinity chromatography. Transition metal chelated by nitrilotriacetic acid (NTA) or other chelates have been successfully applied for purification and detection of oligohistidine-tagged proteins, as well as for immobilization on surfaces.[12-18] Different modifications of this molecular recognition technique have been exploited including target protein detection and protein structure studies[19, 20]. This strategy has been also utilized to introduce a chromophore containing a nitrilotriacetic acid (NTA) moiety into a His-tagged protein. [21-23] Ebright et al. were the first to introduce the NTA unit into a commercially available chromophore for the preparation of fluorescent probes for site-specific hexahistidine-tag-mediated labeling of proteins (Figure 6.1). Simple one-step coupling of the highly fluorescent Cy3 and Cy5 N-hydroxysuccinimide esters with nitrilotriacetic acid gave the NTA functionalized chromophores.[23]
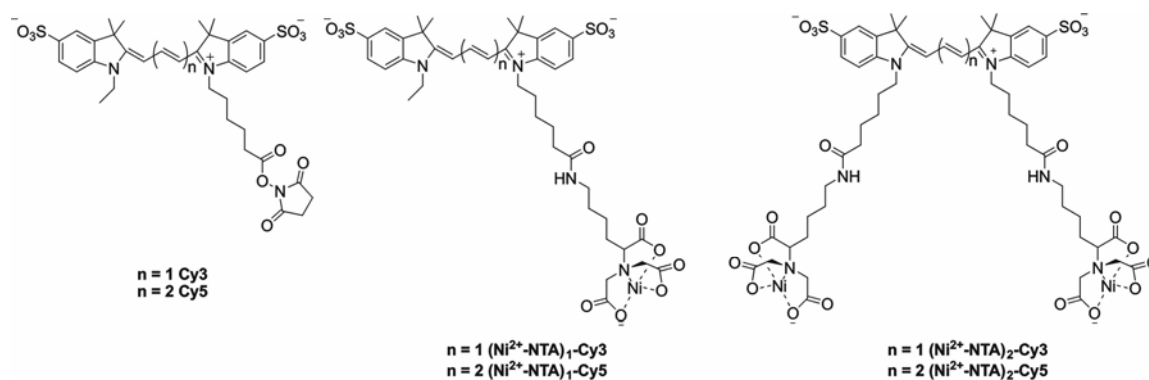
**Figure 6.1. (Ni2+:NTA)n derivatives of cyanine fluorochromes Cy3 and Cy5**

Piehler et al. used different approach and engineered a chemical recognition unit with high affinity for oligohisitidne tagged proteins.[22, 24] Three NTA moieties were grafted on a cyclic scaffold to form tris-NTA, containing an additional functional group for coupling fluorophores. Tris-NTA was coupled to Oregon Green 488, ATTO 565 and the Cy5-analogue FEW 646 (Figure 6.2).[22, 24]
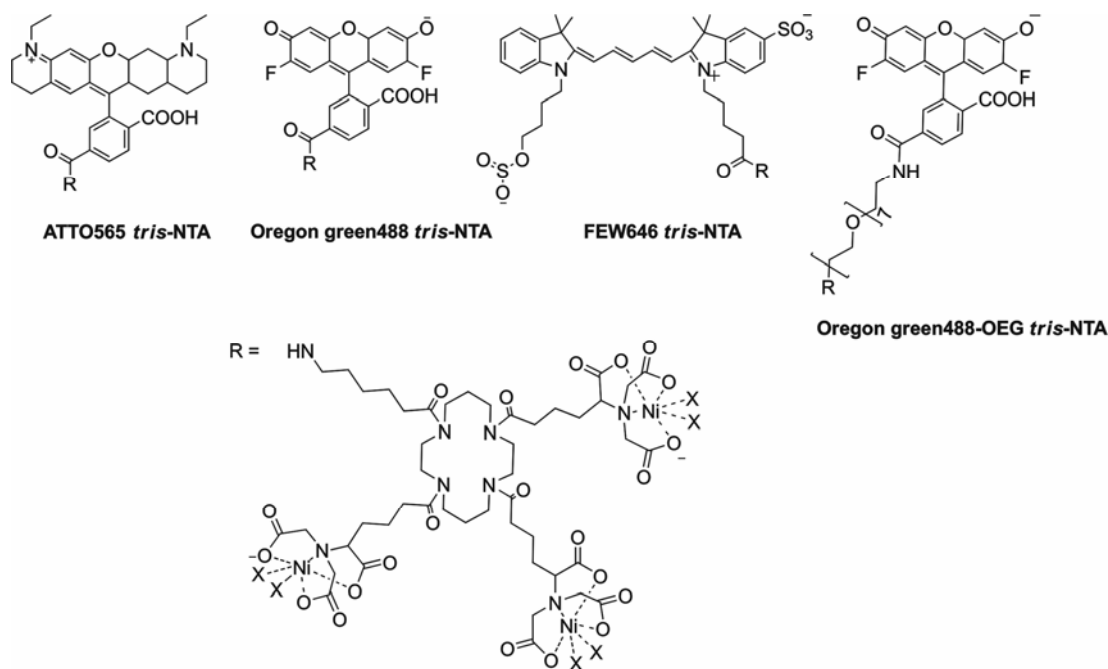


**Figure 6.2. Chemical structures of the tris-NTA/fluorophore conjugates OG488-trisNTA, AT565-trisNTA, FEW646-trisNTA and OG488-OEG-trisNTA. Additional ligands coordinated by the chelated Ni(II) ions are denoted by X.**

It is known that fluorophores proximal to paramagnetic transition metal are liable to alternation in their photophysical properties, primarily quenching of the fluorescence by electron and energy transfer.[25-28] This was the main reason why all of the reported chromophores, possessing NTA moiety, suffer from one drawback – a severe loss of the fluorescence upon binding of the paramagnetic nickel ion. When $Ni^{2+}$ was complexed with the NTA moiety, attached to commercial Cy3 and Cy5 dyes, the fluorescence quantum yield dropped by 75%.[23] Quenching by ~50% for OG488-tris-NTA, ~80% for ATTO565-tris-NTA and ~ 60% for FEW646-tris-NTA was observed upon loading with Ni (II) ions. Although the quenching of the fluorescence is distance dependant, fluorescence quenching was observed even in the OG488-OEG-tris-NTA upon loading with Ni (II) ions, in spite of the introduction of significantly longer spacer between the NTA moiety and the fluorophore.[22]

## 6.2. Preparation of water-soluble perylene containing NTA moiety

Two synthetic strategies were elaborated to attach the NTA moiety to the perylene chromophore. One is based on solution-phase synthesis, while the other relies on a solid-phase approach.

In the first route, the water-soluble perylene N-hydroxysuccinimide ester **3.32** was reacted with t-butyl protected nitrilotriacetic acid (Scheme 6.1). The removal of the t-butyl protective groups was achieved by treatment of **3.48** with trifluoroacetic acid in DMSO and **3.49** was obtained in 70 % yield.

**3.32**            **3.48**            **3.49**
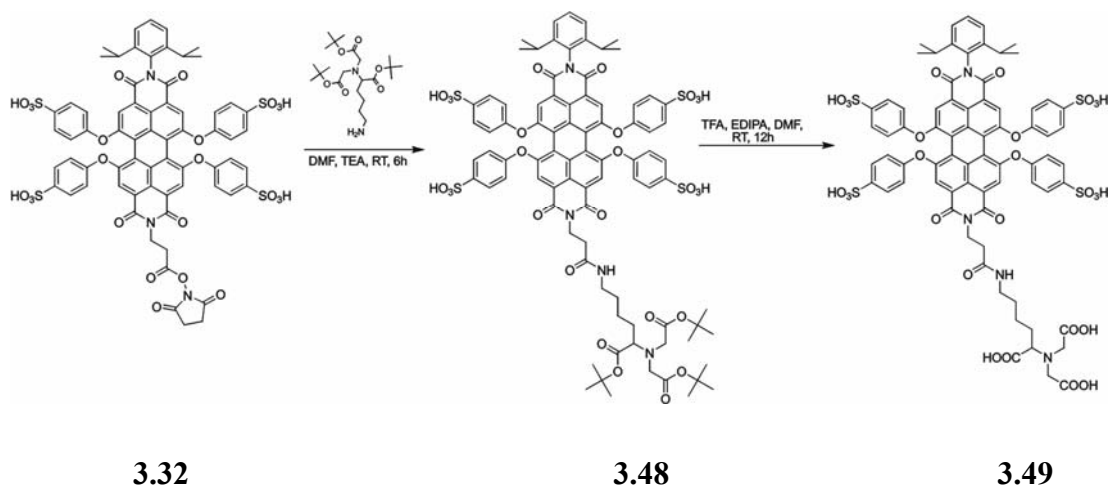
**Scheme 6.1: Solution-phase synthesis of 3.49**

In the second approach we took advantage of a straightforward solid-phase synthesis of a nitrilotriacetic acid moiety that was developed by Meredith et al [29]. The NTA unit was conveniently coupled to a carboxyl functionalized perylene derivative by amide bond formation (Scheme 6.2).



**3.50**            **3.51**            **3.49**
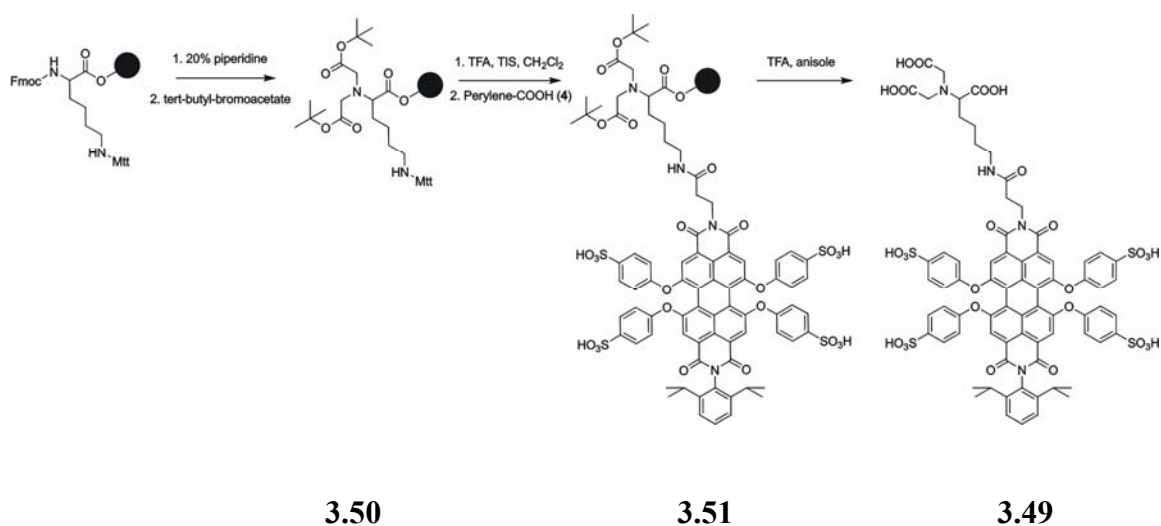
**Scheme 6.2: Solid-phase synthesis of 3.49**

Solid-phase peptide synthesis offers important advantages over synthesis in solution, namely coupling reactions can be carried out more rapidly and nearly to completion, using an excess of the activated amino acid derivative, which is removed at the end of the reaction by simple washing operations.

In our case hydrophilic resins gave better results, in comparison with the classical Merrifield's solid support, which consists of cross-linked poly(styrene-divinylbenzene). Therefore, we have chosen to use a resin that posses PEG chains grafted onto the polystyrene beads due to their high mechanical stability and good solvation behavior. Initially the resin was swollen in dichloromethane, and lysine containing two orthogonal protecting groups (Fluorenylmethoxycarbonyl – *Fmoc* and Methyltrityl - *Mtt*) was loaded onto it. For activation of the carboxy groups was used *FastMoc* chemistry procedure.[30] O-(Benzotriazol-1-yl)-N,N,N,′-tetramethyl uronium hexafluorophosphate (HBTU) was dissolved in a mixture of 1-Hydroxybenzotriazole hydrate (HOBt), diisopropylethylamine (DIPEA) and N,N'-dimethylformamide (DMF). The amino acid was added in this solution in additional DMF. Activated amino acid was formed almost instantaneously and transferred directly to the reaction vessel. After removal of the Fmoc protection group, using repetitive treatments with 20% solution of piperidine in dichloromethane, 20 fold excess of tert-butyl-bromacetate was applied to give **3.51**. Carboxy functionalized perylene(dicarboximide) was activated using again *FastMoc* chemistry and attached to the modified lysine. The product was cleaved from the resin by several treatments with 95% TFA in DCM.

For both solution and solid-phase synthetic routes the isolated product was dissolved in water and purified by size-exclusion chromatography using BioGel as stationary phase and water as eluent. The chemical structure and purity of the final compound was confirmed by $^1$H-NMR and $^{13}$C-NMR spectroscopy.
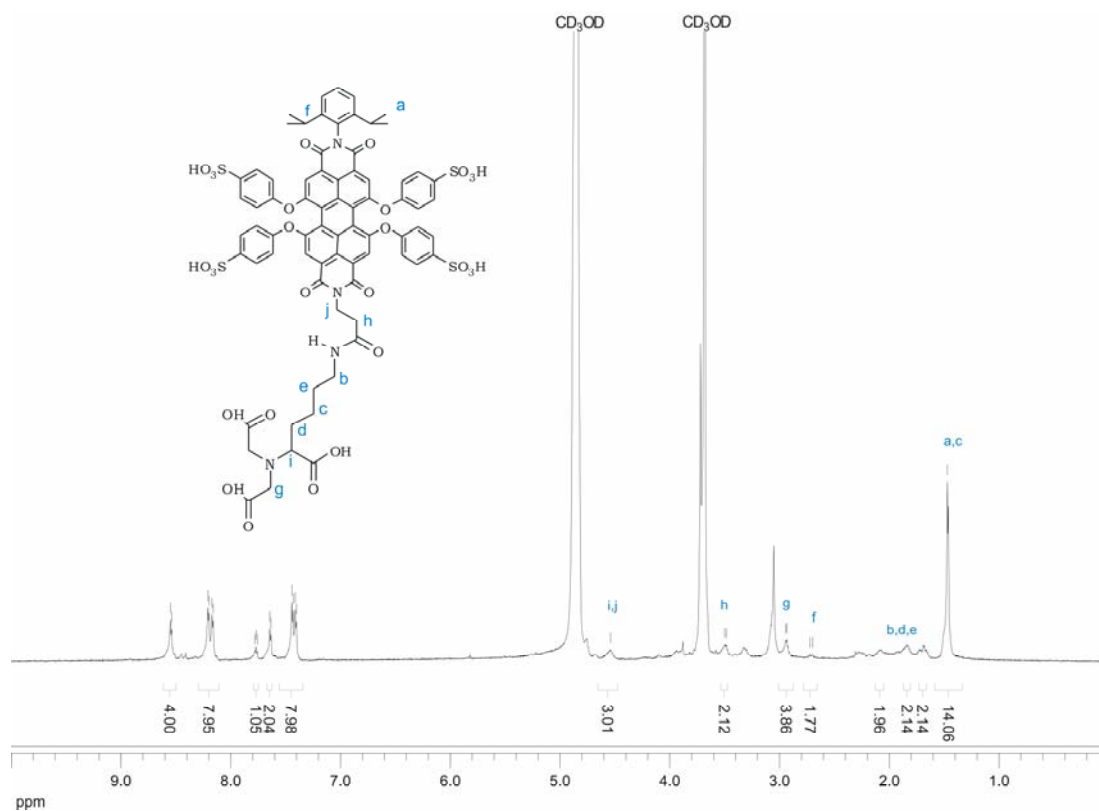
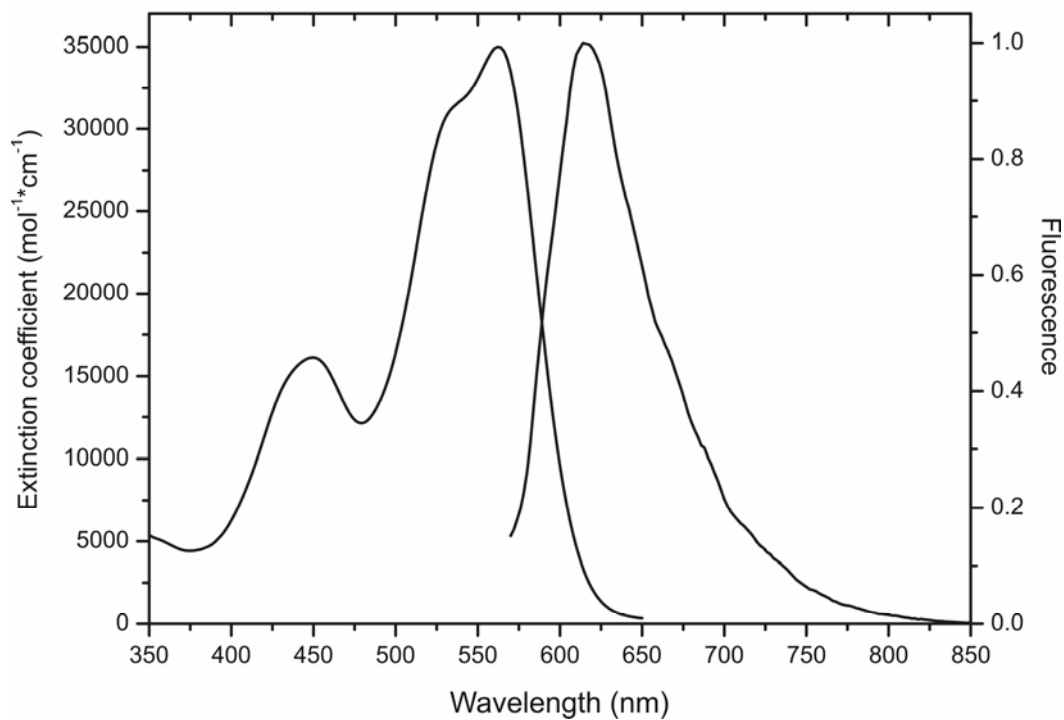**Figure 6.3:** $^1$**H-NMR spectrum (700 MHz) of 3.49 in CD₃OD**



**Figure 6.4: Normalized absorbance and fluorescence spectra of 3.49 in water**

The nitrilotriacetic acid functionalized perylene(dicarboximide) **3.49** has an absorption maximum at 562 nm ($\varepsilon$ = 35 000 $M^{-1}$ $cm^{-1}$). The emission maximum is located at 615 nm (Figure 6.4). A fluorescence quantum yield of 15 % for **3.49** was determined by using Cresyl Violet in methanol as reference.[31] When the same quantum yield measurement was carried out with the $Ni^{2+}$ complexes of **3.49** no decrease in the fluorescence was observed. In addition the absorption and emission maxima remained unchanged.

The new fluorescent reporter has relatively small molecular weight (1555 g/mol), which makes it a good candidate for labeling proteins, at the same time avoiding the limitation of the large size of autofluorescent proteins or quantum dots. Protein labeling with the NTA functionalized perylene(dicarboximide) is successfully demonstrated using His-tagged Small Ubiquitin-Related modifier – 1 and performing FCS experiments with His-tagged ATP synthase.

## 6.3. Site-specific labeling of His-tagged Small Ubiquitin-Related modifier – 1 using NTA functionalized perylene(dicarboximide)

To prove the suitability of the newly synthesized perylene NTA for protein labeling, small histidine-tagged protein was labeled and the conjugate characterized. As a model protein for our study we have chosen the hexahistidine-tagged Small Ubiquitin-Related modifier-1 (SUMO-1). The histidine-tagged SUMO was obtained from BIOMOL International LP.

SUMO-1 belongs to the growing family of ubiquitin-related proteins involved in posttranslational protein modification. Post-translational modification of proteins is an important means to alter their function, activity or localization after their synthesis has been completed.[32-36] In these cases, specific amino-acid residues of target proteins are chemically modified by various molecules, such as phosphate, acetate, lipids or sugars. Modification with ubiquitin represents a unique case

because the modifier itself is a small polypeptide. Ubiquitin is usually attached to lysine side chains of target proteins, resulting in "branched" isopeptide linked ubiquitin-protein conjugates.

Unlike ubiquitin, SUMO-1 does not appear to target proteins for degradation but seems to be involved in the modulation of protein-protein interactions. Independent studies demonstrate an essential function of SUMO-1 in the regulation of nucleo-cytoplasmic transport, and suggested a role in cell-cycle regulation and apoptosis.[33, 37, 38]

The His-tagged SUMO-1 used is a recombinant protein produced in E. coli corresponding to the human sequence encompassing an N-terminal $His_6$-tagged within a leader sequence. The molecular weight of this recombinant material is 16021 Da. The structure of human SUMO1 is depicted on Figure 6.5.
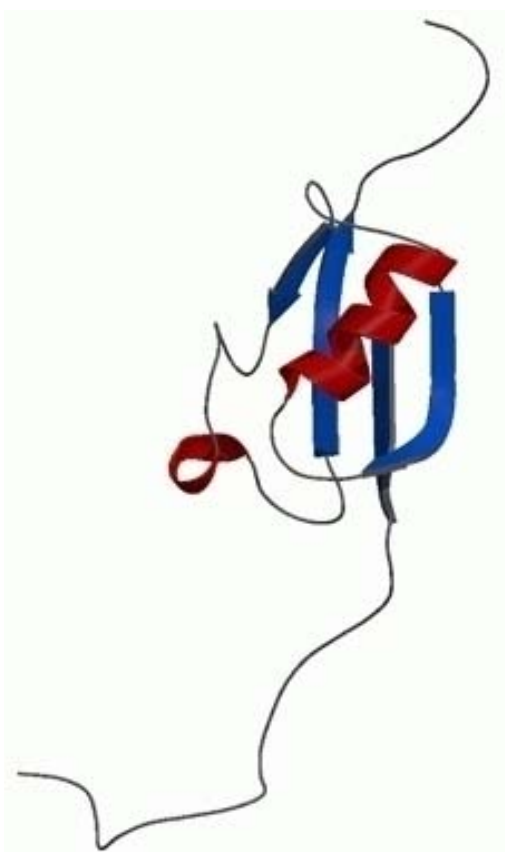


**Figure 6.5.Model of SUMO-1, based on crystal structure and NMR studies[32]**

SUMO-1 is shown as a globular protein with both ends of the amino acid chains sticking out of the protein's centre. The spherical core consists of an alpha helix and a beta sheet. The structure shown is based on NMR analysis in solution, and crystal structure of the protein.[32]

The protein was labeled using the following procedure. The NTA functionalized perylene(dicarboximide) was added to a solution of nickel chloride dissolved in 50 mM sodium acetate buffer solution. Following a reaction time of 30 min, the nickel complex of the dye was applied on Sep-Pak C18 cartridge and eluted with 60% solution of methanol in water and dried. The purification and isolation of the nickel complex by ion exchange as described above avoided the presence of free nickel ions, which can lead to additional quenching of the fluorescence and higher toxicity in further *in vivo* experiments.

Ten fold excess of $Ni^{2+}$:NTA-PDI **3.49** dissolved in 50 mM phosphate buffer (pH 7.5) was added to a solution of the protein in TRIS-HCl buffer (pH 7.5). After a reaction time of 30 min, the reaction mixture was purified by size exclusion chromatography (BioGel P 30) eluted with 50 mM phosphate buffer. Two fractions were isolated from the size exclusion chromatography and analyzed by gel-electrophoresis. The SDS-PAGE gel analysis showed that the first one contained only the labeled proteins and the second one – the free chromophore. The labeling of the protein with PDI-NTA was proven by size exclusion chromatography and SDS-PAGE gel electrophoresis. (Figure 6.6)

**A**



**B**



Lane 6 5 4 3 2 1      6 5 4 3 2 1

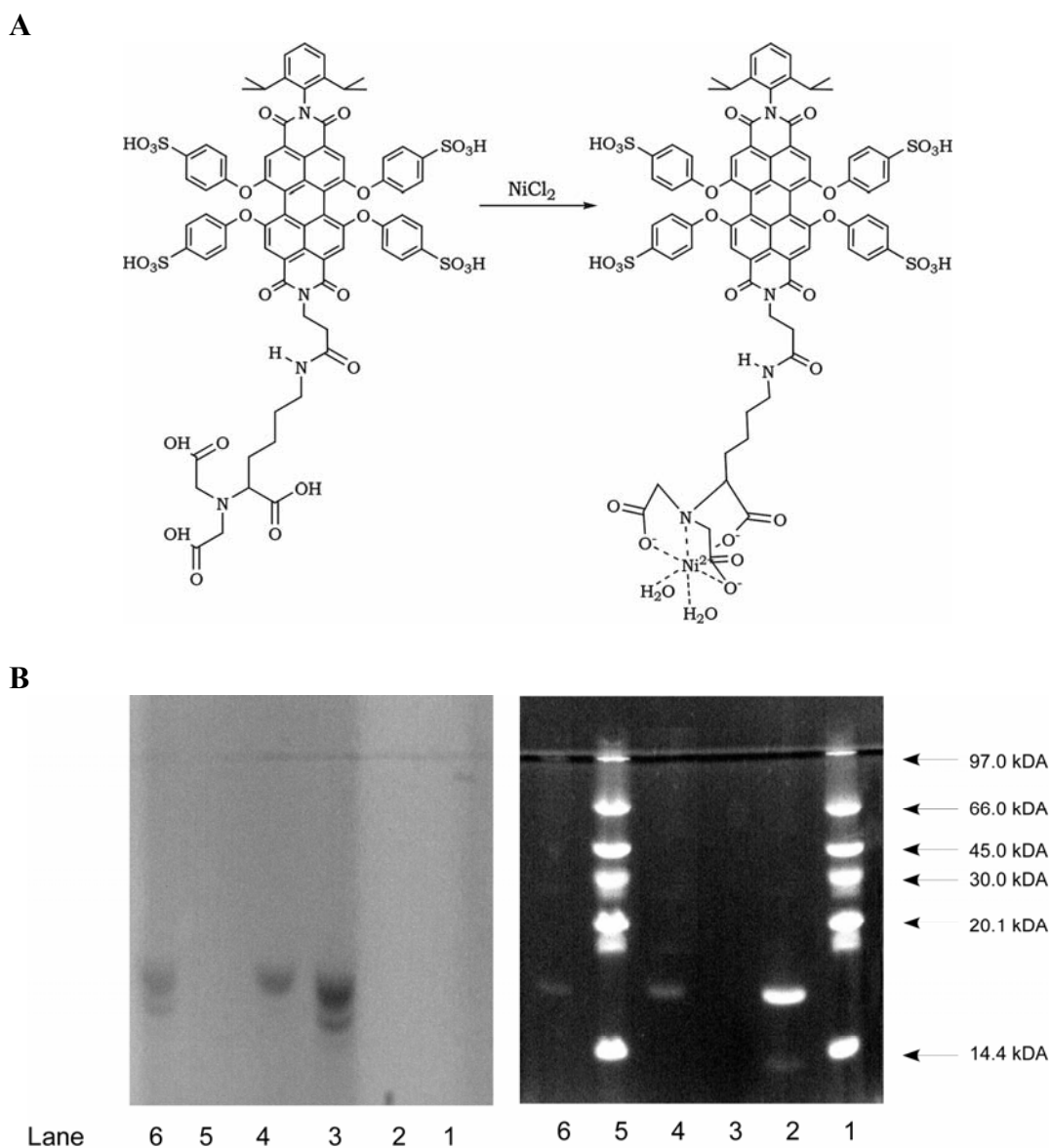**Figure 6.6. A: Formation of the nickel complex; B: SDS-PAGE gel electrophoresis of the labeled SUMO. Gel 1 (left) is shows the fluorescence detection by transillumination at 366 nm, Gel 2 (right) after staining with Coumassie Blue; Lane 1 and 5 - molecular weight marker. Lane 2 - His6-tagged SUMO1, on lane 3 is the perylene NTA, lane 4 shows the labeled and purified SUMO, and lane 6 shows the reaction mixture**

## 6.4. Site-directed labeling of His-tagged ATP synthase using NTA functionalized perylene(dicarboximide)

In order to study the photophysical properties of **3.49** in protein environment and to establish once more its suitability for protein labeling, the Ni-complex of the chromophore was incubated with $His_6$-tagged $F_1$ complex of $F_oF_1$-ATP synthase from *Escherichia coli* and studied using FCS.

$F_oF_1$-ATP synthase catalyzes the formation of ATP from ADP and phosphate in bacteria, mitochondria and chloroplasts, and this reaction is driven by conversion of Gibbs free energy derived from a transmembrane electrochemical proton gradient.[39] The enzyme consists of two parts, $F_1$ and $F_o$, which in E.coli have the subunit composition $\alpha_3\beta_3\gamma\delta\varepsilon$ and $ab_2c_n$ with an expected number n of c subunits between 10 and 12, respectively (Figure 6.7).[40, 41]

A sequential conversion of the conformations of the catalytic sites is caused by rotation of the $\gamma$ subunit, which is located in the centre of the $\alpha_3\beta_3$ complex. Rotation of the $\gamma$ subunit is assumed to be coupled mechanically to proton translocation by a rotational movement of the c-ring of $F_o$. Therefore, the subunits are also defined as "rotor" ($\gamma\varepsilon c_n$) and "stator" ($\alpha_3\beta_3\delta$ $ab_2$)

Much experimental work has focused on the mechanistic events in this molecular rotor, to clarify the central role of energy transduction and the rotary mechanism of $F_oF_1$-ATP synthase. The group of Dr. Börsch has developed a single molecule FRET approach to study intersubunit rotation of membrane bound $F_oF_1$-ATP synthase and associated conformational changes in real time and with subnanometre resolution.[42, 43] Intramolecular single-molecule FRET was used to observe the rotary movement of the $\gamma$ subunit during proton-powered ATP synthesis. (Figure 6.7 b and c) The FRET donor was attached at the rotary $\gamma$ subunit, while the FRET acceptor crosslinked the nonrotating b-subunit dimmer. During catalysis, fluctuating FRET efficiencies indicated the relative movement of the labels because their distances sequentially interchange as a result of the rotation of the $\gamma$ subunit.
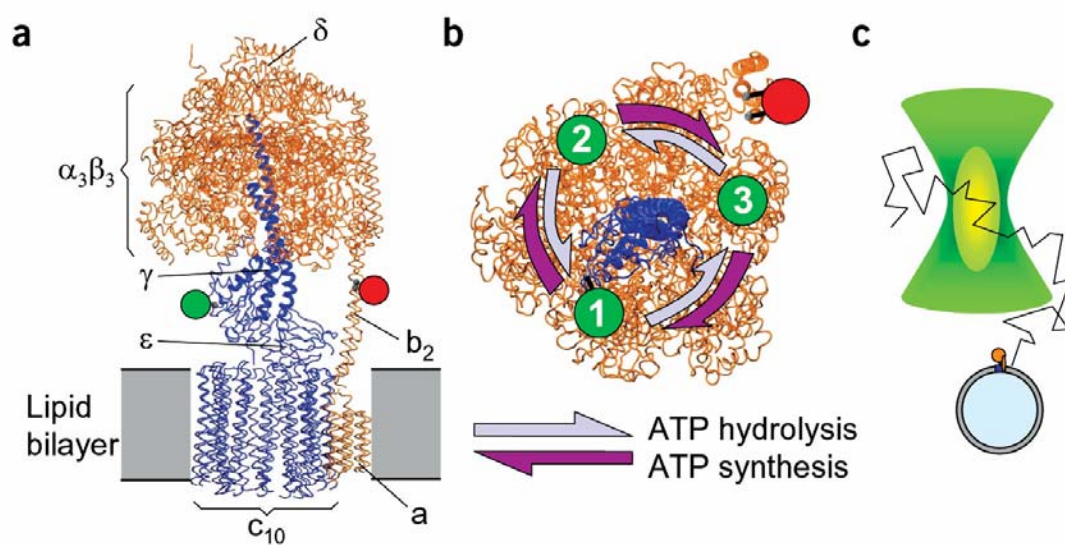
**Figure 6.7. Model of $F_0F_1$ from *E. coli*. (a) Side view. The FRET donor is bound to the $\gamma$ subunit (green circle), the FRET acceptor Cy5 to the b subunits (red circle). 'Rotor' subunits are blue; 'stator' subunits are orange. (b) Cross-section at the fluorophore level, viewed from $F_0$. Cy5bis (red) crosslinks the b subunits. Donor position 1 (green) of cysteine $\gamma$-T106C is farthest away from b-Q64C. Rotation of the $\gamma$ subunit by 120° and 240° results in donor positions 2 and 3, respectively. (c) Photon bursts are observed when a freely diffusing single liposome with a single FRET-labeled $F_0F_1$ traverses the confocal detection volume (yellowish) within the laser focus (green).**

As described above single-molecule FRET was used to investigate nucleotide binding to the different binding sites and conformational changes of the enzyme during ATP hydrolysis. To observe the binding of single nucleotides, the $\gamma$-subunit of holoenzyme $F_0F_1$ was labeled specifically with FRET donor - tetramethylrhodamine (TMR). As the FRET acceptor, ATP-Alexa Fluor 647 was selected. Using confocal single-molecule fluorescence detection, diffusion of the liposome-bound enzyme through the confocal volume was detected by the donor fluorescence (without acceptor), while binding of a single ATP-Alexa Fluor 647 molecule to a single EF0F1 resulted in an intermolecular FRET.

However, some limitations of the single-molecule FRET approach have to be overcome, like the small number of detected photons per time interval, which limits the precision of the distance measurements. Quenching of the protein-bound fluorophores like tetramethylrhodamine, used before, has to be avoided by the use of novel fluorophores with higher quantum yield and better photostability. This would allow further studies, which give a detailed view of structural dynamics and conformational changes.

To prove whether the perylene(dicarboximide) functionalized with NTA can be applied as a better alternative to the commercially available chromophore, we have performed site-selective labeling of $His_6$-tagged $F_1$ complex of $F_oF_1$-ATP and subsequent FCS analysis of the conjugate. Both of the previously used as FRET pair chromophores were bearing maleimide functionality, since the γ- and the β-subunits of the ATP synthase had artificially introduced cysteine residues. The site-selective labeling with fluorophore bearing NTA group required expression of $His_6$-tagged $F_1$ complex of $F_oF_1$-ATP synthase. The expression of the protein was performed by Dr. Thomas M. Duncan (Department of Biochemistry and Molecular Biology, SUNY Upstate Medical, University, Syracuse, NY, USA). The $F_1$ complex with subunit composition $α_3β_3γδε$ contained three $His_6$ tags, one at the N-terminus of each of the β subunits. The βHis6 tags had minimal effect on the specific ATPase activity of F1. These $His_6$ tags have been previously used to attach the $F_1$-ATPase to a glass surface and to demonstrate the ATP-driven rotation of the γ subunit.[44] Ni-complex of **3.49** (Perylene-Ni-NTA) was prepared as described in the previous section and incubated with $His_6$-tagged $F_1$ complex of $F_oF_1$-ATP synthase.

In order to detect the binding of the perylene dye to this rotary motor protein in solution, fluorescence correlation spectroscopy experiments were carried out. Confocal laser excitation at 561 nm was used to match the absorbance maximum of the perylene dye. Different concentrations of $F_1$-ATPase were pre-mixed with 1 nM perylene-Ni-NTA. As a control, the dye was mixed with $F_1$-ATPase in the absence of $Ni^{2+}$. Increasing amounts of $F_1$-ATPase resulted in increasing diffusion times of the perylene-Ni-NTA due to conjugate formation with the His tagged protein (Figure 6.8). In the absence of $Ni^{2+}$, no evidence for binding of the perylene-NTA dye was found by FCS measurements.
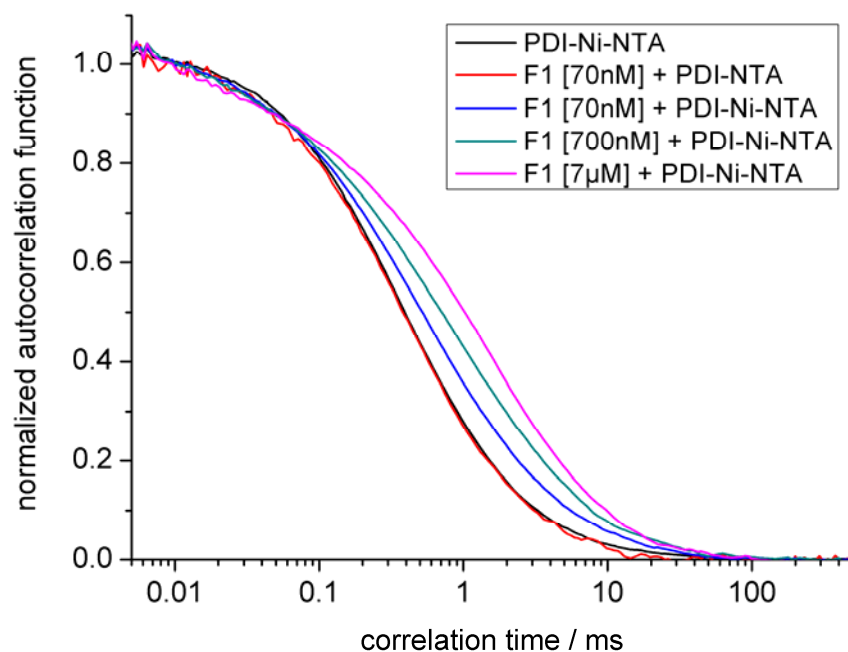
**Figure 6.8: FCS results. Normalized autocorrelation functions of perylene-Ni-NTA and 3.49 in the presence of His$_6$-tagged F$_1$-ATPase**

The fluorescence intensity autocorrelation functions, $g^{(2)}(t_c)$, were fitted with two diffusion times, $t_{D1}$ and $t_{D2}$, for the un-bound and the bound perylene dye, respectively, according to

$$g^{(2)}(t_c) = \frac{1}{N_f}\left\{\alpha\left(\frac{1}{1+t_c/t_{D1}}\right)\left(\frac{1}{1+(\omega_0/z_0)^2(t_c/t_{D1})}\right)^{1/2} + (1-\alpha)\left(\frac{1}{1+t_c/t_{D2}}\right)\left(\frac{1}{1+(\omega_0/z_0)^2(t_c/t_{D2})}\right)^{1/2}\right\}\bullet\{1-T-T\exp(-t_c/t_T\}$$

with $N_F$, average number of fluorescent molecules in the confocal detection volume, $t_c$, correlation time, $\alpha$, fraction of molecules with the shorter diffusion time $t_{D1}$, $\omega_0/z_0$, ratio of the $1/e^2$ radii of the detection volume in radial and axial directions, $T$, average fraction of fluorophores in the triplet state, and $t_T$, lifetime of the triplet state of the fluorophore. The $\omega_0/z_0$ ratio was measured with a Rhodamine 101 solution as the reference and was kept at this value during the subsequent fittings of

the autocorrelation functions of the perylene-Ni-NTA plus $F_1$-ATPase solutions. The triplet state lifetime of perylene-NTA and perylene-Ni-NTA was determined to $t_T = (2 \pm 1)$ μs. The diffusion time of $F_1$-ATPase was measured independently after labeling a cysteine (residue 106 of the γ subunit) with a water-soluble perylene-maleimide. It was used as the diffusion time $t_{D2}$ for the calculation of the binding constant of perylene-Ni-NTA to the His tags at $F_1$.

Using the above described two-component model for bound and un-bound dye to fit the autocorrelation functions of the FCS experiments, a dissociation constant $K_D = 3 \pm 1$ μM was obtained for the perylene-Ni-NTA which is in good agreement with binding constants reported for other Ni-NTA labels [45-47]. In comparison, dissociation constant of $K_D = 14$ μM was reported for fluorescein bearing NTA group and $K_D = 5$ μM for Cy3 functionalized with NTA unit.[23, 24]

In the absence of $Ni^{2+}$, no evidence for binding of the perylene-NTA dye was found by FCS measurements (Figure 6.8).

FCS was also used to determine the mean photon count rate or 'molecular brightness' of a single perylene(dicarboximide)-NTA in the absence of $Ni^{2+}$ (Figure 6.9).[48] Rhodamine 101 and Atto-565 were used as the references. For Rhodamine 101, a maximum fluorescence of about 145 000 counts/s per molecule saturated at an excitation power of 300 μW at the back aperture of the microscope objective was detected. At higher excitation power, photobleaching and increased population of the non-fluorescent triplet state reduced the brightness per molecule. Similar saturation behavior was observed for Atto-565 which was bound to bovine serum albumin (BSA). In contrast, the molecular brightness of the perylene-NTA steadily increased up to an excitation power of 1.2 mW reaching 120 kHz and supporting the high photostability of the perylene chromophore. At this high laser power, the triplet yield was only 11 percent compared to about 45 percent for Atto-565 bound to BSA. In the presence of $Ni^{2+}$, the relative brightness of the perylene derivative was reduced to about 77 percent. Binding of the perylene-Ni-NTA to the His tags of $F_1$-ATPase did not reduce the molecular brightness further but rather increased slightly.
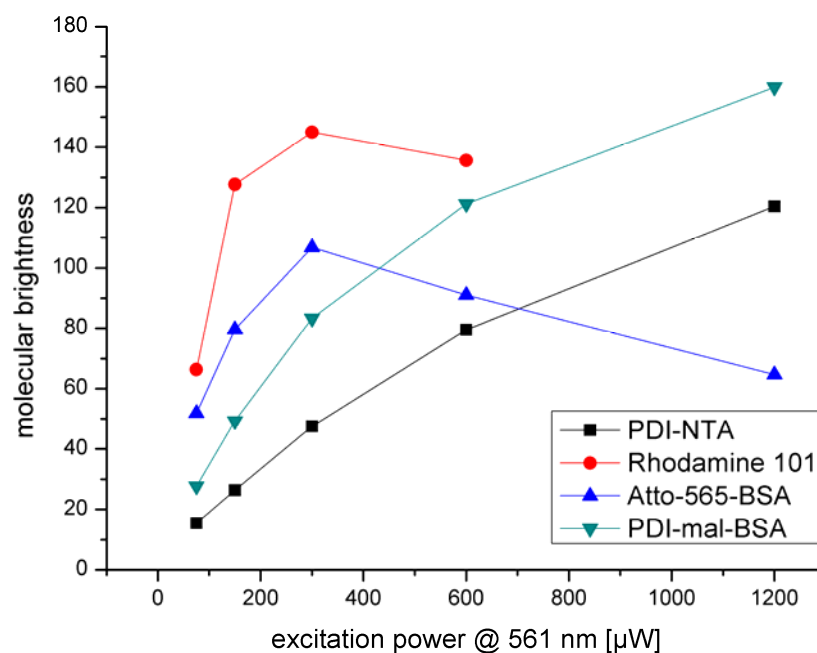
**Figure 6.9: Relative molecular brightness of Perylene-NTA, rhodamine 101 and BSA-bound Atto-565.**

In summary, the synthesis of a new water-soluble perylene chromophore, containing nitrilotriacetic acid functional group was demonstrated, using solution-phase and solid-phase approaches. This new member of the family of the rylene dyes possesses excellent water-solubility and a reactive group for site-selective labeling of proteins. Site-specific labeling of a model protein was successfully demonstrated, the conjugate separated and characterized with size-exclusion chromatography and SDS-PAGE gel electrophoresis.

FCS analysis was used for studying the photophysical properties of the perylene(dicarboximide)-NTA in protein environment, using His-tagged ATPase. FCS studies with NTA functionalized chromophore were performed for the first time, due to the unchaged fluorescence intensity of the nickel complex of the fluorophore. The perylene(dicarboximide)-NTA displayed excellent photostability and improved molecular brightness, in comparison with Rhodamine 101 and ATTO-565. This new chromophore effectively combines numerous advantages such as excellent water-solubility, a reactive group for selective labeling, bright fluorescence not only in the presence of nickel ions, but also in protein environment and excellent photostability.

# 6.5. References

[1] K. L. Holmes, L. M. Lantz, in *Methods in Cell Biology, Vol 63, Vol. 63*, **2001**, pp. 185.

[2] W. L. Hubbell, A. Gross, R. Langen, M. A. Lietzow, *Curr. Opin. Struct. Biol.* **1998**, *8*, 649, *Recent advances in site-directed spin labeling of proteins*.

[3] M. A. Cooper, *Anal. Bioanal. Chem.* **2003**, *377*, 834, *Label-free screening of bio-molecular interactions*.

[4] J. Farinas, A. S. Verkman, *J. Biol. Chem.* **1999**, *274*, 7603, *Receptor-mediated targeting of fluorescent probes in living cells*.

[5] K. M. Marks, P. D. Braun, G. P. Nolan, *Proc. Natl. Acad. Sci. U. S. A.* **2004**, *101*, 9982, *A general approach for chemical labeling and rapid, spatially controlled protein inactivation*.

[6] M. M. Wu, J. Llopis, S. Adams, J. M. McCaffery, M. S. Kulomaa, T. E. Machen, H. P. H. Moore, R. Y. Tsien, *Chem. Biol.* **2000**, *7*, 197, *Organelle pH studies using targeted avidin and fluorescein-biotin*.

[7] I. Chen, A. Y. Ting, *Curr. Opin. Biotechnol.* **2005**, *16*, 35, *Site-specific labeling of proteins with small molecules in live cells*.

[8] I. Chen, M. Howarth, W. Y. Lin, A. Y. Ting, *Nature Methods* **2005**, *2*, 99, *Site-specific labeling of cell surface proteins with biophysical probes using biotin ligase*.

[9] L. W. Miller, V. W. Cornish, *Curr. Opin. Chem. Biol.* **2005**, *9*, 56, *Selective chemical labeling of proteins in living cells*.

[10] T. Ha, T. Enderle, D. F. Ogletree, D. S. Chemla, P. R. Selvin, S. Weiss, *Proc. Natl. Acad. Sci. U. S. A.* **1996**, *93*, 6264, *Probing the interaction between two single molecules: Fluorescence resonance energy transfer between a single donor and a single acceptor*.

[11] C. Jacob, G. L. Giles, N. M. Giles, H. Sies, *Angew. Chem. Int. Ed.* **2003**, *42*, 4742, *Sulfur and selenium: The role of oxidation state in protein structure and function*.

[12] E. Hochuli, H. Dobeli, A. Schacher, *J. Chromatogr.* **1987**, *411*, 177, *New Metal Chelate Adsorbent Selective for Proteins and Peptides Containing Neighboring Histidine-Residues*.

[13] E. Hochuli, W. Bannwarth, H. Dobeli, R. Gentz, D. Stuber, *Bio-Technology* **1988**, *6*, 1321, *Genetic Approach to Facilitate Purification of Recombinant Proteins with a Novel Metal Chelate Adsorbent*.

[14] P. D. Gershon, S. Khilko, *J. Immunol. Methods* **1995**, *183*, 65, *Stable Chelating Linkage for Reversible Immobilization of Oligohistidine Tagged Proteins in the Biacore Surface-Plasmon Resonance Detector*.

[15] E. K. M. Ueda, P. W. Gout, L. Morganti, *Journal of Chromatography A* **2003**, *988*, 1, *Current and prospective applications of metal ion-protein binding*.

[16] C. Hart, B. Schulenberg, Z. Diwu, W. Y. Leung, W. F. Patton, *Electrophoresis* **2003**, *24*, 599, *Fluorescence detection and quantitation of recombinant proteins containing oligohistidine tag sequences directly in sodium dodecyl sulfate-polyacrylamide gels*.

[17] G. B. Sigal, C. Bamdad, A. Barberis, J. Strominger, G. M. Whitesides, *Anal. Chem.* **1996**, *68*, 490, *A self-assembled monolayer for the binding and study of histidine tagged proteins by surface plasmon resonance*.

[18] E. L. Schmid, T. A. Keller, Z. Dienes, H. Vogel, *Anal. Chem.* **1997**, *69*, 1979, *Reversible oriented surface immobilization of functional proteins on oxide surfaces*.

[19] S. A. McMahan, R. R. Burgess, *Anal. Biochem.* **1996**, *236*, 101, *Single-step synthesis and characterization of biotinylated nitrilotriacetic acid, a unique reagent for the detection of histidine-tagged proteins immobilized on nitrocellulose*.

[20] E. W. Kubalek, S. F. J. Legrice, P. O. Brown, *Journal of Structural Biology* **1994**, *113*, 117, *2-Dimensional Crystallization of Histidine-Tagged, Hiv-1 Reverse-Transcriptase Promoted by a Novel Nickel-Chelating Lipid*.

[21] C. R. Goldsmith, J. Jaworski, M. Sheng, S. J. Lippard, *J. Am. Chem. Soc.* **2006**, *128*, 418, *Selective Labeling of Extracellular Proteins Containing Polyhistidine Sequences by a Fluorescein-Nitrilotriacetic Acid Conjugate*.

[22] S. Lata, M. Gavutis, R. Tampe, J. Piehler, *J. Am. Chem. Soc.* **2006**, *128*, 2365, *Specific and Stable Fluorescence Labeling of Histidine-Tagged Proteins for Dissecting Multi-Protein Complex Formation*.

[23] A. N. Kapanidis, Y. W. Ebright, R. H. Ebright, *J. Am. Chem. Soc.* **2001**, *123*, 12123, *Site-specific incorporation of fluorescent probes into protein: Hexahistidine-tag-mediated fluorescent labeling with (Ni2+:Nitrilotriacetic Acid)n-fluorochrome conjugatesfluorescent probes*.

[24] S. Lata, A. Reichel, R. Brock, R. Tampe, J. Piehler, *J. Am. Chem. Soc.* **2005**, *127*, 10205, *High-affinity adaptors for switchable recognition of histidine-tagged proteins*.

[25] S. Hutschenreiter, L. Neumann, U. Radler, L. Schmitt, R. Tampe, *ChemBioChem* **2003**, *4*, 1340, *Metal-chelating amino acids as building blocks for synthetic receptors sensing metal ions and histidine-tagged proteins*.

[26] L. Fabbrizzi, M. Licchelli, P. Pallavicini, D. Sacchi, A. Taglietti, *Analyst* **1996**, *121*, 1763, *Sensing of transition metals through fluorescence quenching or enhancement - A review*.

[27] A. W. Varnes, E. L. Wehry, R. B. Dodson, *J. Am. Chem. Soc.* **1972**, *94*, 946, *Interactions of Transition-Metal Ions with Photoexcited States of Flavins - Fluorescence Quenching Studies*.

[28] H. Masuhara, H. Shioyama, T. Saito, K. Hamada, S. Yasoshima, N. Mataga, *J. Phys. Chem.* **1984**, *88*, 5868, *Fluorescence Quenching Mechanism of Aromatic-Hydrocarbons by Closed-Shell Heavy-Metal Ions in Aqueous and Organic Solutions*.

[29] G. D. Meredith, H. Y. Wu, N. L. Allbritton, *Bioconjugate Chem.* **2004**, *15*, 969, *Targeted protein functionalization using His-tags*.

[30] A. P. PE Applied Biosystems, in *User's Manual, Vol. 2*, Foster city, California, **1997**.

[31] J. R. Lakowicz, *Principles of Photoluminescence Spectroscopy*, 2nd ed. ed., Kluwer Academic/Plenum Publishers, Dordrecht, **1999**.

[32] P. Bayer, A. Arndt, S. Metzger, R. Mahajan, F. Melchior, R. Jaenicke, J. Becker, *J. Mol. Biol.* **1998**, *280*, 275, *Structure determination of the small ubiquitin-related modifier SUMO-1*.

[33] S. Müller, C. Hoege, G. Pyrowolakis, S. Jentsch, *Nat. Rev. Mol. Cell Biol.* **2001**, *2*, 202, *Sumo, ubiquitin's mysterious cousin*.

[34] J. M. P. Desterro, M. S. Rodriguez, R. T. Hay, *Mol. Cell* **1998**, *2*, 233, *SUMO-1 modification of I kappa B alpha inhibits NF-kappa B activation*.

[35] M. S. Rodriguez, J. M. P. Desterro, S. Lain, C. A. Midgley, D. P. Lane, R. T. Hay, *EMBO J.* **1999**, *18*, 6455, *SUMO-1 modification activates the transcriptional response of p53*.

[36] J. Hemelaar, A. Borodovsky, B. M. Kessler, D. Reverter, J. Cook, N. Kolli, T. Gan-Erdene, K. D. Wilkinson, G. Gill, C. D. Lima, H. L. Ploegh, H. Ovaa, *Mol. Cell. Biol.* **2004**, *24*, 84, *Specific and covalent targeting of conjugating and deconjugating enzymes of ubiquitin-like proteins*.

[37] S. Jentsch, G. Pyrowolakis, *Trends in Cell Biology* **2000**, *10*, 335, *Ubiquitin and its kin: how close are the family ties?*

[38] G. Gill, *Genes Dev.* **2004**, *18*, 2046, *SUMO and ubiquitin in the nucleus: different functions, similar mechanisms?*

[39] M. Börsch, P. Graeber, *Biochem. Soc. Trans.* **2005**, *33*, 878, *Subunit movement in individual H+-ATP synthases during ATP synthesis and hydrolysis revealed by fluorescence resonance energy transfer*.

[40] M. Diez, B. Zimmermann, M. Borsch, M. Konig, E. Schweinberger, S. Steigmiller, R. Reuter, S. Felekyan, V. Kudryavtsev, C. A. M. Seidel, P. Graber, *Nat. Struct. Mol. Biol.* **2004**, *11*, 135, *Proton-powered subunit rotation in single membrane-bound F0F1-ATP synthase*.

[41] M. Borsch, M. Diez, P. Graber, *Single Molecules* **2000**, *1*, 180, *Conformational changes of H+ ATP synthase upon ATP hydrolysis detected by fluorescence correlation spectroscopy*.

[42] B. Zimmermann, M. Diez, M. Boersch, P. Graeber, *Biochimica et Biophysica Acta, Bioenergetics* **2006**, *1757*, 311, *Subunit movements in membrane-integrated EF0F1 during ATP synthesis detected by single-molecule spectroscopy*.

[43] B. Zimmermann, M. Diez, N. Zarrabi, P. Graeber, M. Boersch, *EMBO J.* **2005**, *24*, 2053, *Movements of the e-subunit during catalysis and activation in single membrane-bound H+-ATP synthase*.

[44] H. Noji, K. Hasler, W. Junge, K. Kinosita, M. Yoshida, S. Engelbrecht, *Biochem. Biophys. Res. Commun.* **1999**, *260*, 597, *Rotation of Escherichia coli F-1-ATPase*.

[45] A. Armbrüster, C. Hohn, A. Hermesdorf, K. Schumacher, M. Börsch, G. Gruber, *FEBS Lett.* **2005**, *579*, 1961, *Evidence for major structural changes in subunit C of the vacuolar ATPase due to nucleotide binding*.

[46] I. T. Dorn, K. R. Neumaier, R. Tampe, *J. Am. Chem. Soc.* **1998**, *120*, 2753, *Molecular recognition of histidine-tagged molecules by metal-chelating lipids monitored by fluorescence energy transfer and correlation spectroscopy*.

[47] B. Krishnan, A. Szymanska, L. M. Gierasch, *Chem. Biol. Drug Des.* **2007**, *69*, 31, *Site-specific fluorescent labeling of poly-histidine sequences using a metal-chelating cysteine*.

[48] O. Krichevsky, G. Bonnet, *Reports on Progress in Physics* **2002**, *65*, 251, *Fluorescence correlation spectroscopy: the technique and its applications*.

# 7. Summary

Studies of organic fluorescent dyes are experiencing a renaissance related to the increasing demands posed by new microscopy techniques for high resolution and high sensitivity. Such studies aim at a detailed understanding of the chromophores' photophysics, their interactions with the environment and their photochemistry inevitably leading to photobleaching. Single-molecule fluorescence spectroscopy, for example, relies to a large extent on extraordinarily bright and photostable organic fluorescent dyes. While in the last decade single molecule equipment and methodology has significantly advanced and in some cases reached theoretical limits (e.g. detectors approaching unity quantum yields) unstable emission from chromophores and photobleaching become more and more the bottleneck of the advancement and spreading of single-molecule fluorescence studies. The main goal of this work was the synthesis of fluorophores that are water-soluble, highly fluorescent in an aqueous environment, have a reactive group for attachment to a biomolecule and posses exceptional photostability.

In Chapter 3, an approach towards highly fluorescent, water-soluble and monofunctional perylene-3,4,9,10-tetracarboxdiimide and terrylene-3,4:11,12-tetra carboxidiimide chromophores was presented. A new synthetic strategy for the desymmetrization of perylenetetracarboximides was elaborated; water-solubility was accomplished by introducing sulfonyl substituents in the phenoxy ring. Due to their unique properties such as photostability, high fluorescence quantum yields, absorption and emission maxima above 500 nm, such chromophores can be used as high performance fluorescence probes in aqueous media since they allow investigations at single molecule level. This purpose, however, required the synthesis of chromophores bearing an additional reactive anchor group for the

labeling of biologically active macromolecules. Two strategies have been followed relying on either non-specific or site specific labeling. For this purpose a series of new water-soluble monofunctional perylene and terrylene dyes, bearing amine or carboxy group were prepared. The reactivity and photophysical properties of these new chromophores were studied in aqueous medium. The most suitable chromophores were further derivatized with amine or thiol reactive groups, suitable for chemical modification of proteins.



**3.31**            **3.32**            **3.33**



**3.44**            **3.45**
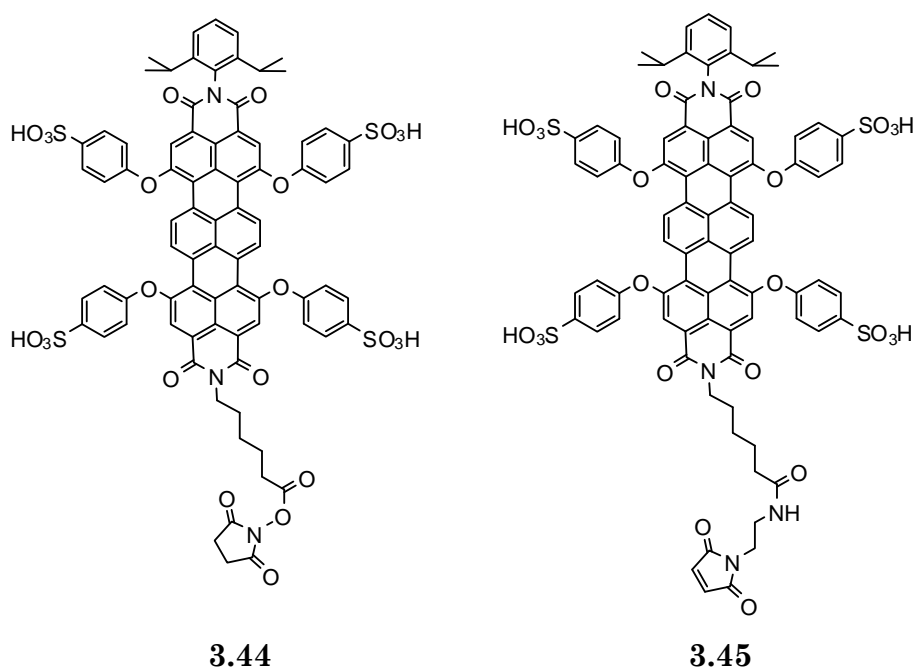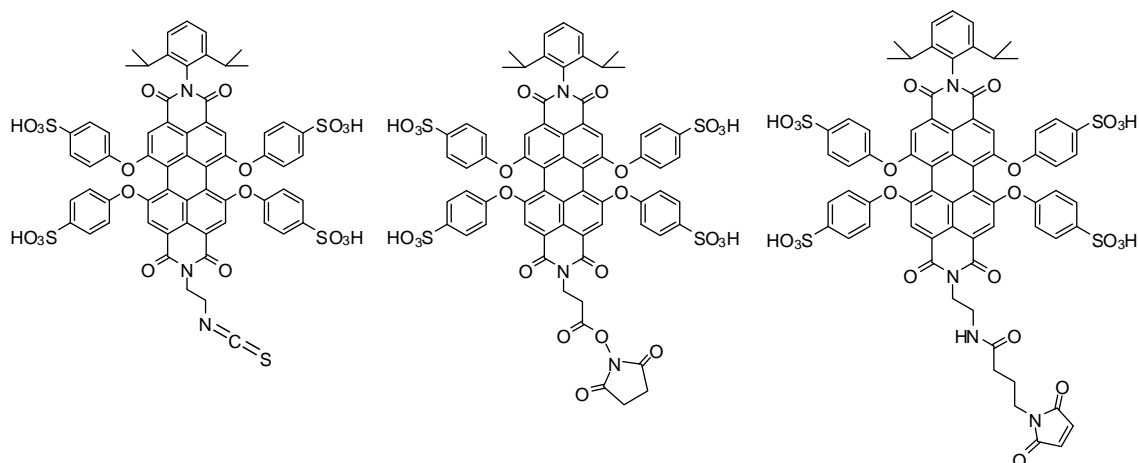
All of the newly presented reactive chromophores displayed high extinction coefficient and high fluorescence quantum yield in water.

In Chapter 4, the performance of the new fluorescent probes was assessed by single molecule enzyme tracking, in this case phospholipase acting on phospholipid supported layers. Phospholipase-1 (PLA-1) was labeled with N-hydroxysuccinimide ester functionalized perylene and terrylene derivatives. The purification of the conjugates was accomplished by novel convenient procedure for the removal of unreacted dye from labeled enzymes, which involves capturing excess dye with a solid support. This novel strategy for purification of bioconjugates allows convenient and fast separation of labeled proteins without the need for performing time consuming chromatographic or electrophoretic purification steps. The application of this approach can be extended to any fluorescent reporter, which contains a functional reactive group. The labeled biomolecule can be recovered very fast and in high purity, thus making this approach one of the most convenient ways of isolating modified biomolecules. Further tests of the bulk activities of the labeled enzyme clearly showed that no activity was lost by the labeling.
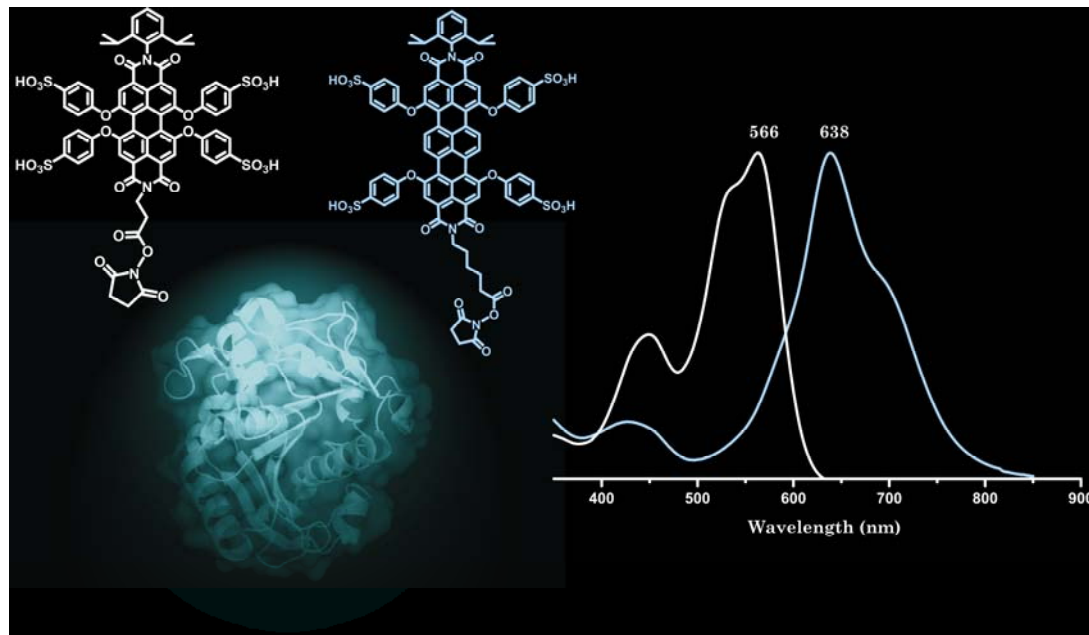


**Figure 8.1. N-hydroxysuccinimide ester functionalized perylene and terrylene, model of PLA-1 based on crystal structure and absorbance spectra of the depicted dyes**

Single-molecule wide-field microscopy measurements revealed that single enzymes could be visualized even on a substrate with fluorescent background. The outstanding photostability of the dyes and, associated therewith, the extended survival times under strong illumination conditions allow a complete characterization of enzyme action on its natural substrates and even connecting enzyme mobility to catalytic activity.
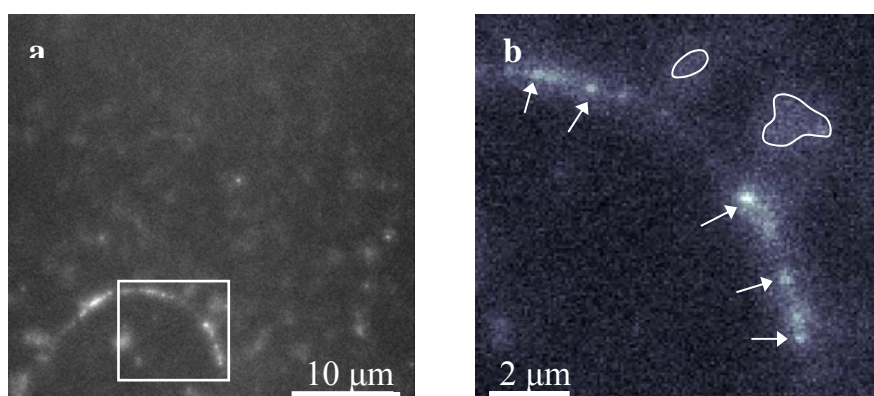


**Figure 8.2. Fluorescence image of individual labeled enzymes on POPC layers. (a) 3.32 labeled PLA1 on a non-labeled POPC layer (b) Magnification of the area in image (a) indicated by the white square. The arrows indicate clearly distinguishable individual enzymes located on the edge of the layer. Note that the signal-to-noise is much higher than for the not adsorbed molecules diffusing in solution (indicated by the circles).**

Enzyme kinetics at the single molecule level have been previously analysed using the conversion of a non-fluorescent substrate into a fluorescent product. However, tracking of single interfacial enzymes with their complex catalytic pathways and modes of operation like phospholipases has not been performed yet.

In the present work, wide-field SMFS was used to gain new insights into the action of phospholipase. The performance of the new fluorescent probes was assessed by single-particle tracking. The measurements revealed that single enzymes could even be visualized on a fluorescently labeled substrate. The outstanding photostability of the dyes and their extended survival times under

strong illumination conditions allow the actions of enzymes to be characterized on their natural substrates, in this case, phospholipase acting on phospholipid-supported layers. By using this approach, enzyme mobilities could be correlated with the catalytic activity. Furthermore, this assay allows the validation of the influence of the layer composition, fluidity, etc. on both parameters (enzyme mobility and activity). A direct relation was established between enzyme mobility on the substrate layers and subsequent hydrolysis for the first time at the single molecule level. By comparing the behavior of active and inactive forms of the enzyme, diffusive motions specifically associated with different parts of the overall catalytic process could be isolated, significantly simplifying the overall kinetic characterization. The success of this approach with combination of the extreme photostability suggests that the rylene chromophores can be applied to study other important interfacial enzymes.

When a protein is being labeled, the goal is to introduce a fluorescent label while preserving the native function and properties of the protein itself. Ideally, one should be able to attach covalently a precise number of chromophores to one or more specific locations on the surface of any molecule in solution. Currently the most general approach is to use electrophilic reagents that can react with nucleophilic groups on the surface of a target protein; however, this tends to yield a heterogeneous mixture of products since almost all proteins carry a number of nucleophilic groups on their surface. To overcome the problem researchers have developed numerous strategies for site-specific labeling of proteins, defining new and efficient ways for attaching a chromophore at precise position. For site-specific attachment of the rylene dyes to proteins the chromophores were functionalized with thioesters or nitrilotriacetic acid groups. This allowed attachment of the emitters to the N-terminus of proteins by native chemical ligation or complexation with His-tagged polypeptides at the N- or C-termini, respectively.

The synthesis of a water-soluble perylenebis (dicarboximide) functionalized with a thioester group was presented in Chapter 5. This chromophore exhibits an exceptional photostability and a functional unit for site-specific labeling of proteins. The suitability of the fluorophore as a covalent label was demonstrated via native chemical ligation with protein containing N-terminal cystein residue.
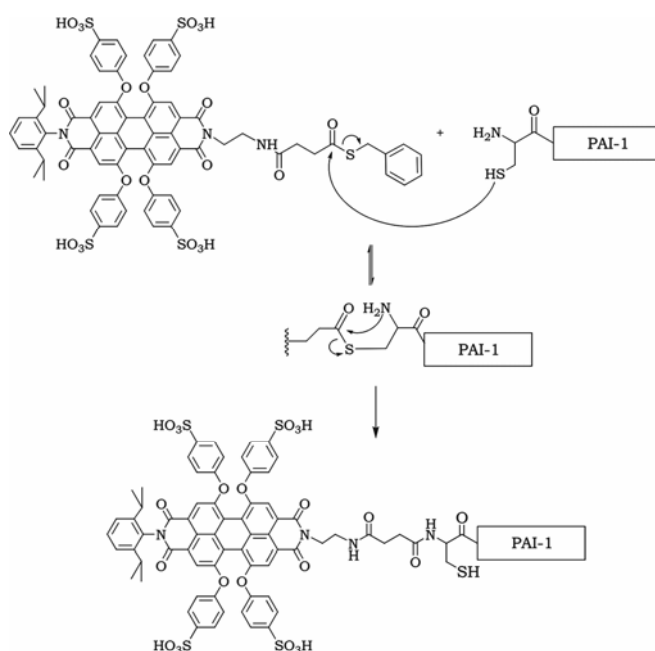
**Figure 8.3 Conjugation between PAI-1 N-terminal cysteine and 3.47**

The PDI-thioester-PAI-1 conjugate was refolded and the photophysical properties of the PDI-thioester studied applying FCS. The excellent photostability, as well as the functional group allowing the introduction of chromophore at precise position established the water-soluble perylene thioester as another attractive member of the family of ultrastable water-soluble perylenebis(dicarboximide)s.

In chapter 6, we exploited oligohisitidine sequences as recognition elements for site-selective labeling.
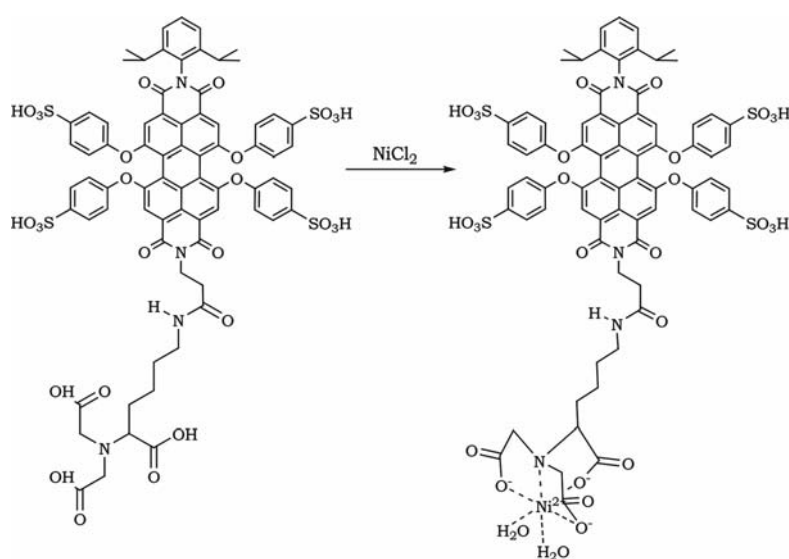


**Figure 8.4. Nitrilotriacetic acid functionalized perylene and its nickel complex**

These genetically encoded tags can be introduced into regions of the amino acid sequence where they do not disturb the protein's structure and function such as at the termini or in loops Oligohisitidine sequences are widely applied in combination with NTA for purification, in vitro detection and surface immobilisation of recombinant proteins.

The synthesis of a new water-soluble perylene chromophore, containing a nitrilotriacetic acid functional group was demonstrated, using solution-phase and solid-phase approaches. This chromophore combines the exceptional photophysical properties of the rylene dyes and a recognition unit for site-specific labeling of proteins. An important feature of the label is the unchanged emission of the dye upon complexation with nickel ions.
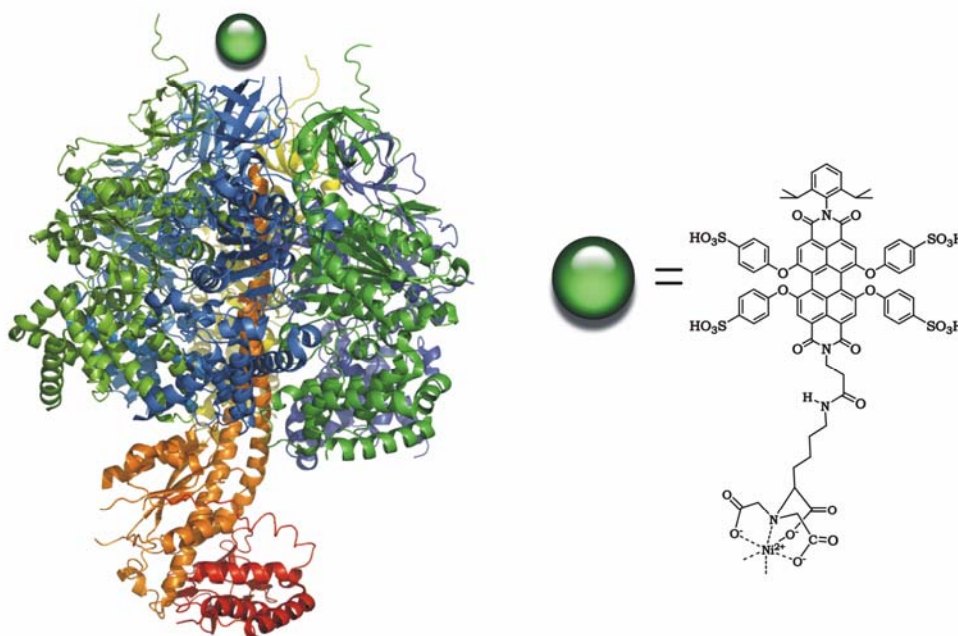


**Figure 8.5. Schematic drawing of the complex between his-tagged ATP synthase and NTA functionalized perylene(dicarboximide)**

FCS analysis was used for studying the photophysical properties of the perylene(dicarboximide)-NTA in protein environment, using His-tagged ATPase. FCS studies with NTA functionalized chromophore were performed for the first time, due to the unchaged fluorescence intensity of the nickel complex of the

fluorophore. The perylene(dicarboximide)-NTA displayed excellent photostability and improved molecular brightness, in comparison with Rhodamine 101 and ATTO-565. Moreover, the suitability of the fluorophore for site-selective labeling was successfully demonstrated using His-tagged SUMO-1 and His-tagged ATP synthase. Due to its small size, its proven exceptional photostability and the possibility for site specific attachment, the perylene-NTA offered great potential for the characterization of protein functions and interactions.

# Experimental Section

## *8.1. General methods*

### *8.1.1 Chemicals and solvents*

All used chemicals and solvents were obtained from the companies ABCR, Acros, Aldrich, Fluka, Lancaster, Merck and Strem. Unless otherwise mentioned, they were used as obtained.

### *8.1.2 Chromatography*

Preparative column chromatography was performed on silica gel from Merck with a grain size of 0.063 – 0.200 mm (silica gel) or 0.04-0.063 mm (flash silica gel, Geduran Si 60). For analytical thin layer chromatography (TLC), silica gel coated substrates "60 F254" from Merck were used. Compounds were detected by fluorescence quenching at 254 nm, self-fluorescence at 366 nm. For eluents, analytically pure solvents (p.a. or technical grade) were distilled prior to the use.

## *8.2 Analytical techniques*

### *8.2.1 Mass spectrometry*

FD mass spectra were obtained on a VG Instruments ZAB 2-SE-FPD spectrometer. MALDI-TOF spectrometry was conducted on a Bruker Reflex II-TOF spectrometer, utilizing a 337 nm nitrogen laser. If not specifically mentioned, tetracyanoquinodimethane (TCNQ) was used as the matrix substance for solid state prepared samples. Varying thicknesses of the prepared sample on the MALDI target reduced the resolution; therefore only integers of the molecular peaks are given. Isotope patterns are given and compared to the calculation, which are usually in agreement.

## *8.2.2 NMR spectroscopy*

$^1$H NMR, $^{13}$C NMR experiments were recorded in the listed deuterated solvents on a Bruker DPX 250, Bruker AMX 300, Bruker DRX 500 or a Bruker DRX 700 spectrometer. The deuterated solvent was used as an internal standard. In complicated cases, spectra were simulated using ACDLabs NMR prediction software to compare the results.

## *8.2.3 Elemental Analysis*

Elemental analysis of solid samples was carried out on a Foss Heraeus Vario EL as a service of the Institute for Organic Chemistry, Johannes-Gutenberg-Universität of Mainz.

## *8.2.4 UV/vis spectroscopy*

Solution UV/vis spectra were recorded at room temperature on a Perkin-Elmer Lambda 100 spectrophotometer. The molar extinctions are given in the unit $m^2 \cdot mol^{-1}$, which is consistent with the SI standard. In order to eliminate aggregation phenomena in solution, spectra of samples of different concentrations were compared to give the properties for the monomeric species in solution, which is usually at a concentration of 10-6 – 10-7 M. The measurement was performed at room temperature.

## *8.2.5 Photoluminescence spectroscopy*

Solution photoluminescence spectra were recorded on a SPEX-Fluorolog II (212) spectrometer. Spectra of samples of different concentrations were compared to extracted aggregation behaviors. Quantum yields of selected compounds were calculated by comparing a known standard (three different concentrations). The measurement was performed at room temperature.

## *8.2.6 Infrared spectorscopy*

Infrared spectra were obtained on a Nicolet FT-IR 320.

### *8.2.7 SDS-PAGE gel electrophoresis*

High-density (20% polyacrylamide gel containing 30% polyethylene glycol) polyacrylamide gel SDS-PAGE was performed using Phast-Gel system (Amersham Biosciences, Uppsala, Sweden). If not specifically mentioned sodium dodecyl sulfate (SDS) was added to the sample buffer before loading the gel. A low molecular weight marker (LMW-SDS), (Amersham, GE Healthcare) consisting of 6 molecular weight markers from 14 - 97 kDa, was used to calibrate the gel. The finished gels were stabilized using a fixative, stained with Coomassie Blue R-350 (Pharmacia, Uppsala, Sweden), destained and stored in 10% glycerol, 5% acetic acid. Gels were imaged using Personal Densitometer SI Software (Molecular Dynamics, Sunnyvale, CA).

## *Materials*

N-(2,6-diisopropylphenyl)-perylene-3,4-dicarboximide, N,N'-(2,6-diisopropyl phenyl)-1,6(7)-dibromoperylene-3,4,9,10-tetracarbox-dianhydride, N,N'-(2,6-di isopropylphenyl)-1,6,7,12-tetrachloro-perylene-3,4,9,10-tetracarboxdianhydride and N,N'-(2,6-diisopropylphenyl)-quaterrylene-3,4,13,14-tetracarboxdiimide are from BASF-AG (Ludwigshafen). All the reported yields are isolated yields.

# *Chapter 3*

### 3.7. <u>1,6,7,12-Tetra[4-sulfophenoxy]-N,N'-(2,6-diisopropylphenyl)-pery lene-3,4,9,10-tetracarboxidiimide:</u>
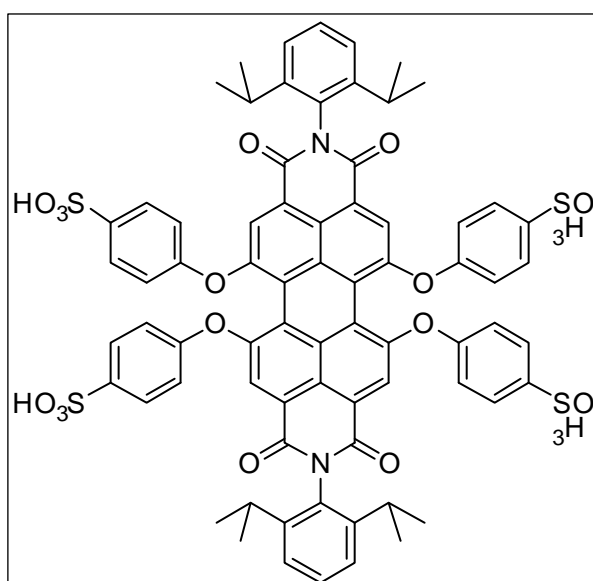


N,N'-Bis(2,6-diisopropylphenyl-1,6,7,12-tetraphenoxyperylene-3,4:9,10-tetracarboxylic acid diimide (2 g, 1.8 mmol) was added to concentrated sulfuric acid (5 mL). The flask was sealed, and the mixture was stirred at room temperature for 15 h. Water (7 mL) was slowly added to the flask to form a precipitate, which was filtered under suction. The solid was washed three times with dichloromethane (50 mL), and was then dried at 120 8C under vacuum to give a red product (2.4 g, 93%)

**Yield:** 93 %

*The analytical data agrees with that in the Ph.D. Thesis of C.Kohl.[1]*

**3.11a). 1,6,7,12-Tetra[4-(2-dimethylamino-ethyl)phenoxy]-N,N'-(2,6-diisopropylphenyl)-perylene-3,4,9,10-tetracarboxidiimide:**
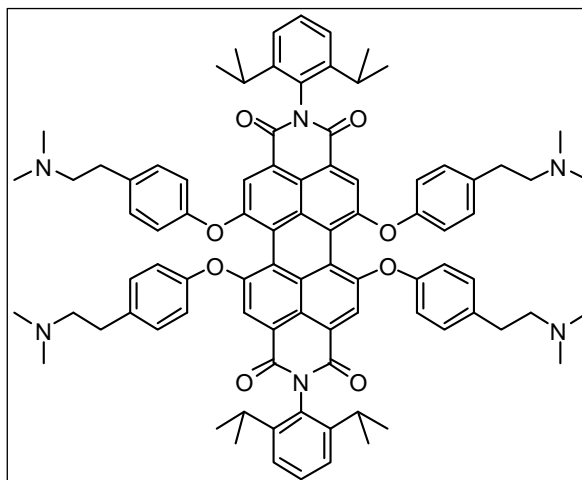


Tetrachloroperylenetetracarboxidiimide **3.8** (2.00 g, 2.32 mmol) was stirred with 4-(2-dimethylamino-ethyl)phenol hydrochloride acid salt (2.36 g, 11.8 mmol) in NMP (200 ml) in a 500 ml round-flask in the presence of powdered anhydrous $K_2CO_3$ (2.0 g, 14.4 mmol) at 100 °C overnight under argon. The reaction mixture was cooled down to room temperature, and then poured into hydrochloride acid (2N). The precipitated product was collected by filtration under suction and then washed with water completely and dried at 75 °C under vacuum. The product was purified by column chromatography with a mixture of triethylamine and dichloromethane (1:9) to get a dark solid **6-9** (1.9 g).

**Yield:** 62 %

*The analytical data agrees with that in the Ph.D. Thesis of J.Qu.*[2]

**3.11b). 1,6,7,12-Tetra[4-(2-trimethylammonio-ethyl)-phenoxy] -N, N'-(2,6-diisopropylphenyl)-perylene-3,4,9,10-tetracarboxidiimide tetraiodide:**
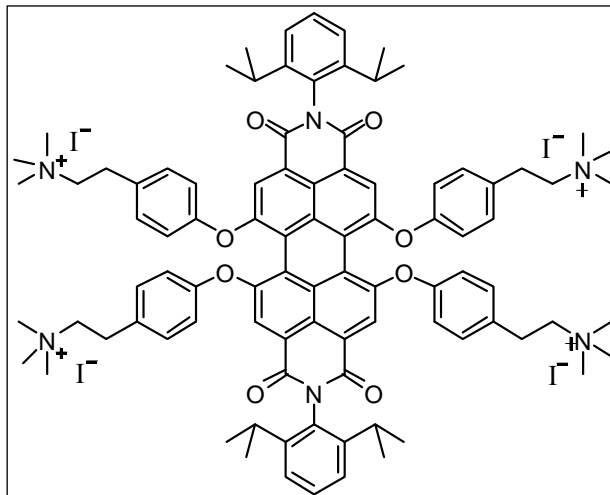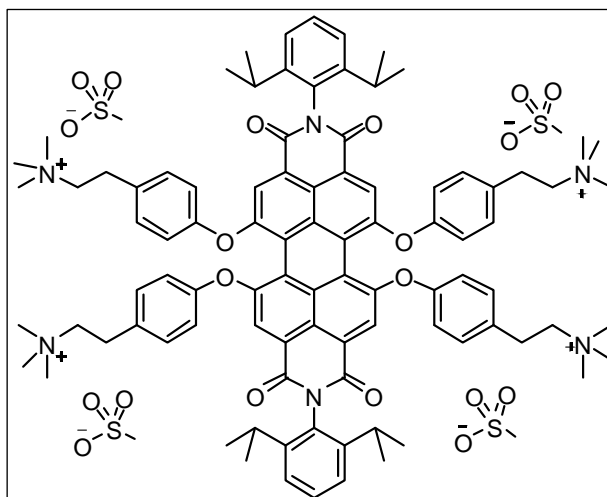


Perylene derivative **3.11a** (1.0 g, 0.73 mmol) and methyl iodide (2ml) in chloroform (100 ml) were added to a 250 ml round flask. The reaction mixture was heated to 60 $^o$C for 1h, resulting in formation of a dark precipitate. After chloroform was removed, the residue was dissolved in methanol (20 ml) with methyl iodide (3 ml). The solution was stirred at 70 $^o$C for 24 h. The solvent and the excess of methyl iodide were removed under reduced pressure to give dark red solid **3.11b**. (1.3 g)

**Yield:** 93%

*The analytical data agrees with that in the Ph.D. Thesis of J.Qu.[2]*

### 3.11. 1,6,7,12-Tetra[4-(2-trimethylammonio-ethyl)-phenoxy]-N,N'-(2,6-diisopropylphenyl)-perylene-3,4,9,10-tetracarboxidiimide tetraiodide:



Ionic perylene derivative **3.11b** (200 mg, 0.103 mmol) and silver methanesulfonate (83 mg, 0.412 mmol) were added to methanol (50 ml). The reaction mixture was stirred for 3 h at room temperature. The white silver iodide was removed by filtration to give a clear red solution. The solvent was removed under reduced pressure to give a dark-red solid **3.11** (180 mg).

**Yield:** 97 %

*The analytical data agrees with that in the Ph.D. Thesis of J.Qu.[2]*

**3.12a).1,6,7,12-Tetra[3-hydroxypyridine]-N,N'-(2,6-diisopropylphenyl)-perylene-3,4,9,10-tetracarboxidiimide:**
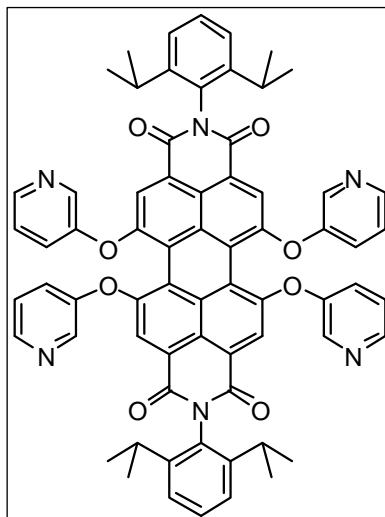


N,N'-Bis(2,6-diisopropylphenyl)-1,6,7,12-tetrachloroperylene-3,4:9,10-tetracarboxylic acid diimide **3.8** (5 g, 5.9 mmol), 3-hydroxylpyridine (4.48 g, 47.2 mmol), and anhydrous K2CO3 (3.45 g, 25 mmol) were added to NMP (600 mL). The solution was stirred at 100 8C under argon for 15 h. The reaction mixture was allowed to cool to room temperature and poured into aqueous hydrochloride acid (1 L, 1m). The precipitated product was filtered under suction and was then washed thoroughly with water and dried at 75ºC under vacuum. The product was purified by column chromatography to give 16 (4.7 g, 74%) as a red solid.

**Yield:** 74 %

*The analytical data agrees with that in the Ph.D. Thesis of J.Qu.[2]*

### 3.12. N,N'-(2,6-diisopropylphenyl)-1,6,7,12-tetra (1-methylpyridinium-3yloxy)-perylene-3,4,9,10-tetracarboxidiimide tetramethanesulfonate (6-11)
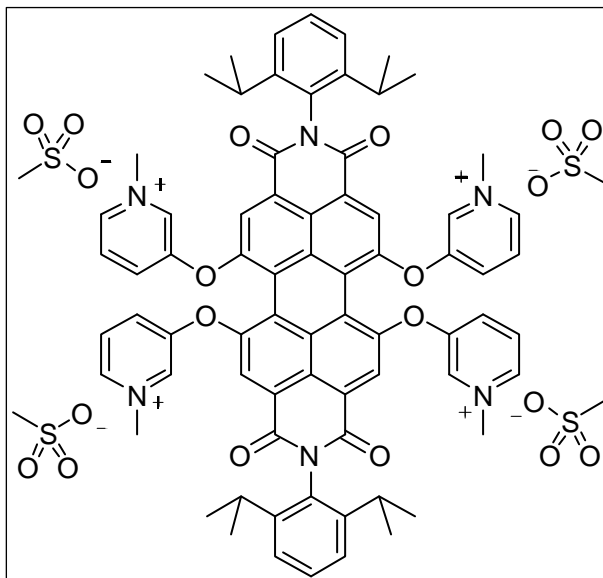


Perylene derivative **6-10** (1.0 g, 0.92 mmol), methyl iodide (3.0 ml) and methanol (150 ml) were added to a 250 ml flask. The reaction mixture was stirred at 80 $^o$C for 24h. After the solvent was removed under reduced pressure, the residue and silver methanesulfonate (743 mg, 3.68 mmol) were added into methanol (100 ml) to form a white precipitate (silver iodide), which was removed to give a clear red solution. The red solid **6-11** (1.4 g) was obtained after evaporating the solvent.

**Yield:** 91 %

*The analytical data agrees with that in the Ph.D. Thesis of J.Qu.[2]*

### 3.18. N-(2,6-diisopropylphenyl)-1,6,7,12-tetraphenoxyperylene-3,4:9,10-tetra carboxy-9,10-monoanhydride-3,4-monoimide:
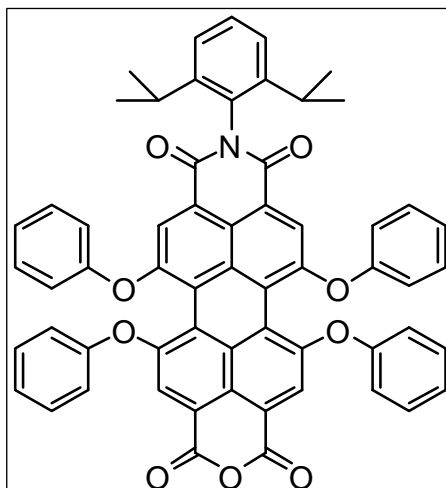


To a solution of N,N'-bis(2,6-diisopropylphenyl)-1,6,7,12-tetraphenoxy perylene-3,4:9,10-tetracarboxy diimide (7.56 g, 7.00 mmol) in 2-propanol (1 L) was added KOH (148 g, 2.64 mol) dissolved in water (130 mL). The reaction was refluxed under argon at 110°C for 12 h. After cooling to room temperature the solution was poured into HCl/H$_2$O (60 mL/3.5 L). The precipitate was filtered and dried under vacuum at 60 °C. The solid was dissolved in acetic acid (100 mL) and refluxed at 80 °C for 30 min. Water (150 ml) was added; the precipitate was filtrated and purified over silica gel using dichloromethane as eluent.

**Yield:** 1,54 g , 24 % red solid

**$^1$H-NMR (250 MHz, DCM-d2 , 300 K):**

δ = 8.16 (s, 2 H), 8.15(s, 2 H), 7.47 (t, J = 7,2 Hz, 1H), 7.35 (d , 2H), 7.33-7.28 (m, 8H), 7.21-7.13 (m, 4 H), 7.03 − 6.97(m, 8H), 2.73-2.62 (sept, J = 6,8 Hz, 2H), 1.08 (d, J = 6,9 Hz, 12H) ppm

**$^{13}$C-NMR (300 MHz, DCM-d2, 300 K):**

δ = 163.54, 160.19, 156.17, 155.60, 146.33, 130.50, 130.42, 128.98, 125.29, 125.17, 124.38, 123.70, 122.49, 120.56, 120.39, 120.33, 118.79, 29.43, 24.04 ppm;

**UV-Vis (CHCl$_3$):** $\lambda_{max}$ ($\varepsilon$) = 443 (14100), 539 (23400), 577 (37300) nm;

**Fluorescence (CHCl$_3$, excitation 570 nm):** $\lambda_{max}$ = 611 nm

**FD-MS spectrum (8 kV):** m/z (rel int.) = 920 (100 %) [M+H]$^+$;
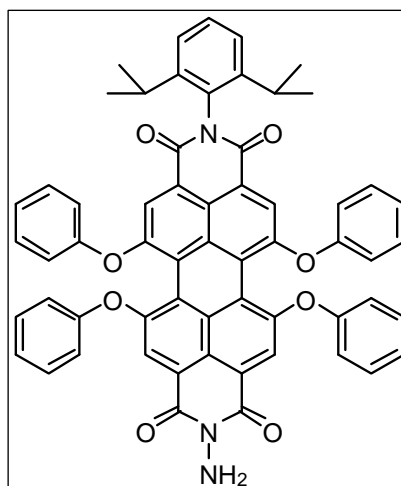
**IR-Spectrum (cm$^{-1}$, ATR):**

$\nu$ = 1769 (C=O), 1735 (C=O), 1708 (C=O), 1673, 1586, 1541, 1508, 1487, 1457, 1404, 1339, 1287 (C=O), 1232, 1200, 1010, 877, 750, 669, 654, 617

**Elemental analysis**

Calc:  78.33 % C, 4.49 % H, 1.52 % N;

Found:  78.36 % C, 4.47 % H, 1.62 % N

### 3.19. N-amino-N'-(2,6-diisopropylphenyl)-1,6,7,12-tetraphenoxy perylene-3,4:9,10-tetracarboxydiimide:



**3.18** (200 mg, 0.2174 mmol) and hydrazine (69 mg, 2.17 mmol) were added to toluene (20 mL). The mixture was stirred under argon at 120°C for 8 h. Following the reduction of the solvent, the material was purified over silica gel using toluene/ethyl acetate 4/1 resulting in 3.19 as a red solid.

**Yield:** 130 mg, 65 % red solid

**$^1$H-NMR (300 MHz, DMSO-d$_6$, 300 K):**

δ = 7.93 (s, 2 H), 7.92 (s, 2 H), 7.67-7.59 (m, 10H), 7.40 (t, J = 15 Hz, 1H), 7.28 (d , J = 9 Hz, 2H), 7.01-6.95 (m, 10 H), 2.73-2.71 (sept, J = 6 Hz, 2H), 1.00 (d, J = 6,9 Hz, 12H) ppm

**$^{13}$C-NMR (300 MHz, DMSO-d$_6$, 300 K):**

δ = 162.50 (C=O), 159.42 (C=O), 154.84, 154.77, 145.44, 144.94, 144.87, 132.06, 127.72, 123.62, 122.71, 122.33, 119.65, 119.55, 118.97, 118.91, 23.67 (CH(CH$_3$)$_2$)

**UV-Vis (CHCl$_3$):** λ$_{max}$ (ε) = 450 (13 550), 540 (26 124), 580 (41 961) nm;

**Fluorescence** (CHCl$_3$, excitation 580 nm): λ$_{max}$ = 618 nm

**FD-MS spectrum (8 kV):** m/z (rel int.) = 934 (100 %) [M+H]$^+$;
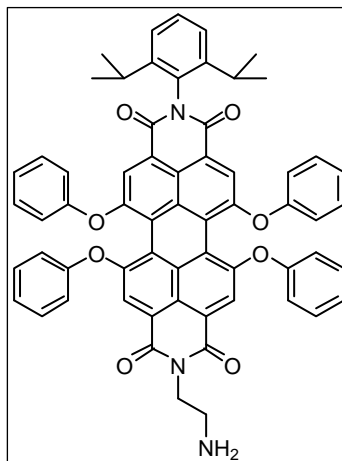
**IR-Spectrum (cm$^{-1}$, ATR):**

ν = 3354 (N-H), 3066 (N-H), 2968 (C-H), 2873, 1701, 1653, 1585 (C=C aromatic), 1512, 1487, 1408 (C-H bend), 1338 (C-N stretch), 1277, 1196, 1161, 1065, 1022, 962, 914, 870, 812, 748 (CH aromatic)

**Elemental analysis:**

Calc %:        76.16 % C, 4.64% H, 4.50 % N;

Found %:       76.04 % C, 4.62 % H, 4.28 % N

### 3.20. N-(2,6-diisopropylphenyl)-N'-(4-aminoethyl)-1,6,7,12-tetra phenoxyperylene-3,4:9,10 tetracarboxydiimide:



**3.18** (600 mg, 0.65 mmol) and 1,2-ethylenediamine (390 mg, 6.5 mol) were added to toluene (60 mL). The mixture was stirred under argon at 60°C for 3 h. Following the reduction of the solvent, the material was purified over silica gel using dichloromethane/acetone 9/1 and dichloromethane/ethanol 10/3 as eluent resulting in **3.20** as a red solid.

**Yield:** 420 mg, 60 % red solid

**$^1$H-NMR (250 MHz, DCM-d2, 300 K):**

$\delta$ = 8.16 (s, 2 H), 8.15(s, 2 H), 7.47 (t, J = 12.5 Hz, 1H), 7.30 (m, 10H), 7.14 (m, 4 H), 6.98 (m, 8H), 4.16 (t, J = 12 Hz, 2H), 2.95 (t, J = 12.5 Hz, 2H), 2.65( m, 2H), 1.08 (d, J = Hz, 7.5H, 12H) ppm

**$^{13}$C-NMR (300 MHz, DCM-d2, 300 K):**

$\delta$ = 163.94, 163.83, 156.32, 156.14, 155.96, 146.55, 133.57, 131.62, 130.52, 129.95, 125.11, 125.08, 124.54, 123.37, 121.44, 121.16, 120.76, 120.63, 120.48, 120.44, 40.66, 31.16, 29.59, 25.34, 24.23 ppm;

**UV-Vis** (CHCl$_3$): $\lambda_{max}$ ($\epsilon$) = 450 (12 348), 538 (21 708), 580 (35 991) nm

**Fluorescence** (CHCl$_3$, excitation 566 nm) $\lambda_{max}$ = 620 nm;

**MS (FD):** m/z (rel.int.) 962 (100 %) [M+];
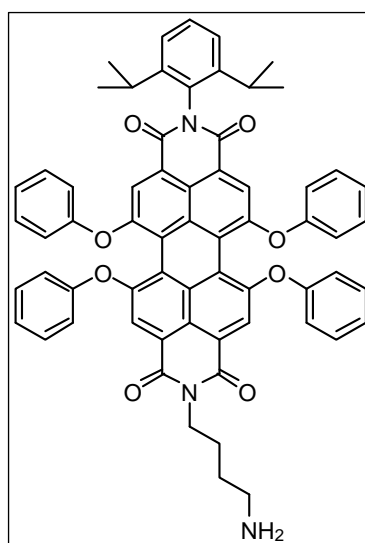
**IR-Spectrum (cm$^{-1}$, ATR):**

$\nu$ = 3425 (N-H), 2925 (C-H), 1701(C=O), 1655, 1589 (C=C aromatic), 1508, 1491, 1414 (C-H bend), 1342 (C-N stretch), 1315, 1282, 1209, 1184, 1124, 1032, 1005, 877, 841, 700 (CH aromatic) cm$^{-1}$

**Elemental analysis:**

Calc %:        77.40 % C, 4.92 % H, 4.37 % N;

Found %:        76.87 % C, 4.86 % H, 4.33 % N

### 3.21. N-(2,6-diisopropylphenyl)-N'-(6-aminoethyl)-1,6,7,12-tetra phenoxyperylene-3,4:9,10 tetracarboxydiimide:



N-(2,6-diisopropylphenyl)-1,6,7,12-tetraphenoxyperylene-3,4:9,10-tetra carboxy-9,10-monoanhydride-3,4-monoimide (214 mg, 0,2334 mmol) and 1,4 – diaminobutane  (2,59 g, 2,59 mol) were added to toluene  (20 ml). The solution was stirred at 60°C under argon for 3 h. Following the reduction of the solvent the mixture was extracted with dichloromethane (25 mL) and washed twice with distilled water (50 mL). The dichloromethane layer was separated, dried over

MgSO₄, and the crude product was purified by column chromatography (silica gel/ CH₂Cl₂ and then CH₂Cl₂/ethanol 10/3) to afford the product as red solid.

**Yield:** 231 mg, 70 %

**¹H-NMR (250 MHz, DCM-d2 , 300 K):**

δ = 8,16 (s, 2 H), 8,15(s, 2 H), 7,47 (t, J = 7,2 Hz, 1H), 7,35 (d , 2H), 7,33-7,28 (m, 8H), 7,21-7,13 (m, 4 H), 7,03 – 6,97(m, 8H), 4,07-4.04 (t, J = 7,5 Hz, 2H), 2,99-2,95 (m, 2H), 2,73-2,62 (sept, J = 6,8 Hz, 2H), 1,66-1,65 (m, 2H), 1,64-1,62 (t, J =  5 Hz, 2 H) 1,08 (d, J = 6,9 Hz, 12H) ppm

**¹³C-NMR (300 MHz, DCM-d2, 300 K):**

δ = 163.83 (C = O), 156.31, 156.11, 146.54, 133.54, 131.61, 130.50, 129.95, 125.11, 124.54, 123.33, 121.39, 121.14, 120.94, 120.37, 29.59, 25.64 (CH(CH₃)₂), 24.23 (CH₃) ppm

**UV-Vis** (CHCl₃): λ$_{max}$ (ε) = 444 (14 097), 538 (24 874), 578 (37 063) nm

**Fluorescence** (CHCl₃, excitation 578 nm) λ$_{max}$ = 614 nm

**MS (FD 8 kV):** m/z = 990 (100 %) [M$^+$] (calc. 990, 11)

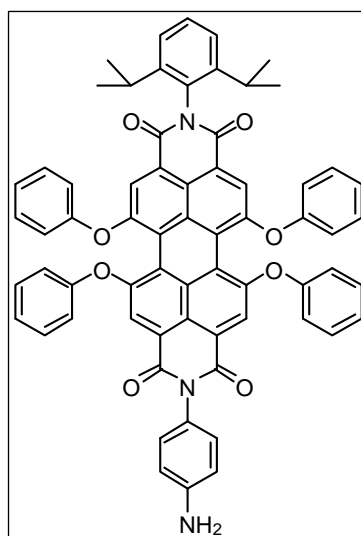**IR-Spectrum (cm$^{-1}$, ATR):**

ν = 3078 (N-H), 2964, 2929 (C-H), 2870, 2156, 2033, 1979, 1701, 1662, 1585 (C=C aromatic), 1510, 1487, 1410 (C-H bend), 1340 (C-N stretch), 1281, 1198, 1165, 1074, 876, 804, 748 (CH aromatic)

**Elemental analysis:**

Calc %:     74.91 % C, 5.40 % H, 4.09 % N;

Found %:     74.38 % C, 4.97 % H, 4.03 % N

### 3.22. N-(2,6-diisopropylphenyl)-N'-(p-aminophenyl)-1,6,7,12-tetra phenoxyperylene-3,4:9,10 tetracarboxydiimide:



N-(2,6-diisopropylphenyl)-1,6,7,12-tetraphenoxy-perylene-3,4:9,10-tetra carboxylicacid-9,10-monoanhydride -3,4-monoimide **3.18** (2.26 g, 2.456 mmol), 1,4 –diaminobenzene (3.14 g, 29.1 mol) and of zing acetate (452 mg, 2.456 mol) were added to quinoline (90 ml). The solution was stirred at 160°C under argon for 8 h. The reaction mixture was allowed to cool down to room temperature and poured into hydrochloride acid (500 ml in 3,5 L water).The precipitated product was filtered under suction and dried at 75°C under vacuum. The product was purified by column chromatography (silica gel/ ethyl acetate/toluene 2/3) to give **3.22** (870 mg, 35 %) as a red solid.

**Yield:** 870 mg, 35 %

**$^1$H-NMR (250 MHz, DCM-d2 , 300 K):**

δ = 8,17 (s, 8 H), 7,34 (t, J = 7,2 Hz, 1H), 7,31 (d , 2H), 7,31-7,28 (m, 8H), 7,21-7,13 (m, 4 H), 7,03 – 6,84(m, 8H), 2,73-2,62 (sept, J = 6,8 Hz, 2H), 1,08 (d, J = 6,9 Hz, 12H) ppm

**$^{13}$C-NMR (300 MHz, DCM-d2, 300 K):**

δ = 164.09, 163.84, 156.33, 156.21, 155.97, 147.67, 146.55, 133.66, 131.62, 130.51, 129.80, 126.10, 125.11, 125.03, 124.55, 123.82, 123.35, 121.45, 120.94, 120.87, 120.57, 120.47, 120.33, 115.63, 29.60, 24.23 ppm

**UV-Vis** (CHCl$_3$): $\lambda_{max}$ ($\varepsilon$) = 446 (12 460), 540 (23 943), 578 (38 160) nm

**Fluorescence** (CHCl$_3$, excitation 578 nm) $\lambda_{max}$ = 616 nm

**MS(FD 8 kV): m/z =** 1010 (100 %) [M$^+$] (calc. 1010, 09)
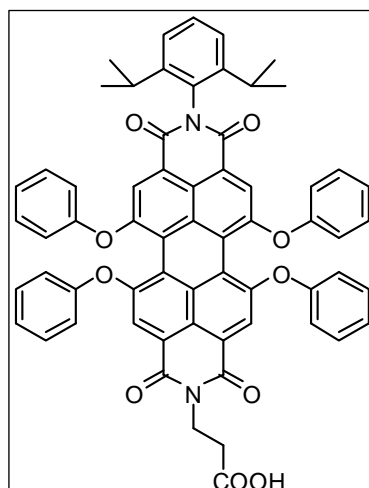
**IR-Spectrum (cm$^{-1}$, ATR):**

$\nu$ = 3369 (N-H), 3070, 2962, 2875, 1702, 1668, 1580 (C=C aromatic), 1520, 1491, 1408 (C-H bend), 1346 (C-N stretch), 1317, 1282, 1196, 1165, 1063, 1030, 960, 881, 759 (CH aromatic)

**Elemental analysis:**

Calc %:    78.48 % C, 4.69 % H, 4.16 % N;

Found %: 78.23 % C, 4.50 % H, 4.02 % N

### 3.23.N-(2,6-diisopropylphenyl)-N'-(4-carboxyethyl)-1,6,7,12-tetra phenoxyperylene-3,4:9,10-tetracarboxydiimide:



**3.18** (500 mg, 0.59 mmol) and 4-aminopropionic acid (532 mg, 5.9 mmol mol) were added to propionic acid (50 mL). The mixture was stirred under argon at 140 °C for 3 h. After cooling the reaction mixture to room temperature, the product was precipitated with water (250 mL). The precipitate was filtered, washed with water and dried under vacuum. Further purification was done by column

chromatography on silica gel with dichloromethane/acetone 9/1 and dichloromethane/ethanol 10/3 as eluent to afford **3.23** in a yield of 65 %.

**Yield:** 380 mg, 65 %

**$^{1}$H-NMR (250 MHz, DCM-d2 , 300 K):**

δ = 8.06 (s, 4 H), 7.37 (t, *J* = 7.5 Hz, 1H), 7.19 (m, 10H), 7.03 (m, 4 H), 6.87 (d, *J* = 7.5 Hz, 8H), 4.26 (t, *J* = 10 Hz, 2H), 2.59 (m, 4H), 1.00 (d, *J* = 7.5 Hz, 12H) ppm

**$^{13}$C-NMR (300 MHz, DCM-d2, 300 K):**

δ = 163.82, 156.37, 146.52, 130.50, 125.12, 125.06, 124.55, 123.35, 123.08, 121.33, 120.48, 31.99, 29.59, 24.22 ppm;

**UV-Vis** (CHCl$_3$): $\lambda_{max}$ (ε) = 450 (13 298), 536 (23 728), 580 (38 132) nm

**Fluorescence (CHCl$_3$, excitation 580 nm)** $\lambda_{max}$ = 620 nm

**MS (FD):** m/z (rel.int.) 990 (100 %) [M$^{+}$];

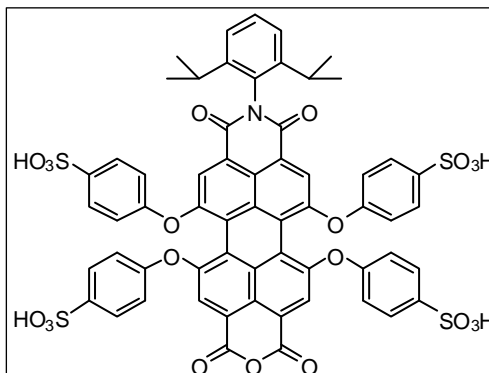**IR-Spectrum (cm$^{-1}$, ATR):**

ν = 3068, 2966, 2935, 2871, 1705, 1662, 1585 (C=C aromatic), 1508, 1487, 1410 (C-H bend), 1342, 1313, 1288, 1203, 1165, 1022, 876, 802, 748 (CH aromatic), 690

**Elemental analysis:**

Calc %:      74.92 % C, 4.78 % H, 2.78 % N;

Found %:      74.38 % C, 4.78 % H, 2.58 % N

### 3.24. N-(2,6-diisopropylphenyl)-1,6,7,12-tetra-(4-sulfo)phenoxy-perylene -3,4:9,10-tetracarboxylicacid-9,10-monoanhydride-3,4-monoimide



Compound **3.18** (100 mg, 0,109 mol) was added to concentrated sulphuric acid (5 ml). The flask was sealed, and the mixture was stirred at room temperature for 24 h. Water (10 ml) was slowly added to the flask to from a precipitate, which was filtered under suction. The solid was washed three times with dichloromethane, and then was dried at 120°C under vaccum to give red solid.

**Yield:** 133 mg, 98 %

**$^1$H-NMR (250 MHz, CD$_3$OD, 300 K):**
δ = 8,13 (s, 2 H), 8,12(s, 2 H), 7,84-7,81 (m, 8H), 7,67 (t, J = 7,2 Hz, 1H), 7,35 (d , 2H), 7,03 − 6,97(m, 8H), 2,73-2,62 (sept, J = 6,8 Hz, 2H), 1,08 (d, J = 6,9 Hz, 12H) ppm

**$^{13}$C-NMR (300 MHz, DCM-d2, 300 K):**
δ =170.46, 169.48, 164.86, 158.53, 158.49, 158.39, 155.95, 155.68, 147.24, 142.68, 142.15, 135.97, 134.17, 133.56, 133.10, 129.39, 125.03, 123.35, 123.30, 121.81, 120.47, 118.95, 30.32, 24.27 ppm

**UV-Vis** (H$_2$O): λ$_{max}$ (ε) = 430 (12 612), 544 (27 647) nm

**Fluorescence** (H$_2$O, excitation 544 nm) λ$_{max}$ = 620 nm

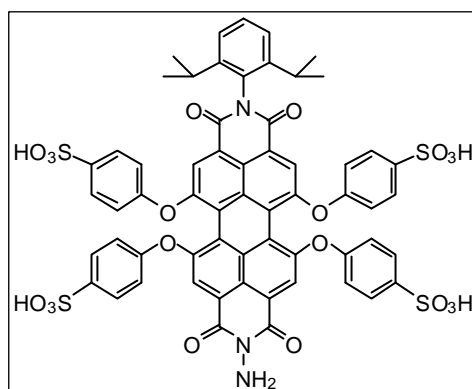**MS (MALDI – TOF): m/z =** 1240 (100 %) [M$^+$] (calc. 1240, 22)

**IR-Spectrum (cm$^{-1}$, ATR):**

ν = 1770 (C=O), 1740 (C=O), 1710 (C=O), 1675, 1585, 1539, 1510, 1490, 1461, 1409, 1282 (C=O), 1232, 1215, 1200, 1010, 879, 751, 669, 654

**Elemental analysis:**

Calc %:     58.11 % C, 3.33 % H, 1.13 % N;

Found %:  57.79 % C, 3.21 % H, 1.02 % N

### 3.25. N-amino-N'-(2,6-diisopropylphenyl)-1,6,7,12-tetra-(4-sulfo)-phenoxyperylene-3,4:9,10-tetracarboxydiimide:



**3.19** (400 mg, 0.31 mmol) was added to concentrated sulfuric acid (12 mL). The flask was sealed, and the mixture was stirred at room temperature for 16 h. Water was slowly added to the flask and the resulted solution was dialyzed in water. The solution was freeze dried to give the product as a red solid.

**Yield:** 377 mg, 94 %

**$^1$H-NMR (300 MHz, DMSO-d$_6$ , 300 K):**

δ = 8.18 (d, J = 3.2 Hz, 4H), 7.88-7.75 (m, 8H), 7.47-7.37 (t, J = 7.21 Hz, 1H), 7.29 (d, J = 7.75 Hz, 2H), 7.17-7.03 (m, 8H), 2.75-2.64 (sept, 2H), 1.09 (d, J = 6.80 Hz, 12H) ppm

**$^{13}$C-NMR (300MHz, DMSO-d$_6$, 300 K):**

δ = 164.56, 158.38, 158.29, 157.28, 156.44, 147.27, 144.84, 142.97, 142.76, 133.97, 132.83, 131.81, 129.55, 129.44, 124.99, 123.40, 121.79, 120.57, 120.47, 30.34, 24.30 ppm

**UV-Vis** (CHCl$_3$): λ$_{max}$ (ε) = 450 (14 795), 532 (28 699), 564 (35 024) nm

**Fluorescence** (CHCl$_3$, excitation 564 nm) λ$_{max}$ = 622 nm

**MS (MALDI – TOF): m/z =** 1254 (100 %) [M$^+$] (calc. 1254, 25)
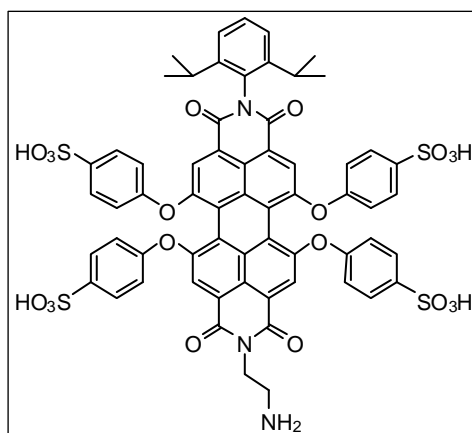
**IR-Spectrum (cm$^{-1}$, ATR):**

ν = 3444 (N-H), 3062 (N-H), 2961 (C-H), 2873, 1702, 1665, 1586 (C=C aromatic), 1511, 1487, 1409 (C-H bend), 1340 (C-N stretch), 1282, 1199, 1161, 1066, 1022, 962, 874, 815, 747 (CH aromatic)

**Elemental analysis:**
Calc %:   57.46 % C, 3.46 % H, 3.35 % N;
Found %: 56.57 % C, 3.30 % H, 3.27 % N

### 3.26. N-(2,6-diisopropylphenyl)-N'-(4-aminoethyl)-1,6,7,12-tetra(4-sulfo phenoxy)-perylene-3,4:9,10-tetracarboxydiimide:



**3.20** (500 mg, 0.5 mmol) was added to concentrated sulfuric acid (15 mL). The flask was sealed, and the mixture was stirred at room temperature for 16 h. Water was slowly added to the flask and the resulted solution was dialyzed in water. The solution was freeze dried to give the product as a red solid.

**Yield:** 622 mg, 97 %

**$^1$H-NMR (250 MHz, DMSO-d6, 300 K):**

δ = 7.97 (s, 2 H), 7.86 (s, 2 H), 7.67 (d, *J* = 7.5 Hz, 5H), 7.57 (d, *J* = 7.5 Hz, 5H), 7.41 (t, *J* = 12 Hz, 1H), 7.38 (d, *J* = 7.5, 2H), 7.01 (d, *J* = 7.5, 4H), 6.93 (d, *J* = 7.5, 4H), 3.08 (t, *J* = 7.5 Hz, 2H), 2.68 (sept, *J* = 10 Hz, 2H), 1.01 (d, *J* = 5 Hz, 12H) ppm

**$^{13}$C-NMR (250 MHz, DMSO-d6, 300 K):**

δ = 163.61, 163.34, 157.38, 157.22, 155.42, 155.07, 146.02, 141.20, 141.10, 132.84, 132.33, 130.59, 129.38, 128.15, 128.03, 123.79, 123.42, 123.19, 121.35, 121.08, 120.89, 120.36, 119.07, 38.80, 37.92, 29.07, 23.08 ppm;

**UV-Vis** ($H_2O$): $\lambda_{max}$ (ε) = 450 (10 850), 534 (21 825), 560 (22 243) nm

**Fluorescence** ($H_2O$, excitation 566 nm) $\lambda_{max}$ = 620 nm;

**MS (MALDI-TOF):** m/z (rel. int.) = 1283 (100 %) [M$^+$] (calc. 1282.30)
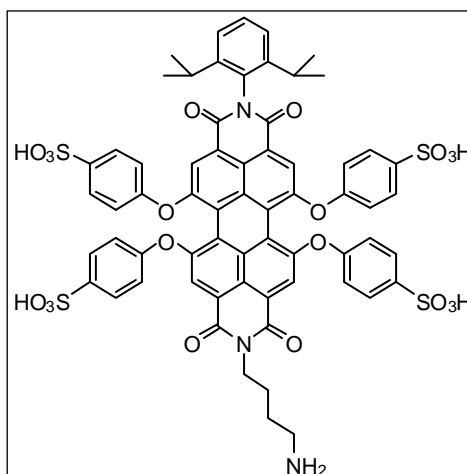
**IR-Spectrum (cm$^{-1}$, ATR):**

$\nu$ = 3078 (N-H), 2968, 2949 (C-H), 2875, 2166, 2036, 1979, 1699, 1664, 1589 (C=C aromatic), 1512, 1485, 1414 (C-H bend), 1342 (C-N stretch), 1309, 1282, 1203, 1169, 1080, 1028, 906, 852, 796, 745 (CH aromatic)

**Elemental analysis:**

Calc %:    58.07 % C, 3.69 % H, 3.28 % N;

Found %:  57.11 % C, 3.53 % H, 3.21 % N

### 3.27.  N-(2,6-diisopropylphenyl)-N'-(6-aminohexyl)-1,6,7,12-tetra(4-sulfo phenoxy)-perylene-3,4:9,10-tetracarboxydiimide:



**3.21** (500 mg, 0.38 mmol) was added to concentrated sulfuric acid (15 mL). The flask was sealed, and the mixture was stirred at room temperature for 16 h. Water was slowly added to the flask and the resulted solution was dialyzed in water. The solution was freeze dried to give the product as a red solid in 96 % yield.

**Yield:** 477 mg, 96 %

**$^1$H-NMR (250 MHz, DMSO-d$_6$ , 300 K):**

δ =7.96 (s, 2H), 7.85 (s, 2H), 7.64 (dd, J = 8.58 Hz, 10H), 7.40 (d, J = 7.51 Hz, 1H), 7.28 (d, J = 7.70 Hz, 2H), 6.99 (m, 10H), 4.01 (m, 2H), 2.73 (sept, J = 6.57 Hz, 2H), 1.72-1.57 (m, 2H), 1.57-1.41 (m, 2H), 1.00 (d, J = 6.66 Hz, 12H) ppm

**$^{13}$C-NMR (300 MHz, DCM-d2, 300 K):**

δ =169.027, 162.755, 162.601, 155.448, 155.249, 155.148, 145.596, 144.731, 144.341, 128.003, 127.901, 123.127, 122.704, 120.241, 119.367, 119.265, 118.933, 28.453, 24.553, 23.840 ppm

**UV-Vis** (H$_2$O): λ$_{max}$ (ε) = 452 (15 593), 530 (30 936), 568 (26 392) nm

**Fluorescence** (H$_2$O, excitation 568 nm) λ$_{max}$ = 616 nm

**MS (MALDI-TOF):** m/z (rel. int.) = 1310 (100 %) [M$^+$] (calc. 1310,36)

**IR-Spectrum (cm$^{-1}$, ATR):**

ν = 3080 (N-H), 2967, 2930 (C-H), 2869, 2154, 2030, 1984, 1702, 1665, 1583 (C=C aromatic), 1509, 1489, 1411 (C-H bend), 1339 (C-N stretch), 1282, 1199, 1163, 1071, 912, 857, 806, 750 (CH aromatic)

**Elemental analysis:**

Calc %:   58.66 % C, 3.92 % H, 3.21 % N;

Found %: 58.18 % C, 3.30 % H, 3.05 % N

### 3.28. N- (2,6-diisopropylphenyl)-N-(4-aminophenyl)-1,6,7,12-tetra-(4-sulfo)-phenoxy-perylene-3,4:9,10-tetracarboxylicacid-9,10-monoanhydride-3,4-monoimide
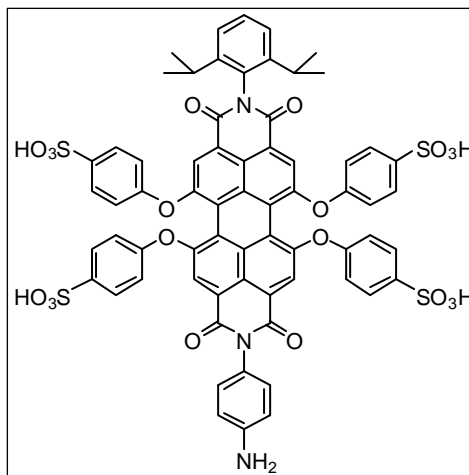


Compound **3.22** (400 mg, 0,4 mol) was added to concentrated sulphuric acid (5 ml). The flask was sealed, and the mixture was stirred at room temperature for 24 h. Water (10 ml) was slowly added to the flask to from a precipitate, which was filtered under suction. The solid was washed three times with dichloromethane, and then was dried at 120°C under vaccum to give red crystals.

**Yield:** 425 mg, 80%

**^{1}H-NMR (250 MHz, DMSO-d6, 300 K)**

$\delta$ = 7.94 (s, 2 H), 7.88 (s, 2 H), 7.67-7.58 (m, 8H), 7.44-7.22 (m, 8H), 7.03-6.99 (d, J = 10 Hz, 4 H), 6.95-6.92 (d, J = 7.5 Hz, 4H), 2,70-2,65 (sept, J = 12.5 Hz, 2H), 1,02-0,99 (d, J = 6,9 Hz, 12H) ppm

**^{13}C-NMR (300 MHz, DCM-d2, 300 K):**

$\delta$ = 164.72, 164.20, 158.30, 158.07, 157.34, 157.01, 156.99, 156.95, 156.54, 156.53, 155.52, 147.42, 143.49, 143.05, 142.94, 136.71, 134.09, 131.98, 129.56, 129.36, 124.51, 124.25, 121.98, 121.92, 120.97, 120.96, 120.46, 30.57, 24.55 ppm

**UV-Vis** ($H_2O$): $\lambda_{max}$ ($\epsilon$) = 450 (6 564), 562 (17 112) nm

**Fluorescence** (H$_2$O, excitation 566 nm) $\lambda_{max}$ = 620 nm

**MS (MALDI-TOF):** m/z (rel. int.) = 1330 (100 %) [M$^+$] (calc. 1330,35)
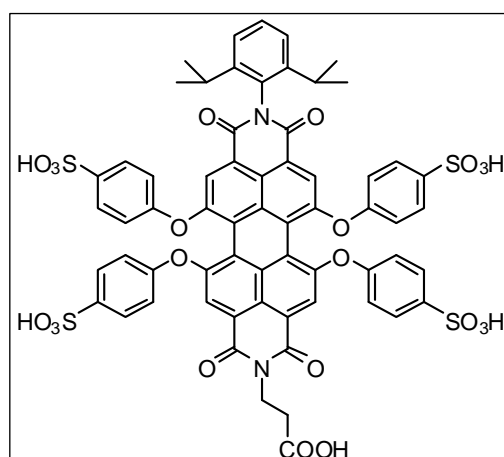
**IR-Spectrum (cm$^{-1}$, ATR):**

$\nu$ = 3462 (N-H), 3381, 3068, 2964, 2873, 1707, 1670, 1589 (C=C aromatic), 1516, 1489, 1410 (C-H bend), 1342 (C-N stretch), 1315, 1286, 1200, 1076, 1024, 957, 879, 808, 752 (CH aromatic)

**Elemental analysis:**

Calc %:    59.59 % C, 3.56 % H, 3.16 % N;

Found %:  58.63 % C, 3.44 % H, 3.03 % N

### 3.29.N-(2,6-diisopropylphenyl)-N`-(3-carboxyethyl)-1,6,7,12-tetra(4-sulfo phenoxy)-perylene-3,4:9,10-tetracarboxydiimide:



**3.23** (400 mg, 0.3 mol) was added to concentrated sulfuric acid (10 mL). The flask was sealed, and the mixture was stirred at room temperature for 48 h. Water was slowly added to the flask and the resulting solution was dialyzed in water. The solution was freeze dried to give the product as a red solid.

**Yield:** 381 mg, 97 %

**$^1$H-NMR (300 MHz, DMSO-d6, 300 K):**

δ = 7.92 (s, 2 H), 7.88 (s, 2 H), 7.66 (m, 4H), 7.60 (m, 4H), 7.40 (t, *J* = 12 Hz, 1H), 7.27 (d, *J* = 9 Hz, 2H), 6.98 (m, 8H), 4.19 (t, *J* = 12 Hz, 2H), 2.68 (sept, *J* = 10 Hz, 2H), 1.00 (d, *J* = 9Hz, 12H) ppm

**$^{13}$C-NMR (300 MHz, DMSO-d6, 300 K):**

δ = 172.25, 162.51, 162.14, 155.26, 155.07, 154.78, 145.43, 144.86, 132.33, 132.03, 130.45, 127.72, 127.69, 123.59, 122.48, 119.87, 119.08, 118.99, 118.88, 31.99, 28.19, 23.64 ppm;

**UV-Vis** ($H_2O$): $\lambda_{max}$ (ε) = 450 (11 454), 534 (22 510), 564 (25 059) nm

**Fluorescence** ($H_2O$, excitation 566 nm) $\lambda_{max}$ = 622 nm;

**MS** (MALDI-TOF): m/z (rel. int.) = 1311 (100 %) [M$^+$]
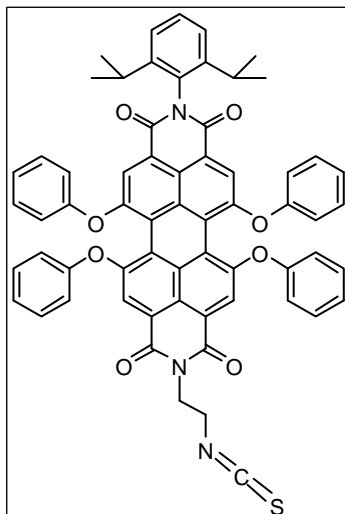
**IR-Spectrum (cm$^{-1}$, ATR):**

ν = 3076, 3047, 2974, 2958, 1730, 1707, 1662, 1583 (C=C aromatic), 1566, 1547, 1512, 1493, 1415 (C-H bend), 1350, 1311, 1288, 1215, 1188, 1165, 1130, 1113, 1038, 881, 845, 704 (CH aromatic), 690

**Elemental analysis:**
Calc %:    57.70 % C, 3.54 % H, 2.14 % N;
Found %: 56.98 % C, 3.40 % H, 2.10 % N

### 3.30. N-(2,6-diisopropylphenyl)-N'-(2-isothiocyanatoethyl)-1,6,7,12-tetra phenoxyperylene-3,4:9,10-tetracarboxydiimide:



**3.20** (100 mg, 0.1 mmol) was dissolved in dry acetone (9 mL). Thiophosgene was added dropwise, and the reaction mixture was stirred at room temperature for 2 h. Following the reduction of the solvent, the mixture was extracted twice with hexane. The hexane layer was separated, dried overnight under vacuum to afford the product as red solid.

**Yield:** 88 mg, 85 %

**$^1$H-NMR (300 MHz, acetone-d6, 300 K):**

δ = 8.10 (m, 4H), 7.33 (m, 11 H), 7.12 (m, 12H), 4.39 (t, J = 6.01 Hz, 2H), 3.97 (t, J = 6.00 Hz, 2H), 2.85 (m, 2H), 1.08 (d, J = 6.81 Hz, 12H) ppm

**$^{13}$C-NMR (300 MHz, acetone-d6, 300 K):**

δ = 164.45, 164.14, 157.51, 157.27, 156.96, 147.37, 134.55, 132.66, 131.56, 130.68, 126.29, 125.16, 124.66, 124.21, 121.85, 121.61, 121.48, 121.05, 120.94, 120.84, 120.75, 120.71, 44.27, 40.55, 29.65, 24.81, ppm;

**UV-Vis** (CHCl$_3$): λ$_{max}$ (ε) = 446 (10 548), 540 (20 870), 578 (33 560) nm

**Fluorescence** (CHCl$_3$, excitation 578 nm) λ$_{max}$ = 616 nm

**MS(FD 8 kV): m/z =** 1004 (100 %) [M$^+$] (calc. 1004.11)

**IR-Spectrum (cm$^{-1}$, ATR):**

ν = 3078, 2968, 2930, 2850 (N=C=S), 2875, 2130, 1707, 1664, 1585 (C=C aromatic), 1547, 1512, 1493, 1485, 1416 (C-H bend), 1350, 1311, 1215, 1189, 1167, 1130, 1111, 1040, 881, 845, 704 (CH aromatic)

### 3.31. N-(2,6-diisopropylphenyl)-N'-(2-isothiocyanatoethyl)-1,6,7,12-tetra (4-sulfophenoxy)-perylene-3,4:9,10-tetracarboxydiimide:
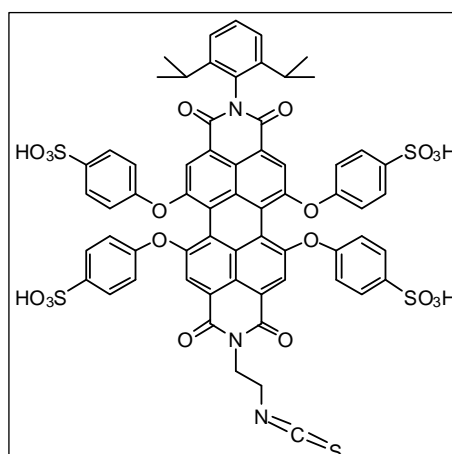


**3.26** (100 mg, 0.078 mmol) was dissolved in mixture of dry DMSO and dry acetone. Thiophosgene was added dropwise, and the reaction mixture was stirred at room temperature for 2 h. Thereafter, the reaction mixture was precipitated in cold ether, the solvent evaporated. The product extracted with methanol, the solvent evaporated and product dried under vacuum and isolated as red solid.

**Yield:** 82 mg, 80 %

**$^1$H-NMR (300 MHz, DMSO-d6, 300 K):**

δ = 7.97 (s, 2 H), 7.86 (s, 2 H), 7.67 (m, 4H), 7.57 (m, 4H), 7.41 (t, *J* = 12 Hz, 1H), 7.28 (d, *J* = 9 Hz, 2H), 6.95 (m, 8H), 4.74 (t, *J* = 12 Hz, 2H), 4.24 (m, 2H), 2.68 (sept, *J* = 10 Hz, 2H), 1.00 (d, *J* = 9Hz, 12H) ppm

**¹³C-NMR (300 MHz, DMSO-d6, 300 K):**

δ =162.82, 162.48, 155.25, 154.99, 154.95, 154.68, 145.39, 144.74, 132.39, 131.75, 130.43, 127.76, 127.63, 123.18, 122.59, 120.15, 119.06, 118.96, 118.48, 54.32, 28.83, 28.21, 24.26, 23.62,  ppm

**UV-Vis** ($H_2O$): $\lambda_{max}$ ($\varepsilon$) = 450 (7 057), 534 (14 225), 566 (15 754) nm

**Fluorescence** ($H_2O$, excitation 566 nm) $\lambda_{max}$ = 620 nm;

**MS** (MALDI-TOF): m/z (rel. int.) = 1324 (100 %) [M⁺]

**IR-Spectrum (cm⁻¹, ATR):**

$\nu$ = 3450, 3020, 2950 (N=C=S), 2930, 2850, 2360, 2340, 1710, 1700, 1685, 1664, 1651, 1643, 1574 (C=C aromatic), 1560, 1547, 1496, 1458, 1437, 1417 (C-H bend), 1342, 1213, 1184, 1122, 1034, 1007, 870, 831, 746

### 3.32.  N-(2,6-diisopropylphenyl)-N'-[3-(N-succinimidyl)carboxyethyl]-1,6,7,12-tetra(4-sulfophenoxy)-perylene-3,4:9,10-tetracarboxydiimide:
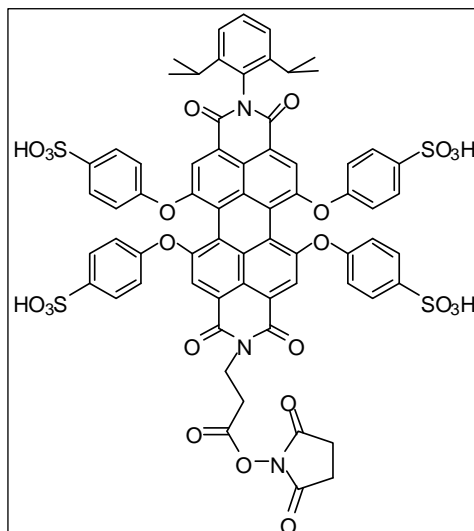


To a solution of **3.29** (50 mg, 0.038 mmol) in DMF (1 mL), dioxane (1 mL) and water (0.5 mL), was added diisopropylethylamine (DIPEA) (7.4 mg, 0.057 mmol) and N,N,N',N'-tetramethyl (succinimido) uronium tetrafluoroborate (TSTU)

(14.3 mg, 0.0475 mmol). After 1 h the mixture was filtered, and the solvents removed under vacuum. Water (2 mL) was added and the solution freeze dried to give the product as red solid.

**Yield:** 45 mg, 85 %

**$^1$H-NMR (300 MHz, DMSO-d6, 300 K):**

$\delta$ = 7.92 (s, 2 H), 7.88 (s, 2 H), 7.66 (m, 4H), 7.60 (m, 4H), 7.40 (t, $J$ = 12 Hz, 1H), 7.27 (d, $J$ = 9 Hz, 2H), 6.98 (m, 8H), 4.30 (t, $J$ = 12 Hz, 2H), 2.76 (m, 4H), 2.68 (sept, $J$ = 10 Hz, 2H), 1.00 (d, $J$ = 9Hz, 12H) ppm

**$^{13}$C-NMR (300 MHz, DMSO-d6, 300 K):**

$\delta$ =169.95, 166.79, 162.58, 162.23, 154.87, 145.50, 144.90, 132.42, 132.10, 130.52, 127.78, 123.67, 123.04, 122.60, 119.96, 199.40, 119.28, 118.97, 53.49, 41.73, 28.28, 25.40, 25.18, 23.72, 18.04, 16.70, 12.35 ppm

**UV-Vis** ($H_2O$): $\lambda_{max}$ ($\varepsilon$) = 450 (9 951), 534 (18 867), 566 (21 071) nm

**Fluorescence** ($H_2O$, excitation 566 nm) $\lambda_{max}$ = 620 nm;

**MS** (MALDI-TOF): m/z (rel. int.) = 1407 (100 %) [M$^+$]

**IR-Spectrum (cm$^{-1}$, ATR):**

$\nu$ = 3440, 3350, 2960, 2924, 2870, 2860, 1732, 1726, 1714, 1699, 1685, 1668, 1651, 1643, 1624, 1574, 1560, 1547, 1504, 1496, 1458, 1437, 1406, 1342, 1311, 1290, 1213, 1184, 1122, 1034, 1007, 870, 831, 746

### 3.33.N-(2,6-diisopropylphenyl)-N'-[N-(4-maleimidobutyryl)aminoethyl]-1,6,7,12-1,6,7,12-tetra(4-sulfophenoxy)-perylene-3,4:9,10-tetracarboxydiimide:
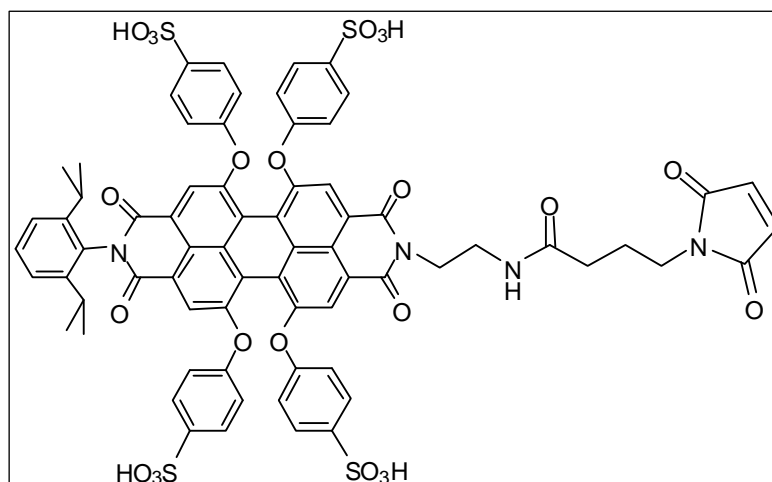


To a solution of **3.26** (50 mg, 0.04 mmol) in dry DMF (3 mL) was a dded triethylamine (0.2 mL) and 4-Maleimidobutyric acid N-succinimidyl ester (GMBS) (10 mg, 0.035 mmol). After 5 h the solvents were removed under vacuum. Dichloromethane (10 mL) was added and the solution filtered. The solvent was removed under vacuum and the product was obtained as a red solid.

**Yield:** 54 mg, 95 %

**$^1$H-NMR (300 MHz, DCM-d2, 300 K):**

δ = 8.15 (s, 2 H), 8.13 (s, 2 H), 7.76 (m, 8H), 7.45 (t, *J* = 12 Hz, 1H), 7.48 (d, *J* = 12 H, 2H), 6.98 (m, 8H), 6.59 (s, 2H), 4.27 (t, *J* = 12 Hz, 2H), 3.53 (m, 2H), 3.41 (t, *J* = 15 Hz, 2H), 2.68 (sept, *J* = 15 Hz, 2H), 2.06 (t, *J* = 15 Hz, 2H), 1.74 (m, 2H), 1.07 (d, *J* = 9 Hz, 12H);

**$^{13}$C-NMR (Spinecho, 300 MHz, DCM-d2, 300 K):**

δ = 173.34, 173.05, 171.50, 163.81, 163.62, 157.14, 157.08, 155.95, 146.58, 142.97, 142.84, 134.66, 133.44, 133.31, 131.52, 129.96, 128.67, 128.57, 124.54, 123.62, 121.55, 121.06, 119.83, 40.43, 38.65, 37.65, 33.78, 29.58, 26.05, 25.00, 24.25 ppm;

**UV-Vis (H₂O):** $\lambda_{max}$ ($\varepsilon$) = 450 (8 367), 534 (16 199), 566 (16 569) nm

**Fluorescence** (H₂O, excitation 566 nm) $\lambda_{max}$ = 620 nm;

**MS** (MALDI-TOF): (100 %) [M$^+$] 1447

**IR-Spectrum (cm$^{-1}$, ATR):**

$\nu$ = 3469, 3406, 3321, 2972, 2937, 2870, 1741, 1720, 1703, 1657, 1649, 1637, 1635, 1626, 1577, 1562, 1547, 1502, 1500, 1439, 1417, 1342, 1311, 1298, 1198, 1128, 1034, 1007, 881, 833, 756

**N-(2,6-Diisopropylphenyl)-4-(bromo)-naphthlene-1,8-dicarboximide, (3.35), and N-(2,6-Diisopropylphenyl)-9-(4,4,5,5-tetramethyl-[1,3,2]dioxaborol an-2-yl)-perylene-3,4-dicarboximide (3.34)**
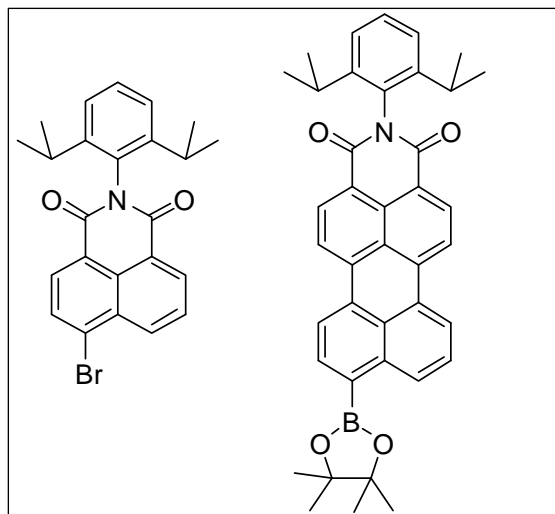


*The synthetic procedure and analytical data are given in the Ph.D. thesis of E. Reuther[3], T. Weil[4]. and C. Kohl[1].*

### 3.38. N,N'-(2,6-Diisopropylphenyl)-terrylene-3,4,11,12-tetracarboxi diimide:
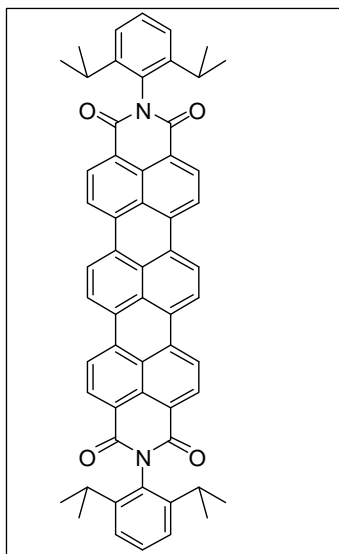
N-iisopropylphenylperylenedicarboximide (4.8 g, 10 mmol), naphthalenedicarboximide **3-5a** (14.2 g, 40 mmol) and *t*-BuONa (19.2 g, 0.2 mol) were added to a 100 ml Schlenk flask. 1,5-Diazabicyclo[4.3.0]non-5-ene (DBN) (30 ml) and diglyme (25 ml) were then injected into the flask under argon. The mixture was stirred at 130 °C for 3h. After cooling to room temperature, the mixture was poured into water (100 ml) to give a precipitate. The dark crude product was washed with ethanol until the color of the filtrate became light red. A pure blue solid was then obtained by recrystallization from chloroform/ethanol. (3.5 g)

**Yield:** 36 %

*The analytical data agrees with that in the Ph.D. Thesis of E. Reuther.[3]*

### 3.39. N-(2,6-Diisopropylphenyl)-N'-(5-carboxpentyl)-terrylene-3,4,11,12-tetracarboxidiimide:
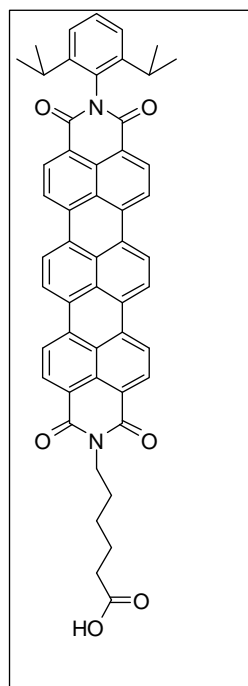
N-Diisopropylphenylperylenedicarboximide (960 mg, 2.0 mmol), naphthalenedicarboximide derivative **49** (1.25 g, 4.0 mmol) and *t*-BuONa (3.84 g, 40 mmol) were added to a 100 ml Schlenk flask. 1,5-Diazabicyclo[4.3.0]non-5-ene (4.0 ml) and diglyme (4.0 ml) were then injected into the flask under argon. The mixture was stirred at 130 °C for 2h. After cooling to room temperature, the mixture was poured into water (100 ml) to give precipitate. The dark crude product was washed with chloroform until the color of the filtrate became light red, and then by methanol (100 ml) three times to give a violet-blue solid (potassium salt). This solid was dissolved in methanol.

When HCl aqueous solution was added, a blue solid was obtained. The product was purified by recrystallization from chloroform/ethanol. (560 mg)

**Yield:** 36 %

*The analytical data agrees with that in the Ph.D. Thesis of J.Qu.[2]*

### 3.40. N-(5-Carboxypentyl)-naphthalene-1,8-dicarboxiimide:
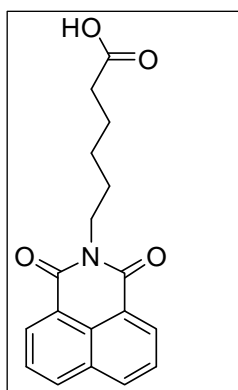
1,8-Naphthaleneanhydride (4.0g, 20.2 mmol), N-(Hexanoic acid)-aniline (5.1 g, 40 mmol) and propionoc acid (250 ml) were added to a 500 ml flask. The reaction mixture was stirred at 140 $^o$C for 15 h. The cooled solution was added to water (1.0 L) to give a white precipitate. The solid was obtained by filtration. The product **3-27** was purified by recrystallization (dichloromethane and ethanol). (5.2 g)

**Yield:** 85 %

*The analytical data agrees with that in the Ph.D. Thesis of J.Qu.[2]*

### 3.41.N-(2,6-Diisopropylphenyl)-N'-(6-hexanoate)-terrylene-3,4,11,12-tetracarboxidiimide:
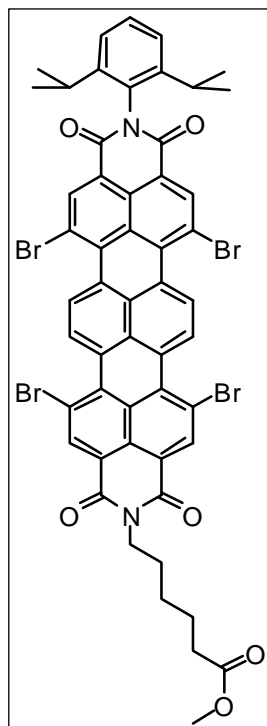
**3.39** (600 mg, 0.74 mmol) was dissolved in chloroform (250 mL). Then bromine was added (12 mL, 0.2 mmol) and the reaction mixture was heated to reflux for 48 h with exclusion of light. Thereafter, the mixture was flushed with nitrogen to remove remaining bromine, and the solvent was evaporated under vacuum. Column chromatography on silica gel with dichloromethane/methanol (9/1) as eluent afforded **3.41** as a blue solid.

**Yield:** 504 mg, 61 %

*The analytical data agrees with that in the Ph.D. Thesis of Fabian Nolde.*[5]

### 3.42.N-(2,6-Diisopropylphenyl)-N´-(6-hexanoat)-1,6,9,14-tetraphenoxy terrylene-3,4,11,12-tetracarboxidiimide:
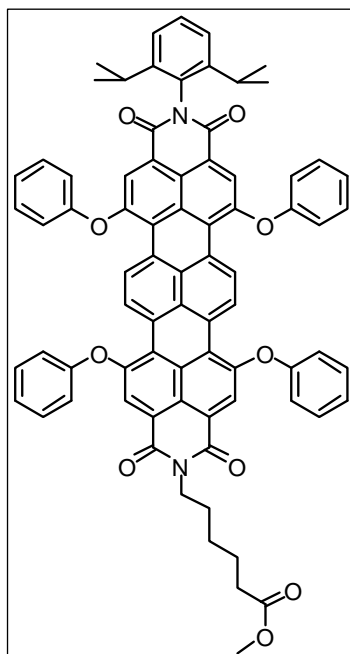
**3.41** (400 mg, 3.6 mmol), phenol (170 mg, 16 mmol), and $K_2CO_3$ (240 mg, 16 mmol) were heated in N-methylpyrrolidone (30 mL) at 90ºC under argon for 17 h. After cooling to room temperature the reaction mixture was poured into HCl (2N, 100 mL). The crude solid was separated under vacuum, dissolved in dichloromethane, and dried over $MgSO_4$.Column chromatography on silica gel with dichloromethane /methanol (9/1) as eluent gave **3.42** as a blue solid.

**Yield:** 307 mg, 73 %

*The analytical data agrees with that in the Ph.D. Thesis of Fabian Nolde.*[5]

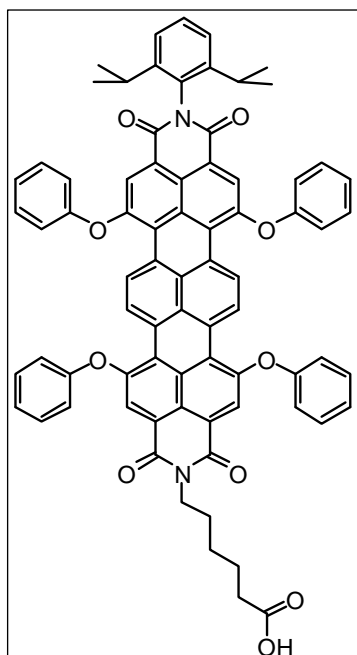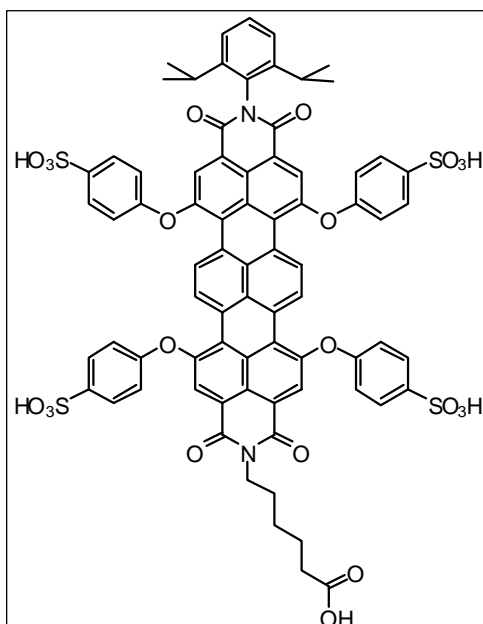### 3.43.N-(2,6-Diisopropylphenyl)-N´-(5-carboxypentyl)-1,6,9,14-tetra phenoxyterrylene-3,4:11,12-tetracarboxidiimide:



To a solution of **3.42** (300 mg, 0.25 mmol) in tetrahydrofuran (15 mL) was added an aqueous solution of LiOH (0.300 mL, 2.3 M) and the mixture was heated at 80 ºC for 12 h under an argon atmosphere. Then the reaction mixture was added to distilled water and the product extracted with dichloromethane (3 x 20 mL). The organic phases were collected, washed twice with water, dried with MgSO4, filtrated and solvent evaporated to give **3.43** as a blue solid. The dried product was used without further purification.

**Yield:** 278 mg, 94 %

### 3.44.N-(2,6-Diisopropylphenyl)-N´-(5-carboxypentyl)- 1,6,9,14-tetra(4-sulfonylphenoxy)terrylene-3,4:11,12-tetracarboxidiimide:



**3.43** (250 mg, 0.21 mmol) was added to concentrated sulfuric acid (10 mL). The flask was sealed, and the mixture was stirred at room temperature for 16 h. Water was slowly added to the flask and the resulted solution was dialyzed in water. The solution was freeze dried to give the product as a blue powder.

**Yield:** 297 mg, 93 %

*The analytical data agrees with that in the Ph.D. Thesis of Fabian Nolde.[5]*

### 3.45.   N-(2,6-diisopropylphenyl)-N'-[5-(N-succinimidyl)carboxypentyl]-1,6,9,14-tetra(4-sulfonylphenoxy)-terrylene-3,4,11,12-tetracarboxidiimide:
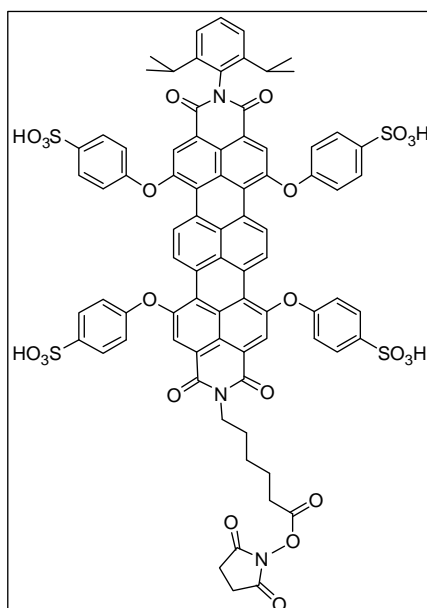


To a solution of **3.44** (200 mg, 0.13 mmol) in DMF (2 mL), dioxane (2 mL) and water (1 mL), was added diisopropylethylamine (12 mg, 0.1 mmol) and TSTU (50 mg, 0.16). After 1 h the mixture was filtered, and the solvents removed under vacuum. Water (2 mL) was added and the solution was freeze dried to give the product as a blue-green solid.

**Yield:** 163 mg, 80%

**$^1$H-NMR (700 MHz, DMSO-d6, 300 K):**

δ = 9.37 (s, 4H), 8.03 (s, 2H), 7.95 (s, 2H), 7.70 (d, *J* = 6.3 Hz, 4H), 7.67 (d, *J* = 6.3 Hz, 4H), 7.42 (t, *J* = 9 Hz, 1H), 7.29 (d, *J* = 9 Hz, 2H), 7.22 (m, 8H), 3.93 (m, 2H), 2.65 (sept., *J* = 13 Hz, 2H), 2.17 (t, *J* = 7.27 Hz, 2H), 1.58 (m, 2H), 1.50 (m, 2H), 1.29 (m, 2H), 1.01 (d, *J* = 6 Hz, 12H) ppm

**$^{13}$C-NMR (500 MHz, DMSO-d6, 300 K):**

δ = 174.03, 168.53, 166.25, 162.22, 155.03, 153.60, 145.32, 144.69, 144.61, 130.52, 128.35, 128.22, 127.76, 125.36, 124.35, 123.48, 122.70, 121.95, 121.53, 118.28, 118.13, 40.33, 33.24, 30.99, 30.96, 28.19, 26.83, 25.74, 23.93, 23.49 ppm;

**UV-Vis (H$_2$O):** λ$_{max}$ (ε) = 426 (4 569), 638 (24 468);

**MS (MALDI-TOF):** 1575 (100 %) [M$^+$]

**IR-Spectrum (cm$^{-1}$, ATR):**

ν = 2962, 2937, 2929, 2870, 1741, 1720, 1703, 1664, 1657, 1649, 1637, 1585, 1562, 1547, 1439, 1417, 1402, 1350, 1311, 1298, 1238, 1173, 1034, 1007, 918, 881, 849, 833, 810

### 3.46. N-(2,6-diisopropylphenyl)-N'-[5-(N-(2-(4-maleimidobutyryl)ethyl)-carboxypentyl]-1,6,9,14-tetra(4-sulfonylphenoxy)-terrylene-3,4,11,12-tetra carboxidiimide :
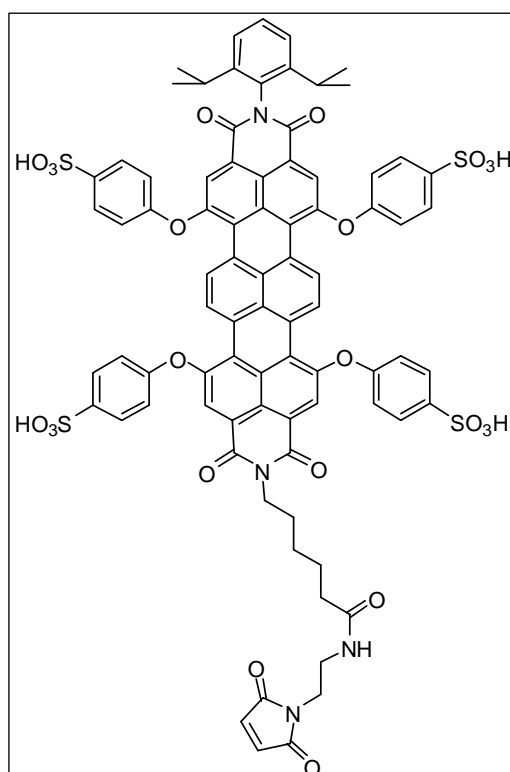


To a solution of **3.45** (100 mg, 0.063 mmol) in dry DMF (3 mL) was added triethylamine (6.36 mg, 0.063 mmol) and 2-maleimidoethylamine trifluoroacetate salt (15 mg, 0.059 mmol). After 5 h the solvent was removed under vacuum. Dichloromethane (10 mL) was added and the solution filtered. The solvent was removed under vacuum and the product was obtained as a blue-green solid.

**Yield:** 91 mg, 90%

**¹H-NMR (700 MHz, DCM-d2, 300 K):**

δ = 9.15 (s, 4H), 8.19 (s, 2H), 7.82 (m, 8H), 7.46 (t, *J* = 9 Hz, 1H), 7.31 (d, *J* = 9 Hz, 2H), 7.15 (m, 8H), 7.03 (s, 2H), 3.91 (m, 2H), 3.36 (m, 4H), 2.65 (sept., *J* = 13 Hz, 2H), 2.17 (t, *J* = 7.27 Hz, 2H), 1.58 (m, 2H), 1.50 (m, 2H), 1.29 (m, 2H), 1.08 (d, *J* = 6 Hz, 12H) ppm

**¹³C-NMR (700 MHz, DCM-d2, 300 K):**

δ = 73.28, 171.53, 163.49, 162.89, 161.47, 161.28, 157.46, 157.42, 154.44, 154.42, 146.78, 143.21, 134.7, 129.03, 128.96, 128.94, 119.15, 116.86, 38.05, 37.98, 36.56, 30.29, 29.67, 26.08, 24.39 ppm

**UV-Vis (H$_2$O):** $\lambda_{max}$ (ε) = 426 (2 782), 638 (16 633) nm

**MS (MALDI-TOF):** 1665 (100 %) [M$^+$+ 3Na$^+$]

**IR-Spectrum (cm$^{-1}$, ATR):**

ν = 2962, 2941, 2929, 2844, 1741, 1720, 1707, 1649, 1633, 1593, 1585, 1561, 1547, 1494, 1439, 1417, 1402, 1350, 1311, 1277, 1238, 1175, 1034, 1007, 918, 881, 849, 833

## *Chapter 4*

Phospholipase A1 (PLA1) was a gift from Novozymes. 1-palmitoyl-2-oleoyl-sn-glycero-3-phosphocholine (POPC) was purchased from Avanti Polar Lipid and used without further purification. 3,3'-dioctadecyloxacarbocyanine perchlorate (DIO) was supplied by Fluka (purity > 99.0%). 5-carboxyfluorescein diacetate single isomer (5-CFDA) was purchased from Molecular Probes. The solutions of 5-CFDA were kept in dimethylsulfoxide (DMSO) (Aldrich 99,9%). Tritom X-100 was purchased from Fluka. ATTO dye 647N NHS ester was supplied by ATTO-Tec.

POPC was purchased from Avanti Polar Lipid and used without further purification. For measurements using non-labeled enzymes, the phospholipid layers were labeled with 5mol% 1,1'-dioctadecyl-3,3,3',3'-tetramethylindocarbocyanine perchlorate (DiI, Molecular Probes). For the two colour experiments, 0.1mol% 3,3'-dioctadecyloxacarbocyanine perchlorate (DIO, Fluka, purity > 99.0%) was used. Chloroform was of spectroscopic grade (Aldrich) and for aqueous solutions; Milli-Q water was used.

Phospholipid layers were prepared using the re-hydration method13. Specifically, 90µl of a POPC solution (10mg/ml) containing dye was spin-coated onto freshly cleaved mica (SPI supplies, V-4 grade).

Enzyme solutions were prepared in a buffer containing 0.01 M Hepes (Fluka, 99.5%), 30 µM calcium chloride (Sigma 99%), 10 µM EDTA (Sigma 95%) and 0.15 M sodium chloride (Sigma-Aldrich 99.99%). The pH of the buffer solution was adjusted to 8 using sodium hydroxide (Sigma-Aldrich 99.998%). PLA1 was a gift from Novozymes.

**Fluorescent labeling of phospholipase (PLA 1) with 3.32:**

Phospholipase A1 (2.56 mg) in 10 mM succinic acid, 0,4M $NH_4SO_4$, pH 6 (400 µL) was reacted at 4 °C for one hour with **3.32** (1.5 mg) freshly dissolved in 0.01 M $NaHCO_3$. TentaGel HL $NH_2$ resin (Rapp Polymere GmbH) (20 mg) was added and the solution shaken for 5 min. The mixture containing the polymer resin was applied to a spin column and filtered. The colored solution containing the labeled enzyme was collected and quantified by 10% SDS-PAGE and by fluorescence correlation spectroscopy (FCS). Solution of the labeled phospholipase in 0.01 M $NaHCO_3$ was stored at -80°C. Sodium dodecyl sulfate polyacrylamide gel electrophoresis (SDS-PAGE) was performed using a Phast-Gel System (Pharmacia Biotech Inc., Piscataway, NJ). The pre-cast gel used was the 12% polyacrylamide gel (Amersham Biosciences, Uppsala, Sweden). A low molecular weight marker (LMW-SDS), (Amersham, GE Healthcare) consisting of 6 molecular weight markers from 14 - 97 kDa, was used to calibrate the gel. Samples were prepared and 1.2 µL of each sample was loaded onto an eightslot applicator and inserted into the Phast-gel system.
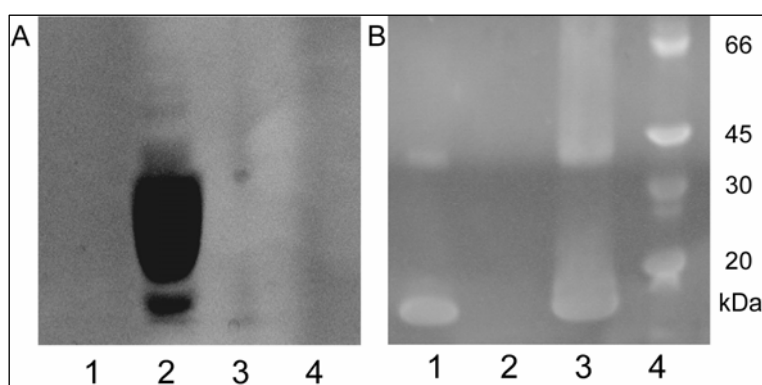


**Figure 8.1.** SDS-PAGE electrophoresis of the labeled enzyme. Panel A corresponds to UV-transillumination visualization and Panel B was stained with Coomassie blue. Lane 4 is the protein molecular weight standard. Lane 2 contains compound **5**. Lane 1 is the phospholipase and lane 3 the labeled phospholipase.

**Fluorescent labeling of phospholipase (PLA 1) with 3.45:**

Phospholipase A1 (2.56 mg) in 10 mM succinic acid, 0,4M $NH_4SO_4$, pH 6 (400 µL) was reacted at 4 °C for one hour with **3.45** (1.5 mg) freshly dissolved in 0.01 M $NaHCO_3$. TentaGel HL $NH_2$ resin (Rapp Polymere GmbH) (20 mg) was added and the solution shaken for 5 min. The mixture containing the polymer resin was applied to a spin column and filtered. The colored solution containing the labeled enzyme was collected and quantified by 10% SDS-PAGE gel electrophoresis. Solution of the labeled phospholipase in 0.01 M $NaHCO_3$ was stored at -80°C. Sodium dodecyl sulfate polyacrylamide gel electrophoresis (SDS-PAGE) was performed using a Phast-Gel System (Pharmacia Biotech Inc., Piscataway, NJ). The pre-cast gel used was the 12% polyacrylamide gel (Amersham Biosciences, Uppsala, Sweden). A low molecular weight marker (LMW-SDS), (Amersham, GE Healthcare) consisting of 6 molecular weight markers from 14 - 97 kDa, was used to calibrate the gel. Samples were prepared and 1.2 µL of each sample was loaded onto an eightslot applicator and inserted into the Phast-gel system.

**Fluorescence Correlation spectroscopy (FCS)**

Fluorescence correlation spectroscopy was performed on Compound **5** itself and enzyme labeled with **5** in aqueous solutions. A green He-Ne laser ($\lambda$ = 543 nm) was used as an excitation source, and the laser light was passed through a 543 nm interference filter. The excitation laser was reflected by a dichroic mirror (z543rdc) and focused into the sample solution by an objective (100x, NA 1.3, Olympus). The excitation power at the focal point was 16.3 µW. The fluorescence was collected by the same objective and filtered with two band pass filters (HQ607/28X, S600/40M).

The fluorescence was detected by an avalanche photo diode (Micro Photon Devices, PDM 50CT) and the active area of the detector (50 µm) was used as a pinhole.

Calibration of the FCS setup was carried out with results of sulforhodamine101 aqueous solution. The diffusion time was estimated to be 30 µs and the form factor of the focal point was to be 5.2 - 6.5 (see the next section).  This form factor was used to analyze FCS curve of water soluble PDI and PDI **5** labeled enzyme.

**Analysis of FCS curve**

The following equation was used to analyze the FCS curve.

$$G(\tau) = 1 + \frac{1}{N} \left\{ \frac{1}{\left(1 + \tau/\tau_1\right)\left(1 + \tau/\tau_1/w^2\right)^{1/2}} \right\} \qquad (1)$$

Where $N$ is number of molecule in the focal volume, $w$ represents the form factor of the focal volume, and $\tau_D$ is FCS diffusion time. On this equation the effect of triplet formation is ignore.

The diffusion constant can be calculated from FCS diffusion time using by the following equation,

$$D = \frac{r_0^2}{4\tau_D} \qquad (2)$$

where $r_0$ is size factor of the focal volume and $\tau_D$ corresponds to the FCS diffusion time. Using the reference compound (the rhodamine derivative in this paper), it is possible to estimate the diffusion constant of the target sample trough the equation (3).

$$D = D_{ref} \times \frac{\tau_{ref}}{\tau_D} \qquad (3)$$

(Using $D_{ref} = 3 \times 10^{-6}$ cm$^2$/s from http://www.biophysics.org/education/schwille.pdf)

This value is in good agreement with the diffusion coefficient calculated from the Stokes-Einstein equation and molecular weight of the enzyme

$$D = \frac{kT}{6\pi\eta a} \qquad (4)$$

where $k$ is the Boltzmann constant, $T$ stands for temperature, $\eta$ corresponds to viscosity of solution, and $a$ is the radius of object. Once more, using a reference, the diffusion constant of the labeled PLA1 can be estimated by

$$D = D_{ref} \times \frac{a_{ref}}{a} \qquad (5)$$

where the radius of enzyme and rhodamine were estimated to be $a \propto (30000)^{\frac{1}{3}} = 31$ and $a_{ref} \propto (606.72)^{\frac{1}{3}} = 8.5$ using their molecular weight, respectively.

The results are summarized in table S1.

**Table 8.1.** Diffusion time and constants for the reference and the target molecules

|  | Diffusion time ($\tau$) ($\mu$s) | Diffusion constant ($D$) (cm$^2$/s) |
| --- | --- | --- |
| Rodamine 101 | 30.0 | 3 x 10$^{-6}$ |
| PDI **5** | 39.7 $\pm$ 1.14 | 2.3 x 10-6 |
| PDI **5 labelled** PLA1 | 90.1 $\pm$ 1.84 | 1 x 10$^{-6}$ |

**Bulk activity measurements**

Bulk activity was measured using SPEX FLUOROLOG 1500 (Spex Industries, Metuchen, NJ). The time base scan experiments were performed with 1Hz acquisition rate. The fluorescent product was excited at 500nm. The fluorescent emission was detected at 520nm.

**Preparation of the layers**

Phospholipid layers were prepared using the re-hydration method.[6] Briefly, a POPC solution containing 0.1 mol% DiO was spin-coated onto freshly cleaved mica (3000rpm for 40s). After drying under vacuum for 2h, the samples were hydrated by immersion in HEPES buffer (pH 8.0) followed by heating in an oven at 80 ◦C for 3 h. Mica was purchased from SPI supplies (V-4 grade).

**Wide-field microscopy**

Imaging of individual single enzymes labeled with **5** on the POPC bilayers has been performed using an inverted wide-field epi-fluorescence microscope (IX71, Olympus). The microscope was equipped with a 60x TIRF (total internal reflection fluorescence) objective and a cooled Electron Multiplying-CCD (cascade 512B, Princeton Instruments Inc.). The PLA1 labeled with **5** was excited with 1-5 kW/cm$^2$ of 532nm laser light (CDPS 532M-50, JDS Uniphase Co.). The enzyme labeled with ATTO 647N was excited using 1kW/cm$^2$ of the 632.8 nm from He-Ne laser (1145P, JDSU & Research Electro-Optics). The POPC layers with DiO were imaged using 1-100 W/cm$^2$ of the 488-nm line from an Ar$^+$ laser (Stabilite 2017, Spectra-Physics). The laser lines of two lasers (488 and 532, for PLA1 labeled with **5** or 488 and 633, for PLA1 labeled with ATTO 647N) were guided onto the sample through a dichroic mirror (z532rdc, or z633rdc, respectively,  Chroma Technology, Inc.) and aligned in the total internal reflection mode (TIRF mode) in order to reduce background scattering form the aqueous solution. The emission from both the enzyme and the membrane were observed through a long-pass filter (HQ545LP for 532 nm and HQ645LP for 633 nm, Chroma Technology, Inc.). In such a way, most of the fluorescence form the POPC layers is rejected by the corresponding long-pass filter such that the fluorescence of individual enzymes can be detected with sufficient high signal-to-noise ratio. Movies were recorded at 20 frames per second over 1800 frames. Tracking of single enzyme molecules was performed using a home-made routine on Matlab®.[7]

## PLA1 labeled with ATTO dye

The enzyme was labeled with ATTO 647N NHS ester by following the procedure suggested by the manufacturer ([www.atto-tec.com](www.atto-tec.com)). The labeling was performed by Susana Rocha (Leuven). Specifically, the concentration of PLA1 solution was adjusted to 1.1 x $10^{-7}$M in sodium bicarbonate buffer (pH 8.3). Two-fold molar excess of reactive dye were added to the solution and incubate for 1h at room temperature. The free dye was removed from the solution using a micro dialysis filter with a cut-off of 7,000 MWCO (Pierce).

Figure S3 is a typical fluorescence image of PLA1 with ATTO dye on a bilayer. 632.8 nm light was used to excite the dye molecules. The bright spots correspond to the labeled enzyme. As compared to PDI labeled PLA1 (Fig. 2 and 3), the spots are less bright and less clear in the image, which makes localization more difficult.

The survival time of the ATTO dye is less than 200 ms with about 1 kW/cm$^2$ of excitation power. This is considerably lower than the survival time of the PDI label (note that the ATTO is excited using a laser power about 5 times lower than the one use for Compound **5**). With such a short survival time, it is hard to track the diffusive motion of the enzymes using single particle tracking. Therefore, such short-lived dye is not suitable for such experiments.
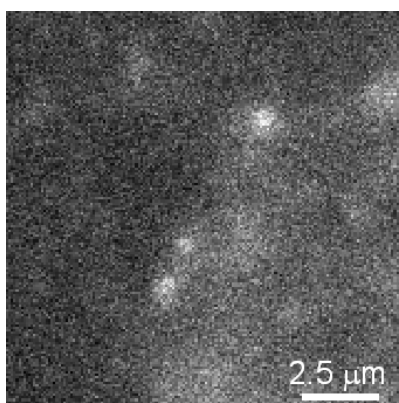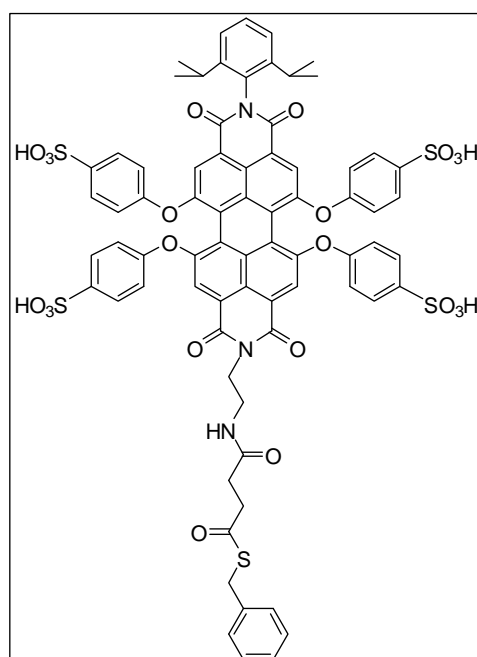


**Figure 8.2.** Fluorescence image of individual labeled enzymes on non-labelled POPC layers.

## *Chapter 5*

**3.47.N-(2,6-Diisopropylphenyl)-N'-[N-aminoethyl]-1,6,7,12-tetra(4-sulfo phenoxy)-perylene-3,4:9,10-tetracarboxydiimide:**



To a solution of N-(2,6-diisopropylphenyl)-N'-(4-aminoethyl)-1,6,7,12-tetra(4-sulfo phenoxy)-perylene-3,4:9,10-tetracarboxydiimide **3.26** (50 mg, 0.04 mmol) in N-methyl pyrrolidinone (NMP) was added thiolane-2,5-dione (6 mg, 0.052 mmol), followed by N,N-diisopropylethylamine (DIPEA) (10 mg, 0.08 mmol). After one hour, the reaction mixture was diluted with 100 mM NaCH3COO buffer (pH 5.2) and cooled to 4°C. Benzyl bromide (14 mg, 0.08 mmol) was added with thorough mixing and additionally reacted for 10 minutes. The product was purified using a Sep-Pak C18 cartridge (Millipore; pre-washed with 10 mL acetonitrile and 10 mL water; washed with 20 mL water; eluted with 1 mL 60 % methanol), dried and isolated as red solid.

**Yield:** 30 mg, 50%

**$^1$H-NMR (250 MHz, DMSO-d6, 300 K):**

δ = 7.95 (s, 2 H), 7.91 (s, 2 H), 7.62 (m, 8H), 7.40 (t, J = 7.5 Hz, 1H), 7.29 (d, J = 7.5, 6H), 6.99 (d, J = 7.5, 4H), 6.96 (d, J = 7.5, 4H), 4.16 (s, 2H), 3.58 (t, J = 12.5, 2H), 3.08 (t, J = 15 Hz, 2H), 2.68 (sept, J = 12.5 Hz, 2H), 2.28 (t, J = 12.5 Hz, 2H), 2.14 (t, J = 12.5 Hz, 2H), 1.00 (d, J = 5 Hz, 12H) ppm

**$^{13}$C-NMR (300 MHz, DMSO-d6, 300 K):**

δ = 178.14 (SC=O), 174.02 (NHC=O), 171.55 (C=O), 162.94 (C=O), 155.48, 155.27, 145.84, 145.24, 132.80, 132.43, 130.87, 128.14, 124.04, 123.69, 122.86, 120.33, 119.33, 53.75 (CH2S), 48.79 (CH2N), 42.07 (CH2N), 36.52 (CH2CO), 30.42 (CH2CO), 24.08 ppm.

**UV-Vis** (H2O): λmax (ε) = 452 (10 643), 536 (19 080), 568 (23 401) nm

**Fluorescence** (H2O, excitation 568 nm) λmax = 622 nm;

**IR-Spectrum (cm$^{-1}$, ATR):**

ν = 3460 (N-H), 3383, 3070, 2968, 2871, 1710, 1670, 1620, 1590 (C=C aromatic), 1516, 1490, 1409 (C-H bend), 1342 (C-N stretch), 1324, 1316, 1282, 1200, 1078, 1026, 957, 879, 812, 752 (CH aromatic)

**Native chemical ligation with N-terminal hexapeptide P1:**
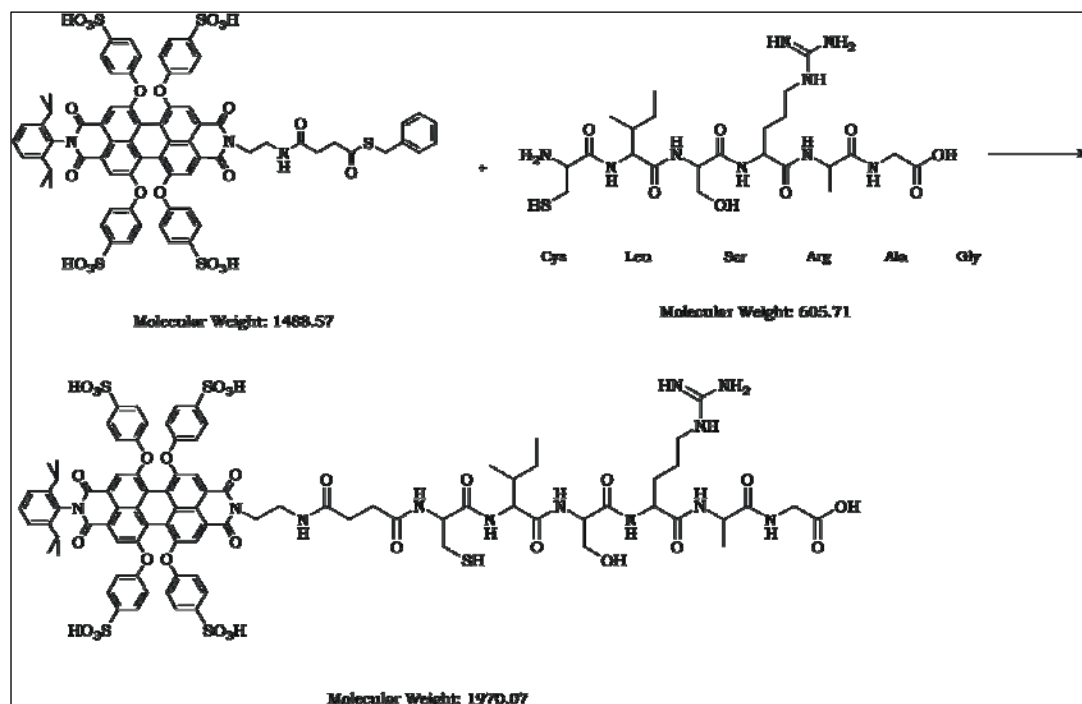


The **P1** peptide was prepared by Dr. Anke Lübbert, Max Planck Institute for Polymer Research, using standard solid-phase synthesis.

The N-terminal cystein containing peptide **P1** (1 mg, 0.0016 mmol) was dissolved in 100 mM phosphate buffer (pH 7.6), and incubated with tris(2-carboxyethyl)phosphine hydrochloride (TCEP) (0.47 mg, 0.0016) for 30 min. Equimolar amounts of **3.47** were dissolved in the same buffer and added to the protein solution and the reaction mixture was allowed to react for 24 hours at room temperature. The reaction mixture was analyzed using SDS-PAGE electrophoresis. Sodium dodecyl sulfate polyacrylamide gel electrophoresis (SDS-PAGE) was performed using a Phast-Gel System (Pharmacia Biotech Inc., Piscataway, NJ).

**Native chemical ligation with N-terminal polypeptide P2:**
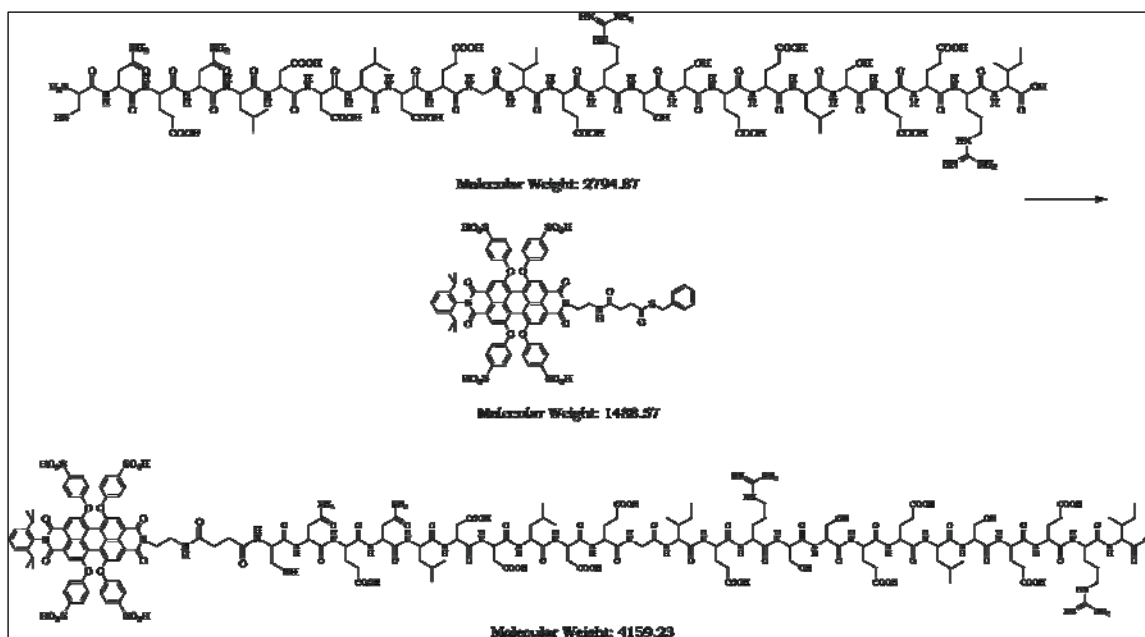


The polypeptide P2 was purchased from Sigma Aldrich Custom Peptide Synthesis.

The N-terminal cystein containing polypeptide **P2** (3 mg, 0.001 mmol) was dissolved in 50 mM HEPES buffer (6 mL, pH 8.5), and incubated with equimolar amount of tris(2-carboxyethyl)phosphine hydrochloride (TCEP) for 30 min. Equimolar amounts of **3.47** were dissolved in the same buffer and added to the protein solution and the reaction mixture was allowed to react for 24 hours at room temperature. The reaction mixture was analyzed using SDS-PAGE electrophoresis. Sodium dodecyl sulfate polyacrylamide gel electrophoresis (SDS-PAGE) was performed using a Phast-Gel System (Pharmacia Biotech Inc., Piscataway, NJ).

## Labeling of PAI-1

PAI-1 N-terminal cysteine was purchased from Oxford Biomedical Research, Inc.

The N-terminal cystein PAI-1, stable mutant was dissolved in 100 mM phosphate buffer, containing 6 M Gn·HCl, 4 % v/v thiophenol and 100 mM sodium phosphate at pH 7.6 to a final protein concentration of 2 mM. Equimolar amounts of PDI-thioester 2 (Scheme 1) were dissolved in the same buffer and added to the protein solution and the reaction mixture was allowed to react for 24 hours at room temperature. The reaction mixture was analyzed using SDS-PAGE electrophoresis. The reaction mixture was analyzed using SDS-PAGE electrophoresis. Sodium dodecyl sulfate polyacrylamide gel electrophoresis (SDS-PAGE) was performed using a Phast-Gel System (Pharmacia Biotech Inc., Piscataway, NJ).
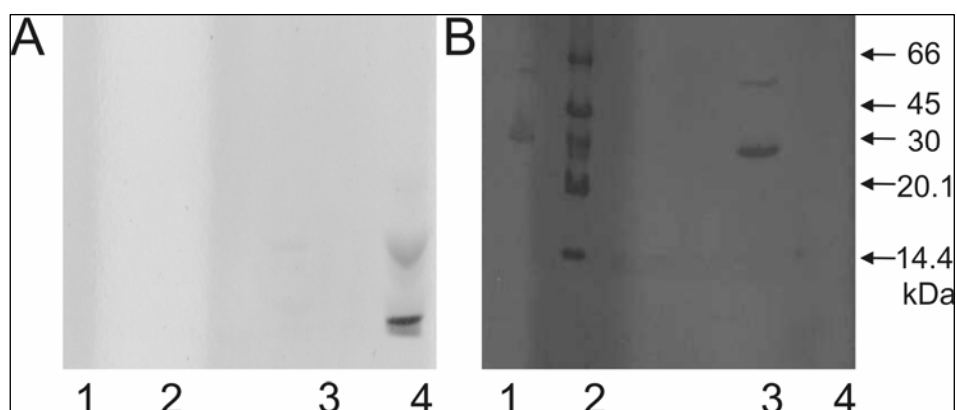


Figure 8.3. SDS-PAGE electrophoresis of the labeled PAI-1. Panel A corresponds to UV-transillumination visualization. Panel B was stained with Coomassie Blue. Lane 1 is the labeled PAI-1. Lane 4 contains **3.47**. Lane 3 is the N-terminal cystein PAI-1 and lane 2 is a molecular weight marker.

## Refolding of the conjugate

Denatured PDI-thioester-PAI-1 conjugate was refolded by dialysis (2 h, 4°C) in 20 mM CH3COONa, 1 M NaCl, 0.01% Tween-80 (v/v), pH 5,6 followed by a second dialysis step (overnight, 4°C). The protein was subsequently concentrated using centrifugal filter devices (Amicon Ultra, Amersham).[8-10]

## Fluorescence correlation spectroscopy (FCS)

FCS measurements were carried out on a confocal setup based on an Olympus IX71 inverted microscope. A solid-state laser (JIVE, Cobolt AB, Stockholm, Sweden) with emission at 561 nm was used and attenuated to 85 µW or 150 µW before focusing into the buffer solution by a water immersion objective (60x, N.A. 1.2, Olympus). The solution was placed on a microscope coverslide as a droplet of 30 µl. Scattered laser light was blocked by a dichroic beam splitter (DCXR 575, AHF, Tübingen, Germany) and out-of-focus fluorescence was rejected by an 150 µm pinhole in the detection pathway. Fluorescence was collected in the spectral range from 575 to 648 nm using an interference filter (AHF). Single photons were detected by an avalanche photodiode (SPCM AQR-14, Perkin Elmer) and registered by a TCSPC device (PC card SPC-630, Becker & Hickl, Berlin, Germany) for software calculation of the autocorrelation functions, g(2)(tc).[11] Sulforhodamine B (Sigma) in H2O was used for the calibration of the confocal volume.

The fluorescence intensity autocorrelation functions, G(tc), were fitted with a single diffusion time, tD, for the sample according to

$$G(\tau_c) = 1/N_f \left[ 1/(1 + \tau_c/\tau_D) \right] \left[ 1/(1 + (\omega/z)_2(\tau_c/\tau_D)) \right]_{1/2} \left[ 1 - T + T\exp(-\tau_c/\tau_T) \right]$$

with $N_F$, average number of fluorescent molecules in the confocal detection volume, $\tau_c$, correlation time, $\omega/z$, the ratio of the $1/e_2$ radii of the detection volume in radial

and axial directions, T, average fraction of fluorophores in the triplet state, and $\tau_T$, lifetime of the triplett state of the fluorophore. The $\omega/z$ was measured with a R6G solution as the reference and was kept fixed at this value during the subsequent fitting of the autocorrelation functions.

## *Chapter 6*

**3.49. N-(2,6-diisopropylphenyl)-N'-[3-(6-(*tert*-butyl-2,2'-(1-*tert*-butoxy-1-oxohexan-2-ylazanediyl)diacetate)carboxyethyl]-1,6,7,12-tetra(4-sulfo phenoxy)-perylene-3,4:9,10-tetracarboxydiimide:**
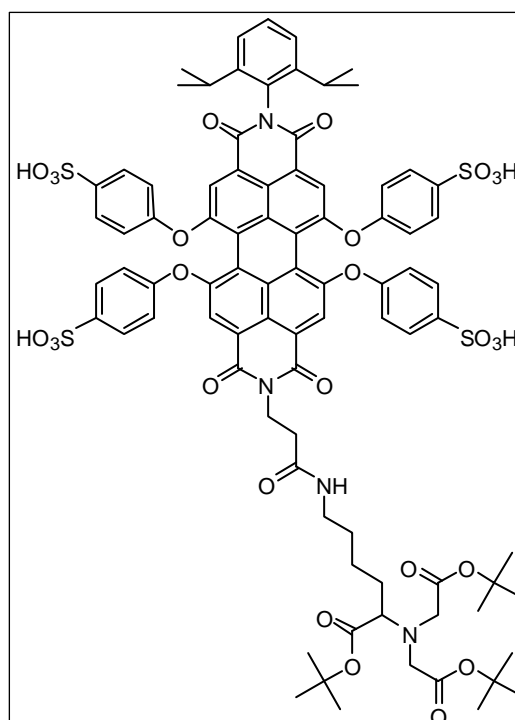


N-(2,6-diisopropylphenyl)-N'-[3-(N-succinimidyl)carboxyethyl]-1,6,7,12-tetra(4-sulfo phenoxy)-perylene-3,4:9,10-tetracarboxydiimide **3.32** (50 mg, 0.035 mmol) and diisopropyl ethylamine (DIPEA) (7.4 mg, 0.057 mmol) were added to a solution of N-(5-Amino-1-carboxypentyl)iminodiacetic acid, Tri-t-butyl Ester (22.8 mg, 0.053 mmol) in dry DMF (3 mL). The reaction vessel was purged with argon and stirred for 16 hours at room temperature. Ethylacetate (15 mL) was added to the reaction mixture to obtain a pink precipitate, which was filtered. The precipitate was washed first with dichloromethane and then three times with ethyl acetate (3x 40 mL) and dried under vacuum to give the product as red solid.

**Yield:** 70 %

**$^1$H-NMR (300 MHz, DMSO-d6, 300K):**

δ = 7.90 (s, 2 H), 7.88 (s, 2 H), 7.63 (m, 8H), 7.39 (t, *J* = 15 Hz, 1H), 7.29 (d, *J* = 9, 2H), 6.97 (m, 8H), 4.14 (t, *J* = 15 Hz, 2H), 3.56 (m, 2H), 3.32 (m, 4H), 3.17 (m, 2H), 2.95 (m 2H), 2.77 (m, 4H), 2.72 (m, 2H), 2.64 (m, 2H),1.35 (s, 27H), 1.00 (d, *J* = 9Hz, 12H);

**$^{13}$C-NMR (300 MHz, DMSO-d6, 300 K, Spinecho):**

δ = 171.89, 170.39, 162.97, 162.55, 155.72, 155.27, 155.21, 145.46, 128.17, 123.55, 122.88, 119.37, 80.30, 40.52, 32.56, 28.07, 22.58 ppm;

**UV-Vis** ($H_2O$): $\lambda_{max}$ (ε) = 450 (13 560), 534 (21 940), 560 (29 087)

**Fluorescence** ($H_2O$, excitation 560 nm) $\lambda_{max}$ = 612 nm;

**MS** (MALDI-TOF): m/z (rel. int.) = 1723 (100 %) [$M^+$]

**IR-Spectrum (cm$^{-1}$, ATR):**

ν = 3450, 3433, 2970, 2939, 2860, 2677, 1736, 1712, 1701, 1648, 1645, 1626, 1593 (C=C aromatic), 1570, 1560, 1518, 1495, 1477, 1433 (C-H bend), 1390, 1338, 1292, 1198, 1153, 1086, 877, 787, 742 (CH aromatic)

### 3.49. N-(2,6-diisopropylphenyl)-N'-[3-(N-(5-Amino-1-carboxypentyl)iminodiacetyl)carboxyethyl]-1,6,7,12-tetra(4-sulfophenoxy)-perylene-3,4:9,10-tetracarboxy diimide:
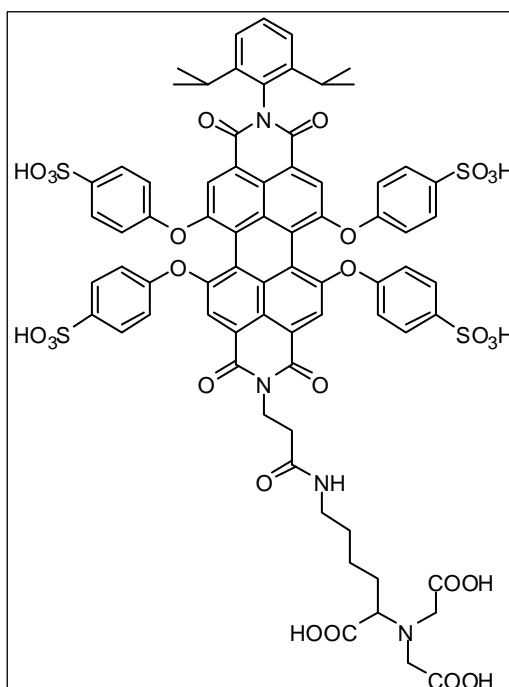


To a solution of **3.48** (40 mg, 0.023 mmol) in dry DMSO (2 mL) were added triisopropylsilane (1 mL) and trifluoroacetic acid (TFA). After stirring the reaction mixture for 3 hours at room temperature, the volatiles were evaporated under reduced pressure. Water (5 mL) was added and the solution applied on a column fill with Biogel P30. The product was eluted with water and freeze dried to give **3.49** as red solid.

**Yield:** 95 %

**$^1$H-NMR (700 MHz, CD$_3$OD, 300K):**

δ = 8.55 (s, 2 H), 8.53 (s, 2 H), 8.18 (m, 8H), 7.76 (t, *J* = 14 Hz, 1H), 7.64 (d, *J* = 7, 2H), 7.43 (m, 8H), 4.54 (t, *J* = 14 Hz, 1H ), 3.87 (m, 4H), 3.49 (m, 3H), 3.32 (m, 4H), 2.70 (m, 2H), 2.28 (m, 2H), 1.83 (m, 2H), 1.68 (t, *J* = 14 Hz, 2H),1.47 (d, *J* = 7,12H);

**¹³C-NMR (700 MHz, CD₃OD, 300K):**

δ = 168.33, 166.58, 158.54, 157.94, 156.52, 156.33, 152.51, 152.47, 149.49, 149.47, 141.82, 138.27, 138.26, 129.84, 124.08, 119.69, 114.20, 113.58, 111.91, 43.04, 38.03, 25.34, 24.71, 21.13, 19.44 ppm;

**UV-Vis (H₂O):** $\lambda_{max}$ ($\varepsilon$) = 448 nm (16 120), 534 nm (31 224), 562 nm (35 000)

**Fluorescence** (H₂O, excitation 562 nm) $\lambda_{max}$ = 614 nm ;

**MS** (MALDI-TOF): 1599.51 (100 %) [M+2Na]

**IR-Spectrum (cm⁻¹, ATR):**

$\nu$ = 3411, 3350, 3074, 2968, 2937, 2864, 1699, 1664, 1651, 1595 (C=C aromatic), 1512, 1479, 1437 (C-H bend), 1400, 1333, 1308, 1271, 1192, 1165, 1066, 1018, 883, 743 (CH aromatic)

## Solid-phase synthesis of 3.49:
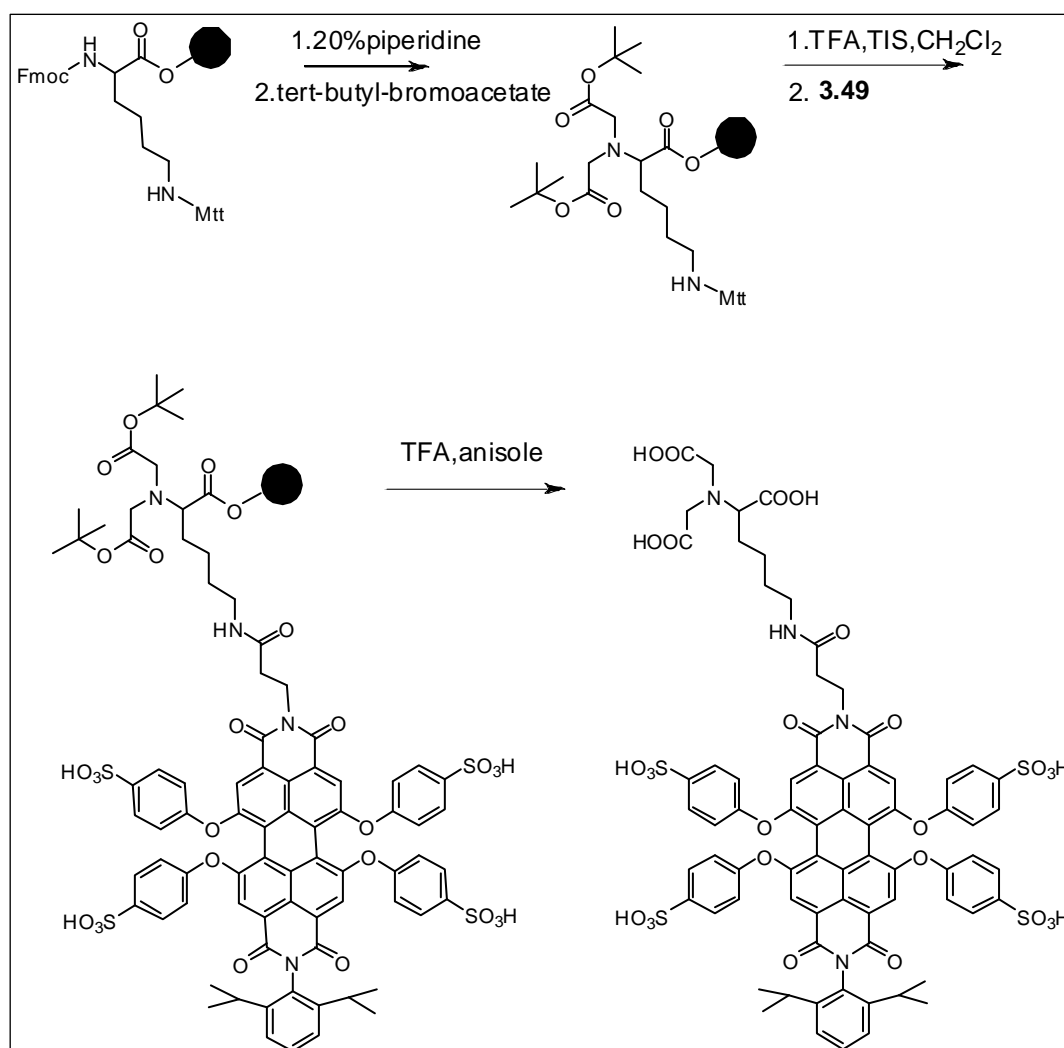


All amine deprotection and coupling steps were monitored with ninhydrine. In a 25 mL manual peptide synthesis reaction vessel, Tenta TGR resin (2 g, 0.64 mmol) was swollen in dichloromethane (DCM) for 1 h. Fmoc-Lys(Mtt)-OH (1.15 g, 1.84 mmol), 1-Hydroxybenzotriazole hydrate (HOBt) (248 mg, 1.84), O-(Benzotriazol-1-yl)-N,N,N′,N′-tetramethyluronium hexafluorophosphate (HBTU) (683 mg, 1.80 mmol), diisopropylethylamine (DIPEA) (237 mg, 1.84 mmol) was dissolved in dry dimethyformamide (DMF) (6.5 mL) added and shaken at 350 rpm at 25°C. After 12 h the resin was washed extensively with DCM. Fmoc deprotection was effected by six successive 15 min treatments of the resin with 20% piperidine in DCM. Afterwards the resin was washed extensively with DCM. To the washed

resin was added a 20-fold excess of *tert*-butyl-bromoacetate (1.79 g, 9.2 mmol) with an equal amount of DIPEA (1.18 g, 9.2 mmol) and DCM (2 ml). The reaction vessel was shaken at 350 rpm at 45°C for 27 h. Fresh reagents were added and the vessel was further incubated at 45°C with shaking for 18 h. The beads were washed successively with DCM, ethyl acetate, and DCM again. The Mtt group was removed by five 3-min treatments with 10 mL of 1% TFA, 5% triisopropyl silane (TIS) in DCM. The beads were again washed extensively with DCM. N-(2,6-diisopropylphenyl)-N-(4-carboxyehtyl)-1,6,7,12-tetrasulfophenoxy perylene-3,4:9,10-tetracarboxydiimide **3.29** (100 mg, 0.076 mmol), HOBt (10 mg, 0.076), HBTU (50 mg, 0.074) and DIPEA (10 mg, 0.076) in dry DMF (0.5 mL) were added to the beads (86 mg, 0.02 mmol) in 2 mL of DMF. The beads were allowed to react with agitation for 24 h at 25°C. After washing of the sample, an equivalent amount of fresh reagents were added and allowed to react for 12 more hours. The beads were washed successively with DCM, ethyl acetate, methanol, DCM again, and dried briefly under vacuum. The product was cleaved from the resin with several 5-min treatments with 10 mL of 95% TFA in DCM. The material was reduced to dryness with rotary evaporation, precipitated with ice-cold diethyl ether, and dried under high vacuum.

The dried off-red material was dissolved in water and purified by size-exclusion chromatography using BioGel as stationary phase and water as eluent. The yield, relative to the amount of Fmoc-Lys(Mtt)-OH was 15%.

## Ni²⁺:NTA-Perylene
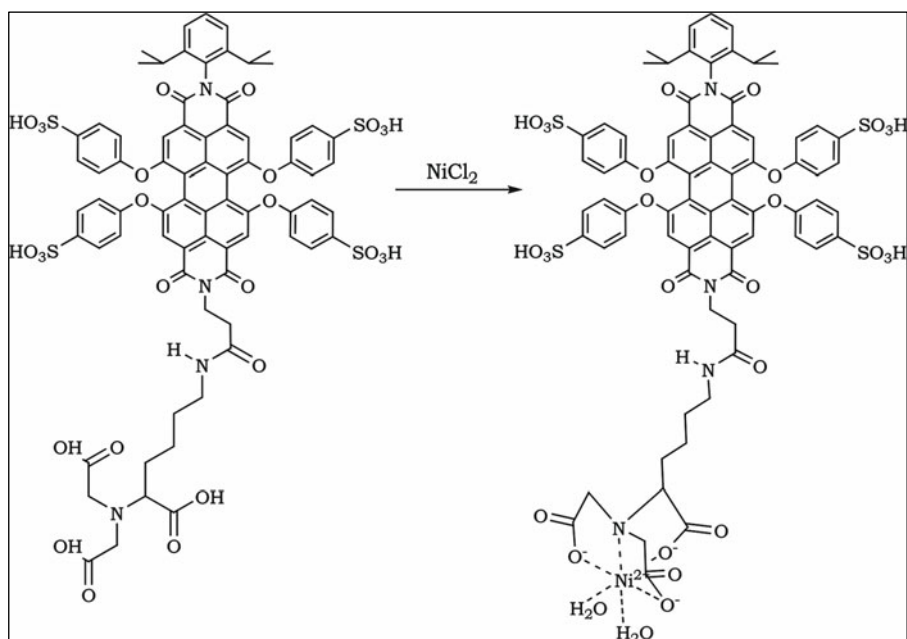


NiCl$_2$ (30 μl, 2.5x10$^{-4}$ M/l solution   in   0.01 N HCl) was added to Perylene NTA **3.49** (1 ml, 5x10$^{-5}$ M/l in water), and the solution was brought to pH 7 by addition of 0.8 mL 50 mM sodium acetate (pH 7), 200 mM NaCl. Following reaction for 30 min at 25°C, the product was purified using a Sep-Pak C18 cartridge (Millipore; pre-washed with 10 mL acetonitrile and 10 mL water; washed with 20 mL water; eluted with 1 mL 60% methanol) and dried.

## Labeling of His tagged Small Ubiqiutin-related Modifier-SUMO

The His-tagged SUMO-1 used is a recombinant protein produced in E. coli corresponding to the human sequence encompassing an N-terminal His$_6$-tagged within a leader sequence. The molecular weight of this recombinant material is 16021 Da. The histidine-tagged SUMO was obtained from BIOMOL International LP. The Ni$^{2+}$: NTA-PDI was dissolved in 50 μl - 50 mM phosphate buffer (pH 7.5), and added to a solution of the protein (using 10 fold excess of the dye). After reaction time of 30 min, the reaction mixture was purified by size exclusion

chromatography (BioGel P 30) eluted with 50 mM phosphate buffer. The labeling of the protein with **3.49** was proved by SDS-PAGE gel electrophoresis. (Figure 8.2)
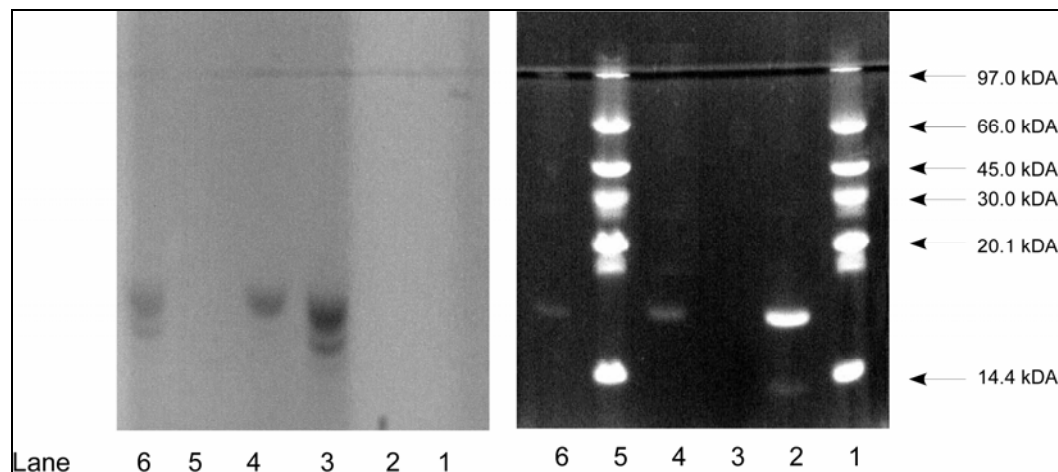


**Figure 8.2 . SDS-PAGE gel electrophoresis of the labeled SUMO. Gel 1 (left) is showing the fluorescence detection by transillumination at 366 nm, Gel 2 (right) after staining with Coumassie Blue; Lane 1 and 5 - molecular weight marker. Lane 2 - His$_6$-tagged SUMO1, on lane 3 is the perylene NTA, lane 4 shows the labeled and purified SUMO, and lane 6 shows the reaction mixture**

### Preparation of His$_6$-tagged *E. coli* F$_1$.

His6-tagged F1 was prepared from Dr. Thomas M. Duncan (Department of Biochemistry and Molecular Biology, SUNY Upstate Medical University, Syracuse, NY, USA), especially for the perylene, bearing nitrilotriacetic acid functionality and for the subsequent FCS experiments.

A His$_6$ tag was inserted at the N-terminus of the β subunit of *E. coli* F$_1$ by a two-step process. First, a PCR-based method[12] was used to create a unique NsiI restriction site (ATG**CA**T) at the 5'-end of the *atpD* gene for β in plasmid p3U[13]. A cassette of complementary, 5'-phosphorylated primers was then ligated into the cleaved, dephosphorylated NsiI site of p3U. Sequencing identified a clone, p3UβH$_6$,

with the cassette in the correct orientation and no other mutations. The modified *atpD* gene encodes β with N-terminal sequence M<u>HHHHHHMH</u>TGK (underlined residues replace wild-type Ala). $F_OF_1$ was expressed from p3UβH$_6$ in strain LE392Δ(*atpI-C*)[14], and βHis$_6$-tagged $F_1$ was purified by standard methods[13]. The βHis$_6$ tags had minimal effect on the specific ATPase activity of $F_1$.

### Fluorescence correlation spectroscopy (FCS) of His-tagged ATPase labeled with 3.49

FCS measurements were carried out on a confocal setup based on an Olympus IX71 inverted microscope. A solid-state laser (JIVE, Cobolt AB, Stockholm, Sweden) with emission at 561 nm was used and attenuated to 150 µW before focusing into the buffer solution by a water immersion objective (40x, N.A. 1.15, Olympus). The solution was placed on a microscope coverslide as a droplet of 25 to 50 µl. Scattered laser light was blocked by a dichroic beam splitter (DCXR 575, AHF, Tübingen, Germany) and out-of-focus fluorescence was rejected by an 100 µm pinhole in the detection pathway. Fluorescence was collected in the spectral range from 575 to 648 nm using an interference filter (AHF). Single photons were detected by an avalanche photodiode (SPCM AQR-14, Perkin Elmer) and registered by a TCSPC device (PC card SPC-630, Becker & Hickl, Berlin, Germany) for software calculation of the autocorrelation functions, $g^{(2)}(t_c)$.

The fluorescence intensity autocorrelation functions, $g^{(2)}(t_c)$, were fitted with two diffusion times, $t_{D1}$ and $t_{D2}$, for the un-bound and the bound perylene dye, respectively, according to

$$g^{(2)}(t_c) = \frac{1}{N_f}\left\{\alpha\left(\frac{1}{1+t_c/t_{D1}}\right)\left(\frac{1}{1+(\omega_0/z_0)^2(t_c/t_{D1})}\right)^{1/2} + (1-\alpha)\left(\frac{1}{1+t_c/t_{D2}}\right)\left(\frac{1}{1+(\omega_0/z_0)^2(t_c/t_{D2})}\right)^{1/2}\right\} \bullet \{1-T-T\exp(-t_c/t_T)\}$$

with $N_F$, average number of fluorescent molecules in the confocal detection volume, $t_c$, correlation time, $\alpha$, fraction of molecules with the shorter diffusion time $t_{D1}$, $\omega_0/z_0$,

ratio of the $1/e^2$ radii of the detection volume in radial and axial directions, *T*, average fraction of fluorophores in the triplet state, and $t_T$, lifetime of the triplet state of the fluorophore. The $\omega_0/z_0$ ratio was measured with a Rhodamine 101 solution as the reference and was kept at this value during the subsequent fittings of the autocorrelation functions of the perylene-Ni-NTA plus $F_1$-ATPase solutions. The triplet state lifetime of perylene-NTA and perylene-Ni-NTA was determined to $t_T = (2 \pm 1)$ µs. The diffusion time of $F_1$-ATPase was measured independently after labeling a cysteine (residue 106 of the $\gamma$ subunit) with a water-soluble perylene-maleimide. It was used as the diffusion time $t_{D2}$ for the calculation of the binding constant of perylene-Ni-NTA to the His tags at $F_1$.

## **Additional photophysics of PDI-NTA and PDI-Ni-NTA :**

The diffusion time of Rhodamine 101 in water was $\tau_D = 251$ µs, the diffusion time of PDI-NTA was $\tau_D = 369$ µs and of PDI-Ni-NTA was $\tau_D = 381$ µs. The diffusion times are related to the effective hydrodynamic radii and, therefore, scale with the molecular mass $M^{1/3}$. As the molecular weight increased by a factor of 3.17 for PDI-NTA (or 3.29 for PDI-Ni-NTA, respectively), the calculated diffusion times for PDI-NTA were $\tau_{D,calc} = 368.7$ µs and for PDI-Ni-NTA $\tau_D = 373.3$ µs which in excellent agreement with the measured FCS data.

# *References:*

[1] C. Kohl, Johannes-Gutenberg University (Mainz), **2003**.

[2] J. Qu, Johannes Gutenberg-University (Mainz), **2004**.

[3] E. Reuther, Johannes Gutenberg-University (Mainz), **2002**.

[4] T. Weil, Johannes Gutenberg-University (Mainz), **2002**.

[5] F. Nolde, Johannes-Gutenberg University (Mainz), **2008**.

[6] A. C. Simonsen, L. A. Bagatolli, *Langmuir* **2004**, *20*, 9720, *Structure of Spin-Coated Lipid Films and Domain Formation in Supported Membranes Formed by Hydration.*

[7] R. Bausinger, K. von Gersdorff, K. Braeckmans, M. Ogris, E. Wagner, C. Brauchle, A. Zumbusch, *Angew. Chem. Int. Ed.* **2006**, *45*, 1568, *The transport of nanosized gene carriers unraveled by live-cell imaging.*

[8] H. Nar, M. Bauer, J. M. Stassen, D. Lang, A. Gils, P. J. Declerck, *J. Mol. Biol.* **2000**, *297*, 683, *Plasminogen activator inhibitor 1. Structure of the native serpin, comparison to its other conformers and implications for serpin inactivation.*

[9] H. J. Lee, H. Im, *Protein Expression Purif.* **2003**, *31*, 99, *Purification of recombinant plasminogen activator inhibitor-1 in the active conformation by refolding from inclusion bodies.*

[10] M. C. Alessi, P. J. Declerck, M. Demol, L. Nelles, D. Collen, *Eur. J. Biochem.* **1988**, *175*, 531, *Purification and Characterization of Natural and Recombinant Human-Plasminogen Activator Inhibitor-1 (Pai-1).*

[11] M. G. Düser, N. Zarrabi, Y. Bi, B. Zimmermann, S. D. Dunn, M. Börsch, *Proceedings of SPIE-The International Society for Optical Engineering* **2006**, *6092*, 60920H/1, *3D-localization of the a-subunit in F0F1-ATP synthase by time resolved single-molecule FRET.*

[12] O. Landt, H. P. Grunert, U. Hahn, *Gene* **1990**, *96*, 125, *A General-Method for Rapid Site-Directed Mutagenesis Using the Polymerase Chain-Reaction.*

[13] T. M. Duncan, V. V. Bulygin, Y. Zhou, M. L. Hutcheon, R. L. Cross, *Proc. Natl. Acad. Sci. U. S. A.* **1995**, *92*, 10964, *Rotation of subunits during catalysis by Escherichia coli F1-ATPase*.

[14] E. M. Schaefer, D. Hartz, L. Gold, R. D. Simoni, *J. Bacteriol.* **1989**, *171*, 3901, *Ribosome-Binding Sites and Rna-Processing Sites in the Transcript of the Escherichia-Coli Unc Operon*.

# List of publications:

## A. Patents:

1. *Water-soluble rylene dyes, methods for preparing the same and uses thereof as fluorescent labels for biomolecules*, **Kalina Peneva**, Andreas Herrmann, Klaus Müllen,  EP07022521, 2007, Max Planck Institute for Polymer Research

## B. Publications:

1. *Energy Transfer in Molecular Layer-by-Layer Films of Water-Soluble Perylene Diimides.* Tingji Tang, Andreas Herrmann, **Kalina Peneva**, Klaus Müllen, Stephen Webber, ***Langmuir***. 2007 Mar 13; : 17352502

2. *Photophysics of Water Soluble Perylene Diimides in Surfactant Solutions.,* Tingji Tang, **Kalina Peneva**, Klaus Müllen, Stephen Webber, ***J Phys Chem A.*** 2007, *Vol. 111* (42), 10609

3. *Water-soluble monofunctional perylene and terrylene dyes: powerful labels for single enzyme tracking,* **Kalina Peneva**, Gueorgui Mihov, Fabian Nolde, Susana Rocha, Jun-ichi Hotta, Kevin Braeckmans, Johan Hofkens, Hiroshi Uji-i, Andreas Herrmann and Klaus Müllen, ***Angew. Chem. Int. Ed.***, 2007,*Vol. 120*, 3420

4. *Exploiting the nitrilotriacetic acid moiety for biolabeling with ultrastable perylene dyes.* **Kalina Peneva**, Gueorgui Mihov, Andreas Herrmann, Nawid Zarrabi, Michael Börsch, Thomas M. Duncan and Klaus Müllen, ***JACS***, 2008, *Vol. 130*, 5398

5. *Site-specific labeling of plasminogen activator inhibitor at amine terminal cysteine with water-soluble perylene thioester*, **Kalina Peneva**, Gueorgui Mihov, Andreas Herrmann, Michael Börsch and Klaus Müllen, ***Organic & Biomolecular Chemistry***, 2008, to be submitted

6. *Linking phospholipase mobility to activity by single molecule wide-field microscopy,* Susana Rocha, James Hutchison, **Kalina Peneva,** Andreas Herrmann, Klaus Müllen, Michael Skjøt, Christian Jørgensen, Allan Svendsen Johan Hofkens, Hiroshi Uji-I, ***PNAS***, 2008, submitted

7. *Tuning single-molecule dynamics in functionalized mesoporous silica,* Timo Lebold, Lea Mühlstein, Julia Blechinger, Melanie Riederer, Heinz Amenitsch, Ralf Köhn, Barbara Platschek, **Kalina Peneva**, Klaus Müllen, Jens Michaelis, Thomas Bein, Christophe Bräuchle, ***JACS,*** 2008, submitted

8. *Macromolecular Scaffolding: Polyisocyanopeptide based multi-chromophoric arrays. A structural analysis*, Erik Schwartz, Vicenzo Palermo, Chris E. Finlayson, Ya-Shih Huang, Matthijs Otten, Sara Trapani, Patrick Brocorens,  Jeroen Cornelissen, **Kalina Peneva**, Klaus Müllen, Frank Spano,

Richard Friend, David Beljonne, Roeland Nolte, Paolo Samori, Alan Rowan, ***JACS***, 2008, submitted

9. *Energy transfer in molecular layer-by-layer films of water soluble perylene diimides.* Tang, Tingji; **Peneva, Kalina**; Mullen, Klaus; Webber, Stephen E.; Abstracts of Papers, 233rd ACS National Meeting, Chicago, IL, United States, March 25-29, 2007

10. *Fluorescence correlation spectroscopy studies of tracer diffusion in polystyrene solutions*; Cherdhirankorn, Thipphaya; Best, Andreas; Koynov, Kaloian; **Peneva, Kalina**; Muellen, Klaus; Fytas, George; *Polymer,* 2008, submitted